PULSED ULTRASONIC DOPPLER VELOCIMETRY FOR

MEASUREMENT OF VELOCITY PROFILES IN SMALL CHANNELS

AND CAPPILARIES

A Thesis
Presented to
The Academic Faculty

by

Matthias Messer

In Partial Fulfillment
of the Requirements for the Degree
Master of Science in the
School of Mechanical Engineering

Georgia Institute of Technology
December 2005

PULSED ULTRASONIC DOPPLER VELOCIMETRY FOR MEASUREMENT OF VELOCITY PROFILES IN SMALL CHANNELS AND CAPPILARIES

Approved by:

Dr. Cyrus K. Aidun, Advisor
School of Mechanical Engineering
Georgia Institute of Technology

Dr. Yves B. Berthelot
School of Mechanical Engineering
Georgia Institute of Technology

Dr. Farrokh Mistree
School of Mechanical Engineering
Georgia Institute of Technology

Dr. Philip J. W. Roberts
School of Civil and Environmental
Engineering
Georgia Institute of Technology

Date Approved: August 8, 2005

Acknowledgements

Table of Contents

List of Tables

List of Figures

List of Equations

Nomenclature

Roman Alphabet:

a	transducer radius
a_a	amplitude absorption coefficient
A	cross section area
A_a	intensity absorption coefficient
c	speed of sound
D_r	directivity function
d	transducer diameter
d_p	piezoelectric receiving coefficient
E	Young's modulus
F	focal distance
f_D	Doppler shift frequency
f_e	emitted frequency
f_r	received frequency
g_p	piezoelectric transmitting coefficient
h	height (distance perpendicular to the flow direction)
I	Intensity
J	Bessel function
K_b	effective dynamic bulk modulus
k	wavenumber
L	characteristic length
L_{NF}	near field length
l	distance along ultrasonic beam axis
P	depth
P_0	atmospheric pressure
N	Prandtl number
R	intensity reflection coefficient
r	amplitude reflection coefficient

S_f	pore shape factor
T	intensity transmission coefficient
T_D	time delay between an emitted burst and its echo
T_d	time delay between the start of transmission and the moment at which the receiver gate opens
T_g	time period for which the receiver gate is open
T_p	pulse duration
T_{prf}	time delay between two emissions
t	amplitude transmission coefficient
U	velocity
V	volume
V_t	flow rate
v_s	velocity of source
v_r	velocity of receiver
W	beam width
Z	acoustic impedance

Greek Alphabet:

α	angle of incidence
α_a	absorption coefficient
β	angle of reflection
$\delta\!f_d$	spectral broadening
δ	phase shift of received echo
ε_p	dielectric constant of piezoelectric material
ϕ	angular excursion
γ	angle of refraction
φ	half angle of beam divergence
λ	wavelength
μ	refractive index

ν	Poisson ratio
θ	Doppler angle
ρ	density
ρ_b	effective dynamic density of material
Ω	Porosity
σ	flow resistivity
ω	Doppler angular frequency

Summary

Pulsed ultrasound Doppler velocimetry proved to be capable of measuring velocities accurately (relative error less than 0.5 percent). In this research, the limitations of the method are investigated when measuring:

- in channels with a small thickness compared to the transducer diameter,
- at low velocities
- and in the presence of a flow reversal area.

A review of the fundamentals of pulsed ultrasound Doppler velocimetry reveals that the accuracy of the measured velocity field mainly depends on the shape of the acoustic beam through the flow field and the intensity of the echo from the incident particles where the velocity is being measured. The ultrasonic transducer turned out to be most critical component of the system. Fundamental limitations of the method are identified.

With ultrasonic beam measurements, the beam shape and echo intensity is further investigated. In general, the shape of the ultrasonic beam varies depending on the frequency and diameter of the emitter as well as the characteristics of the acoustic interface that the beam encounters. Moreover, the most promising transducer to measure velocity profiles in small channels is identified. Since the application of pulsed ultrasound Doppler velocimetry often involves the propagation of the ultrasonic burst through Plexiglas, the effect of Plexiglas walls on the measured velocity profile is analyzed and quantified in detail. The transducer's ringing effect and the saturation region caused by highly absorbing acoustic interfaces are identified as limitations of the method.

By comparing measurement results in the small rectangular channel to numerically calculated results, further limitations of the method are identified. It was not possible to determine velocities correctly throughout the whole channel at low flow rates, in small geometries and in the flow separation region. A discrepancy between the maximum measured velocity, velocity profile perturbations and incorrect velocity determination at the far channel wall were main shortcomings. Measurement results are improved by changes in the Doppler angle, the flow rate and the particle concentration.

Suggestions to enhance the measurement system, especially its spatial resolution, and to further investigate acoustic wave interactions are made.

1 Introduction

At first, the history of pulsed ultrasound Doppler velocimetry, its working principle and other methods to measure velocity profiles in fluids are reviewed. Then, the benefits and the outcome of this research are introduced

1.1 History of Pulsed Ultrasound Doppler Velocimetry

Ultrasound Doppler velocimetry was originally applied in the medical field and dates back more than 60 years. The first use of ultrasound for medical diagnosis came in the 1949 with attempts at ultrasonographic cross-sectional imaging. In 1954, H. P. Kalmus described how flow velocity in fluids could be determined by measuring the phase difference between an upstream and downstream ultrasonic wave. His "upstream – downstream" method was further developed by D. L. Franklin et al. who in 1959 produced a flowmeter that could be mounted directly on blood vessels. The fact that the Doppler frequency shift could be used for the detection of blood velocity patterns was shown by S. Satomura in 1959. In 1964, D. W. Baker and H. F. Stegall presented the first Doppler instrument intended for transcutaneous measurement of blood flow velocity in man using the continuous wave Doppler principle. Approximately five years later, pulsed Doppler instruments were introduced, allowing blood flow velocity measurements at predetermined depths.

The use of pulsed emissions has extended this technique to other fields and has opened the way to new measuring techniques in fluid dynamics. The pulsed ultrasonic flow meter was initially developed to measure the flow in a blood vessel by Wells and Baker around 1970 [20]. Takeda [54] subsequently extended this method to non-medical flow measurements and developed a monitoring system for the velocity profile measurement of general fluids. The method itself was found to be quite useful to flow measurements in general and additionally through years of use has gradually become accepted as a tool to study the physics and engineering of fluid flow [56]. More recently, PUDV was applied

to study fluid flow by Takeda in 1995 [55], by Brito in 2001 [12], by Eckert in 2002 [16], by Alfonsi in 2003 [4], by Kikura in 1999 and 2004 [29-31] and by Aidun in 2005 [64]. Nevertheless, the limitations of pulsed ultrasound Doppler velocimetry are not yet completely investigated, especially when dealing with small channels and capillaries. Therefore, the limitations of pulsed ultrasound Doppler velocimetry especially in the case of small, small compared to the ultrasonic transducer diameter, rectangular channels characterized by a backward facing step are investigated in this research. Before describing this research in more details, the working principle of pulsed ultrasound Doppler velocimetry and other methods to measure velocity profiles are presented in the following sections.

1.2   Working Principle of Pulsed Ultrasound Doppler Velocimetry

The working principle of pulsed ultrasound Doppler velocimetry is to detect and process many ultrasonic echoes issued from pulses reflected by micro particles contained in a flowing liquid. A single transducer emits the ultrasonic pulses and receives the echoes as shown in Figure 1-1. By sampling the incoming echoes at the same time relative to the emission of the pulses, the variation of the positions of scatterers are measured and therefore their velocities. The measurement of the time lapse between the emission of ultrasonic bursts and the reception of the pulse (echo generated by particles flowing in the liquid) gives the position of the particles. By measuring the Doppler frequency in the echo as a function of time shifts of these particles, a velocity profile after few ultrasonic emissions is obtained.
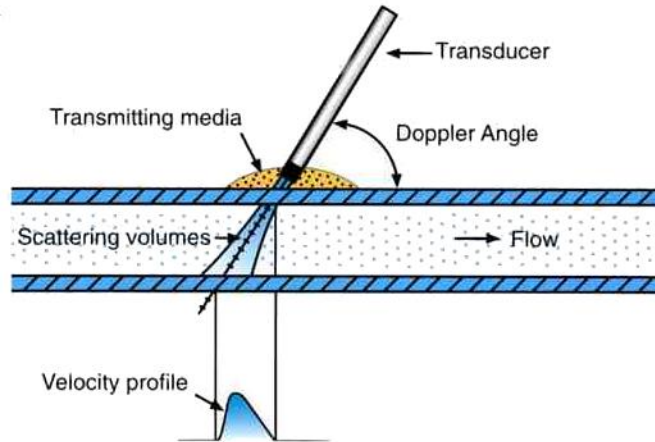
Figure 1-1: Working Principle [51]

1.3 Methods of Measuring the Velocity Profile

The instantaneous velocity profile (illustrated in Figure 1-2) is one of the most fundamental quantities in fluid flow phenomena, and its experimental measurement, especially quantitatively, has long been a demanding and challenging theme in fluid dynamics, fluid engineering, and other engineering fields concerned with fluid flow [55].
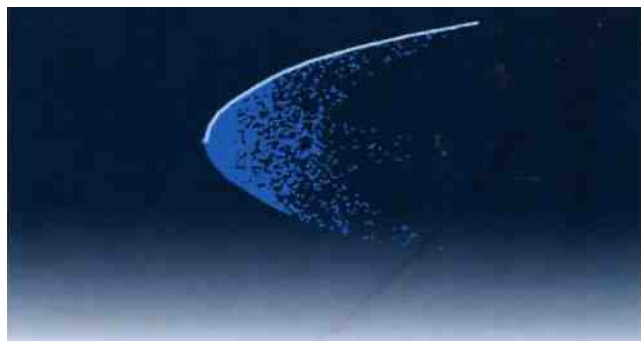
Figure 1-2: Velocity Profile [51]

Various methods and techniques have been applied in investigations where knowledge of flow patterns in enclosures is required. For these purposes flow visualization techniques have mainly been used, in order to obtain spatial information of flows. This method has

the disadvantage of difficulties obtaining quantitative results and real time data handling. Furthermore, its application to opaque fluids is not possible.

Particle image velocimtery (PIV) is the newest entrant to the field of fluid flow measurement and provides instantaneous velocity fields over a global (2- or 3-dimensional) domain with high accuracy. PIV records the position over time of small tracer particles introduced into the flow to extract the local fluid velocity. Thus, PIV represents a quantitative extension of the qualitative flow-visualization techniques that have been practiced for several decades. The basic requirements for a PIV system are an optically transparent test-section, an illuminating light source (laser), a recording medium (film, CCD, or holographic plate), and a computer for image processing. Illuminating particles are a few microns in diameter in gases and perhaps a few tens of microns in liquids [1].

Particle tracking velocimetry (PTV) is a direct descendent of flow visualization using tracer particles in fluid flows. PTV records particle displacements in a single image over a period of time. If the particle is illuminated by two successive bursts of light, each particle produces two images on the same piece of film. Subsequently, the distance between the images can be measured to approximately determine the local Eulerian velocity of the fluid. The charge-coupled device camera integrates the signal over time as the particle travels with the flow. Foreshortened image streaks are created when particles move normal to the light sheet. The centroid of a dot can be located more accurately than the end of streak. In general, velocity measurements determined by particle streaks are less reliable and about 10 times less accurate then particle image velocimetry measurements.

Instead of determining the displacement of individual particles, correlation-based PIV determines the average motion of small groups of particles contained within small regions known as interrogation spots. Essentially, the overall frame is divided into interrogation spots, and the correlation function is computed sequentially over all spots providing one displacement vector per spot. The process of averaging over multiple particle pairs within an interrogation spot makes the technique remarkably noise-tolerant and robust in comparison to PTV.

Tracer particles for PIV must satisfy two requirements. They should be able to follow the flow streamlines without excessive slip, and they should be efficient scatterers of the

4

illuminating laser light. PIV can be accomplished using continuous wave lasers or more optimally, pulsed lasers. The advantage of pulsed lasers is the short duration of the laser pulse, typically a few nanoseconds. As a consequence, a particle traveling at even very high speeds is essentially frozen during the exposure with minimal blurring. However, if the pulse duration is too long, the particle will produce streaks rather than crisp circular images (to a small extent, streaky images can be tolerated in correlation-based PIV).

PIV measurements contain errors arising from several sources: (1) Random error, due to noise in the recorded images; (2) Bias error arising from the process of computing the signal peak location to sub-pixel accuracy; (3) Gradient error resulting from rotation and deformation of the flow within an interrogation spot leading to loss of correlation; (4) Tracking error resulting from the inability of a particle to follow the flow without slip; (5) Acceleration error caused by approximating the local Eulerian velocity from the lagrangian motion of tracer particles [46].

Laser Doppler Velocimetry (LDV) is a non-intrusive measurement device that is sensitive only to velocity. LDV allows a non-invasive measurement of flow velocity by means of the well-known Doppler effect. A laser is spited into two equal-intensity, parallel beams. A lens causes these beams to cross and focus at common point. LDV makes use of the coherent wave nature of laser light. The crossing of two laser beams of the same wavelength produces areas of constructive and destructive interference patterns. The interference pattern, known as a 'fringe' pattern is composed of planar layers of high and low intensity light. Velocity measurements are made when particles 'seeded' in the flow pass through the fringe pattern created by the intersection of a pair of laser beams. These particles scatter light in all directions when going through the beam crossing. This scattered light is then collected by a stationary detector (receiving optics connected to a photomultiplier). The frequency of the scattered light is Doppler shifted and referred to as the Doppler frequency of the flow. This Doppler frequency is proportional to a component of the particle's velocity which is perpendicular to the planar fringe pattern produced by the beam crossing. In order to obtain three components of velocity, three sets of fringe patterns need to be produced at the same region in space.

Compared to laser Doppler velocimetry (LDV), that measures the velocity component, which is perpendicular to the axis of the light beam, Ultrasound Doppler Velocimetry (UDV) measures the component which is in the direction of the axis of the ultrasonic

5

beam. LDV identifies the velocity of a single particle, whereas UDV identifies velocities of a great number of scatters simultaneously and gives therefore the mean value of all the particles present in the sampling volume. In contrast to LDV, the maximum velocity is limited in Pulsed Ultrasound Doppler Velocimetry (PUDV). On the other hand, LDV can not be applied when the liquid contains too many particles or is non transparent, but UDV can. Unlike LDV, UDV gives a complete velocity profile.

1.4   Motivation

As described in the previous section, pulsed ultrasound Doppler velocimetry is almost the unique technique that is capable to measure in real time a velocity profile in liquids containing a great number of particles by processing ultrasonic echoes generated by micro particles flowing in the liquid. It can analyze any opaque or translucent liquid containing particles in suspension such as dust, gas bubbles and emulsions. Moreover it can measure other qualities, such as the echo intensity, the Doppler energy, the spectral density of the Doppler echoes, the spatial intercorrelation, the flow rate, even in presence of very high concentration of particles where optical techniques may be difficult to apply. This technique is fully non-invasive: the ultrasonic beam can cross through virtually any wall material containing the flow. In contrast to conventional techniques, the ultrasound method also offers an efficient flow mapping process and a record of the spatiotemporal velocity field [55]. The main advantage of pulsed Doppler ultrasound is its capability to offer spatial information associated with velocity values instantaneously. Spatiotemporal information (i.e., a velocity field as a function of space and time) can be obtained without prior knowledge of the flow.

Ultrasound Doppler velocimetry is applicable to opaque liquids, such as liquid metals as well as Ferro fluids, food material liquids, and so forth, but the working fluid must be transparent to ultrasound (although it might not be transparent to light). Since this method uses frequency information of the echo, it is in principle not necessary to calibrate the system using any standard velocity field [55]. Although the pulsed ultrasound Doppler velocimetry was developed for measurement of one-dimensional flow, profiles can also be successfully obtained for flow which is essentially multi-dimensional.

Pulsed ultrasound Doppler velocimetry may especially be used for the study of various types of motion within the body. Its major use remains the detection and quantification of flow in the heart, arteries and veins. Moreover, pulsed ultrasound Doppler velocimetry is used in many industrial processes that involve flow of fiber suspension in channels and pipes with various size and shape.

The flow behavior of fiber suspension has been widely studied in the past 50 years because of its important applications in the manufacture of many products such as pulp, paper, food, beverage and polymer materials. The properties of the final product often depend on the flow characteristics, such as the velocity profile and the wall shear stress. Among all of the experimental techniques, velocity profile measurement is one of the most practical methods to characterize fiber suspension flow as well as blood flow behavior. Because there is limited optical access in fiber suspension flow or rather no optical access in blood flow, velocity profile measurements are not trivial. Ultrasound Doppler velocimetry is then the only measurement technique capable of determining the velocity profile in the flow.

Due to its unique characteristics and advantages, pulsed ultrasound Doppler velocimetry already proved to be a feasible method to measure velocity profiles in many areas and especially in the applications mentioned above. Xu [64] for example evaluated and applied pulsed ultrasonic Doppler velocimetry to measure the velocity profile of fiber suspension flow in a 5.08 cm wide and 1.75 cm high rectangular channel at high velocities (Reynolds numbers greater than 10000). The relative error in his measurements caused by velocity fluctuations is less than 0.5 percent. He also showed that the measured velocities for fiber suspension flow in a channel are repeatable and the results are sensitive to small changes in the flow rate (+/- 1 percent). In Figure 1-3, the measurement results of the velocity profile at an average velocity of 4.6 m/s is presented (line B). The flow rate is varied by +/- 1 percent and the resulting velocity profiles are measured and also plotted in Figure 1-3 (line A and C respectively).
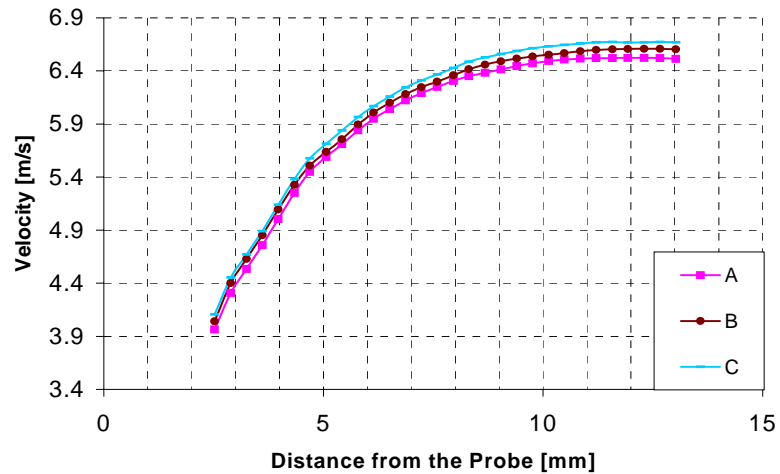
Figure 1-3: Accuracy of Pulsed Ultrasound Doppler Velocimetry [64]

By integrating the area under the velocity profile, the measured mean velocity changes are obtained. The measurement results of a change in bulk flow rate of +/- 1 percent for a suspension at a concentration of 0.5 percent shown in Figure 1-3 are then compared to the changes in the reading of a flow meter. The comparison reveals that changes in the bulk flow rate less than 1 percent can be detected easily with pulsed ultrasound Doppler velocimetry.

Even though pulsed ultrasound Doppler velocimetry proved to be capable of measuring velocities accurately, its limitations have not yet been completely investigated, especially when measuring

- in channels with a small thickness compared to the transducer diameter,
- at low velocities
- and in the presence of a flow reversal area.

Therefore, the desired outcome of this thesis is to determine the limitations of pulsed ultrasound Doppler velocimetry and, if necessary, develop suggestions for improving the measurement of velocity profiles especially in small channels and capillaries where a high spatial and also temporal resolution is required. Application of pulsed ultrasound Doppler velocimetry often involves the propagation of the emitted acoustic field and the returning echo through a Plexiglas wall. Therefore, the effect of Plexiglas walls on the ultrasonic beam shape and on velocity measurements in general is investigated in this research. Moreover, the interaction of pulsed wave packets with porous screens is evaluated. This

8

research may therefore be used to increase the range of application of pulsed ultrasound Doppler velocimetry especially in industrial processes (e.g., paper industry) but also in the medical field and the emerging area of bioengineering.

To determine the limitations of pulsed ultrasound Doppler velocimetry, the fundamentals of this method and the working structure of the utilized instrument as well as other components of the measurement system have been investigated first. In Chapter 2, the fundamentals of ultrasound Doppler velocimetry are reviewed. This part is essential to identify fundamental limitations of pulsed ultrasound Doppler velocimetry, design an experimental setup to investigate further limitations and make suggestions for improvement. At first, the Doppler effect, the basis of ultrasound Doppler velocimetry, is described in Section 2.2. Then continuous and pulsed ultrasound Doppler velocimetry are identified as two complementary modes of ultrasound Doppler velocimetry. In the following, the working structures of the measurement system and its components are analyzed in detail. The fundamentals of the ultrasonic field, acoustic phenomena and the sampling process, necessary for evaluating measurement results at a later point, are identified. The following chapters will build on and refer to the fundamentals reviewed in this chapter.

In Chapter 2, the ultrasonic transducer is identified to be the most critical component of the measurement system. Therefore, the fundamentals of generally available ultrasonic transducers, i.e., single element transducers and transducer arrays, their working principle, architecture, characteristics and potential for focusing the emitted ultrasonic beam have been reviewed especially to make suggestions for improving the currently utilized pulsed ultrasound Doppler velocimeter (described in detail at a later point).

In the Chapter 3, the ultrasonic beam shape is measured. Information about the actual beam shape of various ultrasonic transducers and especially their lateral resolution is gained. The lateral resolution of the pulsed ultrasound Doppler velocimetry system is extremely important in evaluating the flow over a backward facing step in small channels, i.e., when dealing with small geometries. Ultrasonic beam measurements will therefore be used to identify the most appropriate transducer to measure velocity profiles in small channels and capillaries. Moreover, the interaction of walls and porous screens with the emitted ultrasonic wave packet and their effect on measuring the velocity profile with unfocused as well as focused ultrasonic transducers is analyzed. At first, the experimental

setup is described and the ultrasonic beam of various transducers is measured. Since application of pulsed ultrasound Doppler velocimetry often involves the propagation of the emitted ultrasonic burst through a Plexiglas wall, the interaction of the ultrasonic burst with Plexiglas walls of different thicknesses is then investigated and quantified in detail. Finally, the effect of a porous screen, a paper forming screen, is explored.

In Chapter 4, the 8 MHz 5 mm ultrasonic transducer was identified to be the most promising transducer to measure velocity profiles in small channels and capillaries due to its excellent axial and lateral resolution. In Chapter 5, velocity profiles are then non-intrusively measured in a small rectangular channel characterized by a backward facing step to experimentally validate the theoretical limitations of pulsed ultrasound Doppler velocimetry (identified before), investigate further limitations in small channels in a separated flow at low velocities and compare focused with unfocused ultrasonic transducers. At first, the principle of measurement and important parameters of pulsed ultrasound Doppler velocimetry are presented. Then the experimental setup that was solely designed for this purpose is described. Technical drawings of the channel and distributor are shown in Appendix A. After reviewing the fundamentals of flow over a backward facing step, the measurement results are presented and finally evaluated. The effect of Plexiglas walls on the measurement results has been evaluated in detail. Before actually measuring velocity profiles with pulsed ultrasound Doppler velocimetry, the purpose and necessary measurement preparations are described. The effect of Plexiglas walls and various measurement parameters is discussed. Finally, measurement results of focused and unfocused ultrasonic transducers are compared and evaluated.

Based on the fundamentals of pulsed ultrasound Doppler velocimetry, beam shape measurements of various ultrasonic transducers with and without walls and porous screens and measurements of velocity profiles in the flow over a backward facing step in a small rectangular channel, the limitations of pulsed ultrasound Doppler velocimetry are summarized in Chapter 6. After stating the simplifying assumptions of pulsed ultrasound Doppler velocimetry, its accuracy and the effect of artifacts, specific limitations that have been identified by reviewing the fundamentals of pulsed ultrasound Doppler velocimetry and by measuring the ultrasonic beam shape as well as velocity profiles in a small rectangular channel are identified.

Based on the fundamentals of pulsed ultrasound Doppler velocimetry, on the measurements of ultrasonic beam shapes and velocity profiles in the flow over a backward facing step in a small rectangular channel and on the limitations of pulsed ultrasound Doppler velocimetry presented in Chapter 6 suggestions for improving the measurement system and for future research are made in the following. The ultrasonic transducer has been identified as the most critical component of the measurement system. To improve especially the spatial resolution of the measurement system, it is suggested to use annular phased array transducers and modify the measurement system accordingly. Through electronic focusing, ultrasonic beam steering and automatic variations in the aperture size, annular phased array transducers enhance the spatial resolution of the system significantly. Research on a new ultrasonic transducer architecture combining the advantages of standard pulsed ultrasound Doppler velocimetry and the ultrasound phased array technique is therefore crucial. The necessity of future research on the interaction between acoustic waves and acoustic interfaces encountered by the ultrasonic beam and suspended objects in the flow is emphasized in the following sections. A literature review on the interaction of acoustic waves with cylindrical and spherical objects is undertaken to frame future research in this area.

2 Ultrasound Doppler Velocimetry

In this chapter, the fundamentals of ultrasound Doppler velocimetry are reviewed. This part is essential to identify fundamental limitations of pulsed ultrasound Doppler velocimetry, design an experimental setup to investigate further limitations and make suggestions for improvement. At first, the Doppler effect, the basis of ultrasound Doppler velocimetry, is described. Then continuous and pulsed ultrasound Doppler velocimetry are identified as two complementary modes of ultrasound Doppler velocimetry. In the following, the working structure of the measurement system and its components is analyzed in detail. The fundamentals of the ultrasonic field, acoustic phenomena and the sampling process, necessary for evaluating measurement results at a later point, are identified. The following chapters will build on and refer to the fundamentals reviewed in this chapter.

2.1 Introduction to Ultrasound Doppler Velocimetry

In typical applications, where ultrasound Doppler velocimetry is used to measure ambient fluid velocity, the scatterer is presumed to be drifting along with the flow but transmitter and receiver are outside the flow (shown in Figure 2-1). The measurements ordinarily require the idealization that the ambient velocity and acoustical properties appear unidirectional and stratified in the plane that contains transmitter and scatterer and is tangential to the scatterer's velocity vector. The same should apply for the plane containing receiver, scatterer, and the scatterer's velocity [45].
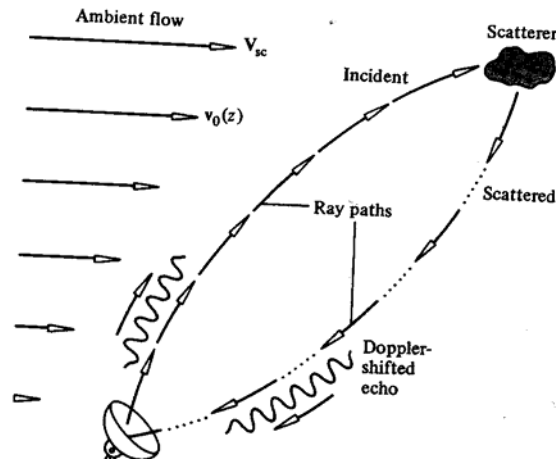
Figure 2-1: Doppler Shift [52]

Two complementary modes of ultrasound Doppler velocimetry are available: continuous and pulsed ultrasound Doppler velocimetry. Both techniques are related to the Doppler effect.

2.2 Doppler Effect

The Doppler effect (Johann Christian Doppler, 1803-1853; Austrian mathematician and physicist) is the shift (change) in frequency of an acoustic or electromagnetic wave resulting from the movement of either the emitter or receptor [8]. For example, if the receiver is approaching the source, it will encounter more waves in unit time than if it remains stationary; thus there is a change in the apparent wavelength. In general, when an observer is moving relative to a wave source, the frequency he measures is different from the emitted frequency. If the source and observer are moving towards each other, the observed frequency is higher than the emitted frequency; if they are moving apart the observed frequency is lower [18].

In general the apparent frequency at the receiver is given by:

$$f_r = \frac{c - v_r}{c - v_s} f_e$$

Equation 1: Frequency at Receiver

where f_e is the frequency of the source, c is the speed of wave propagation, v_r is the velocity of the receiver away form the source and v_s is the velocity of the source in the same direction as v_r.

By convention, the velocity v is considered negative when the target is moving toward the transducer. This equation can be rearranged to give the value $f_D = f_r - f_e$, the Doppler shift frequency, thus:

$$f_D = \left(\frac{c - v_r}{c - v_s} - 1 \right) f_e$$

Equation 2: Doppler Shift Frequency

In ultrasound Doppler velocimetry, the Doppler effect is used to study the movements of reflecting interfaces. When both the source and the receiver are stationary, the reflecting interface alters the direction of the waves in such a way that they appear to originate from a virtual source at a distance from the receiver equal to the total distance traveled by the waves. Thus the effect is the same as if the source and the receiver were moving apart with identical velocities, equal to that of the reflector ($v_r = - v_s = v$). Therefore the change in frequency f_D at the receiver is given by:

$$f_D = -\left(\frac{2v}{c + v} \right) f_e$$

Equation 3: Doppler Shift Frequency (Source and Receiver Stationary)

where v is the absolute velocity of the reflector along the direction of flow. If $c \gg v$, this equation can be simplified to give:

$$v = -\frac{f_D c}{2 f_e}$$

Equation 4: Reflector Velocity (Source and Receiver Stationary Simplified)

In cases where the various velocities do not all act along the same straight line, the appropriate velocity vectors must be used for the calculation of f_D. Thus, if θ_1 is the angle of attack (defined as the angle between the direction of movement and the effective ultrasonic beam direction), the above equation can be modified:

$$v = -\frac{f_D c}{2 f_e \cos\theta_1}$$

Equation 5: Reflector Velocity Modified

The algebraic sign of f_D is not important in a simple system because the Doppler shift detector is sensitive only to the magnitude of f_D.

2.3 Continuous Ultrasound Doppler Velocimetry

In continuous ultrasound Doppler velocimetry, the velocity is measured by finding the Doppler shift frequency in the received signal (for example by quadrature detection [52]). Mathematically, the Doppler shift frequency relation is derived as follows.

Consider an ultrasonic transducer which emits waves of frequency f_e and remains fixed in a medium ($v_s = 0$) where the speed of sound is given by c. A receptor or target in the medium moves with a velocity v. According to Equation 1, if the trajectory of the target is moving toward the transducer and forms an angle θ_1 with respect to the direction of propagation of the ultrasonic wave (as shown in Figure 2-2), the frequency of the waves perceived by the target will be:

$$f_t = f_e - \frac{f_e v \cos\theta_1}{c}$$

Equation 6: Frequency at Target
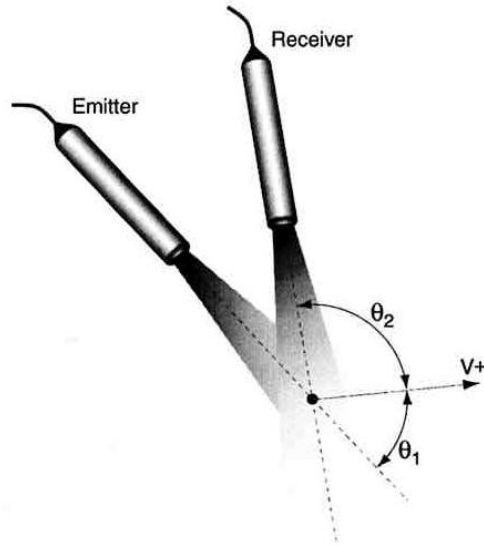
Figure 2-2: Ultrasonic Transducer (Emitter and Receiver) [51]

If the acoustic impedance of the target is different from that of the surrounding medium, the waves will be partially reflected. The target acts as a moving source of ultrasonic signals. The frequency of the waves reflected by the target, as measured by a stationary receiver, is:

$$f_r = f_g - \frac{f_g v \cos\theta_2}{c}$$

Equation 7: Frequency at Receiver

where f_g is the frequency of the reflected wave from the target. When both the source and the receiver are stationary, substitution of the appropriate vector components of v (velocity of target) for v_r and v_s in Equation 2 gives:

$$f_D = \left(\frac{c - v\cos\theta_2}{c - v\cos\theta_1} - 1\right)f_e$$

Equation 8: Doppler Shift Frequency in General

As the velocity of the target is much smaller than the speed of sound ($v \ll c$) it is reasonable to neglect the second order terms:

$$f_D = \frac{f_e}{c}\left(v\cos\theta_1 - v\cos\theta_2\right)$$

Equation 9: Doppler Shift Frequency Simplified

If the same transducer is used for receiving the signals ($\theta_2 = 180° - \theta_1 \Rightarrow \cos\theta_2 = -\cos\theta_1$) the above equation becomes:

$$f_D = \frac{2f_e v\cos\theta_1}{c}$$

Equation 10: Doppler Shift Frequency One Transducer

In continuous ultrasound Doppler velocimetry, the returning ultrasound signal is either a slightly expanded or slightly compressed version of the transmitted signal, due to the motion of the targets. In general, separation of the echo signal and the transmitted signal could be made on the basis of difference in time, by separation of the strong transmitted signal form the weak echo or by recognizing the change in the echo-signal frequency caused by the Doppler effect when there is relative motion between radar and target [53]. In continuous ultrasound Doppler systems the velocity is measured by finding the Doppler shift frequency in the received signal (for example by quadrature detection [52]). Usually two adjacently positioned transducer elements are used. One element constantly emits waves and the other continuously receives reflected signals. The simplest approach to exploit the Doppler shift is to emit a continuous sinusoidal wave and then compare the received with the emitted signal to detect the change in frequency. The received signal is multiplied by a quadrature signal of frequency f_e, the frequency of the emitted signal, to

find the Doppler shift. The result is a signal containing frequency components equal to the sum and difference of the emitted and received signals' frequencies. A band-(low)-pass filter is used for removing the higher frequency signal at twice the emitted frequency. The resulting signal after the band-pass filter contains the Doppler shift of the emitted signal and, thus, the velocity encountered in the medium under investigation. It must be emphasized that although only one frequency is present at this stage, the received signal consists of a continuum of frequencies. Since all the Doppler frequencies fall in the audio range, the velocity distribution can simply be judged by listening to the signal. The simplest quantitative method of characterizing the flow is to detect the most dominant frequency in the signal. This approach should characterize the dominant part of the flow. One technique is to estimate the zero crossing rate of the signal. The zero crossing detector counts the number of times the signal crosses its mean value. This gives a good estimate of the frequency, when the spectrum is essentially monochromatic and contains little noise. The zero crossing detector, thus, has some very significant drawbacks in terms of a biased output and sensitivity to noise. They are, therefore, only used in the simples Doppler instruments today, and more advanced digital techniques are preferred. More flexible, accurate and nearly noise free digital implementations consist of an analog front-end, which quadrature demodulates the Doppler signal. This is then sampled by a pair of analog-to-digital converters and processed by a digital signal processor. A display of the distribution of velocities can be made by Fourier transforming the received signal and showing the result. This display is also called a sonogram [27].

Continuous ultrasound Doppler systems are unable to measure the distance between the transducer and the moving structure. Consequently no information about the range at which movement is occurring is provided. There is no problem with aliasing (velocity ambiguity) of the Doppler shifted signal, since the ultrasound sampling rate (pulse repetition frequency) is very high [28]. Continuous ultrasound Doppler systems are simple and often inexpensive devices and ensure a potential minimal spread in the transmitted spectrum. On the other hand, spillover, i.e., direct leakage of the transmitter and its accompanying noise into the receiver, is a severe problem.

2.4 Pulsed Ultrasound Doppler Velocimetry

In contrast to continuous ultrasound Doppler systems, pulsed ultrasound Doppler systems are able to measure the distance between the transducer and the moving structure. In pulsed Doppler ultrasound, instead of emitting continuous ultrasonic waves, an emitter sends a short ultrasonic burst periodically and a receiver continuously collects echoes from targets that may be present in the path of the ultrasonic beam. Echoes are accepted only for a short period of time following an operator-adjustable delay. The length of the delay determines approximately the range from which signals are gathered [18]. By sampling the incoming echoes at the same time relative to the emission of the series of bursts at the fixed pulse repetition frequency, the shift of positions of scatterers are measured. Instead of making an absolute measurement of frequency as in continuous wave Doppler systems, a relative measurement of phase shift between pulses received is employed in pulsed ultrasound Doppler velocimetry. Pulsed wave Doppler systems are used to obtain Doppler information at a specific range from the face of the transducer.

In general, if P is the distance from the transducer to the target, the total number of wavelengths contained in the two way path between the transducer and the target is $2P/\lambda$. The distance P and the wavelength λ are assumed to be measured in the same units. Since one wavelength corresponds to an angular excursion of 2π radians, the total angular excursion ϕ made by the electromagnetic wave during its transit to and from the target is $4\pi P/\lambda$ radians. If the target is in motion, P and the phase ϕ are continuously changing. A change in ϕ with respect to time is equal to a frequency. This is the Doppler angular frequency ω_D, given by:

$$\omega_D = 2\pi f_D = \frac{d\phi}{dt} = \frac{4\pi}{\lambda}\frac{dP}{dt} = \frac{4\pi v}{\lambda}$$

Equation 11: Doppler Angular Frequency

where f_D is the Doppler frequency shift and v is the relative (or radial) velocity of target with respect to radar. The Doppler frequency shift is:

$$f_D = \frac{2v}{\lambda} = \frac{2vf_e}{c}$$

Equation 12: Doppler Frequency Shift

where f_e is the transmitted frequency and c is the velocity of propagation.

Let's assume a situation, as illustrated in the Figure 2-3, where only one particle is present along the ultrasonic beam. From the knowledge of the time delay T_D between an emitted burst and the echo from the particle, the depth P of this particle could be computed by:

$$P = \frac{cT_D}{2}$$

Equation 13: Depth

where c is the sound velocity of the ultrasonic wave in the liquid.

If the particle is moving at an angle θ relative to the axis of the ultrasonic beam, its velocity v can be measured by computing the variation of its depth (ΔP as shown in Figure 2-3) between two emissions separated in time by T_{prf} (prf stands for pulse repetition frequency):

$$(P_2 - P_1) = \Delta d \cos\theta = vT_{prf} \cos\theta = \frac{c}{2}(T_2 - T_1)$$

Equation 14: Variation in Depth Between Two Emissions
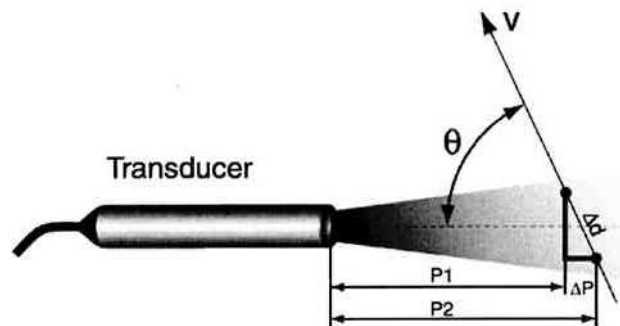
Figure 2-3: Ultrasonic Transducer [51]

The time difference $(T_2 - T_1)$ is always very short, most of the time less than a microsecond. It is advantageous to replace this time measurement by a measurement of the phase shift of the received echo.

$$\delta = \omega t = 2\pi f_e (T_2 - T_1)$$

Equation 15: Phase Shift of the Received Echo

where f_e is the emitting frequency. With this information the velocity of the target is expressed by:

$$v = \frac{c(T_2 - T_1)}{2T_{prf} \cos\theta} = \frac{c\delta}{2T_{prf} \cos\theta \, 2\pi f_e} = \frac{cf_D}{2f_e \cos\theta} \qquad \text{with} \qquad f_D = \frac{\omega_D}{2\pi} = \frac{1}{2\pi} \frac{\delta}{T_{prf}} \ .$$

Equation 16: Velocity Measured

This last equation gives the same result as the Doppler equation but one should always be aware that the phenomena involved are not the same. The term "Ultrasound Doppler Velocimetry" implies that the velocity is measured by finding the Doppler shift frequency in the received signal (for example by quadrature detection [52]), as is the case in Continuous ultrasound Doppler or Laser Doppler velocimetry. In fact, in pulsed ultrasound Doppler velocimetry, this is never the case. Velocities are derived from shifts in positions between pulses and the Doppler Effect plays a minor role.

In pulsed wave systems, a number of pulses are emitted into the fluid or medium under investigation and the backscattered signal received by the transducer is sampled at the same time relative to the pulse emission. The displacement of the backscattered signal, as a consequence of the movement of the particles in the fluid, is then detected. These systems are also called Doppler systems, which is misleading because they do not use the Doppler effect. It is the shift in position of the scatterers, and not the shift in the emitted frequency, that is detected in pulsed ultrasound Doppler velocimetry.

There are two distinct mechanisms affecting the received signal in the demodulation process. The first is that of "classical" Doppler shift where, because of the motion of the

target, each received pulse is either an expanded or compressed version of the transmitted pulse. The second is that because the target in the sample volume (which has a particular "ultrasonic signature") has either moved towards or away from the transducer, consecutive received signals undergo a progressive time shift with respect to the time of transmission. Consecutively received signals are shifted in time compared with the proceeding and preceding sample volume as a result of the scatterers' motion. This time shift gives rise to a progressive change in the phase relationship between the ultrasound signature and the master oscillator, which is exactly what is detected in pulsed ultrasound Doppler velocimetry. As time increases, the time delay of the received signal also increases, as the distance between the transducer and the scattering particle increases. This indicates that if signals from successive emissions were acquired, one would experience a waveform moving slowly away or toward the transducers. Two received signals are compared in order to analyze this situation. Pulses are emitted with a delay of T_{prf} seconds. Identical responses will be received if no movement takes place. Movement will yield a small displacement in position, which can also be perceived as a shift in time relative to the pulse emission. A time delay or corresponding phase shift is observed between consecutive emissions. The received signal is not merely translated in time from pulse to pulse, but does also change shape due to the construction of the signal from the summation of responses from numerous scatterers moving at different velocities. The received signals stem from a summation of contributions from numerous scatterers, each weighted by the field strength and shape, and constructive and destructive interference between the scatterers takes place. Scatterers move at different velocities and their relative position changes over time, modifying the interference between scatterers.

Curiously enough, it can be argued that the "classical" Doppler shift on the ultrasound pulse actually decreases the precision of velocity estimates using a pulsed wave system. Actually the classic Doppler Effect is an artifact in these systems [27]. The important thing to note is that the frequency shift detected due to the changing phase relationship is virtually identical to that detected by a classical continuous wave system, and any differences can be ignored for most practical purposes. Consequently, the basic Doppler equation applies equally in the case of both continuous wave and pulsed wave systems.

Although the demodulated signals from continuous wave and pulsed wave Doppler devices are usually treated and processed in the same way, there are fundamental differences between them which really only become important when considering the effects (or rather the perhaps unexpected lack of effects) on the Doppler signal of such phenomena as frequency-dependent attenuation. Indeed, the surprising fact is that whilst continuous Doppler ultrasound devices measure the "classical" Doppler shift, pulsed Doppler ultrasound devices do not, and indeed could not, because the (wide-band) spectrum of a short pulse of ultrasound changes so significantly as it propagates and is scattered due to dispersion. The detection of a small relative shift is not possible for pulsed instruments that employ a small number of pulses for each detection, because the downshift in frequency due to attenuation will dominate over the Doppler shift. Nevertheless, continuous wave and pulsed wave devices have virtually the same characteristics (leaving aside issues such as aliasing).

Pulsed Doppler systems tend to be used in two distinct fashions. Either the sample volume is made sufficiently large to encompass an entire region containing movement or sufficiently small, such that just a small part of velocity field is probed. In the former case, the range discrimination is used primarily to reject signals from other nearby structures; in the latter, the high spatial resolution is used to extract information about flow or movement in a specific area.

2.5 Architecture of the Velocimeter

In order to determine fundamental limitations and make suggestions for improvement, the working structure of the measurement system is investigated in detail in the following. The general architecture of the Velocimeter used in pulsed ultrasound Doppler velocimetry is shown in Figure 2-4:
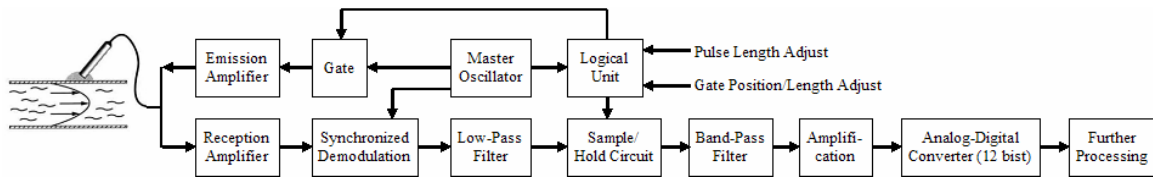
Figure 2-4: General Architecture Velocimeter

2.5.1 Master Oscillator, Gate and Emission Amplifier

The signal coming from the principal oscillator provides the trigger for the emitted signal at the pulse repetition frequency. The signal from the master oscillator is gated under the control of the pulse-repetition-frequency-generator. The length of time the emission gate remains open depends on the required length of the sample volume but is usually sufficient to permit the passage of a number of complete cycles from the oscillator. The resulting pulse is amplified and used to drive the transducer, which emits a burst of ultrasound (the shape and length of the burst is determined both by the exciting pulse and the transducer characteristics).

2.5.2 Transducer

As the length of the transmission burst is very small compared with the reception time, a single crystal transducer can be used. A single transducer operates firstly as a transmitter of ultrasound, and then as a receiver. As the reception path is identical to the transmission path, the problem of alignment is avoided. The ultrasonic transducer is electrically matched to the input impedance of the receiver and is acoustically backed and matched so that it provides an ultrasound burst that matches the electrical excitation voltage produced by the transmitter, i.e. the bandwidth of the probe has to be as large as the bandwidth of the transmitted signal.

Short high-voltage unipolar electrical pulses are used to shock-excite the damped transducer to vibrate in its fundamental resonance thickness expander mode. High-voltage pulses used to increase output energy and overcome transducer damping losses represent a source of electrical interference. The pulse-echo transducer is connected to both transmitting and receiving circuits. Thus, the strong shock pulse also is applied directly to the receiver input. This pulse must not be allowed to enter the high gain amplifiers; it

24

would either blow out circuits or cause a "paralysis" period during which echoes from close reflectors cannot be distinguished. Early analog equipment used diode clipping circuits to limit the transmitted amplitude of the shock pulse while passing low level echoes.

2.5.3   Reception Amplifier

Ultrasonic echoes returning are converted to electrical signals by usually the same transducer. The amplification (time dependent) of the echo signal is increased according to the depth (Time Gain Control) in order to compensate for the attenuation of the waves during their propagation.

Two different operator controls for amplification are used to properly process the echo amplitude signal: overall gain and swept gain. Overall gain is a constant gain level independent of sample volume depth. Time-varying gain (TGC or "swept gain") is used to compensate for attenuation of the sound beam by amplifying echo signals from distal structures more than echo signals from proximal structures. The rate at which the TGC varies with time and the shape of the "gain curve" are under operator control. Since the attenuation coefficient increases with increasing ultrasound frequency, the TGC slope usually has to be steeper for higher-frequency than lower-frequency. Increasing the logarithmic amplifier gain in synchrony with the arrival time of echoes provides a simple means of compression by approximately compensating for attenuation [44].

Constant slope swept gain however can not compensate for echo amplitude variations due to the focused beam pattern. In Figure 2-5 (a) focused beam echo signals obtained from identical reflectors in a uniform sample volume are demonstrated. In this case, the constant slope swept gain has been set to compensate exactly for the attenuation. Each reflector scatters echoes with the same scattering cross section but the incident pressure varies along the focused beam pattern so the echoes from the focal zone are largest. An alternative swept gain control is the use of a set of slide potentiometers to divide the signal depth into equal range increments. Each slide potentiometer determines the swept gain level at the center of a given range in the image. A smooth swept gain control voltage with depth is then automatically generated from the slide potentiometer settings.

In Figure 2-5 (b) the use of the slide potentiometers to compensate for both medium attenuation and the focused beam pattern is shown [44].
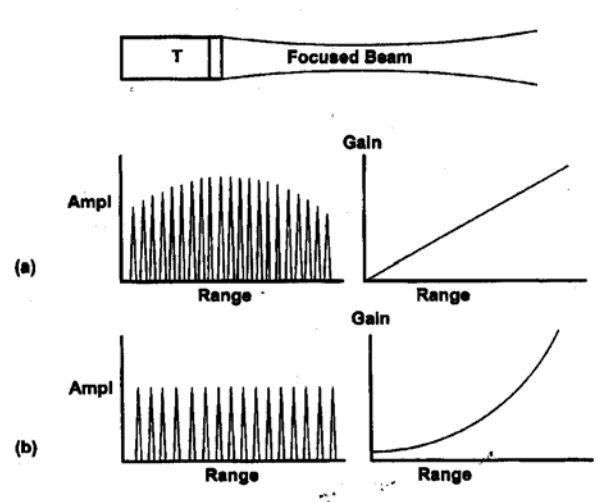
Figure 2-5: Swept Gain [44]

2.5.4 Synchronized Demodulation and Low-Pass Filter

Following the amplification, the echo signals are mixed with a reference signal from the master oscillator, i.e., the echo signals are multiplied by the reference signal of the emitted pulse. These demodulated signals (decomposed into two components of basic frequency and Doppler-shifted frequency) are then filtered to isolate Doppler information, i.e. the sum frequency is removed by a low-pass filter. The demodulation signal contains the range – phase information, i.e. for each burst of ultrasound the difference in phase between the reference signal (provided by the master oscillator) and the received echo at the specified range.

A pulse wave Doppler system has a pulse repetition frequency that is a subharmonic of the carrier frequency. Comparing the carrier frequency against the receive signal in a quadrature phase detector permits the depiction of motion direction. The quadrature demodulation, a phase sensitive demodulation technique as was employed by the continuous wave system, gives both the real and imaginary part of the received signal, which are both 90 degrees out of phase with each other. I is the in phase component and Q is the quadrature component of the output signal. To obtain the direction of the flow,

both output signals from the quadrature detector may be processed by several methods, many of which are now obsolete (such as zero crossing detection). The most widely used method in modern Doppler instruments is digital Fourier spectral analysis. After separation of the various frequency components, the direction of flow is determined by comparing the phase of the real and imaginary parts of the signals. If the real part is 90 degrees ahead of the imaginary part in phase, then flow is directed towards the transducer, and if the real part lags 90 degrees behind, then flow is reversed.

The output from the demodulator covers a frequency spectrum which extends from very low frequencies up to about 10 kHz. Some of the frequency components carry useful information; others do not. It is usual to arrange for unwanted signals to be filtered out whenever this is possible without the loss of useful information. A low pass filter suppresses artifactual frequencies in the spectrum generated by the demodulation. The low pass filter is also used to define the bandwidth and therefore the spatial resolution.

2.5.5 Sample/Hold Circuit

The Doppler signal (output of the demodulator) is then sampled into channels at a specified point in time relative to the onset of the transmission pulse. A receiver gate opens during each transmission cycle after an operator-determined delay, to admit signals to a sample and hold circuit. It is the delay between transmission and the opening of the receiver gate that determines the region from which the signals are gathered, whilst the time for which the gate is left open, together with the length of the transmitted pulse, determines the sample volume length. The time between acquisitions determines the axial spacing between sample volumes, while the delay between the emission and reception determines the distance to the sample volume.

The sample and hold circuit samples the output from the demodulator stage. It is common practice to integrate over the sample period and then hold this integrated value until the next sampling period. The sampling duration, together with the transmitted pulse length, sets the range over which velocity information is gathered. For optimum performance (i.e. the best sensitivity for a given axial resolution), the length of the transmission burst is usually set or the same length as the sampling or receiver gate length [18].

Figure 2-6 is a schematic of the signal-detection process. The train of pulses proportional to the instantaneous phase difference is the input to the sample and hold unit producing a voltage that oscillates at the Doppler frequency [8].
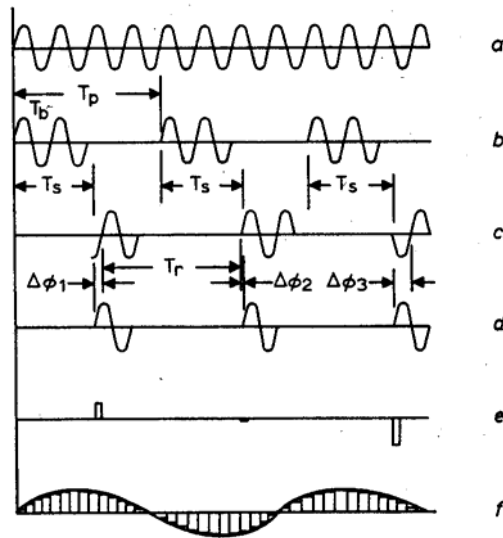
Figure 2-6: The Doppler Frequency and Range Detection Method [7]
a) Master Oscillator
b) Transmitted Burst
c) Range Gated Received Echoes
d) Phase-Coherent Reference Frequency
e) Phase Detector Output
f) Sample and Hold Output Over Many Cycles

2.5.6 Logical Unit

The control logic (logic unit) provides the necessary timing signals to for example implement the transmitter burst or initiate the sample and hold amplifiers at the appropriate time relative to the transmission burst.

An output power control is provided on most systems. This is used to vary the maximum sensitivity of the instrument by increasing or decreasing the amplitude of the acoustic pulse launched by the transducer. This affects the amplitude of the incident and reflected beams at each interface and the size of each echo detected by the transducer. Higher-power levels can result in detection of echo signals from more weakly reflecting interfaces and scatterers [49].

28

2.5.7   Band-Pass Filter, Amplification and Analog-Digital Conversion

The output from the sample and hold circuit is filtered, because it contains not only the Doppler shift frequencies but for example also the sampling frequency which has to be removed. In order that the full range of Doppler shift frequencies can be utilized, i.e. up to half the pulse repetition frequency [18], a very sharp low pass filter is used to eliminate the sampling frequency without degrading the Doppler signal. This filter must also be variable if a variable PRF system is used. Steady and quasi steady components are eliminated by a high pass filter. Thereby, both the sampling frequency and unwanted (often high energy) low frequency components are removed providing the Doppler shift frequency information at the range of interest. After amplification, and analog-to-digital conversion (12 bits), the signal is sent for further processing and display. Finally the frequency of the Doppler signal is estimated. The results may then be used to calculate the velocity.

2.5.8   Signal Processing

The measurement of the velocity is based on the estimation of the mean phase shift of successive echoes coming from a defined depth. Gates are formed by sampling the echo signal. The depth of the gate is computed by measuring the time delay between the emission and reception of the echo. The thickness of all the gates is defined by the burst length and/or the bandwidth or the receiver. In order to compute the velocity in each gate, many emissions are sent. These emissions form an array of time series data values, from which the mean Doppler frequency is computed by an auto-correlation algorithm. The algorithm used is based on the random statistical nature of each echo.

The amplitudes of the echoes reflected by the particles within the flowing fluid are somewhat random in nature, corresponding to the random distribution of the particles in the fluid medium. Thus, the Doppler signals may be treated as random processes. In order to be able to determine the probability of occurrence of this process, one must have access to a great number of actual occurrences of the process. In practice it is difficult to obtain measurements of the exact same process under the exact same condition at several different times. Therefore, a temporal average is preferable to an ensemble average. The

temporal average and the ensemble average will not be the same unless the process is stationary and the analysis time is very long (tending to infinity).

In the algorithm it is assumed that the statistical properties of all collected echoes used in the computation of the mean phase shift are stationary. This allows to transform temporal average into spatial average and to consider all processes stationary. The Doppler frequency calculation algorithm is based on the fact that the inverse Fourier transform of the probability density function of a stationary process is equal to the auto-correlation function. The algorithm computes the auto-correlation of the Doppler echoes. The auto-correlation function is estimated using the complex envelope of the echo signal. The Doppler frequency (f_D) is then computed, and finally the velocity is extracted from the Doppler equation. All velocity profile information is contained in the echo. Thus a velocity profile can be obtained by analyzing the echo signal to derive instantaneous frequencies at each instant. In practice, the echo signal is processed at 128 instants in parallel, and thus a data set which can be converted to the velocity profile is obtained.

Let´s assume that the particles are randomly distributed inside the ultrasonic beam. The echoes returned by each particle are then combined together in a random fashion, giving a random echo signal. A high degree of correlation exists between different emissions. This high degree of correlation is built into all digital processing techniques to extract information, such as velocity [55].

Signal processing may be applied to the echo signals conditioning them suitable for display. Any procedure performed on the echo amplitude signal after transducer reception and before display qualifies as signal processing. The number of emissions per profile, the number of profiles to record, optional filtering (moving average or median filter), scale and units, Doppler angle, the speed of sound as well as the sensitivity may be selected by the user. A change in the sensitivity of the beam of the Doppler unit will alter effective length of the transmitted pulse and the effective beam width [18]. The user can also choose between several computation and display options.

One of the steps involved in signal processing consists of compression. Compression generally refers to reduction of the amplitude range of echo signals for a given range of echo amplitudes at the input to the instrument. The range of echo signals that an instrument is capable of handling properly is referred to as the dynamic range. Different

components of an instrument have different dynamic range capabilities. To allow the display equipment to handle a wider variation in echo signal amplitudes, signal compression is applied in the receiver. Most instruments allow selection of additional signal processing through choice of preprocessing and post processing control settings.

Preprocessing refers to special signal processing applied before echo signals are stored in the instrument's memory. There are mainly two possibilities for preprocessing. Logarithmic compression amplifies low-amplitude echo signals more than high-amplitude signals. Thus amplitude variations among the low signal levels are emphasized. The S-shaped curve on the other hand emphasizes variations over the middle of the echo signal range. Preprocessing usually also includes a preamplifier, since small single element transducers or the individual elements in multielement arrays cannot drive long lengths of coaxial cable. Thus a preamplifier close to the piezoelectric crystal is used for some initial signal amplification to overcome cable capacitance. Also, the preamplifier output is electrically impedance matched to standard 50 Ohm cable impedance. Further manipulation of echo data can be done using post processing.

Post processing refers to signal conditioning that operates on signals already stored in memory, just before they are directed to the display. Post processing does not provide new data but simply allows the same echo image data to be displayed differently.

2.5.9   Architecture DOP 1000 and DOP 2000

In Figure 2-7 and 2-8, the architecture of the pulsed ultrasound Doppler velocimeters DOP2000 and DOP1000 from Signal Processing is presented. Differences in performance characteristics between the two systems are emphasized by italic letters in the figure of the architecture of the DOP1000 velocimeter.
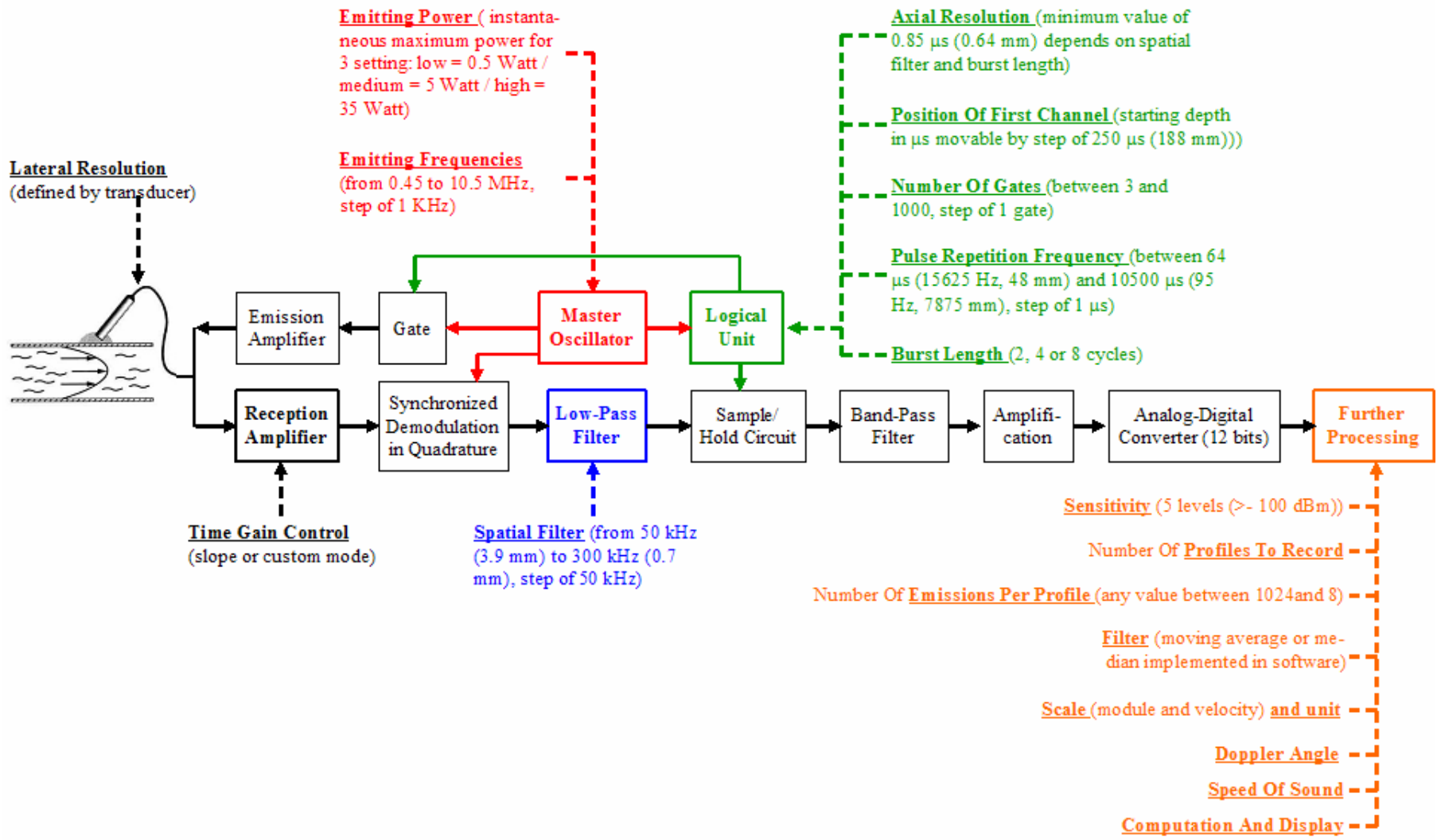
Figure 2-7: Architecture Signal Processing DOP2000 Velocimeter
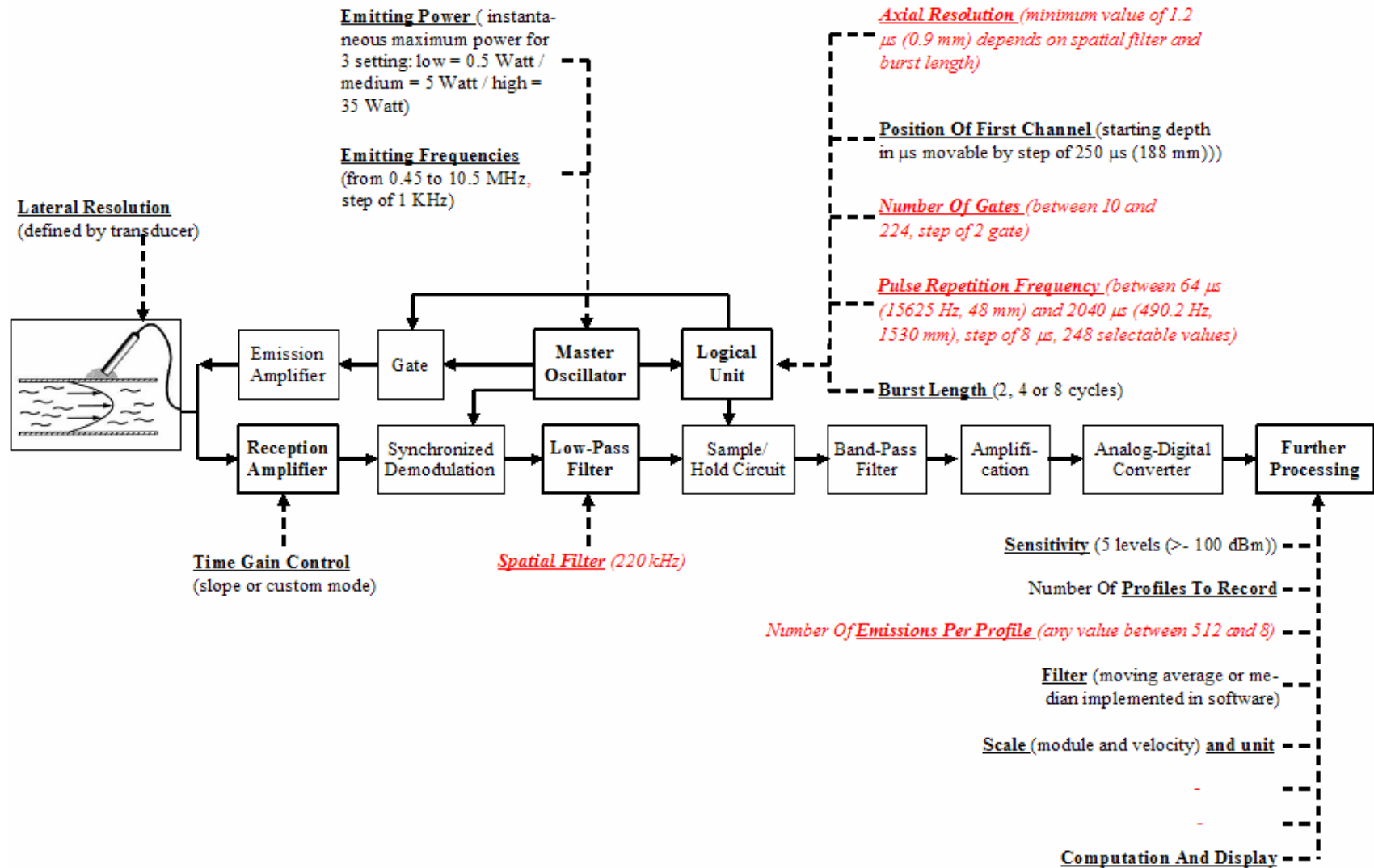
Figure 2-8: Architecture Signal Processing DOP1000 Velocimeter

Evaluating the architecture of the velocimeter, the ultrasonic transducer turns out to be the most critical component of the measurement system especially when measuring the velocity in small channels. The ultrasonic transducer mainly determines the lateral resolution of the measurement system. Consequently the sensitivity of the velocimeter and its spatial resolution, which is crucial to measure the velocity in small channels more accurately, mainly depend on the ultrasonic field emitted by transducer and consequently on the transducer itself. Suggestions to improve the measurement system will be based on improving the transducer architecture. Therefore, the fundamentals of the ultrasonic field emitted by the transducer are reviewed in Section 2.6. These fundamentals are also crucial to evaluate ultrasonic beam measurements presented in Chapter 4 and velocity measurements in small channels presented in Chapter 5. Fundamentals of commonly used transducer architectures are then further investigated in Chapter 3.

2.6 Ultrasonic Field

The generation of ultrasonic waves as well as their transformation into an electrical signal is of obvious importance to the quality of the information which may be obtained concerning the flow field. For the measurement of velocity profiles in small channels and capillaries, a good spatial resolution of the Doppler system is crucial. Therefore, this chapter explores ultrasound, its characteristics and propagation, and especially the ultrasonic field emitted by the transducer in more detail.

In a pulsed Doppler system, short bursts of acoustic energy are transmitted by amplitude modulation of a carrier frequency. The returning signal is sampled at a specific delay time from transmission of each pulse. As a consequence, the sampled portions of the returning signal correspond to a back-scattered acoustic energy originating from a specific region of space in the ultrasonic field called the sample volume, whose range from the transducer is determined by the delay time. As a first approximation, this measurement volume is a disk-shape and has a diameter d and a thickness h as shown in Figure 2-9 [31].
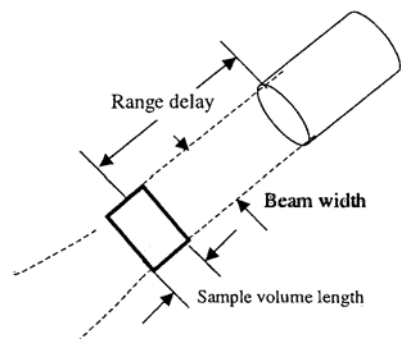
Figure 2-9: Acoustic Sample Volume for a Pulsed Doppler System [64]

In Equation 16, the velocity v of a single sound scatterer is described. If the pulsed Doppler detector possessed sufficient spatial resolution to sample just a single particle at a time, this equation would describe the process. However, the actual acoustic burst is a 3-dimensional region of sound intensity. Any flow particles passing through this region, called the "sample volume", produce Doppler signals which are detected at the receiver. If the particles have different velocities, the received signal is a spectrum of frequencies containing the Doppler shifts of each particle.

The spatial resolution of a Doppler system is determined by the size of the sample volume. The lateral size of the sample volume is determined by the ultrasonic beam size. The length of the sample volume corresponds to the distance sound travels. Consequently the spatial resolution is of the order of the ultrasound wavelength in the shooting direction and depends upon the width of the ultrasonic beam in the perpendicular directions [12].

2.6.1 Ultrasound

Compared to subsonic noise (f_{sn} < 20 Hz) and the range of audibility (20 Hz < f_{ra} < 20 kHz), the frequencies of ultrasonic noise exceed 20 kHz (f_{un} > 20 kHz). Consequently any sound generated above the human hearing range (typically 20 kHz) is called ultrasound. The acoustic spectrum in Figure 2-10 breaks down sound into 3 ranges of frequencies. The ultrasonic range is then broken down further into 3 sub sections. However, the frequency range normally employed in general ultrasonic applications (nondestructive testing, thickness gaging, …) is 100 kHz to 50 MHz [43]. In Doppler applications in medicine the usual range of frequencies used is between 2 MHz and 10 MHz (although higher frequencies are used in specialist applications). The lower limit is determined by

wavelength considerations (the longer the wavelength the poorer the spatial resolution – both axial and transverse) and the upper limit by acceptable power levels (attenuation rises very rapidly with frequency and so a very small proportion of the transmitted power is returned to the transducer at high frequencies) [18]. Although ultrasound behaves in a similar manner to audible sound, it has a much shorter wavelength. This means it can be reflected off very small surfaces such as defects inside materials or particles suspended in fluids. It is this property that makes ultrasound useful for either nondestructive testing of materials or the determination of velocity profiles in fluids.
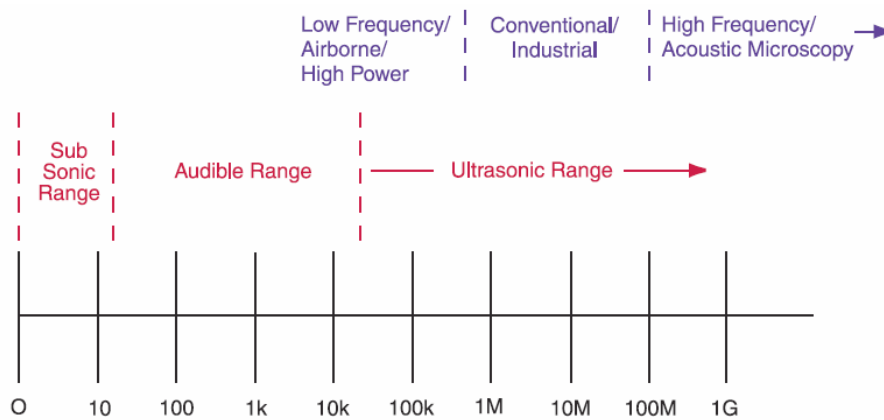
Figure 2-10: Acoustic Spectrum [43]

Sound waves are mechanical vibrations that propagate in a host medium. They are coupled modes between medium particles oscillating about equilibrium positions and a traveling ultrasonic wave. The velocity of ultrasound c in a perfectly elastic material at a given temperature and pressure is constant and can be determined by: $c = \lambda f = \lambda/T$, where λ is the wavelength, f the frequency and T the period of time:

Ultrasonic vibrations travel in the form of a wave, similar to the way light travels. However, unlike light waves, which can travel in a vacuum (empty space), ultrasound requires an elastic medium such as a liquid or a solid. The most common methods of ultrasonic diagnostics utilize either longitudinal waves or shear waves. Other forms of sound propagation exist, including surface waves and Lamb waves.

Solids support the propagation of both longitudinal waves (compressional waves in which the particles are oscillating parallel to the wave propagation direction) and transverse

(shear) waves (particles oscillating perpendicular to the wave propagation direction. Figure 2-11 provides an illustration of the particle motion versus the direction of wave propagation for longitudinal waves and shear waves. Surface (Rayleigh) waves have an elliptical particle motion and travel across the surface of a material. Their velocity is approximately 90% of the shear wave velocity of the material and their depth of penetration is approximately equal to one wavelength. Plate (Lamb) waves have a complex vibration occurring in materials where thickness is less than the wavelength of ultrasound introduced into it. Fluids (gases and liquids) only support longitudinal wave propagation.
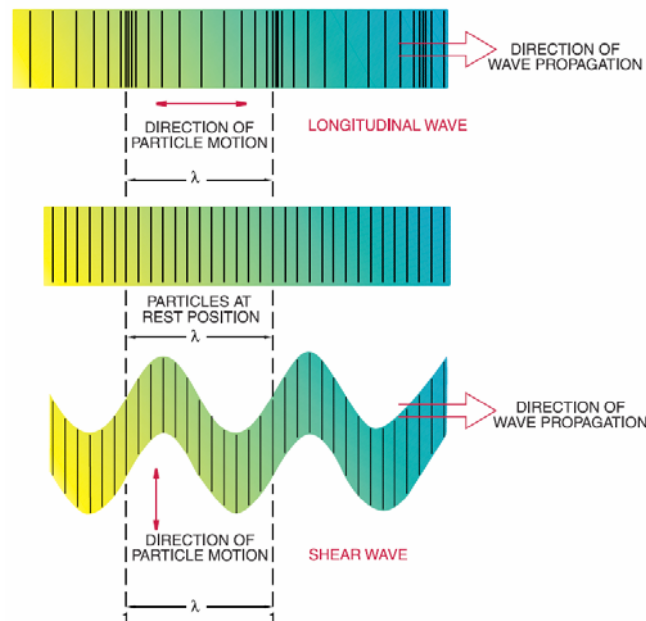
Figure 2-11: Longitudinal and Shear Waves [43]

Pulsed ultrasound, as in the case of pulsed ultrasound Doppler velocimetry, is produced by applying electric pulses to an ultrasonic transducer. The number of pulses produced per second is called the pulse repetition frequency. The spatial pulse length is the length of space over which a pulse occurs. It is equal to the wavelength times the number of cycles in the pulse. It decreases with increasing frequency.

2.6.2 Acoustic Phenomena

Ultrasound Doppler velocimetry requires some amount of scatterers suspended in the liquid, which may disturb its flow or change its fundamental properties. In this section, the effect of the required scatterers on the ultrasonic beam is evaluated and basic acoustic phenomena are described.

Ultrasound attenuates as it progresses through a medium, i.e. its amplitude and intensity decrease gradually with increasing distance of travel. Assuming no major reflections, there are the following causes of attenuation: scattering, diffraction and absorption. The amount of attenuation through a material can play an important role in the selection of a transducer for an application. Attenuation is important because it limits the depth range especially with high-frequency sound beams. The rate of attenuation, or attenuation coefficient, depends on both the matter traversed and the ultrasound frequency. The rate of attenuation increases with increasing frequency. Attenuation can be compensated in the receiving amplifier by electronic circuitry which applies increasing gain as signals are received from increasing depths. Solid plaque attenuates ultrasound strongly owing to high reflection and refraction and therefore casts shadows in the region behind it. The frequency dependence of attenuation results in the high frequency components of an ultrasonic pulse being preferentially reduced in amplitude relative to the low frequency components [18]. The attenuation coefficient increases with increasing frequency.

The ultrasonic waves generated by the standard single-element transducer (described in detail in chapter 3) are more or less confined in a narrow cone. As they travel in this cone they may be scattered when they touch a particle having different acoustic impedance. The acoustic impedance of a material is the opposition to displacement of its particles by sound and occurs in many equations. The characteristic impedance is defined by: $Z = \rho\,c$, where ρ is the density of the medium and c the sound velocity. The boundary between two materials of different acoustic impedances is called an acoustic interface.

When an ultrasonic wave traveling through a medium strikes an acoustic interface, i.e., a discontinuity or any variation from uniformity in the medium of dimensions similar to or less than a wavelength, some of the energy of the wave is scattered in many directions. Scattering is the process of central importance, since it provides most of the signals for echo Doppler techniques as in the case of pulsed Doppler ultrasound velocimetry. It

occurs at rough boundaries and within heterogeneous media. The discontinuities may be changes in density or compressibility or both. Of particular interest is the differential cross-section of the target of volume of material at 180 degrees to the direction of the incident ultrasound. This is known as the backscatter cross-section and determines the size of the signal back to the transducer. Three general types of scattering can occur: scattering (reflection) from large flat boundaries, known as specular reflection; scattering from point reflectors (or local variation in tissue structure or density), known as diffuse scattering; and scattering from structures whose dimensions are commensurate with the wavelength, known as resonance scattering.

When sound strikes an acoustic interface, some amount of sound energy is reflected and some amount is transmitted across the boundary and consequently refracted as shown in Figure 2-12.
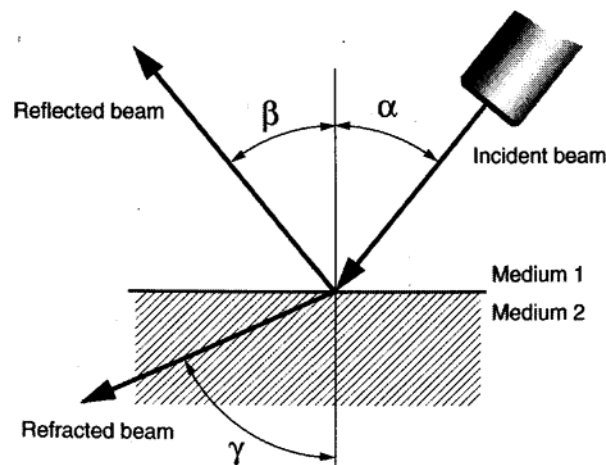
Figure 2-12: Reflection and Refraction [51]

Reflection is a special case of scattering which occurs at smooth surfaces on which the irregularities are very much smaller than a wavelength. When a wave front strikes a smooth surface at an oblique angle of incidence, it is reflected at an equal and opposite angle. Point reflectors (structures whose dimensions are small compared to the wavelength) undergo Rayleigh scattering, which has a pressure scattering cross section proportional to frequency squared. Diffuse scattering produces low-amplitudes, omni directional echoes.

Refraction is the deviation of a beam when it crosses a boundary between two media in which the speeds of sound are different. The resultant angle of propagation is given by the familiar Snell's Law: $\sin\alpha/\sin\gamma = c_1/c_2 = \mu_2/\mu_1$, where μ_i is the refractive index, α is the angle of incidence and γ is the angle of refraction. Greater deviations are to be expected when a wall is more rigid due to the presence of plaque [18].

Deriving the transmission and reflection coefficients, it is assumed that both the incident wave and the boundary between the media are planar and that all media are fluids. For normal incidence, a large class of solids obeys the same equations developed for fluids. The only modification needed is that the speed of sound in the solid must be based on the bulk modulus rather than Young's modulus. The ratios of the pressure amplitudes and intensities of the reflected and transmitted waves to those of the incident wave depend both on the characteristic acoustic impedance and the speeds of sound in the two media and on the angle of incident wave makes with the normal to the interface. As a consequence of the conservation of energy, the power in the incident beam must be shared between the reflected and the transmitted beams so that the intensity transmission coefficient T and the reflection coefficient R are connected by: $1 = T + R$ [34].

Based on the assumption of continuity of pressure at the boundary and continuity of particles' velocities on both sides of the boundary between two media, the intensity transmission and reflection coefficients can be derived. The interface pressure reflection coefficient r is given by Kino [33]:

$$r = \sqrt{R} = \frac{\rho_2 c_2 \cos\alpha - \rho_1 c_1 \cos\beta}{\rho_2 c_2 \cos\alpha + \rho_1 c_1 \cos\beta} = \frac{Z_2 \cos\alpha - Z_1 \cos\beta}{Z_2 \cos\alpha + Z_1 \cos\beta}$$

Equation 17: Reflection Coefficient

where α is the angle of incidence, β is the angle of transmission, Z_1 is the acoustic impedance of the first medium and Z_2 is the acoustic impedance of second medium.

The magnitude of the interface pressure reflection coefficient r depends on differences of the acoustic impedance Z of the medium at the interface. If $Z_1 = Z_2$, the reflection coefficient is zero and only transmission occurs at the interface. This condition is called impedance matching. The larger the difference between Z_1 and Z_2, the larger is the

reflection coefficient. This condition is called impedance mismatching. If $Z_1 < Z_2$, the reflected wave has no phase change upon reflection and if $Z_1 > Z_2$, the reflected wave has a π radian phase change upon reflection. Since pulse-echo ultrasonic imaging is performed with a single transducer, the high-amplitude, directionally dependent specular reflections are only received by the transducer if the ultrasonic beam is normal to the medium interface (or very close to normal).

The intensity transmission coefficient T, which is equal to the ratio of the refracted intensity to the incident intensity, is given by Kino [33]:

$$T_R = \frac{4 Z_1 Z_2 \cos^2(\alpha)}{(Z_2 \cos(\alpha) + Z_1 \cos(\gamma))^2}$$

Equation 18: Transmission Coefficient

According to the principle of acoustic reciprocity, transmission coefficients are independent of the direction of the wave. Transmission coefficients are small whenever the acoustic impedances of both media have widely separated values.

These equations may also be used to predict the amount of ultrasonic energy that will penetrate in the liquid. In other words, they predict the amount of energy that tends to remain in the wall. The dB loss of energy on transmitting a signal from medium 1 to medium 2 at normal incidence is given by Panametrics [43]:

$$dB_{loss} = 10 \log_{10} \left[\frac{4 \cdot Z_1 \cdot Z_2}{(Z_1 + Z_2)^2} \right]$$

Equation 19: dB Loss Due to Transmission

The dB loss of energy of the echo signal in medium 1 reflecting from an interface boundary with medium 2 at normal incidence is given by Panametrics [43]:

$$dB_{loss} = 10 \log_{10} \left[\frac{(Z_2 - Z_1)^2}{(Z_1 + Z_2)^2} \right]$$

Equation 20: dB Loss Due to Reflection

When dealing with transmission through a layer at normal incidence, the calculation of the reflection and transmission coefficient becomes more complex. It is assumed that a layer of uniform thickness L lies between two fluids and that a plane wave is normally incident on its boundary. When an incident signal arrives at a boundary between the fluid and the layer (or vice versa) some of the energy is reflected and some is transmitted. If the duration of the incident signal is less than $2L/c_L$ (c_L is the sound velocity in the layer), an observer on either side of the layer will detect a series of echoes separated in time by $2L/c_L$. The echo amplitude can then be calculated by applying the formulas given above the appropriate number of times. On the other hand, if the incident wave train is long compared to $2L$ and monofrequency can be assumed, the various transmitted and reflected waves combine resulting in standing waves within the layer. In the steady-state condition assuming continuity of the normal specific acoustic impedance at both boundaries, the intensity transmission coefficient T is given by Kinsley [34]:

$$T = \frac{1}{1 + \frac{1}{4}\left(\frac{Z_L}{Z_W} - \frac{Z_W}{Z_L}\right)^2 \sin^2(k_2 L)}$$

Equation 21: Intensity Transmission Coefficient (Simplified)

where $k = \omega/c$ is the wave number, $\omega = 2\pi f$ is the angular frequency, c is the speed of sound, L is the layer thickness, Z_L is the acoustic impedance of the layer and Z_W is the acoustic impedance of the fluid on both sides of the layer (the initial equals the final fluid).

Absorption is the process of conversion of wave motion energy into heat. Absorption increases rapidly with frequency. In practice, absorption on its own is rarely of interest, since other processes are simultaneously contributing to the total attenuation of the acoustic wave. These processes are scattering, reflection, refraction, non-linear propagation and beam divergence. Since many of these factors are strongly frequency dependent, it is not surprising that attenuation rises rapidly over the frequency range 1 – 20 MHz [18]. Absorption and attenuation are very important in Doppler techniques and their influence on any examination must be considered.

2.6.3 Ultrasonic Field Emitted by Transducer

A pulsed ultrasonic Doppler flow meter for detailed measurements of velocity profiles projects a beam of ultrasonic bursts. The back-scattered signals are processed to produce a signal corresponding to the mean velocity over a small region of the flowing stream. The size and shape of this sample volume determines the flow meter sensitivity and accuracy. The velocity profile obtained from this instrument is a weighted average of the ultrasonic intensity and the flow field velocity over the sample volume.

The sound-field characteristics are determined by the ultrasonic transducer's focal characteristics, the sound scatterers and the sensitivity of the receiver circuitry. A sufficient description of the characteristics of the sound field requires quantitative information about the sample-volume geometry and intensity distribution, the focused beam shape and the amplitude of the back-scattered signal as a function of range. The sample-volume geometry and intensity are important because they influence the spectral content of the back-scattered signal. The focused beam shape indicates how the geometry of the sample volume varies with range.

In Doppler echography, the object is not to make use of a plane longitudinal wave, but rather an ultrasonic beam that is as thin as possible throughout the measurement depth. The geometry of the acoustic field is governed by the diameter D of the emitter and the wavelength λ, which is equal to the ratio of the speed of sound in the analyzed medium and the emitting frequency.

Using Huygen's principle, one may predict the geometry of the acoustic field. In the following approach, the ultrasonic single-element transducer is modeled as a combination of several adjacent point sources, each generating a spherical wave. The typical shape of the ultrasonic field is illustrated in Figure 2-13:

Near Field   Far Field
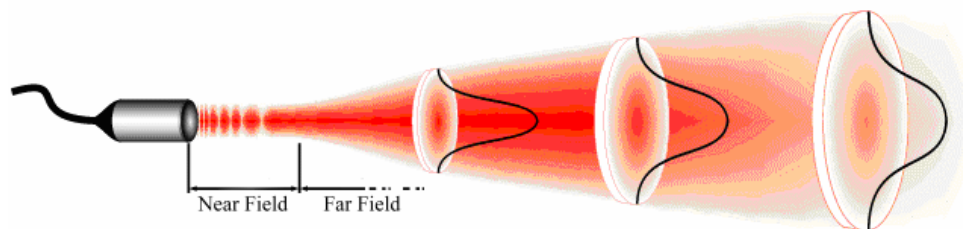
Figure 2-13: Ultrasonic Field [51]

For a circular transducer of radius a operating in a piston-like manner, the intensity of the acoustic field I along the axis is given by Kino:

$$\frac{I_z}{I_0} = \sin^2\left[\frac{\pi}{\lambda}\left(\sqrt{a^2 - x^2} - x\right)\right]$$

Equation 22: Intensity of the Acoustic Field

where I_0 is the maximum intensity, x is the distance from the transducer and λ is the wavelength [33]. The acoustic field generated by a transducer possesses two characteristic regions, separated by the distance of the furthermost maximum of the above function: the cylindrical near field and the conical far field.

In the near field (Fresnel zone), the region that is located near the transducer surface, the acoustic field is nearly cylindrical, with a diameter slightly less than the diameter of the emitter. The intensity of the acoustic waves oscillates along the axis of the transducer. The echo amplitude goes through a series of maxima and minima. As the characteristic distances of these oscillations are much smaller than the dimensions of the measured volumes, they do not significantly affect Doppler information collected in this region. The length of the near field L_{NF} is given by Kino [33]:

$$L_{NF} = \frac{4d^2 - \lambda^2}{4\lambda}$$

Equation 23: Length of the Near Field

where d is diameter of the transducer. The length of the near field is defined by the position of the last maximum of the acoustic intensity as shown in Figure 2-14. The near field distance is the natural focus of the transducer and a function of the transducer frequency, element diameter (aperture size) and the speed of sound velocity in the medium.

In the far field (Frauenhofer zone), the zone lying beyond L_{NF}, the intensity of the acoustic waves along the axis decreases as the inverse of the square of the distance from the transducer (according to the inverse-square law for point sources). Small oscillations

appear in the radial direction (perpendicular to the axis of propagation) as shown in Figure 2-14. The sound field pressure gradually drops to zero.
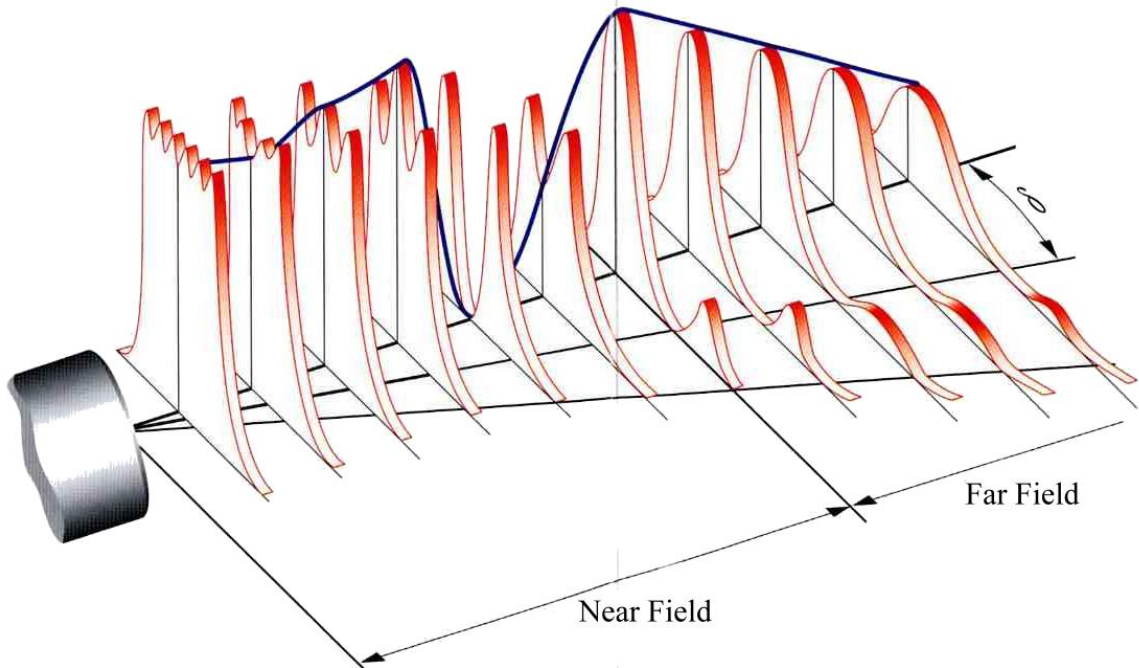
Figure 2-14: Near and Far Ultrasonic Field [51]

Most of the acoustic energy is contained in a cone. The relationship between the acoustic field intensity and the angle off the transducer axis depends on the directivity function:

$$D_r(\gamma) = \frac{2J_1(k\,a\sin\gamma)}{k\,a\sin\gamma}$$

Equation 24: Directivity Function

where J_1 is the first order Bessel function of the first kind, and $k = 2\pi/\lambda$ the wave number [33]. The half angle of divergence of the main lobe φ (-6 dB pulse-echo beam spread angle) is characterized by the wavelength and the diameter of the emitter and is given by Signal Processing [51]:

45

$$\varphi = \sin^{-1}\left(\frac{1,22\lambda}{d}\right) = \sin^{-1}\left(\frac{1,22c}{f \cdot d}\right)$$

Equation 25: Half Angle of Beam Divergence

It can be seen from this equation that beam spread from a transducer can be reduced by selecting a transducer with a higher frequency or a larger element diameter or both.
All ultrasonic beams diverge. In other words, all transducers have beam spread. In the near field, the beam has a complex shape that usually narrows. In the far field the beam diverges. The divergence of the ultrasonic beam depends on the diameter of the emitter and the wavelength. Most of the time, a compromise between these two parameters has to be established in order to achieve the thinnest beam possible at a defined distance. A higher frequency gives a better axial resolution but also often induces higher attenuation of the ultrasonic waves.

There are a number of sound field parameters that are useful in describing the characteristics of an ultrasonic transducer. Especially knowledge of the beam width and focal zone may be necessary in order to determine whether a particular transducer is appropriate for the given application. The geometry of the acoustic field generated by the ultrasonic wave determines the lateral resolution of the ultrasonic transducer. The characteristics of the acoustic field depend on the size and shape of the piezoelectric element. A transducer's sensitivity is affected by the beam diameter at the point of interest. The smaller the beam diameter, the greater the amount of energy that is reflected by particles. By definition, the starting and ending points of the focal zone are located where the on-axis pulse-echo signal amplitude drops to − 6 dB of the amplitude at the focal point [43].

2.6.4 Sample Volume

In ultrasound Doppler velocimetry, the back-scattered signals are processed to produce a signal corresponding to the mean velocity over a small region of the flowing stream. The size and shape of this "sample volume" determines the flow meter sensitivity and accuracy. The velocity profile obtained is a weighted average of the ultrasonic intensity

and the flow field velocity over the sample volume, and is mathematically described by a convolution integral.

Pulsed ultrasound Doppler velocimetry systems emit short bursts of ultrasound several thousand times every second, usually at regular intervals. After each pulse has been transmitted there is a delay before one or more gates in the receiving circuit are opened for a short period of time to admit signals returning from a small volume. The delay between transmission and opening the gate may be altered by the operator to determine the depth from which the signals are gathered, whilst the time for which the gate is left open (and to some extent the receiver bandwidth), taken together with the length of the transmitted pulse, determines the length of the sample volume. Specifically the distance from the transducer to the beginning of the range cell, P_1, will be given by:

$$P_1 = c \frac{T_d - T_p}{2}$$

Equation 26: Distance Transducer to Beginning Sample Volume

where c is the velocity of the ultrasound in the specific medium, T_p is the pulse length and T_d is the time delay between the start of transmission and the moment at which the receiver gate opens. The distance from the transducer to the end of the range cell, P_2, will be given by:

$$P_2 = c \frac{T_d + T_g}{2}$$

Equation 27: Distance Transducer to End of Sample Volume

where T_g is the period for which the gate is open. The length of the range cell may therefore be written:

$$P_r = P_2 - P_1 = c \frac{T_d - T_p}{2}$$

Equation 28: Length Sample Volume

As described above, the spatial resolution of a standard pulsed wave system is related to the length of the transmitted pulse and it follows from this equation (the last equation) that to achieve very short range cells, or very good spatial resolution, it is necessary to use very short pulses. The signal-to-noise ratio of a Doppler system is, however, related to the average transmitted power and therefore, if the pulses are made shorter in order to maintain the signal-to-noise ratio, it is necessary to increase their amplitude (the pulse repetition frequency cannot be arbitrarily increased because of the need to avoid range ambiguity by only having one pulse in flight at a given time). For a more general Doppler system it is the signal bandwidth rather than the signal duration that determines the range resolutions.

The axial dimension of the measured volumes is defined by the instrument that analyzes the Doppler echoes (the duration of the emitted burst and the bandwidth of the receiver) and their lateral size by the amount of acoustic energy reflected by the particles. Due to the spatial dependence of the acoustic intensity, the lateral dimension of the measured volumes depends on their position as simplified by the disks in Figure 2-13. More exactly, the shape of the sample volume of a pulsed wave beam is often described as a teardrop (Figure 2-17). This arises from the combination of the three dimensional shape of the transmitted pulse and gated range [18].

A sufficient description of the characteristics of the sound field requires quantitative information about the sample volume geometry and intensity distribution, the focused beam shape and the amplitude of the back-scattered signal as a function of range. The sample length and intensity are functions of the transducer bandwidth. In Figure 2-15 the nature of the transducer response to an input pulse is shown [8].
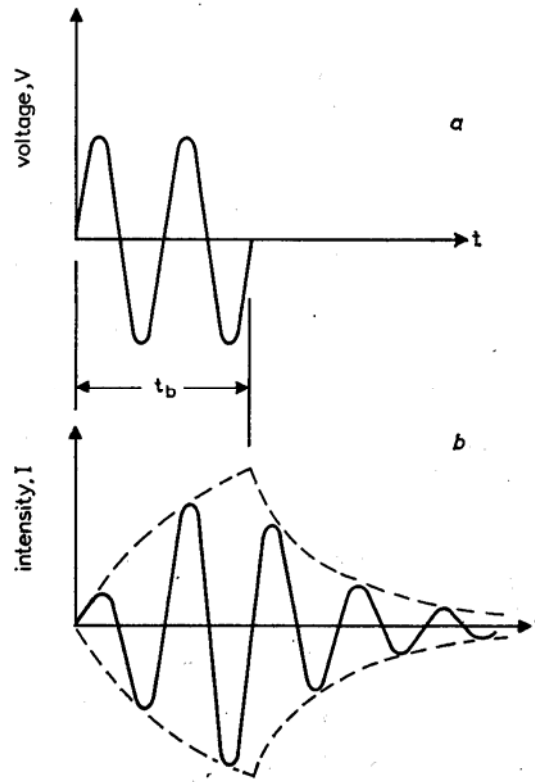
Figure 2-15: Piezocrystal Transducer Response [8]
   a) Driving Burst
   b) Acoustic Burst

The tail of the acoustic burst is due to transducer ringing, or the gradual decay of the stored energy, and represents the free response characteristics of the transducer. Transducer ringing increases the length of the sample volume, and therefore decreases the spatial resolution of the Doppler detector. In Figure 2-15 the expected intensity envelope with the characteristic tail due to transducer ringing is shown. The envelope can mathematically be described as two exponentials. In Figure 2-16 the two functions which describe the general shape of the acoustical intensity envelope are plotted [8].
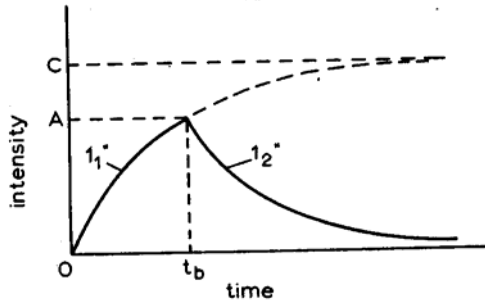
Figure 2-16: The Acoustic Intensity Envelope [8]

Owing to noise levels it can be concluded that the sample volume will have a finite length. Thus curve $1_2''$ must be a truncated exponential. In addition to the finite length of the actual acoustic burst there is also a finite width of diameter, since the sample volume is 3-dimensional. The 3-dimensional sample volume is simply the envelope curve revolved about the time axis as shown in Figure 2-17 [18].
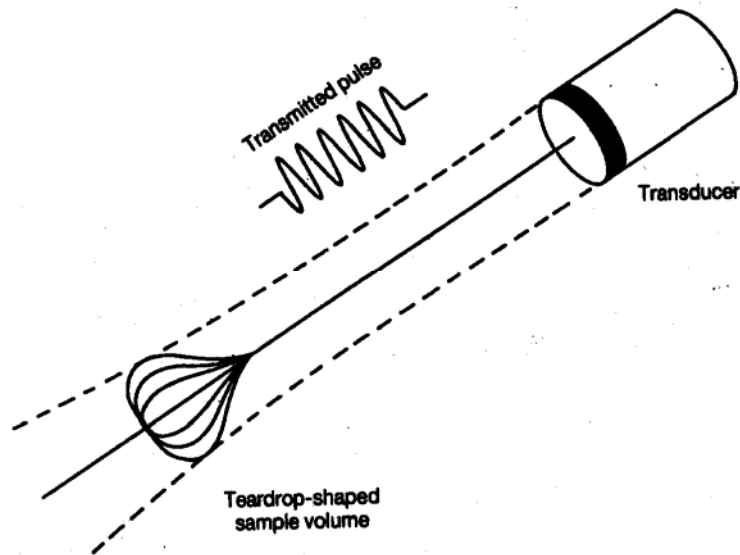
Figure 2-17: Teardrop Shape Sample Volume [18]

The size of the sample volume also depends on the sound scatterers and the focusing characteristics of the transducer. The sample volume length now varies with both range position and the signal intensity. The mathematical description of the sample volume (expressions for the intensity distribution along the axis of the sample volume and equations describing the sample volume geometry (radius)), which includes this variation

in effective length with trigger level, are derived in [8]. The maximum intensity at any cross-section normal to the sound axis will occur on the axis and the intensity will decrease radially outward.

Experimental studies [8] indicate that the sample volume has an envelope intensity curve which can be described as two truncated exponentials. Since the sample volume is a 3-dimensional packet of sound intensities, the exponential envelope can be revolved about its axis to describe a body of revolution. The accuracy of this assumption depends on the type of transducer used. If a single-crystal transducer is used for both transmitting and receiving then the assumption is accurate.

It should be noted, that the range cell is not equally sensitive throughout, and its effective distribution will depend on the shape of the ultrasound pulse, the relative lengths of the transmitted pulse and the sample gate, and the bandwidth of the receiving electronics. Furthermore, due to the properties of the ultrasound transducer and the limited bandwidth of the receiving electronics, the ideal rectangular pulse and rectangular receiving gate shapes will not be attained in practice.

The dimensions of the pulsed Doppler sample volume are determined by the factors given in Figure 2-18. Their optimal values coupled with the proper transmitting frequency will give the best sensitivity to resolution ratio for flow sensing at various depths.
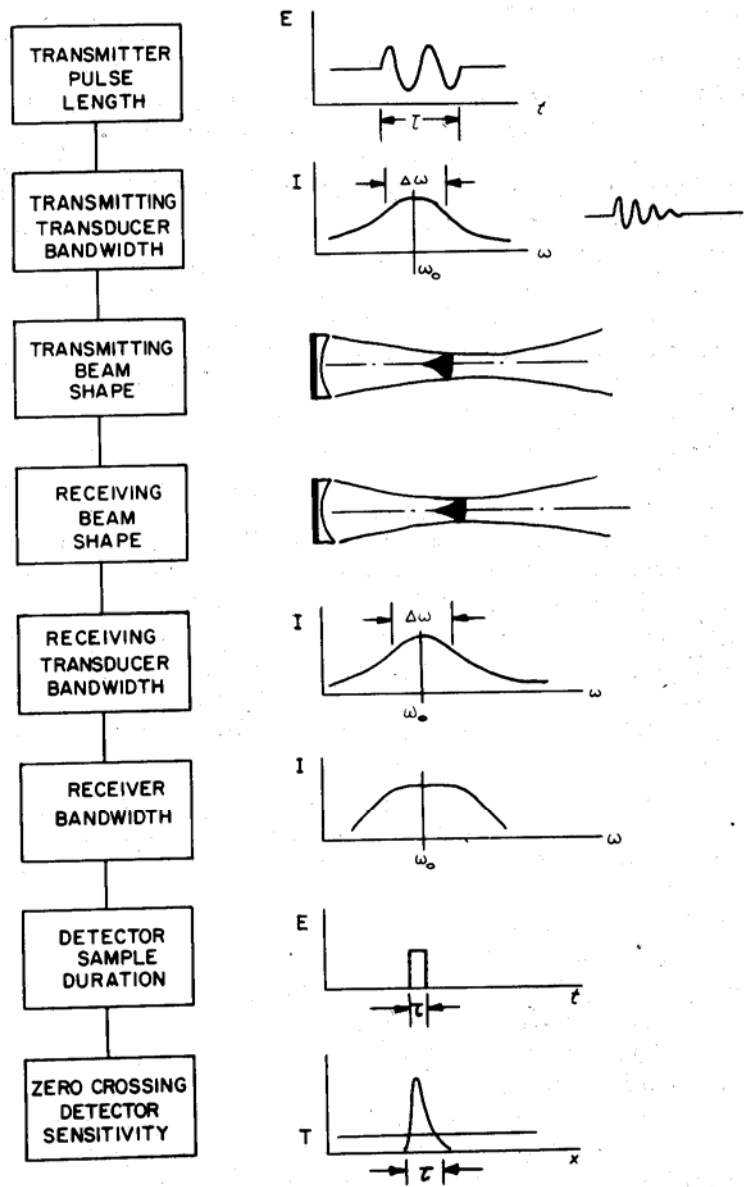
Figure 2-18: Dimensions Sample Volume [20]

By selecting the appropriate frequency, diameter and ultrasonic beam shape of the
transducer, it is possible to define the optimum sizes of the sample volumes (the volumes
from which particles contribute to the measurement of a single velocity value) for each
application. In order to realize the best compromise between the noise level and the
desired resolution, both the burst length and the bandwidth of the receiver stage can be
modified (bandwidth reduction defines the minimum thickness of the sampling volume).
The beam shape indicates how the geometry of the sample volume varies with range.

2.6.5 Sampling Process

A 3-dimensional convolution technique can be used to simulate the Doppler velocity detection process. The frequencies in the backscattered signal depend on the acoustic sample volume dimensions as well as the scatterer velocities. The nature of this dependence can be shown with the aid Figure 2-19 [8]:
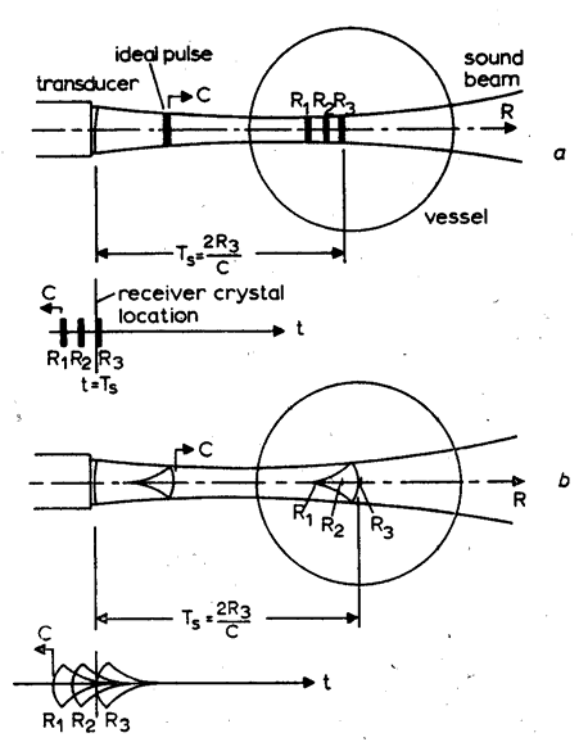
Figure 2-19: The Sampling Process [8]

In Figure 2-19 *a* the ideal case is presented in which the acoustic sample volume has infinitesimal geometry but very high intensity; i.e. the sample volume approximates an ideal impulse. As the impulse propagates through the flow field the sound scatterers lying in its path each reflect a portion of the acoustic energy with a similar impulse. Points R_1, R_2 and R_3 are ideal impulses. There is no overlap between echoes. Thus, if the receiver gate is turned on for an instant, after a delay $T_s = 2\ R_3/c$ seconds, corresponding to the transit time of the impulse to point R_3 and back, the only information reaching the receiving crystal at this instant is the echo from point R_3. The signal therefore contains only the single frequency due to the Doppler shift by scatterers moving through the point R_3.

The actual sample volume, of course, has finite geometry. This case is shown in Figure 2-19 *b*. Again as the sample volume enters the flow field, the scatterers lying in the sound field each reflect a portion of the acoustic energy; the echoes each have the shape of the transmitted pulse. If it is desired to sample the echo from point R_3, the range gate is turned on for an instant at time $T_s = 2R_3/c$ seconds. Since the echoes are finite in length, overlapping occurs so that the signal reaching the receiver at time T_s contains information from points R_1 and R_2 as well as point R_3. In fact, the signal reaching the receiver at this instant contains information from scatterers spread throughout the sample volume. The frequency content of the signal therefore corresponds to the velocities throughout the sample region. The selected frequency is a weighted average of the signal spectrum. Mathematically a true weighed average is determined by the convolution integral. The expression used as the basis of the 3-dimensional convolution or weighted average technique for the analytical model can be found in [8]. The goal of the analytical model is to simulate the sound field velocity interaction using the convolution process by taking into account the sample volume and focusing characteristics of the transducer, the signal detection and frequency-meter characteristics and the general parameters which describe a given test situation.

If, however, the sample volume is only partially within the flow field, as occurs during entry and exit of the channel, then only a portion of its energy contributes to the backscattered signal. The intensity of the signal is therefore zero when the sample volume is out of the flow field, and gradually rises to the level indicated by the focusing characteristics as it enters the flow field. This is illustrated in Figure 2-20.
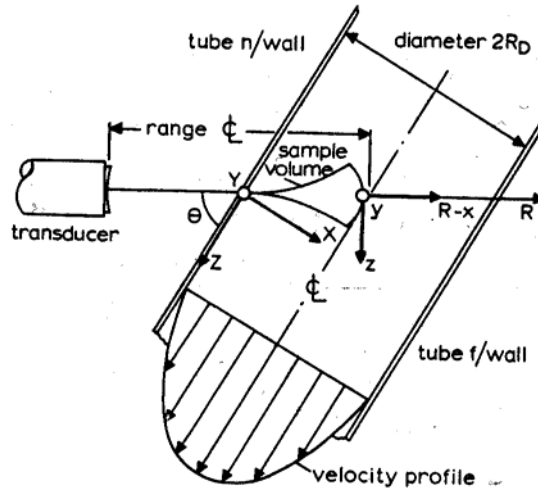
Figure 2-20: Sample Volume Flow Entry/Exit [8]

2.6.6 Doppler Spectrum

Equation 16 describes the Doppler frequency shift due to the velocity of a single sound scatterer. If the pulsed Doppler detector possessed sufficient spatial resolution to sample just a single particle at a time, this equation would describe the process. However, the actual acoustic burst is a 3-dimensional region of sound intensity. Any flow particles passing through this region, the sample volume, produce Doppler signals which are detected at the receiver. If the particles have different velocities, the received signal results in a spectrum of frequencies containing the Doppler shifts of each particle, the Doppler spectrum. The sample-volume geometry and intensity are important because they influence the spectral content of the back-scattered signal.

The Doppler shift frequency estimate is proportional to velocity. Under ideal uniform sampling conditions the power in a particular frequency band of the Doppler spectrum is proportional to the volume of fluid moving with velocities that produce frequencies in that band. Therefore the Doppler power spectrum should have the same shape as a velocity distribution plot for the flow. In Figure 2-21 the effect of the sample volume on the Doppler power spectrum and the generation of the velocity profile v_w is shown schematically [59]. The effect of the sample volume can also be seen the experimental results presented in Chapter 4 and Chapter 5. Among other thing, this effect causes the

wall effect, identified by Aidun and Xu in [64]. This wall effect is presented detail in chapter 5.5.
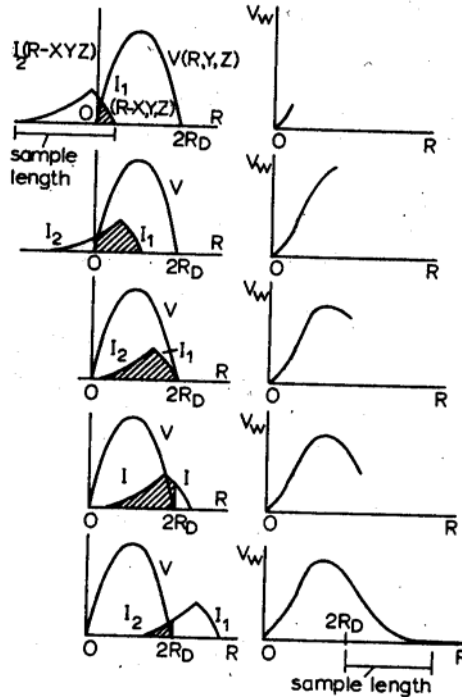
Figure 2-21: Doppler Power Spectrum and Velocity Profile [8]

In practice, the shape of the velocity profile is modified by a number of mechanisms, including non-uniform sampling, scattering, attenuation, intrinsic spectral broadening, filtering and the limitation of spectral estimation techniques.

The spectra corresponding to flat velocity profiles have much of the power concentrated in a relatively small range of frequencies, whilst those corresponding to parabolic profiles are almost flat. In turbulent flow, the velocities of the targets in the ultrasound field fluctuate rapidly with time. This causes a broadening of the spectrum that would otherwise be obtained from flow with the same temporal average velocity profile. Gross disturbances, such as large vortices, may cause irregular spectra with large isolated forward and reverse components.

Since pulsed wave systems use higher peak pressures compared to continuous wave systems (because they only transmit for a small percentage of the time and therefore to achieve an adequate signal-to-noise ratio, the short bursts they use must have greater

56

amplitude), non linear propagation may occur. Non linear propagation leads to changes in the spectral content of ultrasound pulses, which will in turn influence the Doppler spectrum. However, studies that have examined this potential source of error have shown that non-linear effects to make little or no difference to measured Doppler shift frequencies [18].

2.6.6.1   Spectral Broadening

Spectral broadening of Doppler power spectrum occurs where a very short sample volume length is used and it is difficult to distinguish between broadening caused by a true distribution of velocities in the sample volume and the intrinsic broadening. For this reason it is necessary to exercise caution in the interpretation of reports concerning the ability to resolve spectral broadening due to turbulence using high spatial resolution measurements.

The sample volume in which the velocity is measured is of a finite dimension. Each particle, which traverses the ultrasonic beam, backscatters the acoustic waves for a short time. The duration of the backscattering time depends on the angle of incidence as well as on the particle velocity, and is referred to as the transmit time. If the fluid contains small particles possessing different acoustic properties than the fluid, the echo signal amplitude will evolve over time depending on the passage of a group of particle through the sample volume. This results in a modulation of the echo signal which serves to broaden its frequency spectrum. The signal is further modulated by the non-homogeneity of the fluid-particle medium. This spectral broadening depends on the velocity at which the particles traverse the ultrasonic beam. The higher the velocity, the faster the signal will be modulated and its spectrum broadened.

Since the Doppler signal is related to the velocity, it is possible to evaluate the effect of the transit time as a function of the Doppler frequency. Spectral broadening δf_d can be estimated by [51]:

$$\frac{\delta f_d}{f_d} = \frac{K\lambda}{D}\tan\theta$$

Equation 29: Spectral Broadening

where K is a constant between 2 and 3, depending on the ratio of the intensity of the acoustic wave at its center to its intensity near the periphery, λ is the wavelength and D is the diameter of the ultrasonic beam.

The spectral broadening created by the modulation of the echo signal amplitude may also be explained based on geometric considerations. The finite dimension of the sample volume implies that each particle contained within it is viewed from a slightly different Doppler angle. This results in a spread of Doppler frequencies corresponding to this small angle change.

2.6.6.2 *Spectral Broadening Due to Attenuation and Scattering*

The use of pulses with large bandwidths creates additional problems in that, as both scattering and attenuation are frequency dependent, the shape of an ultrasound pulse, and hence its Doppler replica, can be considerably distorted.

Attenuation may effectively modify the shape of a pulsed wave Doppler beam, but this will normally only be of importance with long-gate Doppler systems where the objective is to insonate relatively large sample volumes uniformly. For short-gate Doppler systems it is the frequency dependent nature of attenuation, rather than attenuation itself, that is important in distorting the Doppler power spectrum. In general, attenuation of ultrasound increases with increasing frequency. Therefore, the higher frequency components of the transmitted pulse are attenuated more rapidly and scattered more strongly than the lower frequencies. This leads to an increase in the center frequency of the pulse which, depending on the Doppler estimator employed, may in turn result in an overestimate of the Doppler shift frequency. Fortunately, even for estimators that are sensitive to this source of error, it only becomes significant for extremely high bandwidth pulses [18]. It is more difficult to generalize over the effects of frequency dependent attenuation than frequency-dependent scattering, because the former is only determined by the Doppler frequency estimator used and the pulse bandwidth, but also by the attenuation coefficient of the matter through which the pulse travels (and its frequency dependence) and by the depth of the target. In general the errors can be somewhat larger than those introduced by frequency-dependent scattering, but are not sufficient to cause practical difficulties unless the pulse bandwidth is large and/or the target is deep. To some extent any increase in the

mean Doppler shift frequency due to scattering is partially compensated for by the decrease due to frequency dependent attenuation.

2.6.6.3 Spatial Versus Velocity Resolution

In general, a compromise between the length of the range area (spatial resolution) and the velocity resolution must be made. If a short and narrow pulse is used, a small area is probed, but the pulse spectrum and resulting velocity spectrum are wide and give a low velocity resolution, i.e., increasing the spatial resolution decreases the accuracy of the estimation of the Doppler frequency. For a longer and wider pulse the reverse is true, i.e., an accurate estimation of the target velocity requires a narrow spectrum, and thus a long (and wide) emitted pulse. Such an emission will decrease the depth resolution. A long range gate is employed, and a narrow spectrum evolves. The spectral resolution is also determined by the number of pulses (N) used, as the bandwidth of the narrow spectra is proportional to f_{prf}/N. A long observation time, NT_{prf}, yields a small bandwidth.

The fundamentals of the ultrasonic field emitted by the transducer have been identified in this section. In Section 2.5, the ultrasonic transducer was identified to be the most critical component of the measurement system. In Chapter 3, commonly used transducer architectures will be investigated. The transducer selection to measure the velocity in small channels and suggestion for improving the measurement system are based on the previous sections and the fundamentals of transducer architectures identified in Chapter 3.

3　Ultrasonic Transducer

In Section 2.5, the ultrasonic transducer was identified to be the most critical component of the measurement system. It directs transmitted ultrasonic energy and receives the returning echoes. Its beam pattern determines the velocity profile resolution. The sensitivity of the velocimeter to weak echoes, the spatial resolution achievable and the ultrasound frequencies used depend on the transducer. The generation of ultrasonic waves as well as their transformation into an electrical signal is of obvious importance to the quality of the information which may be obtained concerning the flow field. Therefore, the fundamentals of generally available ultrasonic transducers, i.e., single element transducers and transducer arrays, their working principle, architecture, characteristics and potential for focusing the emitted ultrasonic beam have been reviewed in this chapter especially to make suggestions for improving the currently utilized pulsed ultrasound Doppler velocimeter. The following chapters build on and refer to the fundamentals identified in this chapter.

A transducer is any device that converts one form of energy to another. An ultrasonic transducer converts electrical energy to mechanical energy, in the form of sound, and vice versa. The generation and reception of ultrasonic waves is usually accomplished using piezoelectric crystals.

Pulsed Doppler probes are usually excited with peak-to-peak voltages of between 20 and 100 Volt and with a burst length ranging between 1 and 10 µs. The main constraint on the transmitter is that it has to have a sufficient bandwidth to cope with such a signal. Also because a single element transducer is normally permanently connected to the receiver input, the output noise from the transmitter must be kept to an absolute minimum. An on-off ratio of greater than 150 dB is usually adequate [18].

3.1 Piezoelectric Effect

In the application of ultrasound in fluid velocity measurement, the generation and detection of ultrasound depend on the piezoelectric effect, in which mechanical energy is converted to electrical energy and vice versa. The strain produced in a piezoelectric material by the application of unit electric field is called the piezoelectric coefficient d_p, usually known as the transmitting constant of the material. A second piezoelectric coefficient g_p, known as the receiving constant is defined as the electric field produced, in open-circuit conditions, for unit applied stress. These two coefficients are related to the dielectric constant ε_p of the material of the transducer by: $\varepsilon_\pi = d_p/g_p$. In general, a large value of the transmitting constant d_p is desirable for a transmitter, and a large value of g_p is necessary for a sensitive receiver. If a transducer is to operate both as a transmitter and as a receiver, it is desirable for both d_p and g_p to be large.

The mechanical vibration based on the piezoelectric effect can generate ultrasound. The application of a potential difference across the ends of a piezoelectric ceramic results in a change in thickness. The movement of the faces of the transducer radiates energy into the media in contact with both the front and back faces. This mechanical oscillation can be used to set up an ultrasonic wave in material coupled to the transducer, producing the energy transfer:

<center>electrical pulse ↔ mechanical oscillation ↔ ultrasonic wave</center>

The application of a sinusoidal electrical driving signal to a transducer results in a corresponding variation in the thickness of the transducer. The energy reflected at each face of the transducer travels back across the transducer toward the opposite face. When the crystal vibrates, its two surfaces will move periodically toward and away from each other. If the distance between the surfaces is equal to half the wavelength of the internal sound wave, the waves from the two surfaces will coincide in phase and reinforce each other. The two surfaces will vibrate in synchrony, i.e., in resonance. The so-called "fundamental resonant frequency" of an ultrasound transducer is the transmit frequency that corresponds to the half-wavelength crystal thickness.

The received echo voltage across the piezoelectric crystal is proportional to the average echo pressure incident on the crystal front surface. This pressure sensitivity explains the

fact that the transducer is a coherent detector as well as a coherent transmitter of ultrasonic radiation.

Some materials, such as quartz, are naturally piezoelectric; quartz was used for transducers during the early years of diagnostic ultrasound. However, most modern transducers are formed using piezoelectric ceramics, such as lead zirconate titanate or lead metaniobate. These materials offer advantages of greater sensitivity and shorter pulse durations than previous materials. The ceramic is somewhat brittle, so a transducer can be damaged if dropped.

Some modern transducer elements are composites. These elements are formed out of piezoelectric ceramics whose faces have been diced, forming a grid arrangement with the piezoelectric material sticking out like posts. The area between the posts is backfilled with a type of epoxy. Piezoelectric composites have the advantage of large frequency bandwidths, improved sensitivity and resolution.

Piezoelectric ceramic materials must be polarized before they will work as ultrasonic transducers. This is done when the element is manufactured by heating the element, applying a strong electrical voltage, and cooling. A transducer could become depolarized, and hence lose its piezoelectric properties, if it were inadvertently heated excessively. For this reason, transducers are never heat sterilized for cleaning. The temperature at which depolarization might occur is usually a few hundred degrees centigrade. The housing on which the piezoelectric transducer is mounted has heat-sensitive bonds; these also would be damaged by excessive heat [49].

3.2   Transducer Architecture

In general, two transducer architectures are predominant in pulsed ultrasound Doppler velocimetry: single element transducers and transducer arrays.

3.2.1   Single Element Transducer

Essential components of single element ultrasonic transducers, namely the active element (transducer), backing layer and wear surface, are shown in Figure 3-1. The thin

piezoelectric (active element) crystal is bonded to a rear backing material and a front plastic wear surface and the three components fit inside an external housing. The piezoelectric crystal has electroded surfaces that are connected to both transmission and reception circuits.
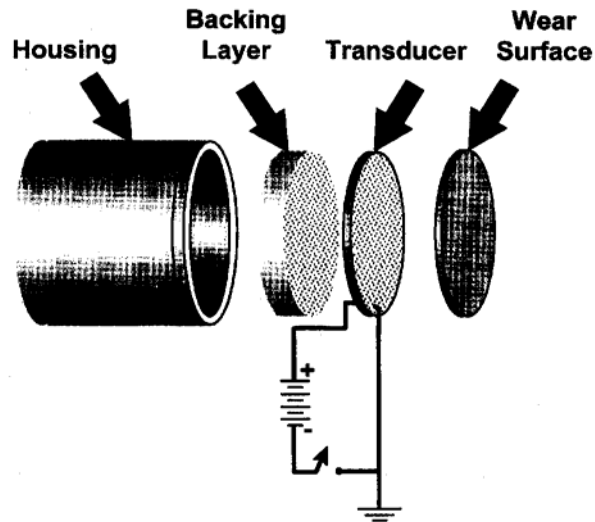
Figure 3-1: Main Components Ultrasonic Transducer [44]

The active element, which is piezoelectric or ferroelectric material, converts electrical energy such as an excitation pulse from a flaw detector into ultrasonic energy. The most commonly used materials are polarized ceramics which can be cut in a variety of manners to produce different wave modes. New materials such as piezoelectric polymers and composites are also being employed for applications where they provide benefit to transducer and system performance.

The piezoelectric crystal is energized into transmission by the application of an electrical voltage across its electroded surfaces that cause the crystal to deform slightly in thickness. When the voltage terminates, the deformed crystal surfaces attempt to recover to an undeformed state; this generates two longitudinal ultrasonic waves, one propagating into the crystal and the other one propagating into the adjacent bonded layer. The two in-going longitudinal waves may reinforce each other as they reflect back and forth from the electroded surfaces, causing resonant thickness oscillations of the crystal. These resonance oscillations occur at a frequency at which the crystal thickness is half an acoustic wavelength or odd multiples of this frequency. The outgoing wave that

propagates into the wear surface will pass through it and into the patient. The outgoing wave that propagates into the backing material will be absorbed without reflection back into the crystal.

The purpose of the backing layer is to absorb ultrasonic energy, causing the transmit time (or output pulse length) to be as short as possible [44]. The backing layer acts as an absorber dampening the crystal oscillations, producing a short output pulse. Usually a highly attenuative, high density material is used to control the vibration of the transducer by absorbing the energy radiating from the back face of the active element. The choice of the material for the backing determines the type of acoustic impulses which may be emitted by the transducer. When the acoustic impedance of the backing matches the acoustic impedance of the active element, the result will be a heavily damped transducer that displays good range resolution but may be lower in signal amplitude. For a highly absorbent material, most of the energy is absorbed, tending to produce a short emission. If there is a mismatch in acoustic impedance between the element and the backing, more sound energy will be reflected forward into the test material. For a weakly absorbing material, the energy at the rear of the transducer is returned to the front face, thereby increasing the energy transmitted out in the medium. The end result is a transducer that is lower in resolution due to a longer waveform duration, but may be higher in signal amplitude or greater in sensitivity.

The basic purpose of the transducer wear surface is to protect the transducer element from the testing environment. It also functions as an electrical insulator and as part of its focusing mechanism. In many applications, the wear plate has the additional purpose of serving as an acoustic transformer between the high acoustic impedance of the active element and the water, the test piece or medium, which are of lower acoustic impedance. This is accomplished by selecting a matching layer that is ¼ wavelength thick and of the desired acoustic impedance (the active element is nominally ½ wavelength). The choice of the wear surface thickness is based upon the idea of superposition that allows waves generated by the active element to be in phase with the wave reverberating in the matching layer. When signals are in phase, their amplitudes are additive, thus a greater amplitude wave enters the test piece. If a transducer is not tightly controlled or designed with care and the proper materials and the sound waves are not in phase, it causes a

disruption in the wave front [43]. By placing an additional layer (wear surface) between the two given media (piezoelectric element and surrounding medium), the energy transfer may consequently be optimized. Because of its very low impedance, even a very thin layer of air between the transducer's face and the test piece or medium would reflect virtually all the sound, preventing penetration into the medium.

3.2.2   Transducer Arrays

In many instruments transducer arrays are used rather than single-element transducers. An array transducer assembly consists of a group of piezoelectric elements, each of which can be excited individually and whose echo signals can be detected and amplified separately. Dividing the transducer into individual elements that can be independently fired and utilized in reception provides great flexibility in the design of transmit and receive beam patterns. The elements are rectangular in shape and arranged in a line (linear array) or are ring shaped and arranged concentrically (annular array).

Advantages offered by all arrays are their potential for electronic focusing and automatic variations in the aperture size. These two features can be exploited to enhance the spatial resolution. The position of the focus can be electronically controlled and hence moved very rapidly. Array transducer can be made fairly small, but it is difficult to produce very high frequency array transducers.

A sound beam is produced by a transducer array by sending individual electrical excitation signals to each element used to form the beam. The number of elements involved varies with the type of array and the design. The emerging sound beam is the sum of individual beams from each of the elements. Small elements are used because they have much larger beam divergence angles. It is this large angle which opens up the useful features of arrays such as dynamic focusing and beam steering. Another feature of small elements is their energy transfer efficiency. Smaller elements take less energy to excite and are more efficient receivers due to the lower mass to be energized.

Commonly used array transducer systems are shown in Figure 3-2 [49]. Views are from the bottom with sound beams traveling out of the plane of the diagram.

SEQUENTIAL   SECTORED   ANNULAR
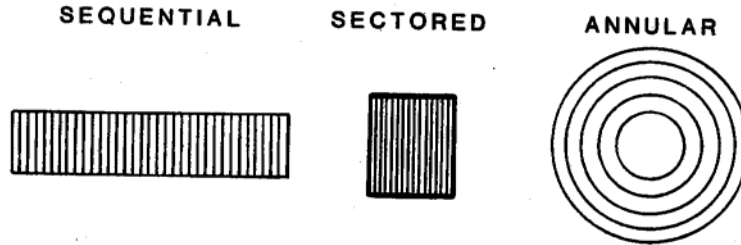
Figure 3-2: Transducer Arrays [49]

Linear array transducers are widely used for imaging. A linear array is a series of transducer elements aligned in a single housing, typically a rectangular single element that has been segmented into smaller individual elements. Linear arrays typically contain up to 256 piezoelectric elements whose operation is under computer control. Introducing curvature to linear arrays has proven to be popular in imaging since the field of view is increased. Moreover, the curved array can be used to produce a desired beam shape or conform to the geometry of the experimental setup. Phased array transducers (curved or linear) find widespread use in both imaging and Doppler modes. A modern phased array transducer typically consists of 128 thin linear elements (element sized are from 0.05 mm to 0.25 mm) and has a length of $1 - 2$ cm [18].

A phased array is a multi-element linear array that uses all of its elements to form each image line. If the elements are fired simultaneously, an unfocused "plane wave" ultrasonic pulse will be transmitted parallel to the normal of the array surface. This is because the cylindrical waves from each small element combine at a distance from the array to form a plane wave parallel to the array surface and in a homogeneous medium the direction of wave propagation is normal to the surfaces of constant phase. The direction of wave propagation may be changed by firing the elements along the array with a constant time delay between element transmissions. Then the cylindrical waves will combine at a distance from the array to form a plane wave tilted at an angle commensurate with the array geometry and the constant time delay. This is called beam steering [44]. The transmitted ultrasonic pulse may be focused at any depth by timing the element firings such that the cylindrical waves all arrive at the chosen focal point at the same instant of time. Phased array transducers contrast with linear array transducers where all elements "fire" with the same phase lag to form a beam that is directed

66

perpendicular to the transducer face. Besides the advantages of array transducer discussed above, especially phased array transducers require circuit complexity caused by the large number of individual elements and the need for different focus time delays at each beam steered angel. Phased array image quality also falls off at large beam-steering angles.

Annular arrays using a smaller number of elements can achieve symmetrical electronic focusing about the axis of the transducer at selected depths. An annular array is a series of concentric ring elements contained in a single housing. In other words, an annular array is a single round element divided into multiple individual concentric rings. Theoretical modeling of the beam shape from an annular array indicates that at least five ring elements are necessary to generate a good quality focused beam [18]. Most modern annular phased array transducers consist of 2 to 5 annuli with active element diameters ranging from 6 to 19 mm. Focal ranges of 1 to 10 cm are typical. The emitted frequency of phased array transducers in general ranges from 0.5 to 25 MHz.

Single element piezoelectric transducers have a large ratio of width to thickness, so the frequency bandwidth of their thickness-expander mode vibrations is well separated from undesired modes of vibration. This permitted the use of shock-excitation voltage pulses with large frequency bandwidths. The small array elements have small width to thickness ratios with overlapping of the frequency bandwidths of desired (thickness-expander) and undesired (shear, lateral and surface wave) modes of vibration. Excitation of these undesired modes of vibration: (1) wastes energy, which reduces element sensitivity; (2) degrades the single element directivity by distorting the shape of the radiating face; and (3) leads to acoustic cross talk between elements, which degrades the beam shape. The higher the desired operating frequency, the lower the width to thickness ratio.

Composite piezoelectric structures were designed to reduce these effects. They are fabricated using a dice-and-fill technique, described by Papdakis [44]. This results in a width to thickness ratio of the small array elements to much less than unity, which separates their desired and undesired mode frequency bandwidths and reduces the deleterious effects of the undesired modes. There is an accepted trade-off associated with the use of composite piezoelectrics. Since the electroded area of piezoelectric material is reduced (due to the fill), the element sensitivity is reduced proportionately. An important feature of composite piezoelectrics is the reduction of element acoustic impedance and

therefore a reduction of the required acoustic matching. New acoustic matching techniques such as acoustic matching by micro machined graded volume fraction silicon structures and active piezoelectric layers (described by Papdakis [44]) provide improved transmission and reception characteristics. Besides increased element sensitivity, the improved acoustic impedance matching produces better near-field image quality, broader bandwidth operation and less energy dissipated within the transducer (very important when transducer is pulsed rapidly).

Only the focal zone portion of a focused ultrasonic beam pattern is narrow enough to be effective applications where high spatial resolution is required. Use of the complex interference pattern near-field and the wide far-field beam portions leads to reduced spatial and contrast resolution. In analog static imaging, the single-element transducers were weakly focused to lengthen the focal zone and minimize this problem. Modern imaging equipment with fast digital circuitry uses zone focusing to eliminate the undesirable portions of the beam pattern.

The first attempt to improve image quality at all depths was selectable zone focusing (Figure 3-3 (a)). For each image there were three possible focused beam patterns: a near-depth focus, a mid-depth focus, or a far-depth focus. The operator selected the focal depth for each image with a three-way switch. High image quality occurred only at the selected image depth.

A further refinement eliminated the undesirable portions of each depth's focused beam pattern. As shown in Figure 3-3 (b) with three depth zone, for each image line the transducer sequentially transmits the three different focal patterns. After each transmission, only the echoes from that beam's focal zone are acquired. Then the acquired focal zone echoes are combined to form an effective beam pattern that is a composite of the three separate transmissions and partial receptions (Figure 3-3 (c)).

68
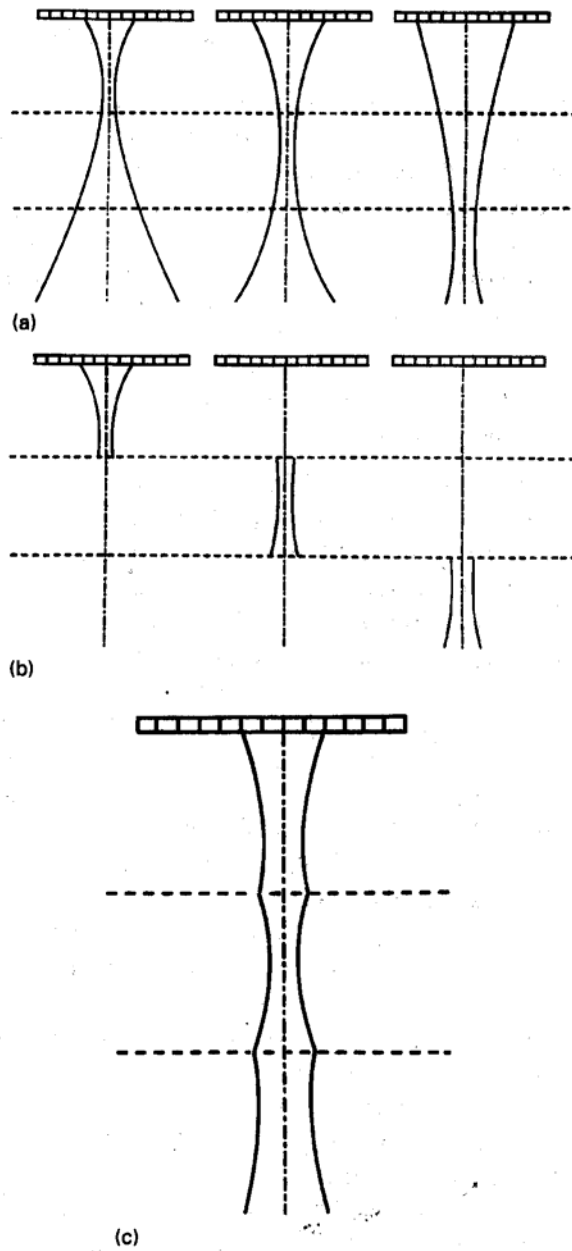
Figure 3-3: Zone Focusing [18]

Once an ultrasonic beam is transmitted, its focal properties cannot be changed. During echo reception, however, it is possible to sequentially change the array element time delays such that the receive beam pattern is continuously focused at the depth of origin of the echoes being received. In other words, the receive focus moves outward at half the acoustic velocity. This switching of array element time delays is performed in discrete steps using fast digital circuitry. Dynamic receive focusing is accompanied by dynamic

aperture and dynamic apodization. That is along with changing the focus time delays, as echoes are being received the aperture is increased stepwise (element by element) such that the receive beam spot size remains approximately constant. Since the pulse-echo beam pattern is the product of transmit and receive beam patterns, it is narrowed considerably by the use of dynamic receive focusing with a commensurate lengthening of its effective focal zone [44].

3.3   Transducer Characteristics

A transducer has a resonance frequency, or a frequency at which it operates most efficiently. This frequency is determined by the thickness of the piezoelectric element. The thicker the element, the lower the transducer frequencies, i.e. low frequency piezoelectric transducer elements are thick and high frequency elements are thin.

The near field distance is the natural focus of the transducer and a function of the transducer frequency, element diameter (aperture size) and the sound velocity of the test material. With a constant aperture, increasing the frequency increases the length of the near-field and decreases the angle of divergence in the far-field, producing a more directional beam pattern. Decreasing the aperture size at a constant frequency causes a shorter near-field and a larger angle of divergence, producing an omni directional beam pattern. The near zone is longer for larger diameter transducers and for higher frequency transducers

Sensitivity is the ability of an ultrasonic system to detect reflectors at a given depth in a test material. The greater the signal that is received from these reflectors, the more sensitive the transducer system.

There are two types of resolution: spatial and echo amplitude resolution. Spatial resolution allows one to identify two adjacent structures in the image. It is usually associated with high-contrast objects in the image (such as two point reflectors). Near surface resolution is the ability of the ultrasonic system to detect reflectors located close to the surface of the test piece. Echo amplitude resolution allows one to identify a region of echoes (reflectors) whose amplitude is slightly greater or less than the amplitude of the surrounding echoes (reflectors). Echo amplitude resolution is also called contrast

resolution and is usually associated with low contrast objects in the image [44]. Amplitude resolution mainly depends on circuit complexity considerations.

Spatial resolution refers to how closely positioned two reflectors or scattering regions can be to one another and still be "seen" as separate reflectors on a display [49]. It also compares to the smallest object of a given echo contrast compared with the background matter, that can be detected. Spatial resolution is very closely tied to the properties of the transducer.

Axial or range resolution refers to how closely positioned two reflecting targets can be along the sound beam axis and still be distinguished on the display as shown in Figure 3-4. In other words, axial resolution is the ability of an ultrasonic system to produce simultaneous and distinct indications from reflectors located at nearly the same positions with respect to the sound beam. It depends mainly on the duration of each ultrasound pulse emitted by the transducer. Optimum axial resolution is achieved by using transducer that produce short-duration acoustic pulses [49].
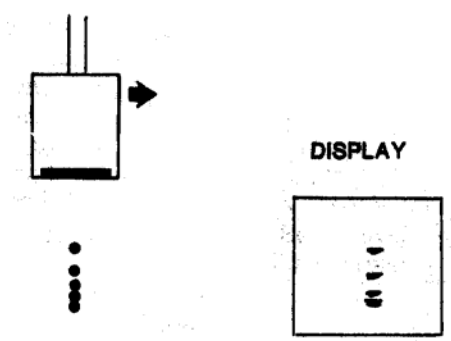
Figure 3-4: Axial Resolution [47]

The pulse duration must be kept as low as practical to obtain good axial resolution. The pulse duration is minimized by damping the vibration of the transducer as quickly as possible following excitation. The backing layer absorbs sound waves at the back surface of the piezoelectric element resulting in a short duration pulse and good axial resolution. The greater the amount of damping, the shorter will be the pulse duration and the better will be the axial resolution.

Besides the degree of damping, the ultrasonic frequency also influences the axial resolution. For the same relative amount of damping the acoustic pulse produced by a

high-frequency transducer is shorter in duration than that produced by a low-frequency transducer. Therefore, higher-frequency transducers result in better axial resolution than lower-frequency transducers.

Lateral resolution refers to how closely spaced two reflectors can be along a line perpendicular to the sound beam and still be seen as separate reflectors as shown in Figure 3-5 [49].
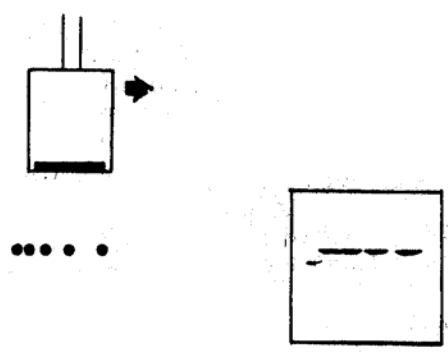
Figure 3-5: Lateral Resolution [47]

Lateral resolution depends on the effective beam width at the position of the reflector. According to Signal-Processing [49], the beam width W at axial distance x in the far field of an unfocused transducer (transducer radius a as shown in Figure 3-6) may be approximated by:

$$W = 1.22 \frac{\lambda x}{2a}$$

Equation 30: Beam Width Unfocused Transducer
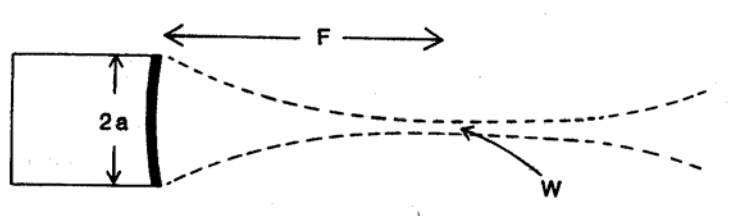
Figure 3-6: Focused Beam Shape [18]

At a given transducer radius, the beam width decreases with decreasing wavelength λ. Because wavelength is inversely proportional to frequency, beam width decreases with increasing frequency. The beam width in the far field also decreases with increasing transducer size (greater radius a).

For a given transducer frequency the near field length is greater for larger diameter transducer. Beam divergence in the far field is less for larger diameter than smaller diameter transducers.

For a given transducer diameter the near field length is greater for higher-frequency transducers. Beam divergence in the far field is less for higher-frequency than lower-frequency transducers.

Axial and lateral resolutions depend on pulse length and pulse width, respectively. The shorter the pulse is, the better the axial resolution is. The narrower the pulse is, the better the lateral resolution is. Damping and the use of higher frequencies shorten the pulse, improving the axial resolution. Focusing narrows the pulse, improving the lateral resolution (at least in the focal region). The smallest axial resolution is equal to one half the pulse length. The lateral resolution is equal to the pulse width. Improved resolution with higher frequency is accompanied by decreased penetration depth as a result of increased attenuation.

3.4 Focused Transducers

Immersion transducers are available in three different configurations: unfocused ("flat"), spherically ("spot") and cylindrically ("line") focused. The beam's diameter at any point depends on the frequency, transducer diameter, and distance from the transducer. It is important to realize that even for flat, unfocused transducer elements, there is some beam narrowing or "focusing". Most transducers are focused to achieve better lateral resolution than would be found with unfocused probes.

The sound may be focused by using a curved transducer element, a lens, an acoustic mirror system or a (phased) transducer array. The addition of a lens is the most common way to focus a transducer. An unfocused transducer may be used in general applications or for penetration of thick materials. A spherically focused transducer is commonly used

73

to improve sensitivity to for example small flaws or small scatterers. A cylindrically focused transducer is typically used in the inspection of tubing or bar stock.

By definition, the focal length of a transducer is the distance form the face of the transducer to the point in the sound field where the signal with the maximum amplitude is located. In an unfocused transducer, this occurs at a distance from the face of the transducer which is approximately equivalent to the transducer's near field length, because the last signal maximum occurs at a distance greater than its near field.

When focusing a transducer, the type of focus (spherical or cylindrical), focal length and focal target (point or flat surface) need to be specified. Based on this information, for example the radius of curvature of the lens for the transducer can be calculated which varies based on above parameters.

3.4.1 Single Element Transducers

Focusing at a fixed range can be done using an acoustic lens, an acoustic mirror system or using a curved (concave) piezoelectric element. Three different methods are shown in Figure 3-7. In the later case, to provide a flat face on the transducer and hence easier coupling, a weak convex lens can be attached to the front of the concave element. The combined effect of the concave element and the convex lens is designed to give focusing at the desired range.
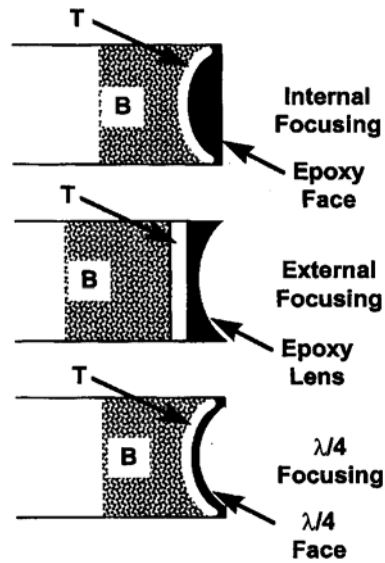
Figure 3-7: Focusing Methods Single Element Transducer [44]

Focusing reduces the beam width over a volume called the focal zone. The resulting beam is rather wide at distances close to the transducer. It narrows and increases in intensity along the axis near the focal distance. Beyond the focal distance the beam gradually diverges. The focal length is the distance from the transducer to the center of the focal region. It cannot be greater than the near zone length of the comparable unfocused transducer.

Substituting z by the focal length F in the formula given above (Equation 30), the beam width at the focal distance can be estimated. This equation shows that in the focal region the lateral resolution is improved as larger-diameter transducers are employed. For a fixed-transducer diameter the lateral resolution is improved if higher-frequency transducers are used.

With a single-element transducer the focal distance is fixed during the manufacturing process

3.4.2   Transducer Arrays

The transmitted beam from an array may be focused by introducing time delays in the appropriate sequence to the excitation pulses applied to individual elements. Precision electronic delay circuits are available and are provided in an instrument for this purpose.

With the time delays in action, the situation is as though a focusing lens or a curved piezoelectric element were producing the beam.

A distinct advantage of an array over a single-element transducer is that the array's focal distance can be varied, simply by selecting a different delay sequence for pulses applied to individual elements. Thus, an array is not locked into a fixed focal distance as is a single-element transducer. Most array instruments allow the user to select the transmit focal distance. It also is possible to provide simultaneous, multiple transmit focal distances. If the latter is available, the instrument automatically changes the transmit focus while scanning, optimizing the resolution throughout the depth range of the scan. On transmission, the size of the excitation signal to each element, the timing of the excitation of each element and the number of elements excited can all be controlled and altered rapidly.

Array transducers also allow focusing of received echo signals. When echo signals are picked up by elements in an array, signals from individual elements are added together in the receiver, yielding a net signal for each reflector. An echo from a discrete target located in the beam may arrive at individual elements of the array at slightly different times because of slight differences in distance. This could lead to variations in the phase of signals from individual elements. The individual signals might be brought back into precise synchronization or phase before summing with the help of electronic delays whose settings are adjusted for the depth of the reflector. Focusing during echo detection is usually done dynamically. The focal distance of the array during reception may be varied electronically. Each time a sound pulse is launched, the receiving focal distance of the array is set (initially at a shallow depth). As the time after the transmitted pulse increases, the receiver focus changes automatically, "keeping up" with or tracking the position of the sound pulse as it encounters deeper reflectors. The result of using dynamic focus is an extended focal region that is considerably greater than that achievable with a single-element transducer or with a single focal distance applied to an array. On reception, the echo signal at each element can be digitized accurately and rapidly to preserve amplitude and phase information. The gain of each receiver, the delay applied to each signal and the number of elements in use can also be controlled.

For most focused transducers or transducer arrays the beam width varies with distance from the transducer. Variations of beam width with depth can be minimized with array transducer assemblies that also provide dynamic aperture. The aperture refers to the size of the transducer surface involved in producing and detecting echoes for each sound beam. Variation of beam width with depth may be minimized by changing the variable a in Equation 30, the aperture size, with reflector depth. This may be done by varying the number of elements involved in echo detection while echo signals are being picked up by the transducer. As echoes return from deeper and deeper structures the number of elements used to pick up echo signals and hence the aperture is increased. This keeps lateral resolution nearly constant over the entire image region.

Dynamic focusing, beam steering and better energy transfer efficiency are significant advantages of phased array transducers over single element transducers. So far, phased array transducer cannot be used with pulsed ultrasound Doppler velocimetry instruments. The feasibility of using phased array transducers in combination with pulsed ultrasound Doppler velocimetry is further investigated in Chapter 7. Since so far, only single element transducer are available for measuring velocities with pulsed ultrasound Doppler velocimetry, measurements of the ultrasonic beam emitted by various single element transducers are performed. The results of these ultrasonic beam measurements are presented in Chapter 4. Especially the actual beam shape and echo intensity is investigated to select the most promising transducer to measure velocity profiles in small channels. Since application of pulsed ultrasound Doppler velocimetry often involves the propagation of the transmitted acoustic field and the returning echo through a Plexiglas wall, the effect of Plexiglas walls on the beam shape and echo intensity is evaluated. Moreover, the effect of porous screens is investigated and focused transducers are compared to unfocused transducers.

4 Ultrasonic Beam Measurements

In Chapter 2, the ultrasonic transducer was identified to be the most critical component of the measurement system. In Chapter 3, the transducer architecture was then investigated in detail. The ultrasonic transducer mainly determines the lateral resolution of the measurement system. In this chapter, the ultrasonic beam shape and echo intensity is measured. Consequently, information about the actual beam shape of various ultrasonic transducers, especially their lateral resolution, is gained. The lateral resolution of the pulsed ultrasound Doppler velocimetry system is extremely important in evaluating the flow over a backward facing step in small channels, i.e., when dealing with small geometries. Ultrasonic beam measurements will therefore be used to identify the most appropriate transducer to measure velocity profiles in small channels and capillaries. Since application of pulsed ultrasound Doppler velocimetry often involves the propagation of the transmitted acoustic field and the returning echo through a Plexiglas wall, the effect of Plexiglas walls on the beam shape and echo intensity is evaluated in detail. Moreover, the interaction of porous screens with the emitted ultrasonic wave packet and their effect on measuring the velocity profile with unfocused as well as focused ultrasonic transducers is analyzed.

In Chapter 4, the experimental setup is described and the ultrasonic beam of various transducers is measured at first. Then the interaction of the ultrasonic burst with Plexiglas walls of different thicknesses is investigated and quantified in detail. Finally, the effect of a porous screen, a paper forming screen, is explored.

Measurement of the ultrasonic field (transmission zone) of a transducer is undertaken by moving a small detector systematically in the region in front of the transmitting element at various distances. The transducer face and the detector are immersed in water. It should be remembered that the beam characteristics measured in water are different from those in water with suspended fibers or particles. Nevertheless, a great deal can be deduced about a beam in water with suspended fibers or particles from a plot obtained in water.

4.1 Experimental Setup

The pulsed Doppler ultrasound velocimetry instrument DOP2000 model 2125 (by Signal-Processing) is used to measure the ultrasonic field generated by various ultrasonic transducers. The effect of Plexiglas walls and forming screens placed between the ultrasonic transducer and a target reflecting the ultrasonic wave packet emitted by the transducer (in this case a plastic sphere) is evaluated. The plastic sphere is mounted on a xy-positioner. Ultrasonic transducer and plastic sphere are submerged in water as shown in Figure 4-1 and 4-2.
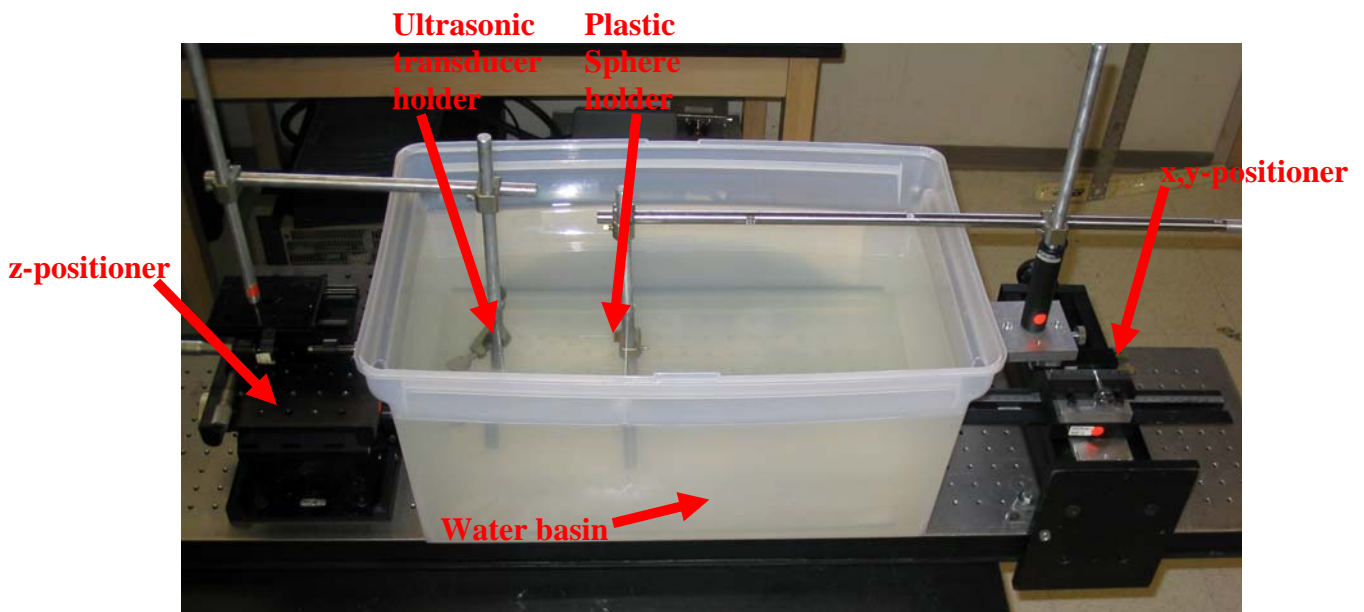
Figure 4-1: Ultrasonic Field Experimental Setup Front View
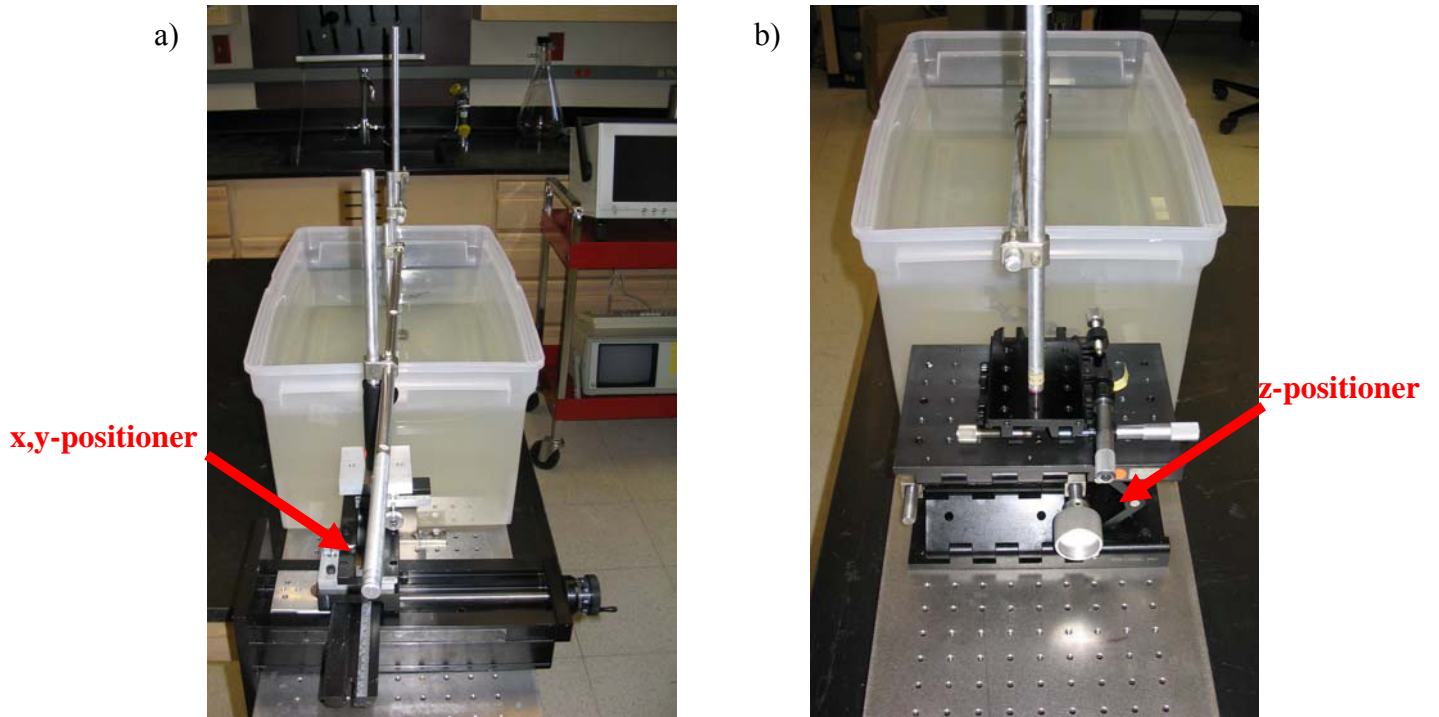
Figure 4-2: Ultrasonic Field Experimental Setup Side Views
   a) x-y-Positioner
   b) z-Positioner Including x,y-Fine-Positioner

In Figure 4-3 the basic experimental setup used to measure the ultrasonic field is shown. The ultrasonic signal propagates along the x-axis. Therefore, the ultrasonic beam is symmetric about the x-axis (or ultrasonic beam axis). Δx is defined as the distance between the sphere and the surface of the transducer on the x-axis. Movements along the y- and z-axis are movements perpendicular to the ultrasonic beam axis.
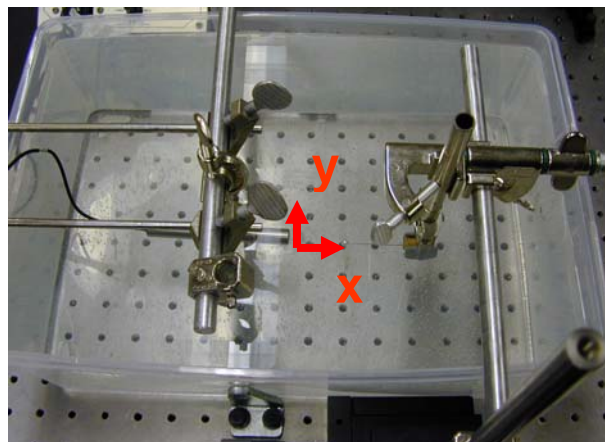
Figure 4-3: Basic Experimental Setup

The plastic sphere is handled by a small rigid rod (1/3 of the diameter of the sphere). The length of the rod is 5 cm. The system, rod and sphere, is mounted on a x,y-table, which is capable of positioning the sphere with a minimum resolution of 0.1 mm. The system sphere-transducer is completely submerged. The depth of the liquid surrounding the sphere-transducer system is at least twice the distance between the sphere and the transducer in order to avoid the influence of the free surface of the liquid.

4.2 Principle of Measurement

The measurement of the ultrasonic field generated by an ultrasonic transducer is realized by measuring the intensity of an echo coming from the plastic sphere. By moving the position of the sphere along a line (y-axis) perpendicularly to the axis of the ultrasonic beam (x-axis) the intensity of the echo for different positions of the sphere on the y-axis is measured. The acoustic intensity distribution is used to measure the -3dB and -6dB width of the ultrasonic beam, from which the size of the sampling volume can be estimated. In Figure 4-4 the principles of the method is illustrated:
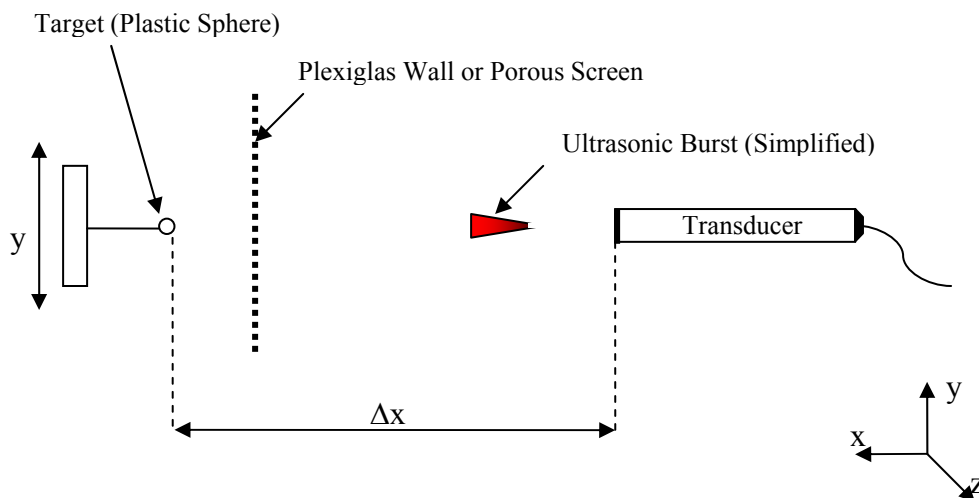
Figure 4-4: Principle Beam Shape Measurements

After selecting various control parameters, centering and placing the sphere at the desired depth, the intensity of the ultrasonic field can be measured. Figure 4-5 shows the three panels on the screen of the instrument. The panel on the left is reserved to the display of the measured ultrasonic beam width. The panel on the right displays the intensity of the echo coming from the sphere and the panel located on the bottom of the screen contains the control parameters.
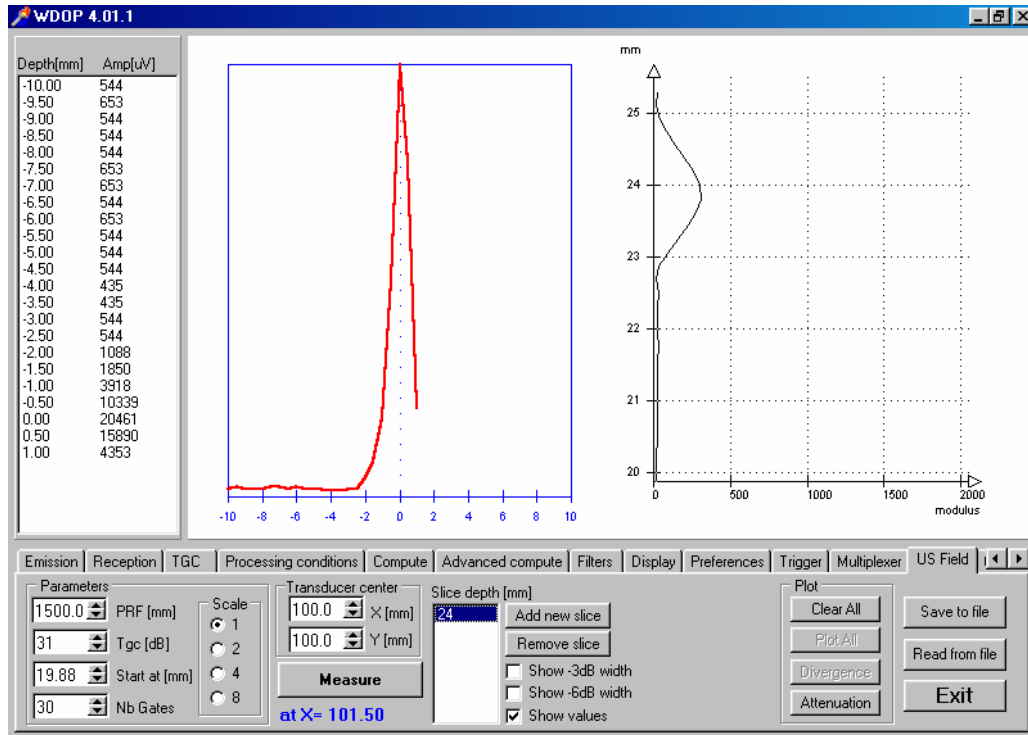
Figure 4-5: Interface Beam Shape Measurements

At first, ultrasonic beam shape measurements of three different transducers are conducted. Then a Plexiglas wall is placed between the transducer and the target (plastic sphere). Finally the Plexiglas wall is replaced by a porous screen, a paper forming screen described in Section 4.5.

4.3 Ultrasonic Beam Measurements of Various Ultrasonic Transducers

The ultrasonic beam shape of the following transducers has been measured:

- Transducer 1: 2 MHz emitting frequency, 10 mm transducer diameter
- Transducer 2: 4 MHz emitting frequency, 5 mm transducer diameter
- Transducer 3: 8 MHz emitting frequency, 5 mm transducer diameter
- Transducer 4: 4 MHz emitting frequency, 8 mm transducer diameter, focused

The experimental setup is shown in Figure 4-3. The principle of measurement is explained in the previous section. After evaluating the measurement results, figures of the general ultrasonic beam divergence and echo intensity plots of each transducer are presented (Figure 4-6 to 4-13). In the beam divergence profiles, the 3 dB and 6 dB width of the ultrasonic beam, derived from the acoustic intensity distribution perpendicular to the ultrasonic beam axis, is plotted along the position of the plastic sphere on the ultrasonic beam axis. In all echo intensity plots, the echo intensity is plotted over the distance between the plastic sphere and the transducer center perpendicular to the ultrasonic beam axis for various distances between the plastic sphere and the transducer face along the ultrasonic beam axis (Δx). For example in Figure 4-6, the echo intensity distribution perpendicular to the ultrasonic beam axis is plotted at distances of 20 mm, 25 mm, 30 mm, 40 mm, 50 mm, 75 mm, 100 mm and 150 mm between the plastic sphere and the transducer face along the ultrasonic beam axis.

4.3.1 Evaluation of Results

Ultrasonic beam measurements are conducted to gain information about the actual beam shape of the given ultrasonic transducers and especially their lateral resolution. A good lateral resolution is essential to measure velocity profiles in small channels and capillaries. In the following chapters, ultrasonic beam measurements will then be used to analyze the effect of walls and porous screens on measuring the velocity profile. Before investigating the ultrasonic beam shape with walls or porous screens between the

transducer and the target (plastic sphere), the beam shape of various transducers is determined.

At a certain minimal distance between the transducer and the plastic sphere on the x-axis, measurements of the ultrasonic beam shape become impossible due to the transducer's ringing effect (described in section 2.6.4). Further decreasing Δx beyond this minimal distance between the transducer and the plastic sphere on the ultrasonic beam axis (x-axis) does not yield any useful measurement results of the ultrasonic beam shape. This is due to the fact that the ultrasonic echo of the plastic sphere can not be recognized in between the high echo intensities caused by the transducer's ringing effect. The ringing noise follows the emission of the ultrasonic burst by transducer. Ringing noise can never be completely removed. Ringing effects following the emission of the ultrasonic wave packet cause a region of strong echoes (saturation) at depths located just after the surface of the transducer. In this region, the ultrasonic field can consequently not be measured. In the following, the region of high echo intensities caused by the transducer's ringing effect is called "saturation region". The distance between transducer and plastic sphere at which the saturation region begins is called "minimal distance".

The effect of the saturation region on the echo intensity can be seen in Figure 4-6 (echo intensity plot of the 2 MHz 10 mm transducer). The echo intensity usually forms a maximum located on the ultrasonic beam axis. As soon as Δx becomes smaller than the minimal distance the magnitude of the maximum echo intensity decreases while the overall echo intensity level increases. Further decreasing Δx leads to a straight line at relatively high echo intensities. In this case, the echo of the plastic sphere can not be recognized in between this "saturation region". Therefore, at a certain minimal distance, beam shape measurements become impossible.

Using a 2 MHz ultrasonic transducer, the saturation region is usually 10 – 15 mm wide. In the following, the effect of Plexiglas walls and forming screens placed between the ultrasonic transducer and the plastic sphere is evaluated. Since walls or forming screens absorb and reflect acoustic energy, the measurable echo intensity of the plastic sphere is reduced. To clearly recognize the echo coming from the plastic sphere behind the forming screen or Plexiglas wall, a high amplification must be used. Increasing the amplification in the instrument consequently increases the transducer's ringing effect. Therefore

increasing the amplification increases the saturation region and the minimal distance. Because of the high amplification that must be used to recognize the echo of the sphere behind the screen, the saturation region of the 2 MHz transducer is therefore about 20 mm wide (instead of 10 – 15 mm). Using a 4 MHz transducer, the region of strong echoes is usually 3 – 8 mm, depending on the chosen amplification. In our case with increased amplification, the minimal distance is 5 mm for the unfocused 4 MHz transducer and 4 mm for the focused 4 MHz transducer. For the 8 MHz transducer, values of ideally 3 – 5 mm can be obtained. In our case, the minimal distance for the 8 MHz transducer is 8 mm. In general, the minimal distance decreases with increasing frequency. Since the ultrasonic signal emitted by the 8 MHz transducer is much stronger attenuated than the ultrasonic signal emitted by the 4 MHz transducer, a higher amplification had to be used. Consequently, the minimal distance of the 8 MHz transducer was increased and is higher than the minimal distance for the 4 MHz transducer.

Looking at Figure 4-7, 4-9 and 4-11, it can clearly be seen, that at a given transducer diameter, the beam width decreases with decreasing wavelength. Because wavelength is inversely proportional to frequency, beam width consequently decreases with increasing frequency. It can also be seen that the beam width in the far field decreases with increasing transducer size (greater aperture).

In the same way as the beam width, the beam divergence decreases with increasing frequency. The half angle of beam divergence (calculated by the instrument) for the 2 MHz 10 mm transducer is 2.27 degrees, 2.23 degrees for the 4 MHz 5 mm transducer, 1.22 degrees for the 8 MHz 5 mm transducer and 2.33 degrees for the 4 MHz 8 mm focused transducer. Theoretically beam divergence in the far field should be less for larger than smaller diameter transducers [18]. It can be seen that the angle of beam divergence is smaller for the unfocused 4 MHz 5 mm than for the focused 4 MHz 8 mm transducer. Consequently, the claim that beam divergence in the far field should be less for larger diameter than smaller transducers is not justified when comparing focused and unfocused transducers. Unfortunately unfocused ultrasonic transducers of the same frequency with different diameters were not available to experimentally validate this theoretical claim. Theoretically, for a given transducer frequency the near field length should also be greater for larger diameter transducers [18]. Moreover, for a given

transducer diameter the near field length should theoretically be greater for higher-frequency transducers [18].

The fact, that for large ratios of diameter to piezoelectric element thickness the ultrasonic beam is focused, can clearly be seen in the figures given above and especially in Figure 4-11. The 4 and 8 MHz transducer both have a transducer diameter of 5 mm. Since the thickness of the piezoelectric element equals half a wavelength (discussed in detail in chapter 3), the ratio of the diameter to the piezoelectric element thickness for the 8 MHz 5 mm transducer is larger than for the 4 MHz 5 mm transducer. Therefore, the originally unfocused 8 MHz 5 mm ultrasonic transducer is focused in contrast to the unfocused 4 MHz transducer. This effect can clearly be seen in Figure 4-9 and 4-11.

In the ultrasonic beam divergence profile of the 2 MHz transducer (Figure 4-7), it can be shown that this transducer is not suitable for measuring velocity profiles in small channels due to the relatively large minimal measurable distance of 20 mm and the poor lateral resolution. The 2 MHz transducer could be placed at a distance of 20 mm away from the region of interest, but acoustic coupling and for example wall effects decrease the quality of achieved measurement results. The 8 and 4 MHz transducers are best suited for measuring the velocity profile in small channels when dealing with small geometries. Due to the better lateral and axial resolution (smaller beam diameter and short ultrasonic pulse length) of the unfocused 8 MHz transducer, compared to the MHz transducer, the unfocused 8 MHz transducer is best suited for measurements in small channel described above.

To compare measurement results of unfocused and focused ultrasonic transducers, a focused 4 MHz 8 mm transducer is compared to an unfocused 4 MHz 5 mm transducer. The focal point of the ultrasonic beam of the unfocused 8 MHz 5 mm transducer (due to the large ratio of diameter to piezoelectric element thickness) at a Δx of approximately 15 mm (Figure 4-11) makes the use of specifically manufactured focused 8 MHz ultrasonic transducers dispensable for this application. The focal point of the focused 4 MHz 8 mm transducer is approximately 20 mm away from transducer face. The beam width of the focused transducer is approximately half of the beam width of the unfocused transducer at the focal point. Due to focusing the ultrasonic beam and consequently the ultrasonic energy, the intensity of the received echo from the focused transducer is increased by

approximately 500 percent at the focal point, compared to approximately 20 percent at the focal point of the unfocused 8 MHz 5 mm transducer. The echo intensity before and after the focal point is of the same order of magnitude for the focused and unfocused transducer. The minimal distance at which measurements are possible is approximately of the same order for the focused and unfocused transducer. It can clearly be seen that the beam width in the far field is smaller with the focused transducer. This is also due to the larger aperture of the focused transducer.

Having evaluated the measurement results, figures of the general ultrasonic beam divergence and echo intensity plots of each transducer are presented in Section 4.3.2 (Figures 4-6 to 4-13).

4.3.2 Echo Intensity and Beam Divergence Plots
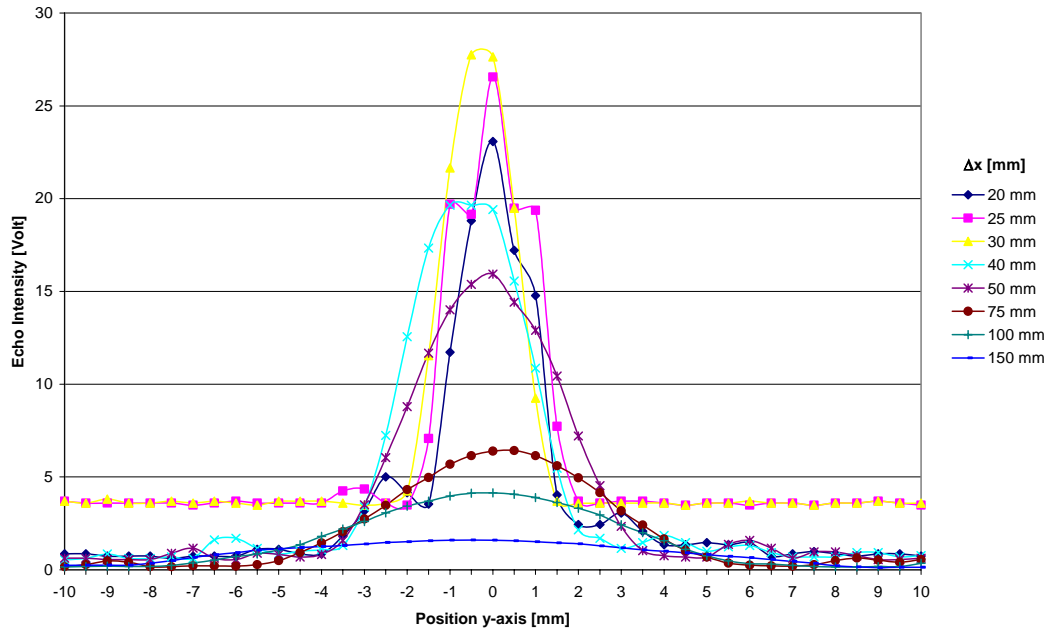
Transducer 1:

Figure 4-6: Echo Intensity 2 MHz 10 mm Transducer
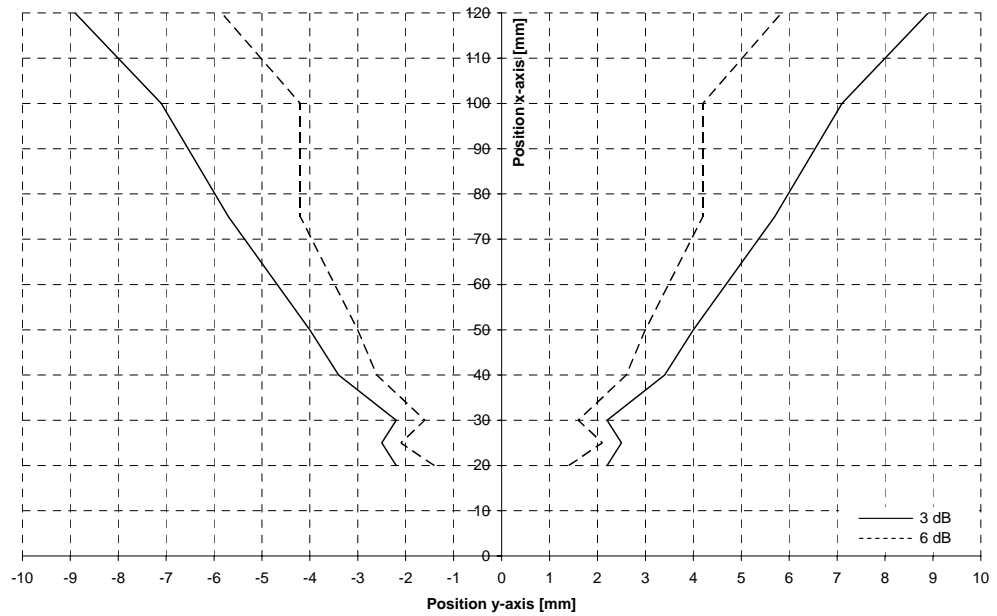
Figure 4-7: Divergence 2 MHz 10 mm Transducer

Transducer 2:
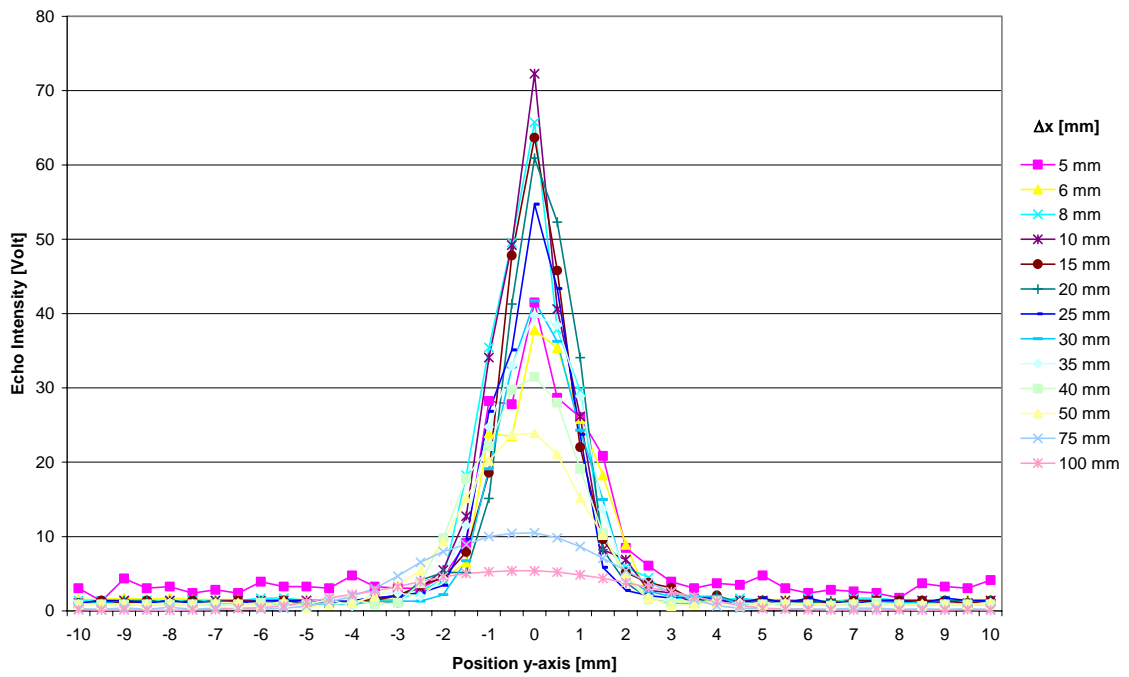
Figure 4-8: Echo Intensity 4 MHz 5 mm Transducer
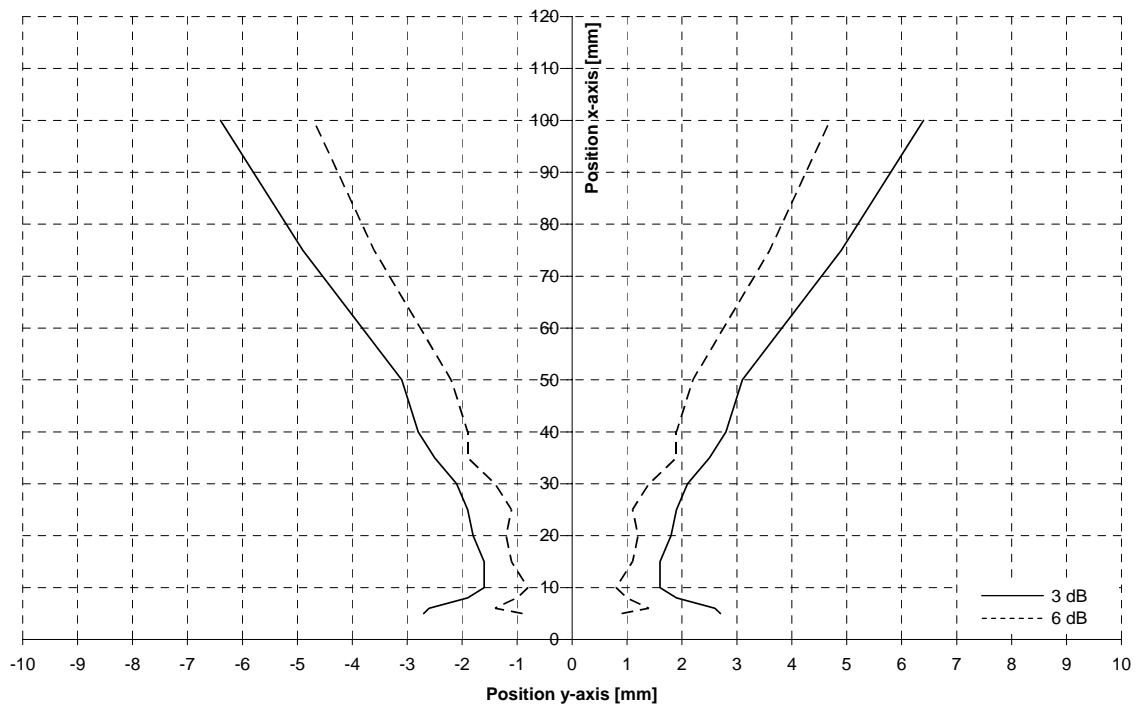
Figure 4-9: Divergence 4 MHz 5 mm Transducer

Transducer 3:
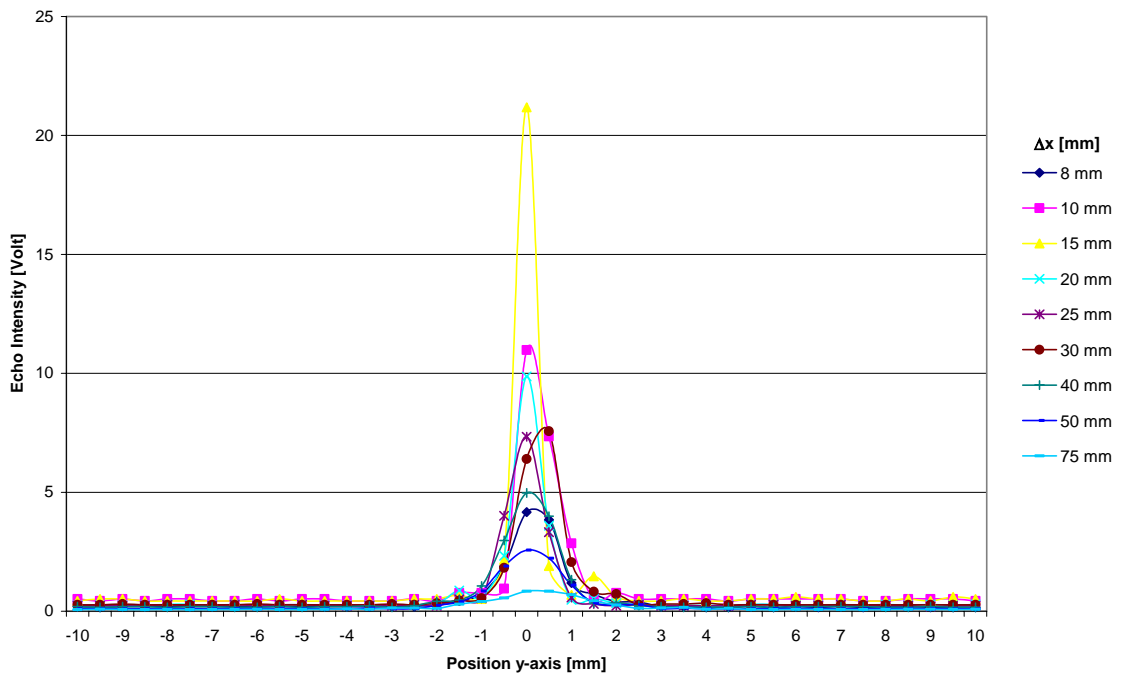
Figure 4-10: Echo Intensity 8 MHz 5 mm Transducer
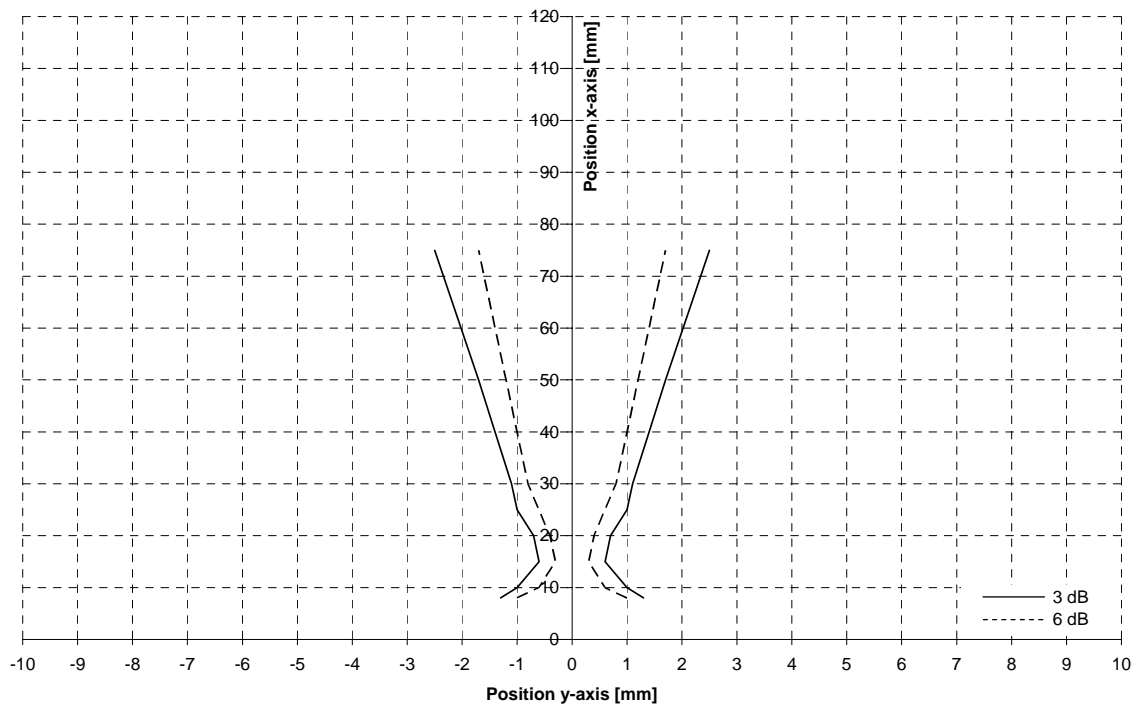
Figure 4-11: Divergence 8 MHz 5 mm Transducer

Transducer 4:
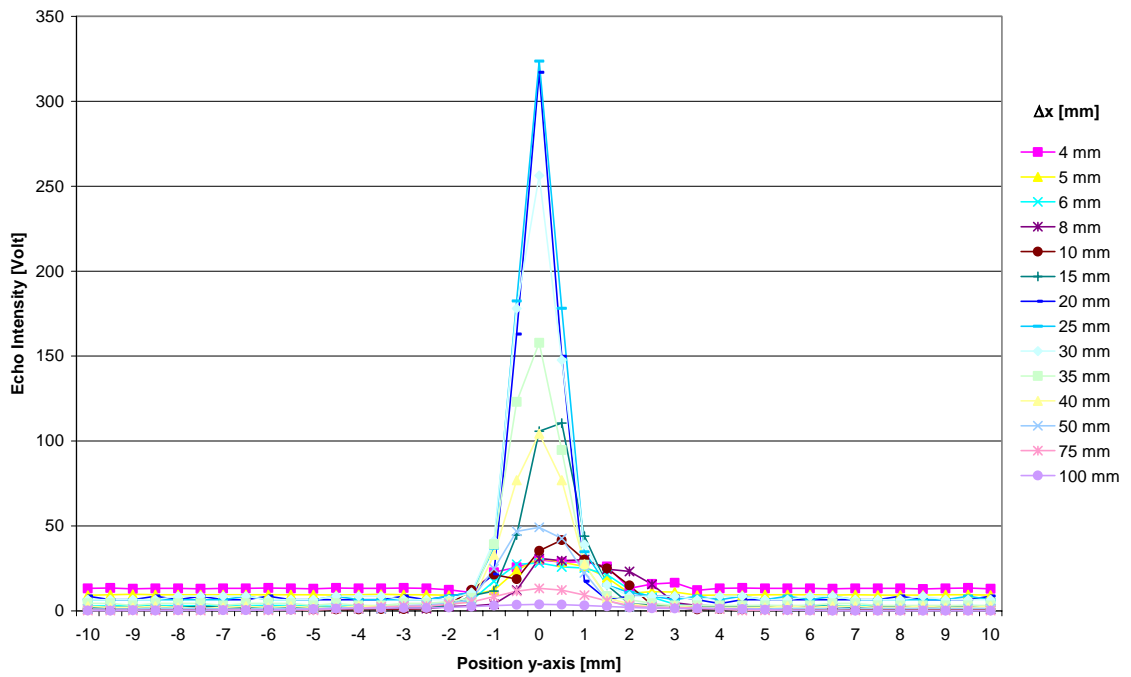
Figure 4-12: Echo Intensity 4 MHz 8 mm Focussed Transducer
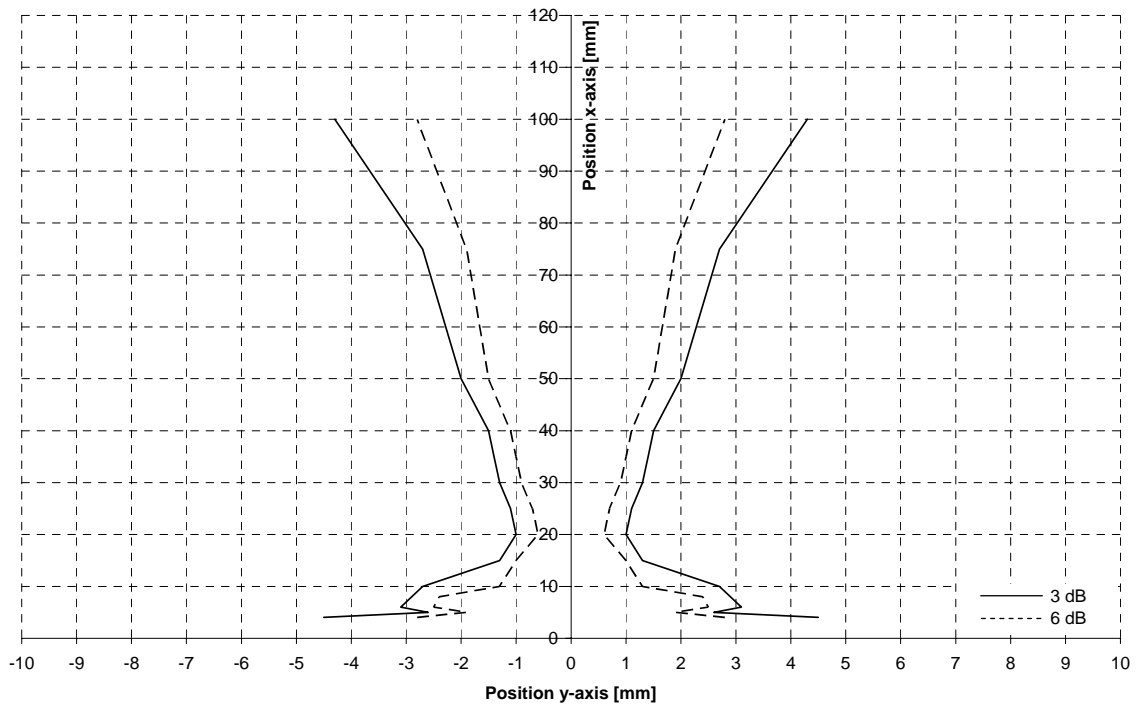
Figure 4-13: Divergence 4 MHz 8 mm Focussed Transducer

4.4　Effect of Plexiglas Walls

Since application of pulsed ultrasound Doppler velocimetry often involves the propagation of the transmitted acoustic field and the returning echo through a Plexiglas wall, the basic experimental setup is modified to evaluate the effect of Plexiglas walls. In the context of measuring the velocity profile in the small channel described in chapter 5, a Plexiglas wall as shown in Figure 4-14 is used:
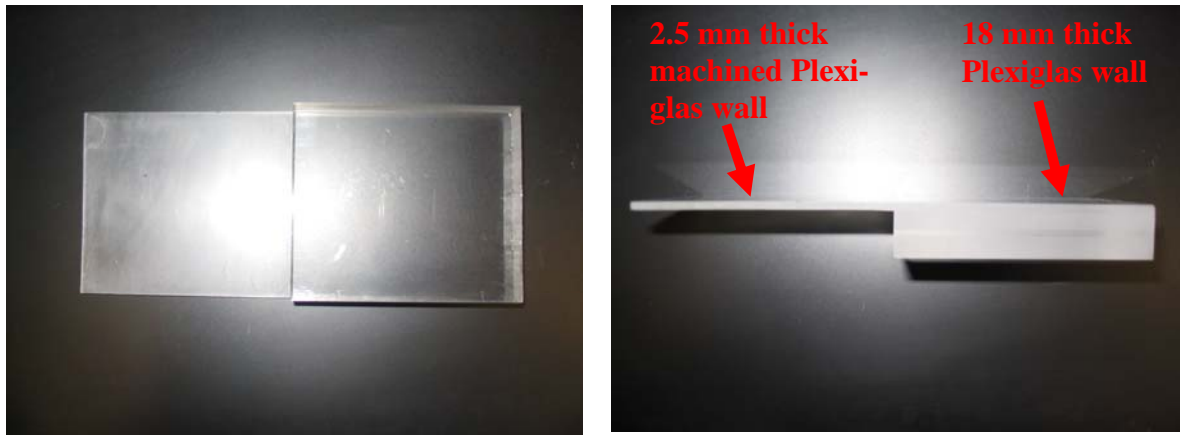
Figure 4-14: Plexiglas Wall

The thin side of the Plexiglas wall is a 2.5 mm thick machined surface (according to the 2.5 mm thick machined top wall measurement area of the channel used in the following chapter). The other side is 18 mm thick and not machined (according to the side of the channel used in the following chapter). The Plexiglas wall is placed between the ultrasonic transducer and the plastic sphere as shown in Figure 4-15:

After measuring the ultrasonic beam shape with both sides of the Plexiglas wall, the effect on the ultrasonic beam shape and the echo intensity is evaluated in the following for each transducer introduced in the previous section. All echo intensity and beam divergence plots are presented in Section 4.4.2 (Figures 4-18 to 4-33).
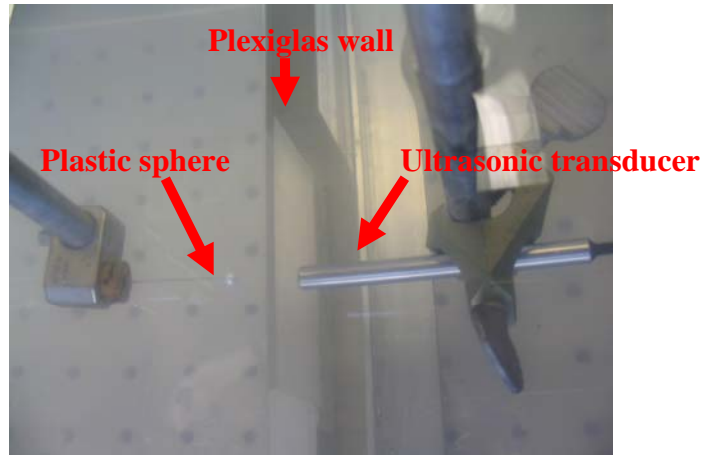
Figure 4-15: Experimental Setup Plexiglas Wall

4.4.1 Evaluation of Results

Comparing the results of the beam shape measurements with a Plexiglas wall with the results given in Section 4.3 the most obvious effect of placing a Plexiglas wall between the ultrasonic transducer and the plastic sphere is a reduction in the measured echo intensity. According to the measurement results, the 18 mm thick Plexiglas wall leads to an echo intensity reduction of approximately 90 percent for the 2 MHz transducer, approximately 97 percent for the 4 MHz transducer, approximately 98 percent for the 8 MHz transducer and approximately 95 percent for the 4 MHz focused transducer. The 2.5 mm thick machined Plexiglas wall leads to a reduction in echo intensity of approximately 40 percent for the 2 MHz transducer on average. The echo intensity of the 4 MHz unfocused transducer is reduced by approximately 45 percent, the echo intensity of the 8 MHz transducer is reduced by approximately 80 percent and the echo intensity of the 4 MHz focused transducer is reduced by approximately 60 percent in the case of the 2.5 mm thick Plexiglas wall.

In general, placing a Plexiglas wall between the ultrasonic transducer and the plastic sphere reduces the received echo intensity. To clearly recognize the echo of the plastic sphere behind the Plexiglas wall, the amplification of the received echo has to be increased. Increasing the amplification increases the transducers ringing effect as discussed in Section 4.3.1. Therefore, the measurable minimal distance increases.

In order to evaluate the effect of Plexiglas walls on the measurable minimal distance, it must be taken into account that different values of the speed of sound in Plexiglas and water cause a distance offset along the ultrasonic beam axis displayed in the instrument. Inserting a Plexiglas wall has therefore a great effect on the distance between the plastic sphere and the transducer face displayed in the instrument. This effect can be seen in Figure 4-22, Figure 4-26 or Figure 4-30. In Figure 4-22 for example, the measurable minimal distance given by the instrument is 14 mm even though the Plexiglas wall is 18 mm thick.

In the following, the distance offset displayed by the instrument is calculated. Since the lateral dimensions of the Plexiglas wall are much larger than the wavelength, Equation 31 [25] is used to calculate the speed of sound, i.e., the speed of longitudinal waves, in Plexiglas.

$$c_L = \sqrt{\frac{E(1-\upsilon)}{\rho_W (1-\upsilon-2\upsilon^2)}}$$

Equation 31: Speed of Propagation of Longitudinal Waves in Solids

For Plexiglas, Young's modulus E is 4200 MPa, the density ρ_W is 1.19 g/cm^3 and the Poisson ratio υ is 0.4. Calculating the sound velocity in Plexiglas consequently yields 2750 m/s.

Calculating the time required for sound to travel through the Plexiglas wall and subtracting it from the time needed for sound to travel the same distance in water yields the offset displayed by the instrument as a function of the Plexiglas wall thickness. The distance offset is given in Figure 4-16. It is seen, that values of the distance offset displayed by the instrument increase with increasing Plexiglas wall thickness.
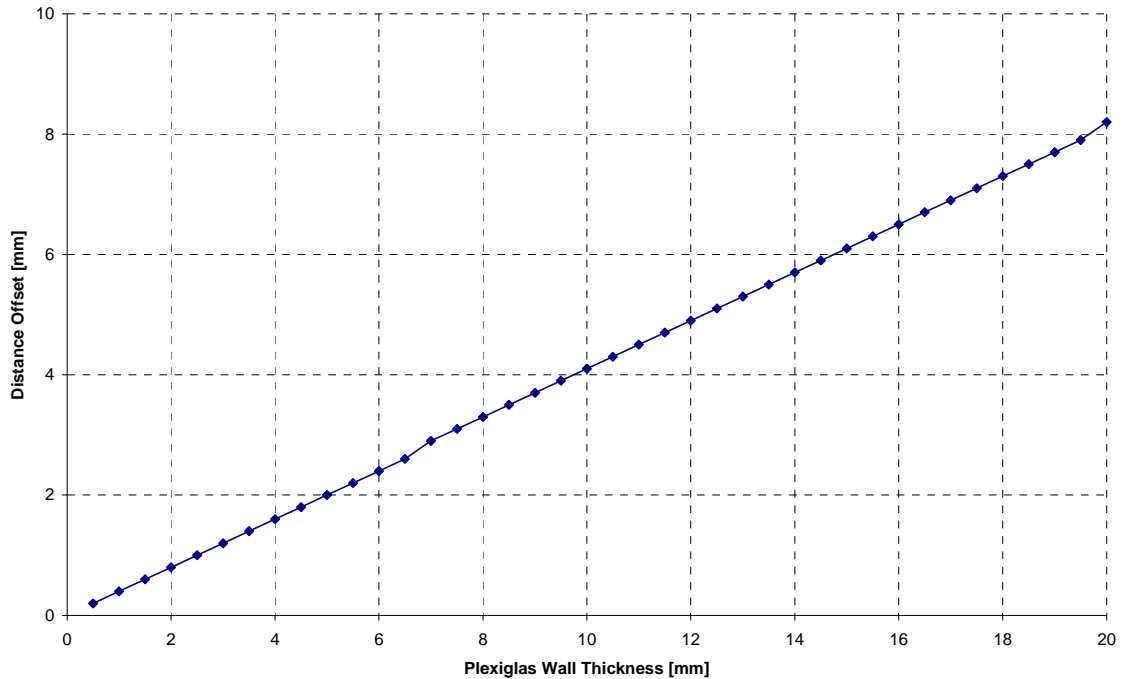
Figure 4-16: Distance Offset

Placing a 2.5 mm thick Plexiglas wall between the transducer and the target (plastic sphere) therefore yields a distance offset of 1 mm whereas the 18 mm thick Plexiglas wall yields a distance offset of 7.5 mm. This offset must be taken into account when evaluating the measurement results, especially changes in the measurable minimal distance caused by the Plexiglas wall.

At distances between transducer and plastic sphere smaller than the minimal distance, the echo of the plastic sphere is in the saturation region caused by the transducer's ringing effect and the effect of the Plexiglas wall. The saturation region leads to an increase in the general echo intensity level of the plastic sphere. This effect can be seen in Figure 4-30 for distances of 15 mm and 14 mm between the transducer and the plastic sphere. The width of saturation region increases with increasing Plexiglas wall thickness.

Comparing the measurement results given in Section 4.4.2 with those given in Section 4.3.2, it can be seen that the measurable minimal distance increases as a result of placing a Plexiglas wall between the ultrasonic transducer and the plastic sphere. The lower the frequency of ultrasound, the larger is the minimal measurable distance. Consequently the smallest measurable minimal distance was achieved with the 8 MHz transducer. With the

18 mm thick Plexiglas wall in place, the broadening of the saturation region caused by the Plexiglas wall is 2.5 mm, with the 2.5 mm thick Plexiglas wall only 1 mm (see Figure 4-17). For example with the 2 MHz ultrasonic transducer and the 18 mm thick Plexiglas wall in place, the broadening of the saturation region caused by the Plexiglas wall is 12.5 mm, with the 4 MHz transducer and 2.5 mm thick Plexiglas wall in place 4 mm.
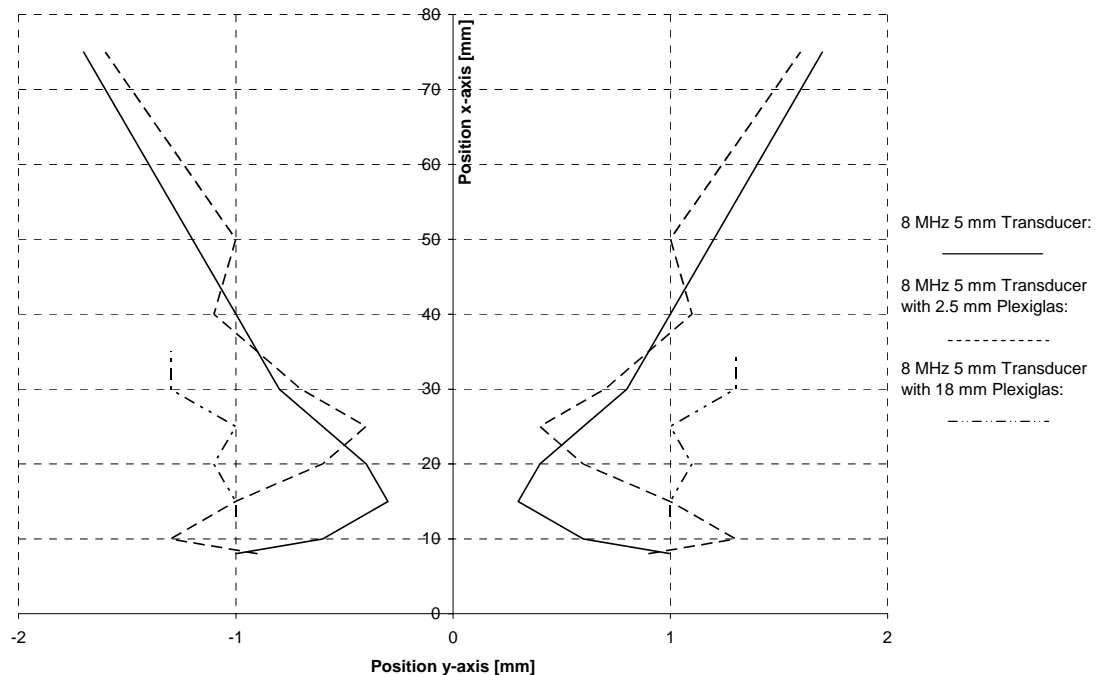
Figure 4-17: Beam Shape 8 MHz 5 mm Transducer With/Without Plexiglas Wall

Placing a Plexiglas wall between the ultrasonic transducer and the plastic sphere also leads to distinct changes in the divergence of the ultrasonic beam. Obviously, a Plexiglas wall modifies the general beam shape (Figure 4-17). In general, the Plexiglas wall disturbs the beam shape (Figure 4-17). In the case of the "naturally" focused 8 MHz 5 mm ultrasonic transducer the focal point is shifted away from the transducer face. Considering the distance offset caused by the Plexiglas wall, the focal point is shifted further away, the thicker the Plexiglas wall is. The focal point of the 8 MHz 5 mm transducer is shifted approximately 10 mm away from the transducer when the 2.5 mm thick Plexiglas wall is in place and approximately 16 mm when the 18 mm thick Plexiglas wall is in place (Figure 4-17). For the focused 4 MHz 8 mm transducer, the focal point is almost completely removed after inserting the Plexiglas wall (Figure 4-30).

Placing a Plexiglas wall between the transducer and the plastic sphere also increases the overall divergence angle of the ultrasonic beam displayed by the instrument. Measurement results reveal that placing an 18 mm thick Plexiglas wall between the transducer and the plastic sphere increases the divergence angle of the ultrasonic beam much more than placing a 2.5 mm thick Plexiglas wall between the transducer and the plastic sphere.

Besides changing the general beam shape, Plexiglas walls absorb ultrasonic energy. The maximum measurable distance decreases with increasing frequency due to the frequency proportional attenuation of ultrasound. The echo intensity from the plastic sphere far away from the transducer becomes so small, that it cannot be recognized by the system. In the following, the experimentally determined reduction of echo intensity due to the Plexiglas walls given in the beginning of this section is calculated. Having determined the speed of longitudinal waves in the Plexiglas, the length of the ultrasonic pulse (incident wave train) emitted by the instrument must be determined in order to make the right assumptions when calculating the reduction in the echo intensity due to the Plexiglas wall. The length of one ultrasonic burst cycle (incident wave train) is given by its wavelength λ: $\lambda = c/f$, where c is the speed of sound propagation and f is the ultrasonic frequency. In the following calculation, a speed of sound in water (c_W) at 20 degrees Celsius of 1480 m/s is used. In Table 4-1 the length of one ultrasonic burst cycle in the Plexiglas wall as well as in water is given.

Table 4-1: Length of One Ultrasonic Burst Cycle in Plexiglas and Water

Frequency of Ultrasound	Length of One Ultrasonic Burst Cycle	
	Plexiglas Wall	Water
2 MHz	1.375 mm	0.74 mm
4 MHz	0.688 mm	0.37 mm
8 MHz	0.344 mm	0.185 mm

Since the duration of the incident signal is less than $2L/c_L$ (when using two ultrasonic burst cycles for measuring velocity profiles), Equation 18, described in detail in chapter

2.6.2, has to be used to calculate the transmission coefficient of Plexiglas. Because $Z_{Plexiglas}$ is 3.26 x 10^6 MKS Rayls, Z_{Water} is 1.483 x 10^6 MKS Rayls and normal incidence of the ultrasonic signal exists, the intensity transmission coefficient for Plexiglas T_P is 0.55.

This transmission loss calculation only accounts for the transmission loss due to reflection at boundaries of different acoustic impedances. To calculate the reduction in echo intensity of the backscattered ultrasonic signal, the absorption of ultrasound in the Plexiglas wall must be predicted. Absorption of ultrasound depends on its frequency and the Plexiglas wall thickness. In the following, the absorption is calculated for the 2.5 mm and 18 mm thick Plexiglas wall as well as for the 2 MHz, 4 MHz, and 8 MHz ultrasonic transducer. Absorption coefficients α are found in the literature [60] and are given in Table 4-2:

Table 4-2: Intensity Absorption Coefficients

Frequency of Ultrasound	Absorption Coefficient [dB/mm]	
	Water	Plexiglas
2 MHz	0.00088	0.4
4 MHz	0.00352	0.8
8 MHz	0.01408	1.6

The pressure amplitude of a plane wave propagating in the x-direction can be expressed in the form:

$$p(x,t) = P_0\, e^{-a_a x}$$

Equation 32: Pressure Amplitude of a Plane Wave

where a_a is the amplitude absorption coefficient, x is the distance, p is the pressure and P_0 is the pressure amplitude. Therefore, the absorption coefficient α_α, amplitude absorption coefficient a_a and intensity absorption coefficient A_a are related to each other as follows [60]:

$$\alpha_a = 20\log_{10}\left(e^{a_a}\right) = 10\log_{10}\left(e^{A_a}\right) = 8.686\,a_a = 4.343\,A_a$$

Equation 33: Absorption Coefficients

Consequently, placing a 2.5 mm or 18 mm Plexiglas wall between the ultrasonic transducer and the target (plastic sphere) reduces the intensity of the ultrasonic burst emitted by the 2, 4 or 8 MHz ultrasonic transducer as given in Table 4-3:

Table 4-3: Reduction in Acoustic Intensity Due to Plexiglas Walls

		2.5 mm Thick Plexiglas Wall	18 mm Thick Plexiglas Wall
2 MHz	Intensity Reflected at Plexiglas Boundaries	45 %	45 %
	Intensity Absorbed in Plexiglas	36.9 %	96.4 %
	Intensity Reduction General	65.3 %	97.9 %
4 MHz	Intensity Reflected at Plexiglas Boundaries	45 %	45 %
	Intensity Absorbed in Plexiglas	60.2 %	99.9 %
	Intensity Reduction General	78.1 %	99 %
8 MHz	Intensity Reflected at Plexiglas Boundaries	45 %	45 %
	Intensity Absorbed in Plexiglas	84.2 %	99.9 %
	Intensity Reduction General	91.3 %	99 %

Since the absorption coefficient of water is small (0.2 percent of the absorption coefficient of Plexiglas), its effect will be neglected in this calculation. When dealing with much longer distances between transducer and plastic sphere than in this case, the absorption of ultrasound in water should be taken into account.

Comparing the calculated and measured intensity reduction, it can be seen that for relatively small frequencies (2 MHz), the calculated reduction is bigger than the measured reduction in echo intensity, especially for the thin Plexiglas wall. This can be explained by the fact, that for smaller frequencies and especially for thinner Plexiglas walls, the threshold of the formula used to calculate the transmission coefficient (Equation 18) is reached. The duration of the incident signal is then of the order of $2L/c_L$. If the duration of the incident signal is less than $2L/c_L$, in other words if the incident wave train is long compared to $2L$, Equation 21 should be used to calculate the transmission coefficient. Calculating the transmission coefficient with Equation 21 leads to a much smaller reduction in echo intensity for relatively small frequencies and thin Plexiglas walls. Using Equation 21 the following reduction in echo intensity can be calculated for the 2.5 mm thick Plexiglas wall: 46 percent for the 2 MHz transducer, 66 percent for the 4 MHz transducer and 86 percent for the 8 MHz transducer. These values better match the measurement results. The still slightly higher calculated than measured reduction in echo intensity can be explained by the effect of reflections of the Plexiglas wall from previous ultrasonic burst emissions that are received by the ultrasonic transducer without having completely propagated through the Plexiglas wall.

After having evaluated the effect on the ultrasonic beam shape and the echo intensity for each transducer introduced, the echo intensity and beam divergence plots are presented in Section 4.4.2 (Figures 4-18 to 4-33).

4.4.2 Echo Intensity and Beam Divergence Plots

Transducer 1:

18 mm Plexiglas Wall:
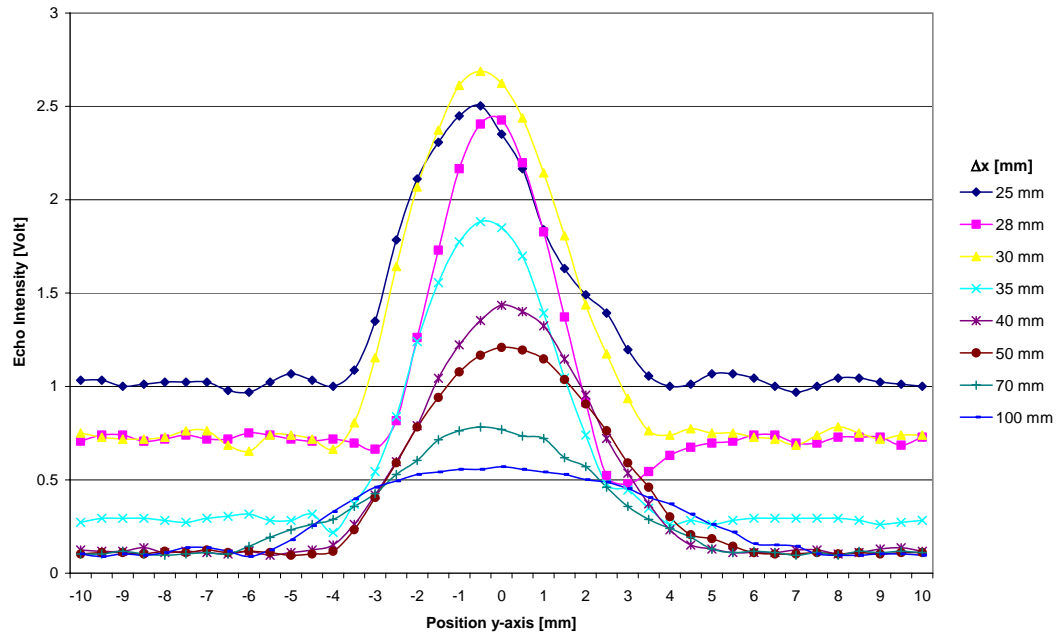
Figure 4-18: Echo Intensity 2 MHz 10 mm Transducer 18 mm Plexiglas Wall
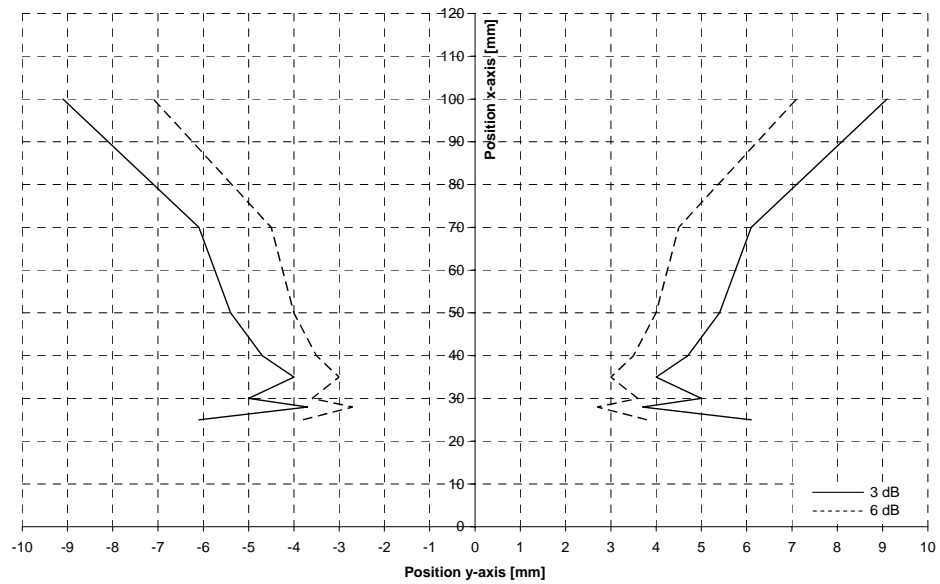
Figure 4-19: Divergence 2 MHz 10 mm Transducer 18 mm Plexiglas Wall

101

2.5 mm Plexiglas Wall:
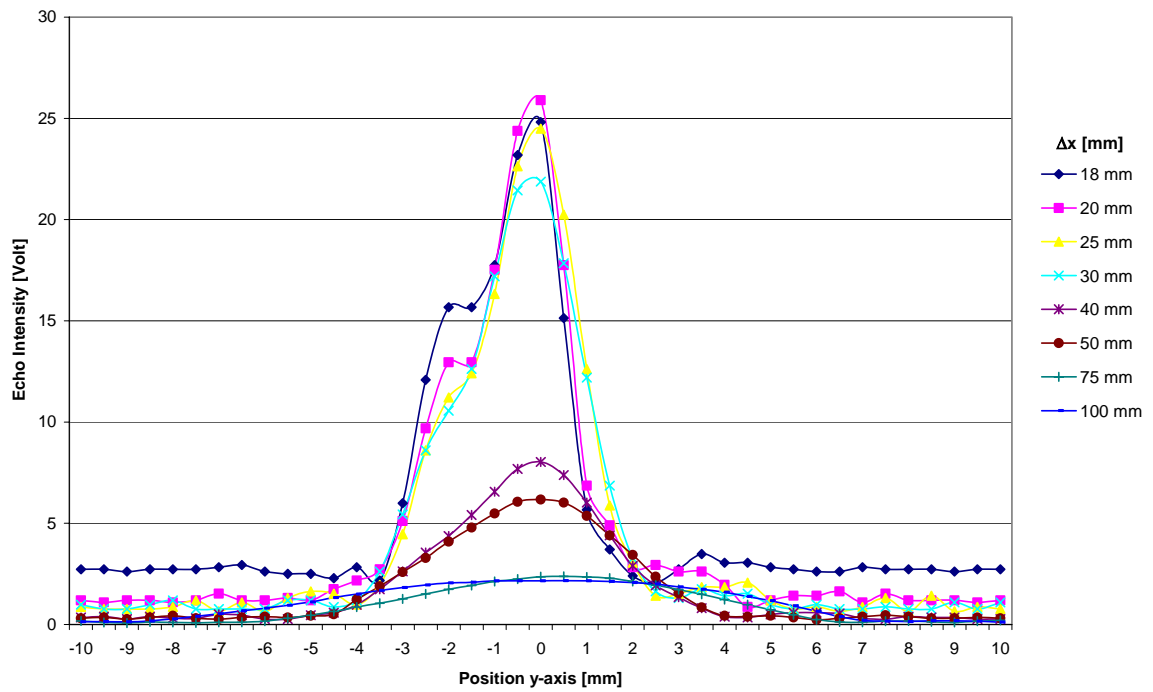
Figure 4-20: Echo Intensity 2 MHz 10 mm Transducer 2.5 mm Plexiglas Wall
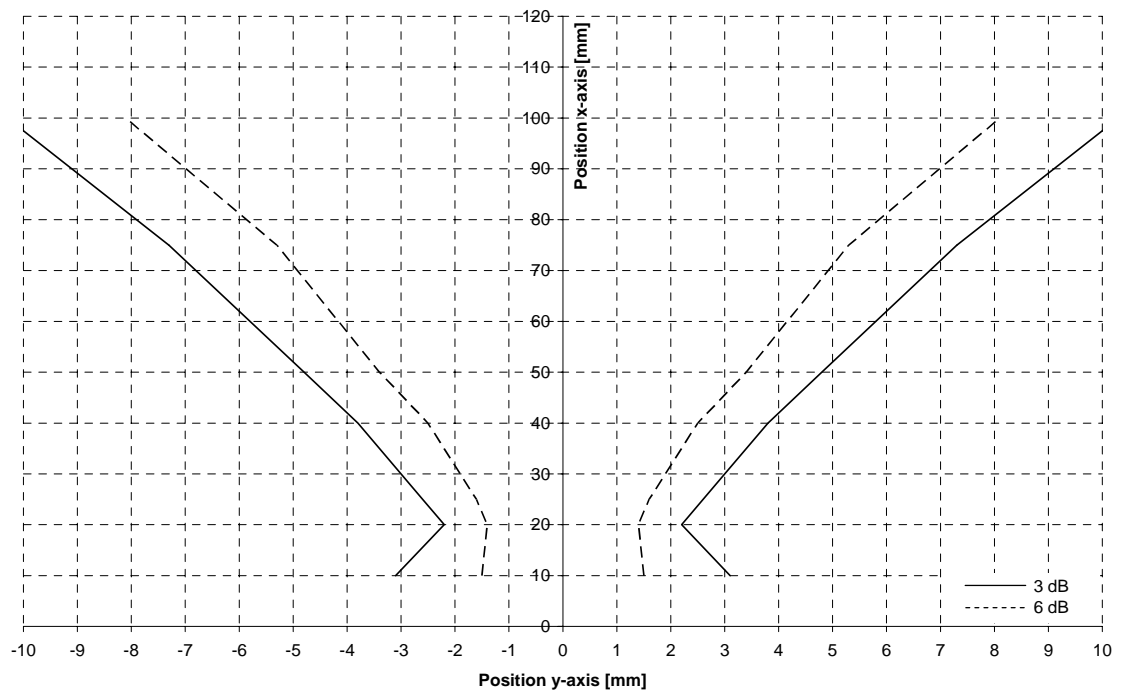
Figure 4-21: Divergence 2 MHz 10 mm Transducer 2.5 mm Plexiglas Wall

Transducer 2:

18 mm Plexiglas Wall:
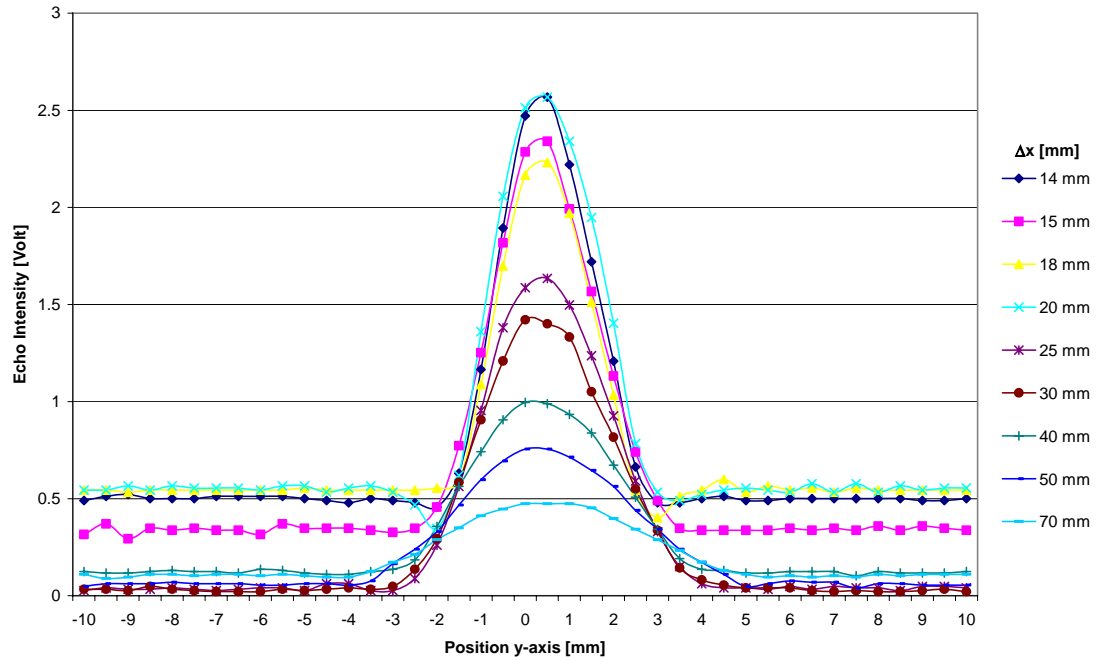
Figure 4-22: Echo Intensity 4 MHz 5 mm Transducer 18 mm Plexiglas Wall
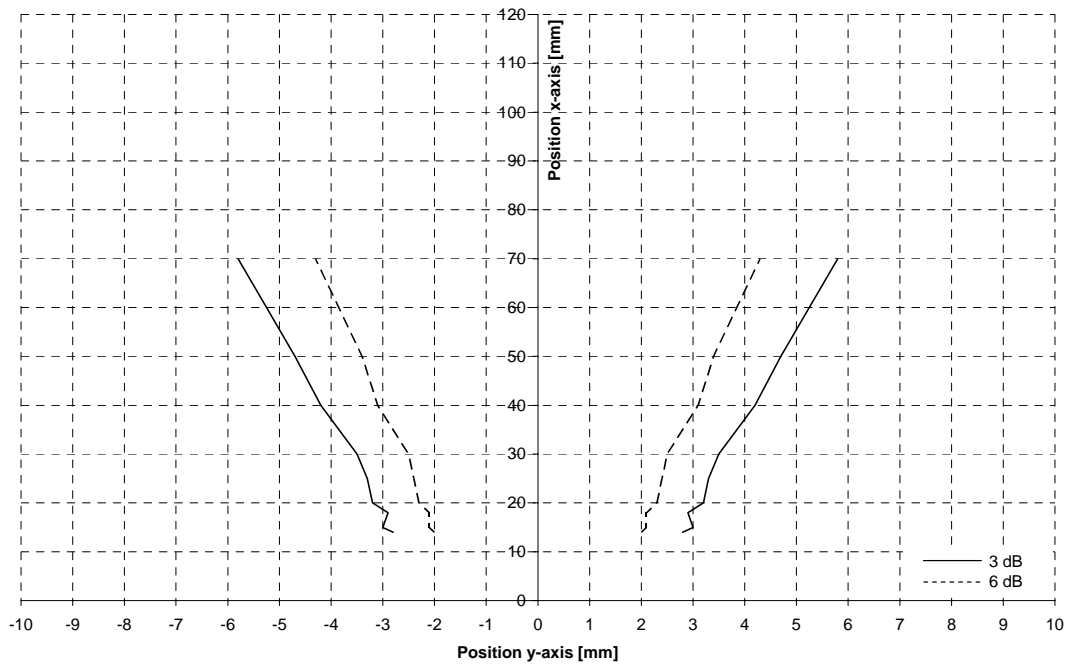
Figure 4-23: Divergence 4 MHz 5 mm Transducer 18 mm Plexiglas Wall

2.5 mm Plexiglas Wall:
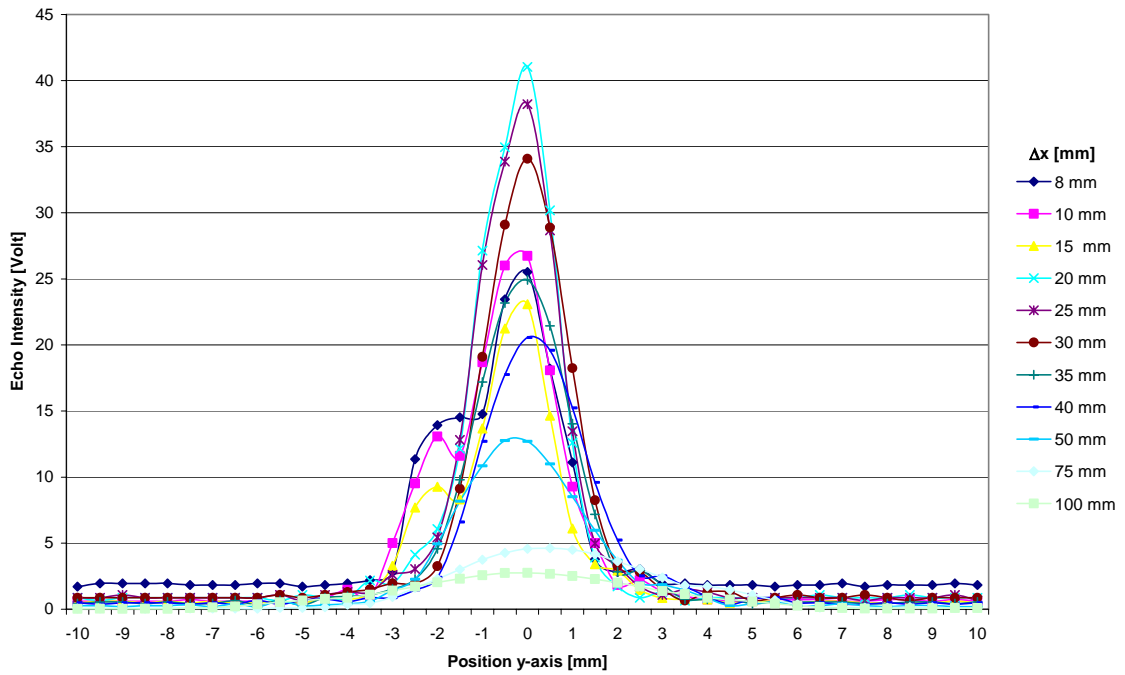
Figure 4-24: Echo Intensity 4 MHz 5 mm Transducer 2.5 mm Plexiglas Wall
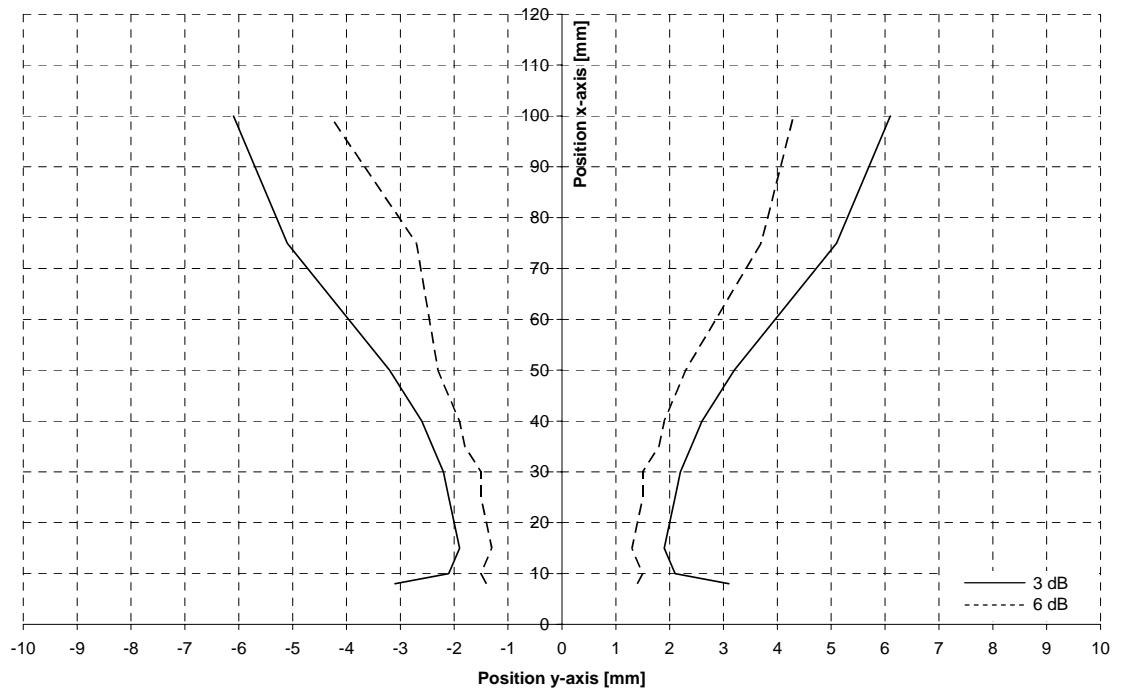
Figure 4-25: Divergence 4 MHz 5 mm Transducer 2.5 mm Plexiglas Wall

104

Transducer 3:

18 mm Plexiglas Wall:
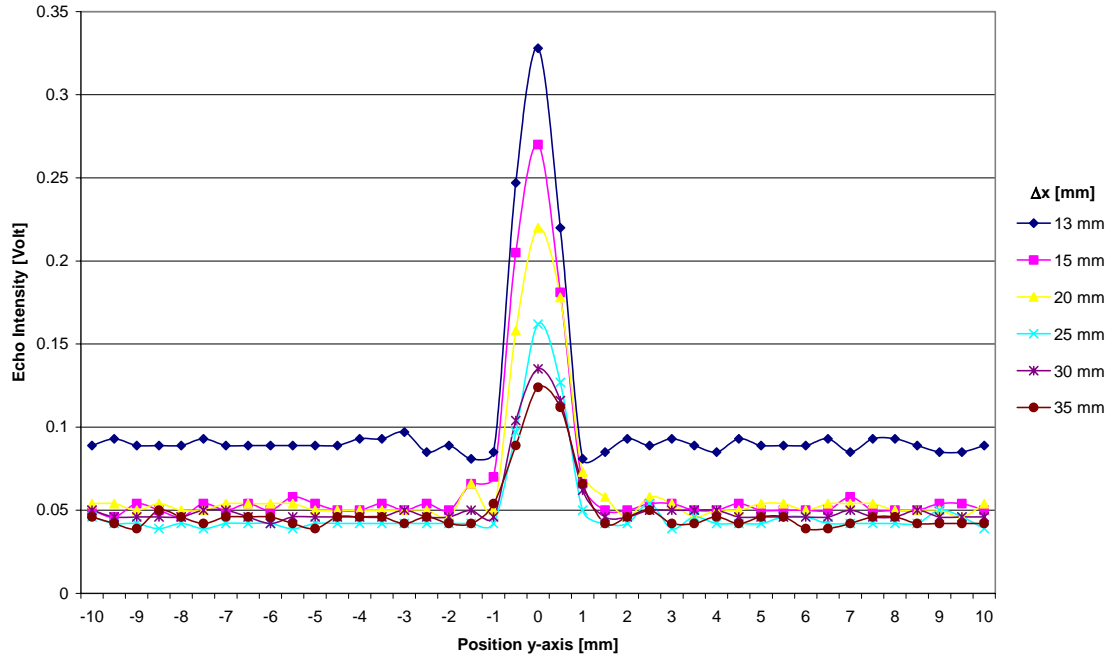
Figure 4-26: Echo Intensity 8 MHz 5 mm Transducer 18 mm Plexiglas Wall
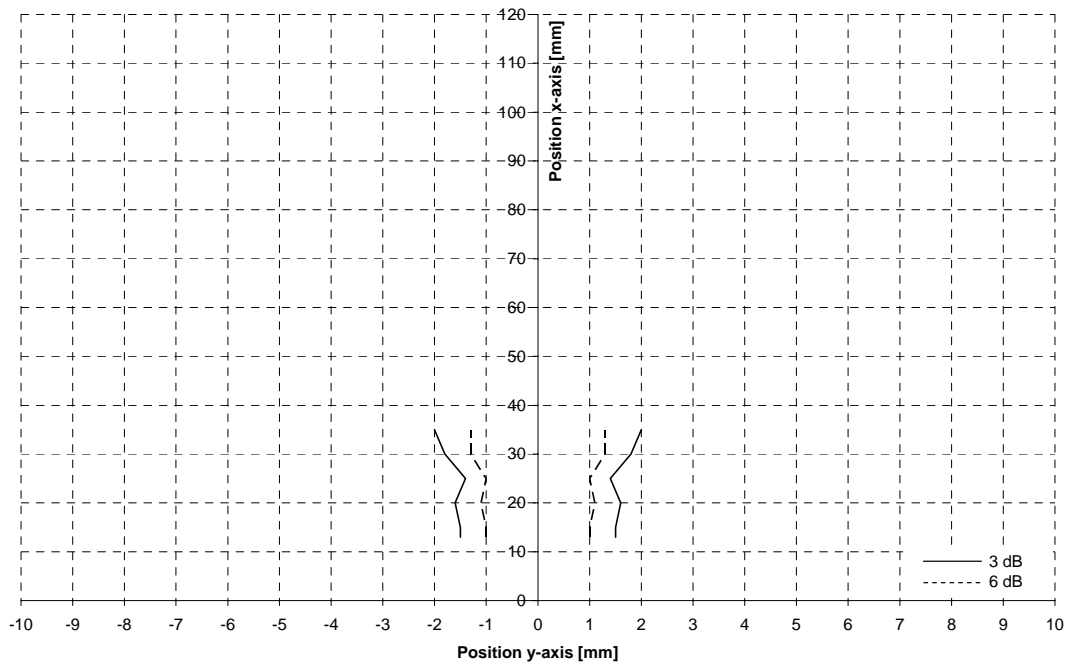
Figure 4-27: Divergence 8 MHz 5 mm Transducer 18 mm Plexiglas Wall
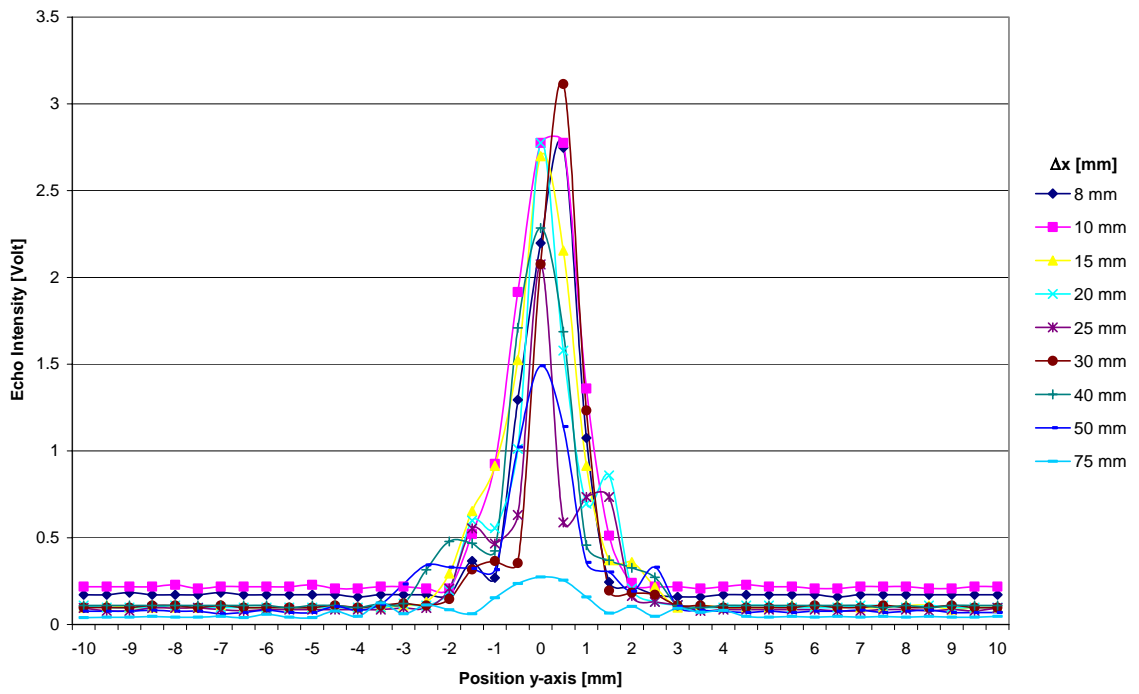
Figure 4-28: Echo Intensity 8 MHz 5 mm Transducer 2.5 mm Plexiglas Wall
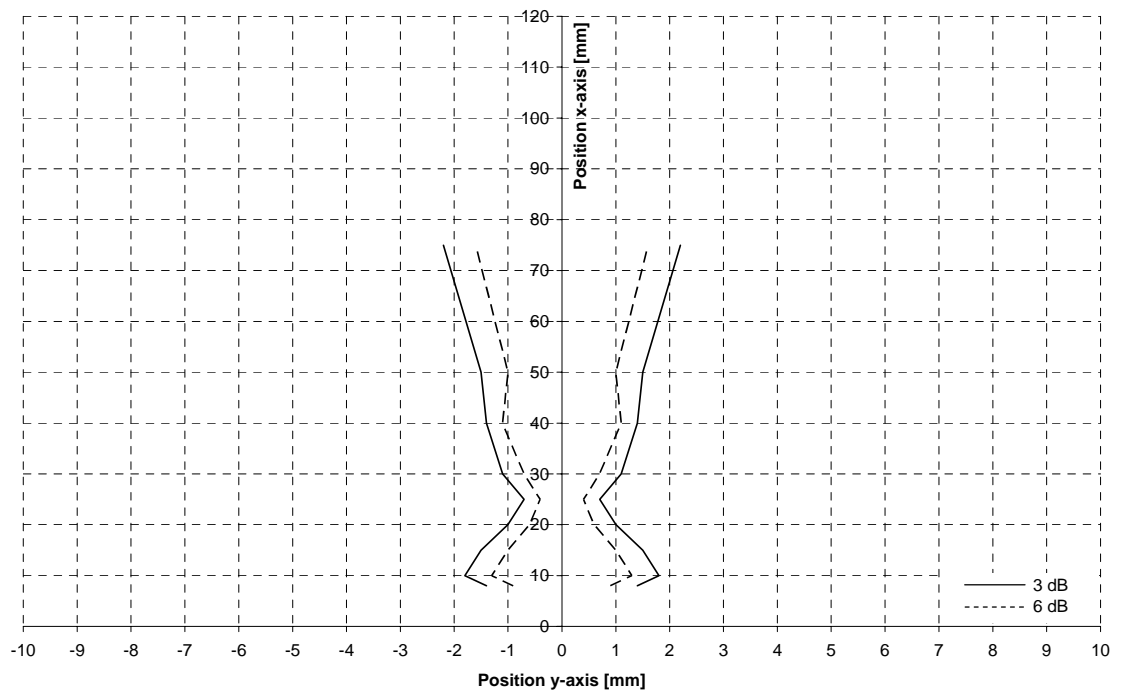
Figure 4-29: Divergence 8 MHz 5 mm Transducer 2.5 mm Plexiglas Wall

Transducer 4:

18 mm Plexiglas Wall:
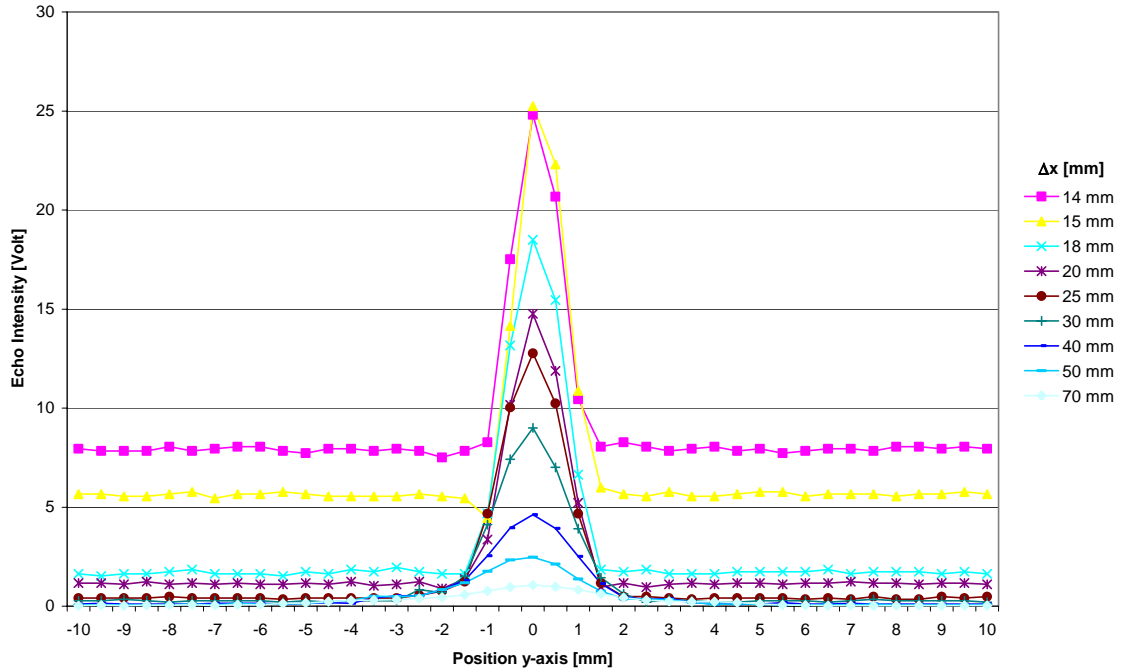
Figure 4-30: Echo Intensity 4 MHz Focussed Transducer 18 mm Plexiglas Wall
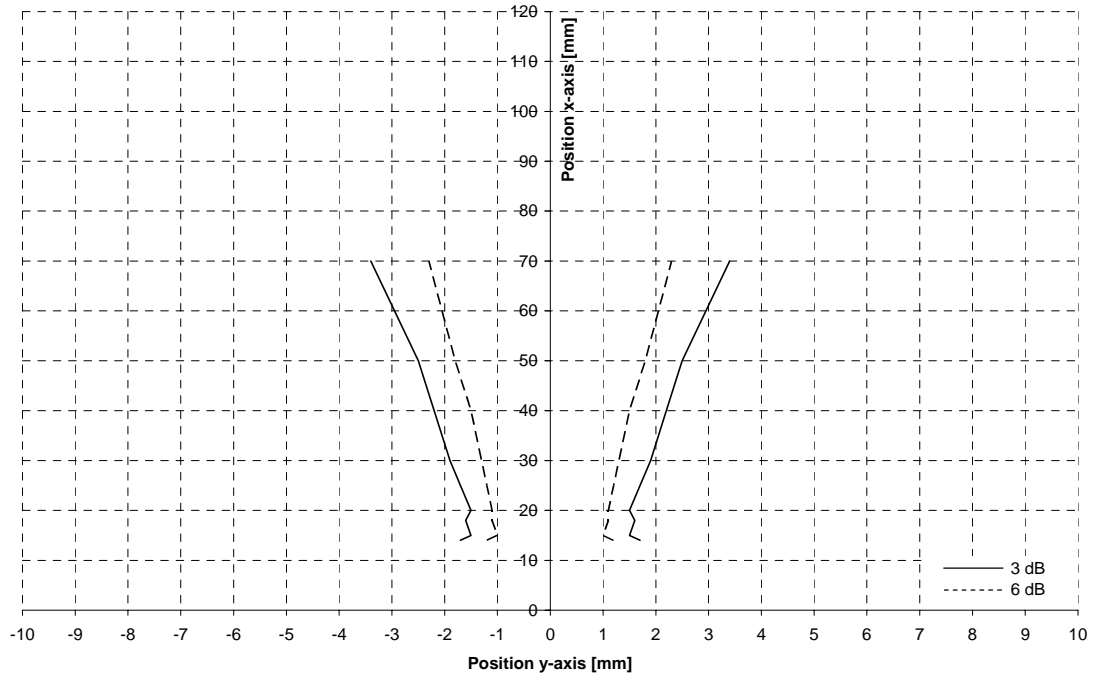
Figure 4-31: Divergence 4 MHz Focussed Transducer 18 mm Plexiglas Wall

2.5 mm Plexiglas Wall:
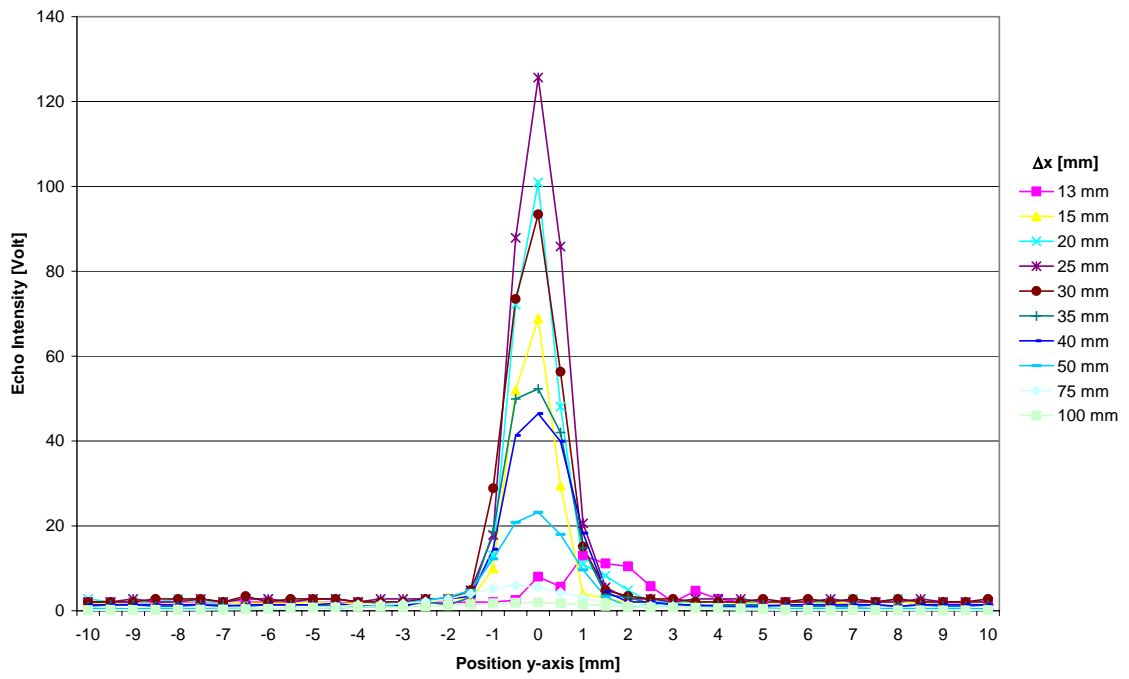
Figure 4-32: Echo Intensity 4 MHz Focussed Transducer 2.5 mm Plexiglas Wall
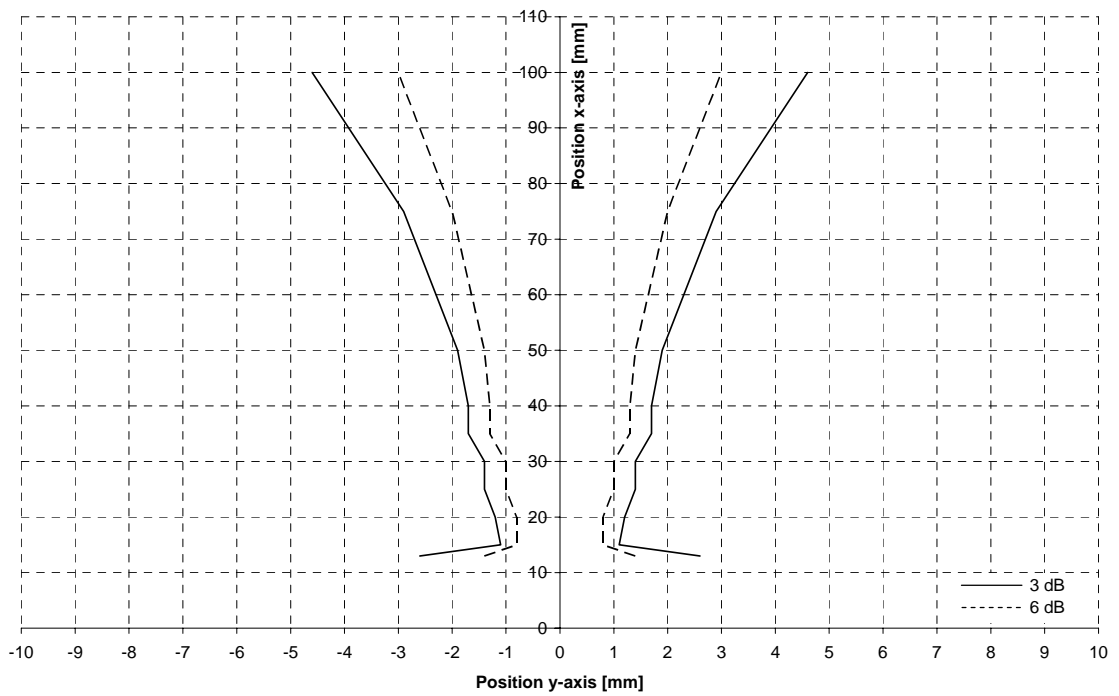
Figure 4-33: Divergence 4 MHz Focussed Transducer 2.5 mm Plexiglas Wall

4.5 Effect of Forming Screens

In industrial applications, the measurement of velocity profiles in the area close to porous forming screens is most important. Therefore, the distance from the forming screen to the plastic sphere at which the echo of the plastic sphere can still be recognized must be as small as possible. In evaluating the measurement results, emphasis is laid on finding the closest distance from the plastic sphere to the screen over the widest range of transducer-screen-distances (Δx) that produces detectable echoes of the plastic sphere behind the forming screen. The long term goal is to use pulsed ultrasound Doppler velocimetry to measure velocity profiles closely behind a forming screen. This is described in detail in Section 7.2.

To evaluate the effect of forming screens, the basic experimental setup is modified. A forming screen is placed between the ultrasonic transducer and the plastic sphere as shown in Figure 4-34.
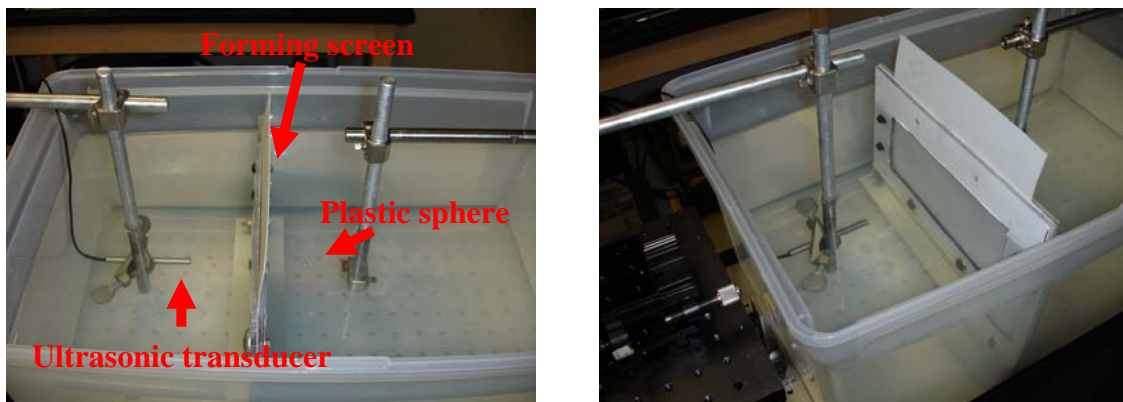
Figure 4-34: Experimental Setup Forming Screen

The following parameters of the forming screen sample have been identified:

- Material: Polyester
- Density Polyester: 1.35 g/cm^3 = 1350 kg/m^3
- Fiber volume: 0.38 cm^3

- Pore volume: 0.36 cm^3
- Porosity: 0.95
- Sample weight (in air):   0.57 g
- Sample weight (in water):   0.873
- Sample volume: 0.74 cm^3
- Apparent density (in air):   0.77 g/cm^3 = 770 kg/m^3
- Apparent density (in water):   1.18 g/cm^3 = 1180 kg/m^3
- Thickness: 0.022 in = 0.00056 m
- Mesh: 60 wires/inch = 2362 wires/meter
- Pore shape factor: 1 (cylindrical pores ≈ cubical pores)
- Double layer:
    i. Fiber diameter ply 1:   0.2 mm
    ii. Fiber diameter ply 2:   0.4 mm
- Specific flow resistance: 95.5 MKS Rayls
- Speed of Sound [13]: 1700 m/s

Figure 4-35 is a picture of the forming screen. The composition of the forming screen is shown in the microtomographic cross-section views in Figure 4-36 (4 µm resolution).

Figure 4-35: Forming Screen
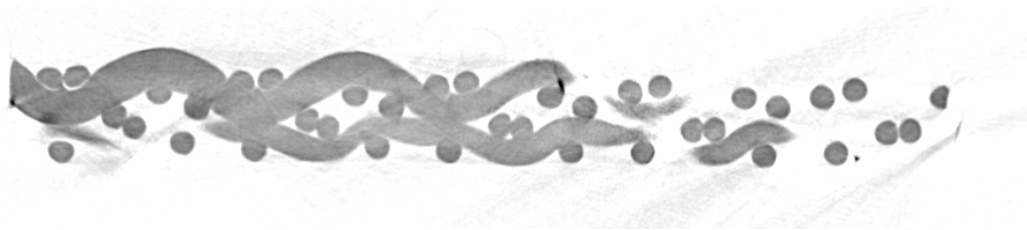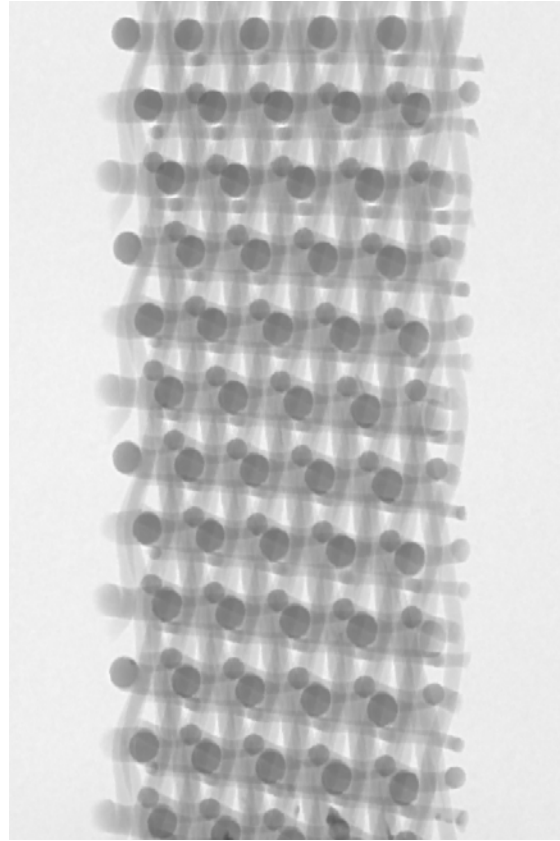
Figure 4-36: Microtomographic Cross-Section View Forming Screen

Varying the distance between the screen and the face of the ultrasonic transducer on the x-axis for each transducer, different measurements were performed. The effect of forming screen on the ultrasonic beam is evaluated in the following. Echo intensity plots and figures of the ultrasonic beam divergence are given in section 4.5.3 (Figure 4-38 to 4-59).

4.5.1 Evaluation of Results

Comparing the results of the ultrasonic beam shape measurements (with the forming screen) with the results given in chapter 4.3, it becomes obvious that placing the forming screen between the plastic sphere and transducer forces the echo intensity to decrease due to the absorption of the ultrasonic waves by the screen. When placing the forming screen

between the transducer and plastic sphere, the foremost effect seen is a sharp decrease in the intensity of the echo. For the 2 MHz 10 mm transducer, the decrease in the intensity of the echo is 60 percent when the screen is between the plastic sphere and the transducer. For the 4 MHz 5 mm transducer, the decrease in echo intensity is 85 percent, and with the 4 MHz 8 mm focused transducer, the decrease in the intensity of the echo is approximately 94 percent. The 8 MHz 5 mm transducer had a decrease of 98 percent in echo intensity. It can clearly be seen that the echo intensity decreases with increasing frequency since attenuation of acoustic waves increases with increasing frequency. Therefore, the 8 MHz 5 mm transducer did not yield useful results. The echo intensity decreases with increasing distance between the transducer and the screen. All measurements reveal a significant decrease in echo intensity when the forming screen is between the plastic sphere and transducer.

As the echo intensity decreases due to the presence of the forming screen, the gain of the system must be increased to achieve a measurable signal. As the gain of the system is increased, the ringing effect is also increased. This ringing effect causes the minimal measurable distance to increase.

Using the 2 MHz 10 mm transducer and placing it 20 mm away from the screen, the closest distance that the plastic sphere produced a detectable echo was when it was 28 mm away from the transducer (8 mm away from the screen). Placing the same transducer 40 mm away form the screen, the closest detectable distance of the plastic sphere was 46 mm away from the transducer (6 mm away from the screen). Placing the screen 60 mm away from the same transducer, the closest measurable distance from the screen was reduced to 4 mm (64 mm away from the transducer). Increasing the distance between the 2 MHz transducer to the screen to 80 mm, the closest measurable distance from screen was increased to 9 mm (89 mm away from the screen). Consequently, using the 2 MHz 10 mm transducer, the closest distance from the plastic sphere to screen that produced detectable echoes was 4 mm. It was achieved when the screen was placed 60 mm away from the transducer.

Using the 4 MHz 5 mm transducer and placing it 20 mm away from the screen, the closest distance that the plastic sphere produced a detectable echo was when it was 22 mm away from the transducer (2 mm away from the screen). Placing the same transducer

112

40 mm away form the screen, the closest detectable distance of the plastic sphere was 44 mm away from the transducer (4 mm away from the screen). Increasing the distance between the 4 MHz transducer to the screen to 60 mm, the closest distance that the pin produced a detectable echo was when it was 3 mm away from the screen (63 mm away from the transducer). Using the 4 MHz 5 mm transducer, the closest distance from the plastic sphere to the screen that produced detectable echoes was 2 mm.

The 8 MHz 5 mm transducer did not produce any detectable echoes at any distance away from the transducer and away from the screen. This is due to the increased attenuation of this high frequency transducer.

Using the 4 MHz 8 mm focused transducer and placing it 20 mm away from the screen, the closest distance that the plastic sphere produced a detectable echo was when it was 23 mm away from the transducer (3 mm away from the screen). Placing the same transducer 40 mm away form the screen, the closest detectable distance of the plastic sphere was 43 mm away from the probe (3 mm away from the screen). Increasing the distance between the 4 MHz transducer to the screen to 60 mm, the closest distance that the plastic sphere produced a detectable echo was when it was 4 mm away from the screen (64 mm away from the probe). Using the 4 MHz 8 mm focused transducer, the closest distance from the plastic sphere to the screen that produced detectable echoes was 3 mm.

The closest distance from the plastic sphere to the screen over the widest range of transducer-screen-distances that produced detectable echoes was achieved with the 4 MHz transducer. The 4 MHz transducer turned out to represent a good tradeoff between the high attenuation of the 8 MHz transducer and the low resolution (measurable depth and velocity) of the 2 MHz transducer. Keeping in mind the simplicity of the experimental setup, the 2 mm distance from the plastic sphere to the screen could possibly be further decreased using a more sophisticated setup.

The shape of the beam of the ultrasonic transducer changes when the screen is inserted in the field. When the screen is in place between the plastic sphere and the transducer, the beam seems to have two distinct regions. The "near screen field" is the region on the opposite side of the screen from the transducer, which is approximately 20-40 mm in length for the 2 MHz transducer and 20 mm in length for both of the 4 MHz transducers. The "far screen field" is the region that is on the opposite side of the screen as the

transducer and is past the "near screen field" (> 40 mm for the 2 MHz transducer and > 20 mm for the 4 MHz transducers). In all cases, the beam shape and width in the far screen field are very close to the same with and without the screen as shown in Figure 4-37.
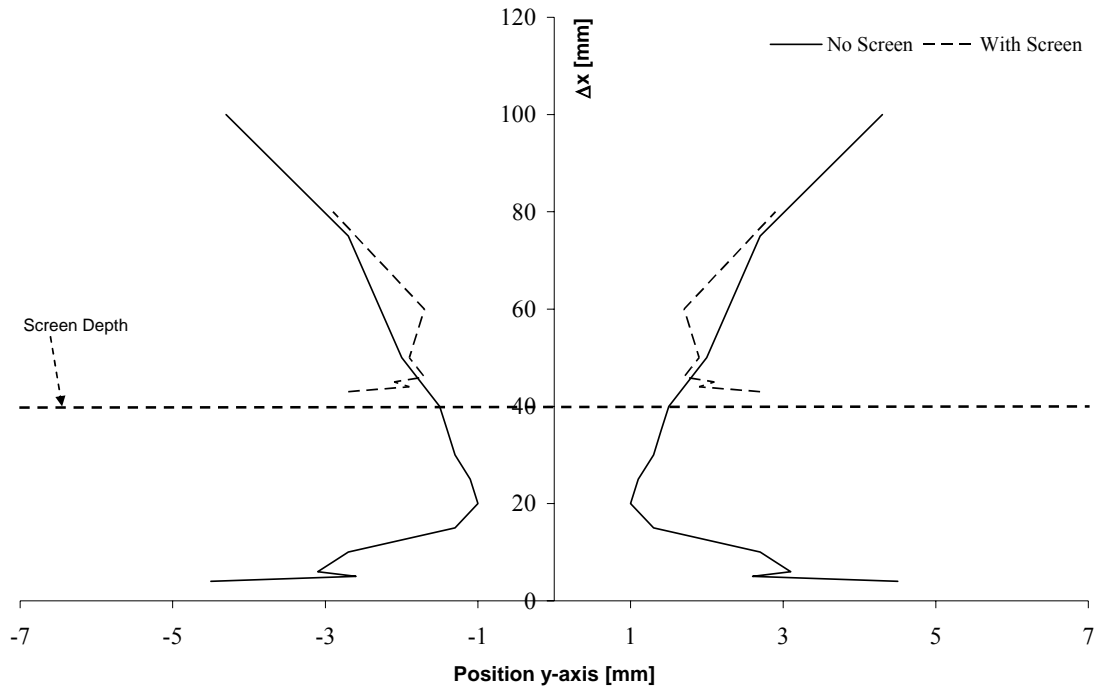
Figure 4-37: 4 MHz Focused Transducer With/Without Screen at 40 mm (6 dB)

In the near screen field, there is a common trend of beam convergence (narrowing of beam width) followed by beam divergence (widening of the beam width) as the beam gets closer to the far screen field (Figure 2-1). The beam width in the near screen field is generally slightly smaller (no more than 2 mm) than the beam width when the screen is not present (Figure 2-1). For the 4 MHz 8 mm focused transducer, the focal point without the screen is at 20 mm, but with the screen placed 20 mm away from the transducer, the focal point shifts back approximately 10 mm. This does not happen when the screen is at any other position that was tested with the 4 MHz focused transducer. Since the far screen field beam width and shape are very similar with and without the screen present, the angle of divergence for the transducers is similar in both cases. With the screen in place, the beam shape changes dramatically with different transducers so that the trends are different for different transducers at different screen depths.

114

4.5.2 Effect of the Forming Screen on the Echo Intensity

To calculate the frequency dependent absorption of acoustic energy due to the forming screen and compare this reduction of echo intensity to the reduction of echo intensity due to the Plexiglas wall, the acoustic impedance and consequently the transmission coefficient of the porous forming must be determined.

Different approaches were used to calculate the acoustic impedance of porous forming screens. As a first approximation, the measured apparent density of 1.18 g/cm^3 of the forming screen sample (described in section 4.5) and the sound speed of 1700 m/s measured by Brodeur [13] were multiplied to get a vague value of the acoustic impedance. Consequently the order of magnitude of the acoustic impedance is 2 x 10^6 MKS Rayls.

In order to predict the acoustic impedance of the forming screen more accurately, the Delany-Bazley-model, a fundamental model in the area of sound propagation in fibrous materials, and the Allard-Champoux-model, new expressions that can be used instead of the phenomenological equations of Delany and Bazley, were used. Using the Delany-Bazley-model an acoustic impedance which is approximately the same magnitude as the acoustic impedance of water was predicted. This would lead to a transmission coefficient of nearly 100 %, which is simply not realistic. The Allard-Champouc-model did not yield useful results as well. Especially the high porosity of the forming screen and the pore saturation with water instead of air may be the reason why both models do not yield useful results. As a reference, both models and the results are described in Appendix J.

For now, it is not possible to predict the acoustic impedance with adequate accuracy. Therefore, the reduction in echo intensity caused by placing a forming screen between the ultrasonic transducer and the target is not calculated. The evaluation of the echo intensity reduction is therefore solely based on the measurement results given above.

4.5.3 Echo Intensity and Beam Divergence Plots

Transducer 1:

Screen at x = 20 mm:
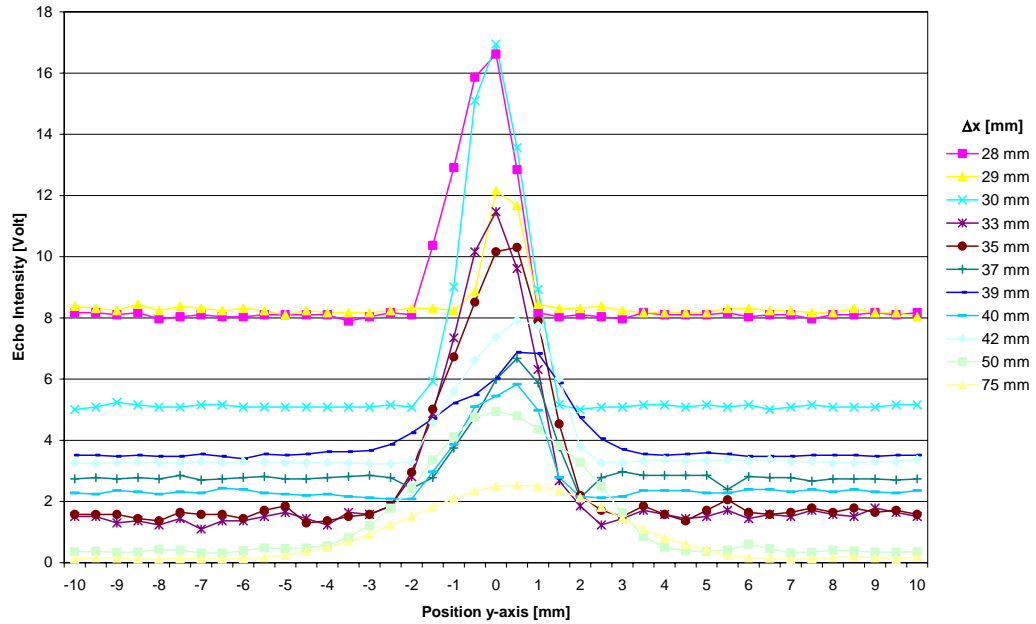
Figure 4-38: Echo Intensity 2 MHz 10 mm Transducer With Screen at x = 20 mm
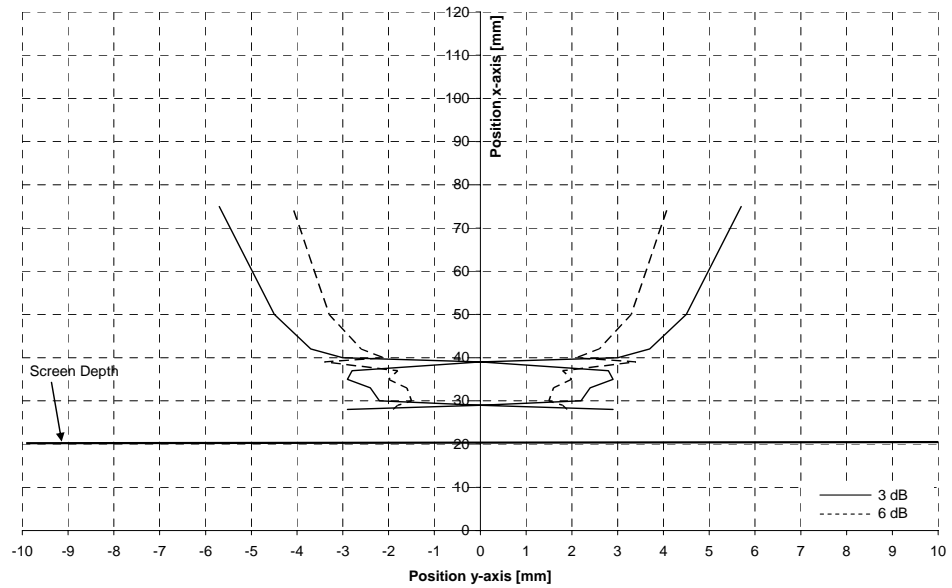
Figure 4-39: Divergence 2 MHz 10 mm Transducer With Screen at x = 20 mm

116
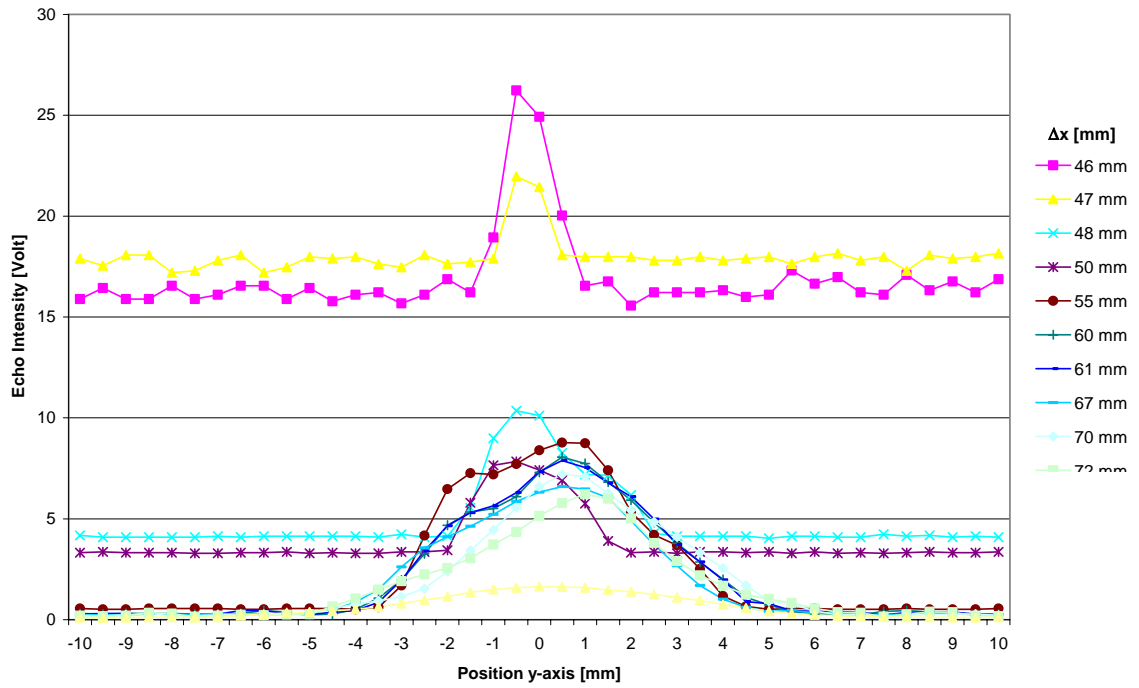
Screen at x = 40 mm:

Figure 4-40: Echo Intensity 2 MHz 10 mm Transducer With Screen at x = 40 mm
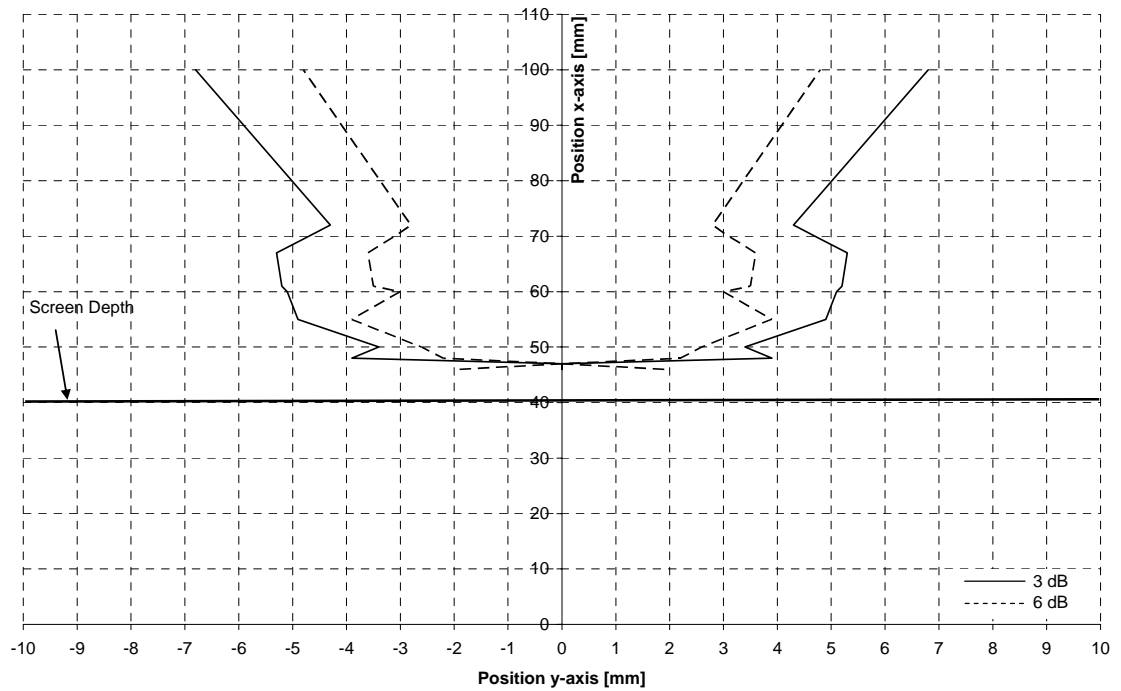
Figure 4-41: Divergence 2 MHz 10 mm Transducer With Screen at x = 40 mm

Figure 4-42: Echo Intensity 2 MHz 10 mm Transducer With Screen at x = 60 mm
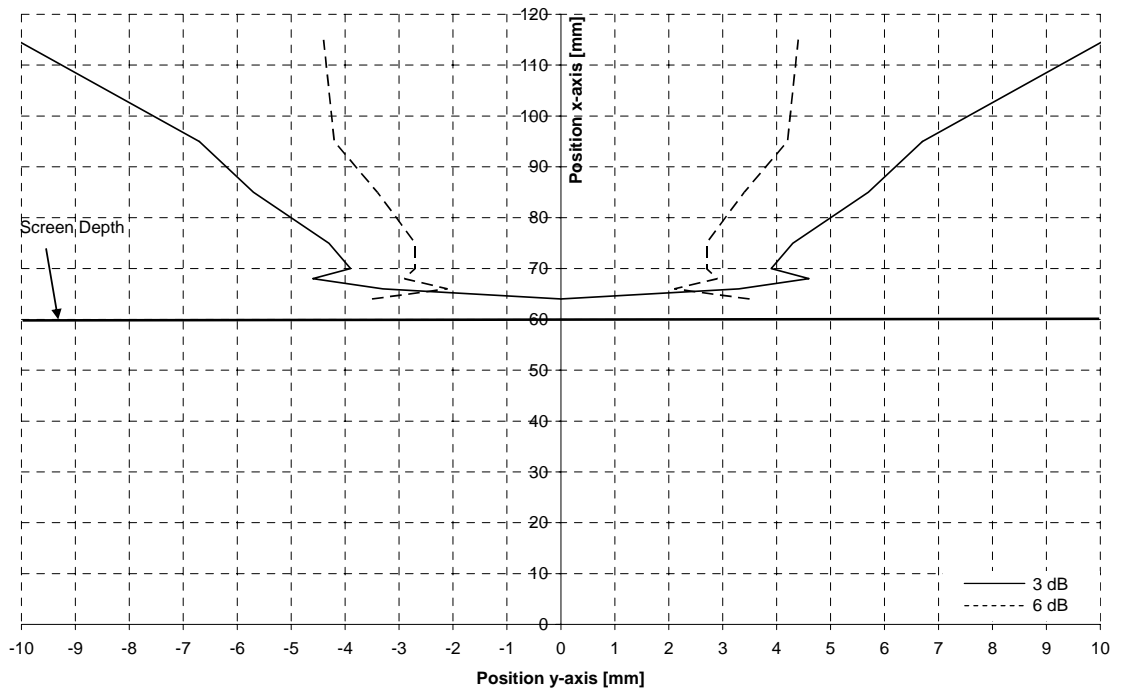
Figure 4-43: Divergence 2 MHz 10 mm Transducer With Screen at x = 60 mm

Screen at x = 80 mm:
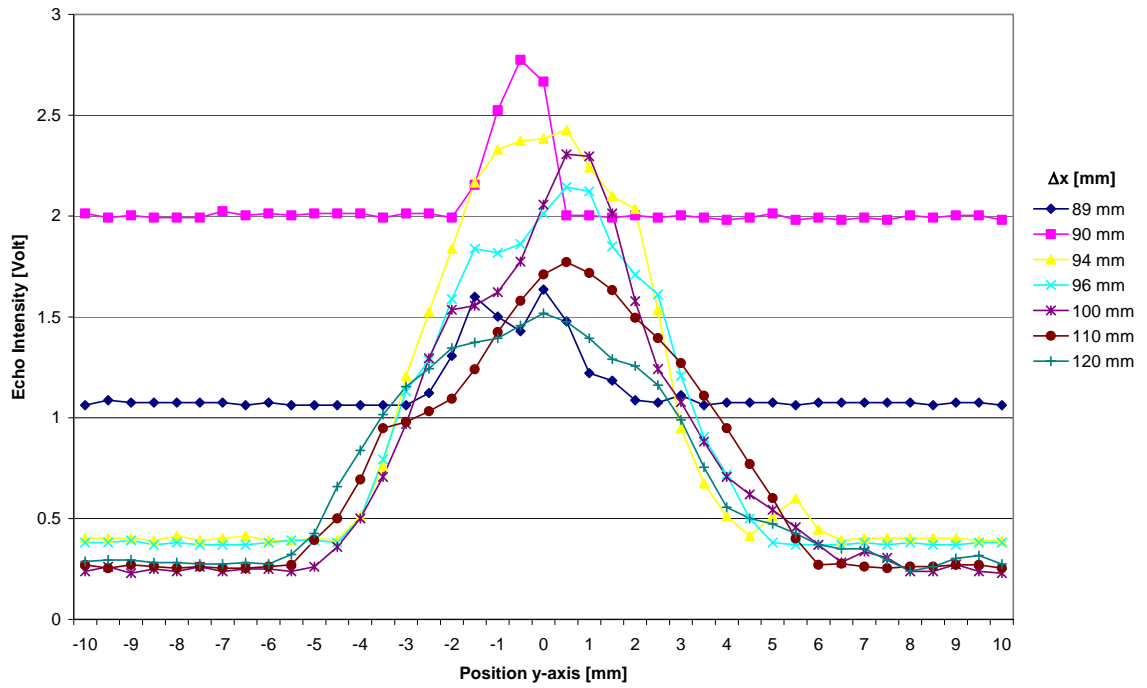
Figure 4-44: Echo Intensity 2 MHz 10 mm Transducer With Screen at x = 80 mm
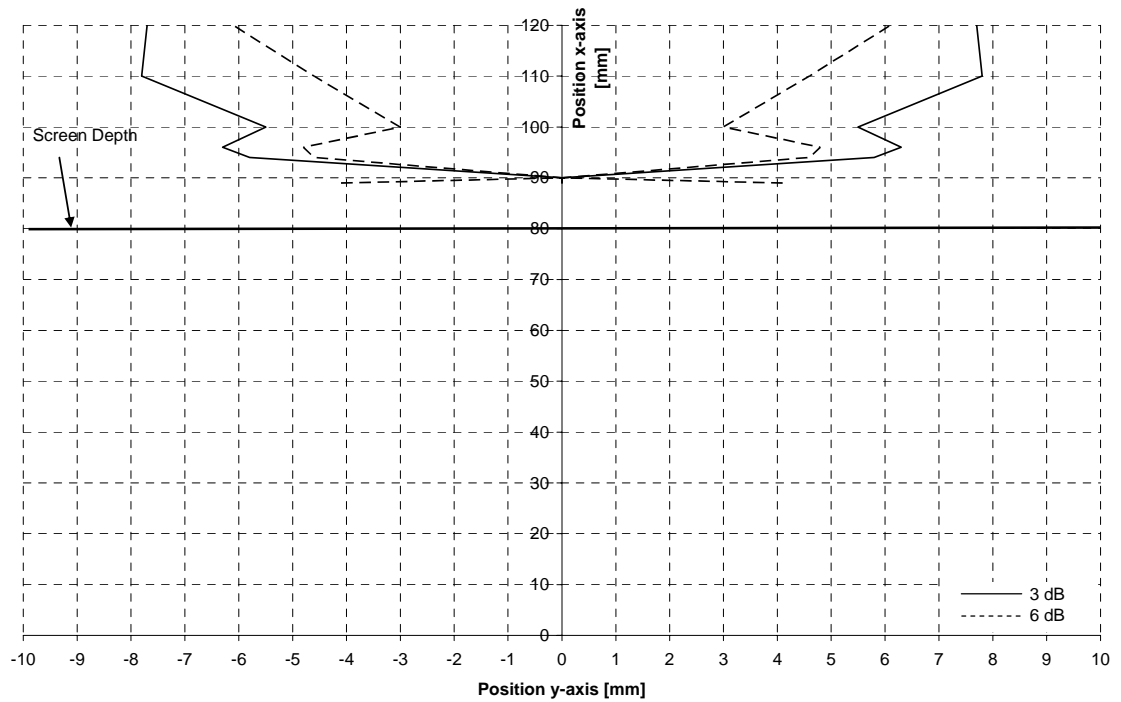
Figure 4-45: Divergence 2 MHz 10 mm Transducer With Screen at x = 80 mm

119

Transducer 2:

Screen at x = 20 mm:
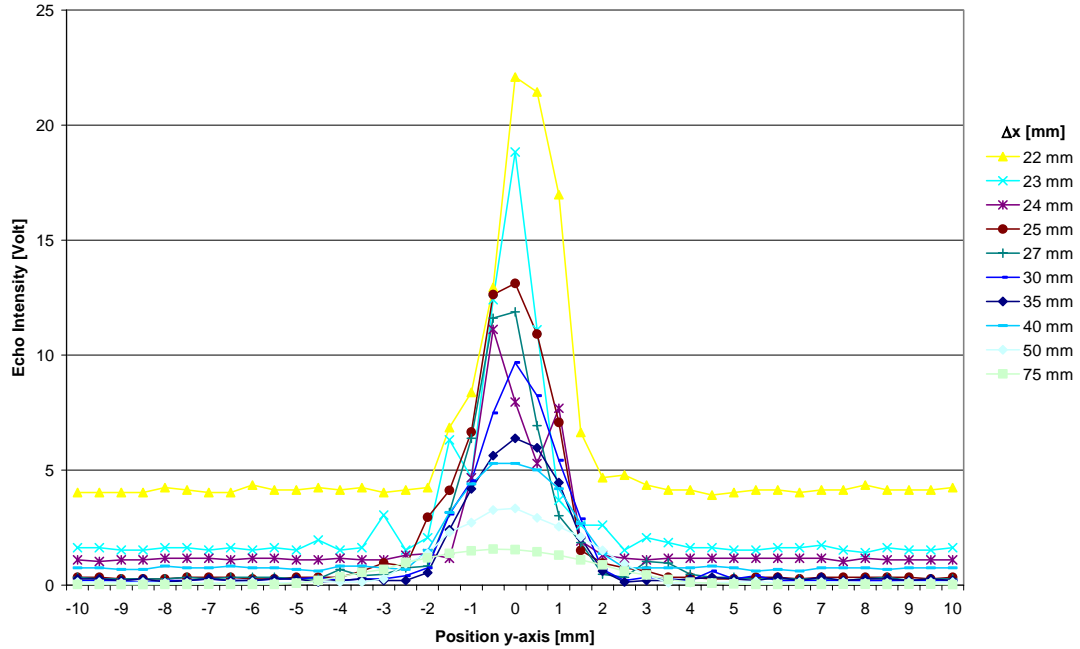
Figure 4-46: Echo Intensity 4 MHz 5 mm Transducer With Screen at x = 20 mm
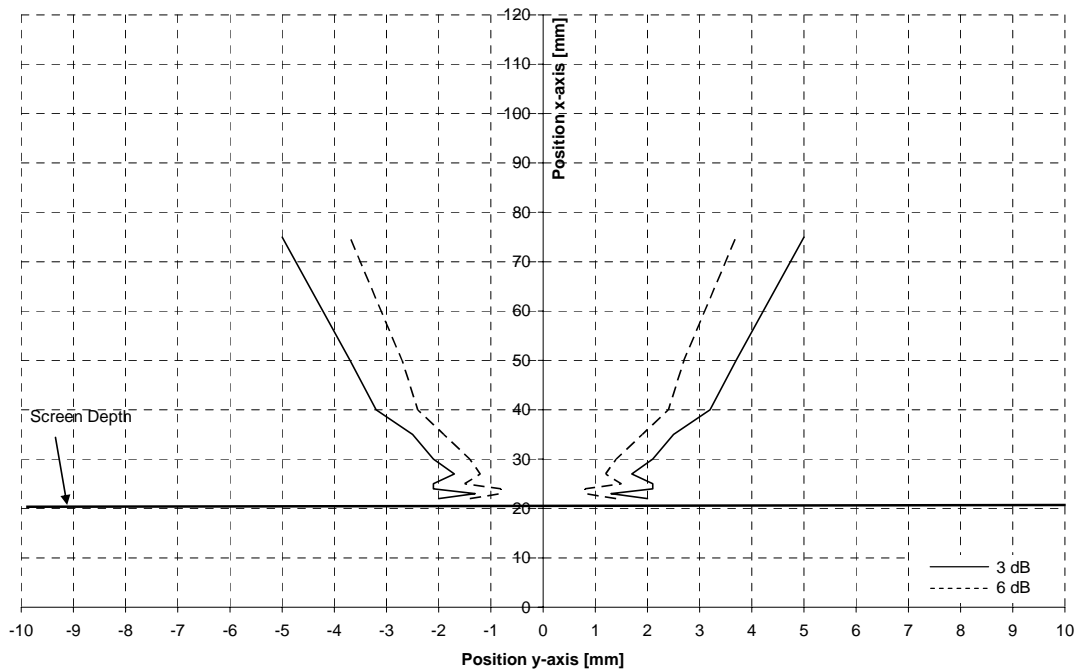
Figure 4-47: Divergence 4 MHz 5 mm Transducer With Screen at x = 20 mm
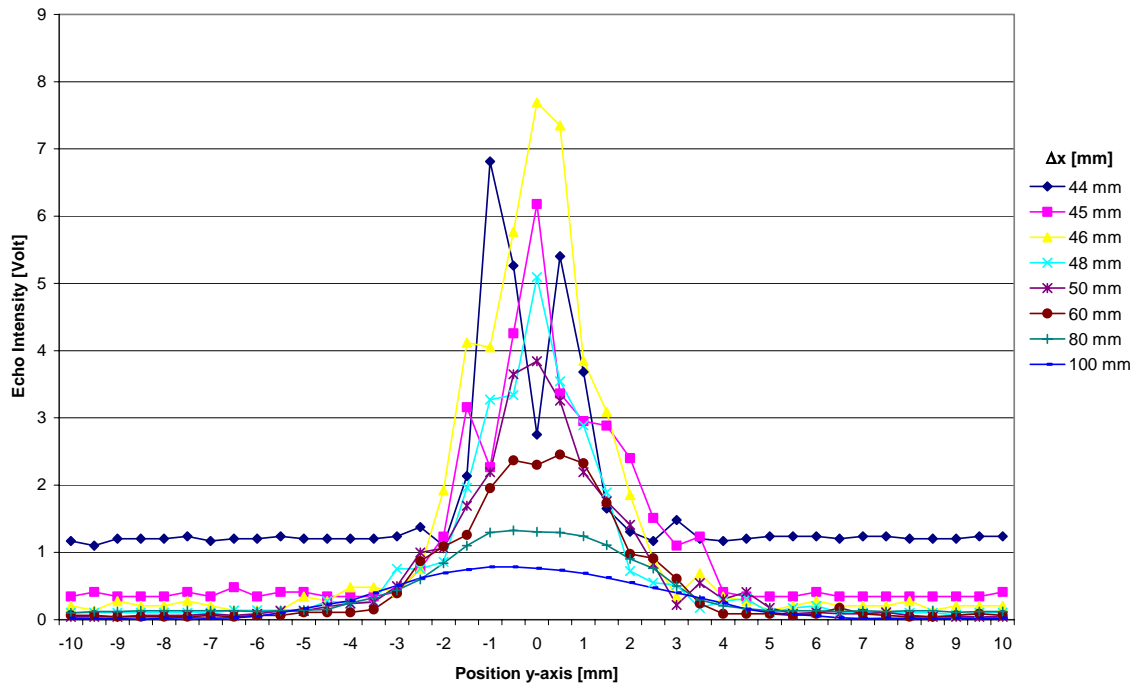
Screen at x = 40 mm:

Figure 4-48: Echo Intensity 4 MHz 5 mm Transducer With Screen at x = 40 mm
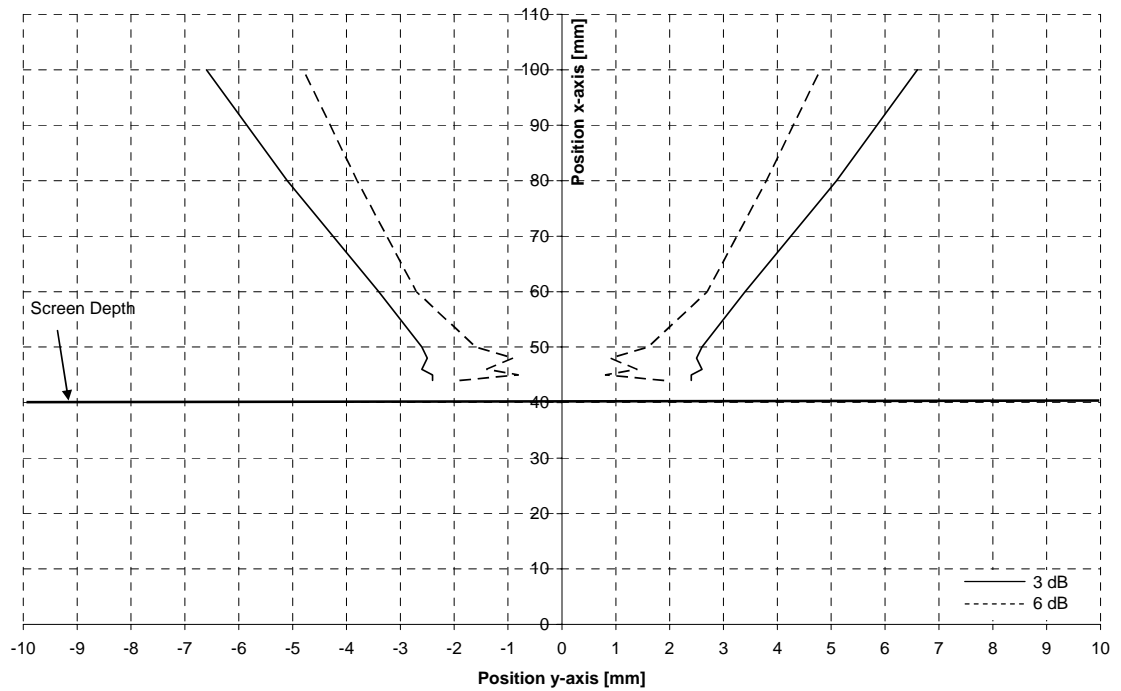
Figure 4-49: Divergence 4 MHz 5 mm Transducer With Screen at x = 40 mm

121

Screen at x = 60 mm:

Figure 4-50: Echo Intensity 4 MHz 5 mm Transducer With Screen at x = 60 mm
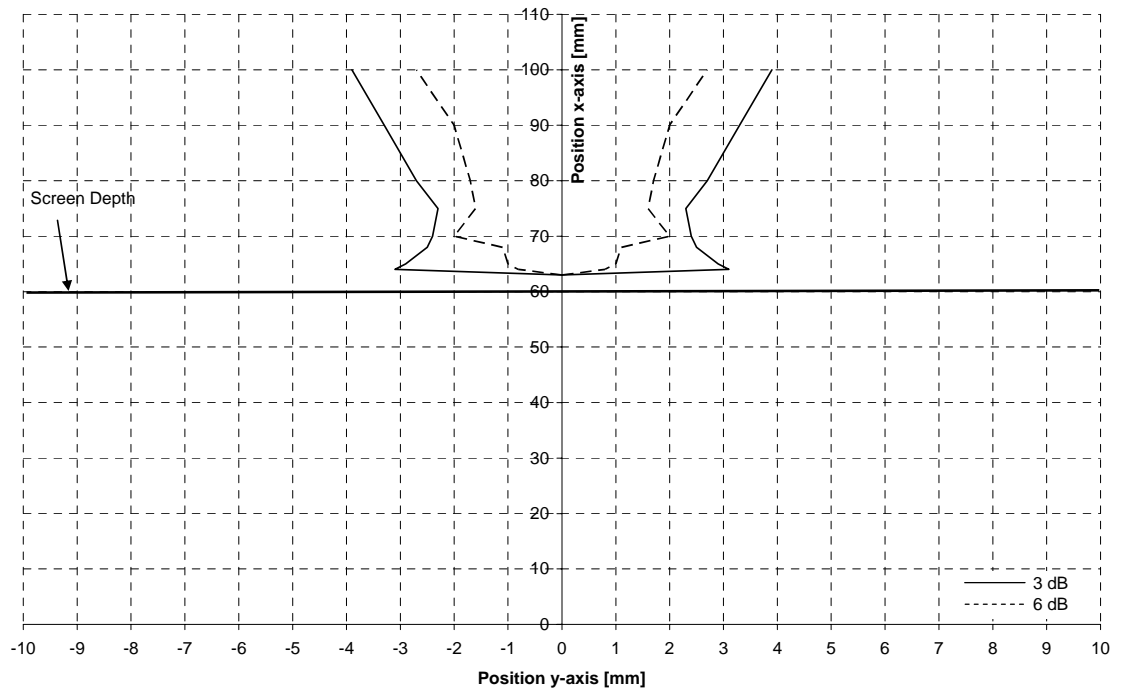
Figure 4-51: Divergence 4 MHz 5 mm Transducer With Screen at x = 60 mm

Transducer 3:

Using the 8 MHz 5 mm transducer, the ultrasonic echo of the plastic sphere behind the forming screen could not be recognized. Due to high absorption, useful results could not be obtained for this transducer.
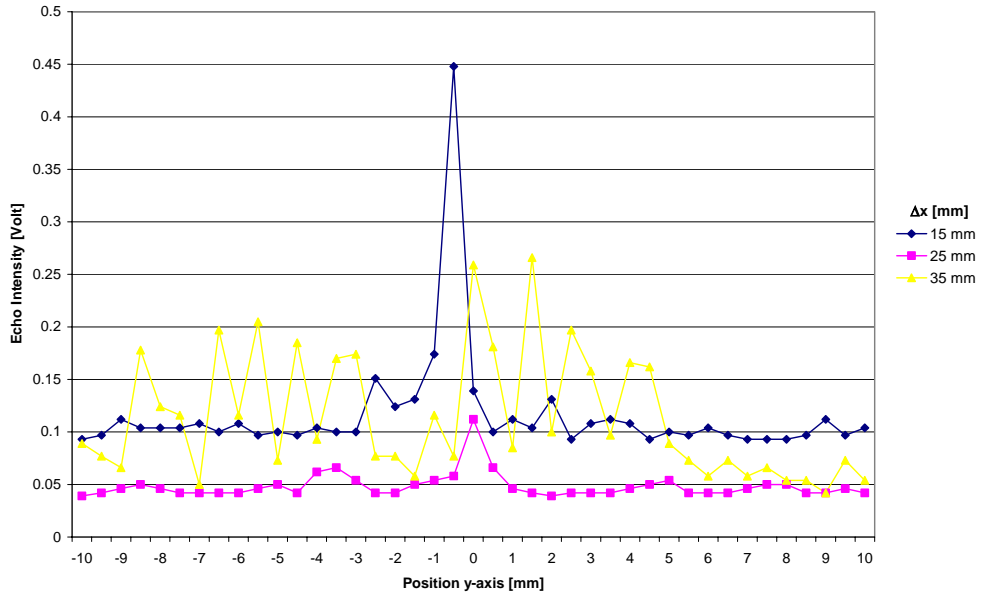
Figure 4-52: Echo Intensity 8 MHz 5 mm Transducer With Screen at x = 10 mm
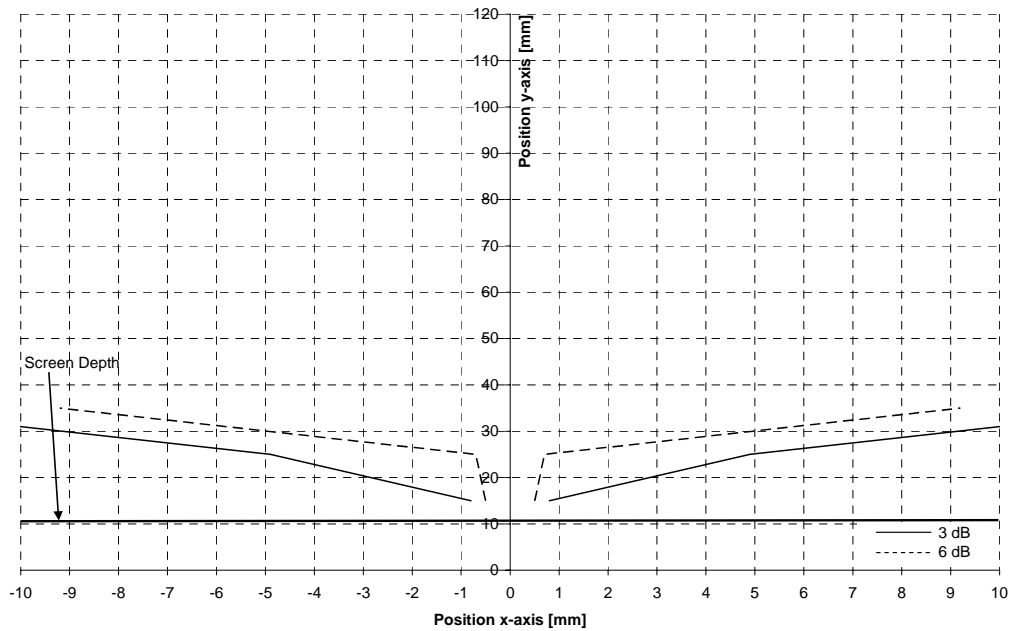
Figure 4-53: Divergence 8 MHz 5 mm Transducer With Screen at x = 10 mm

Transducer 4:

Screen at x = 20 mm:
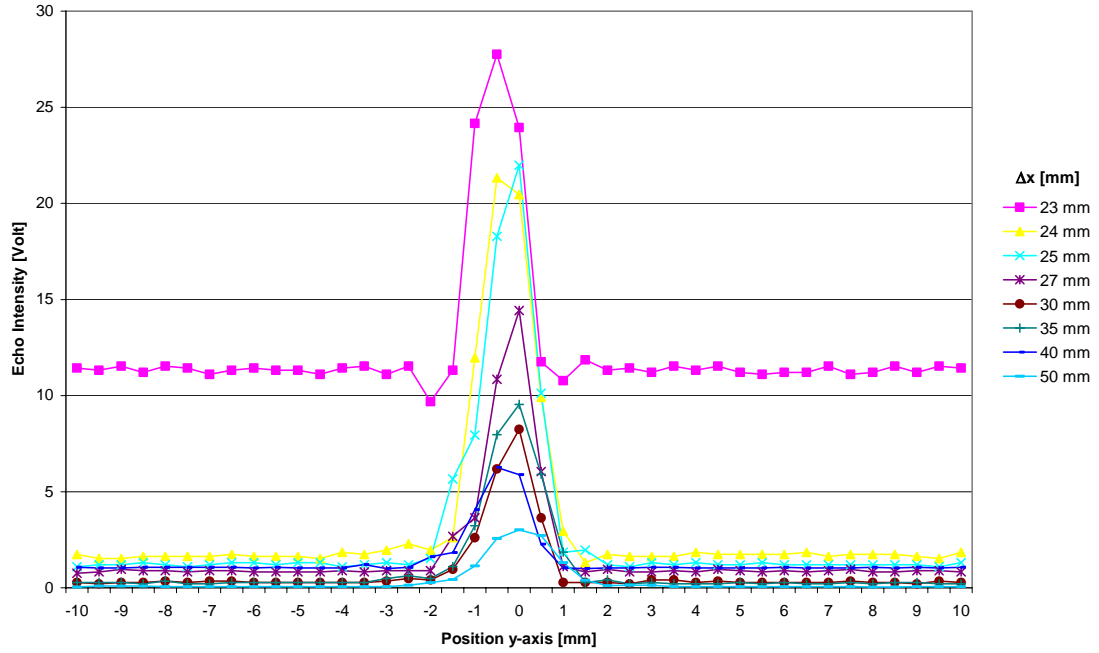
Figure 4-54: Echo Intensity 4 MHz Focussed Transducer With Screen x = 20 mm
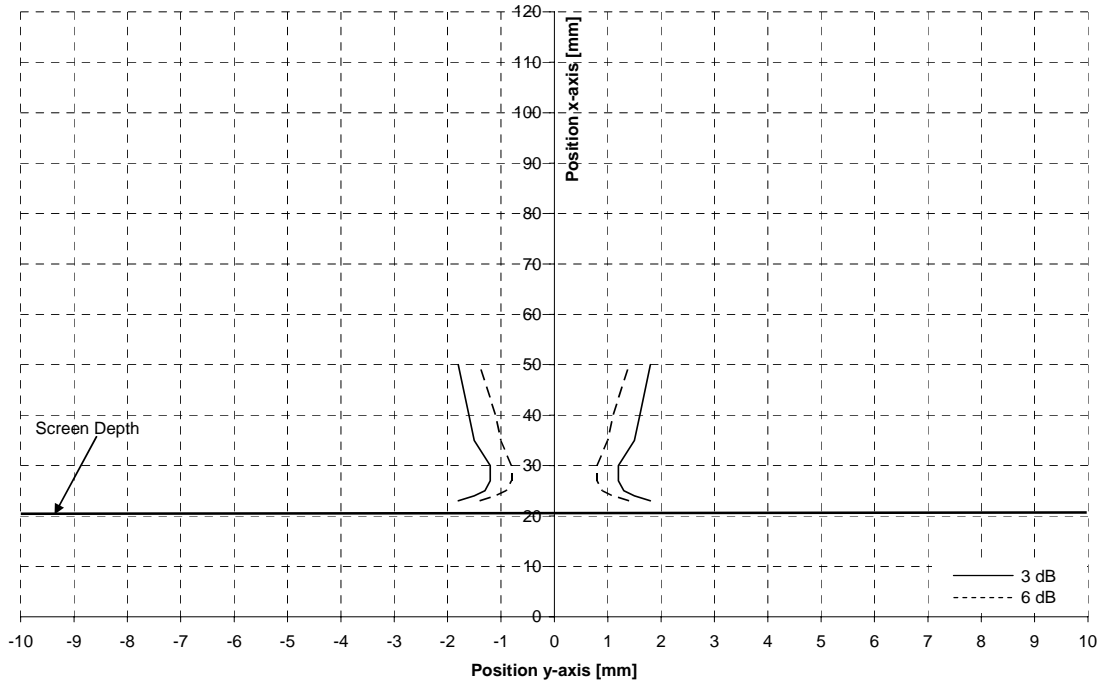
Figure 4-55: Divergence 4 MHz Focussed Transducer With Screen at x = 20 mm
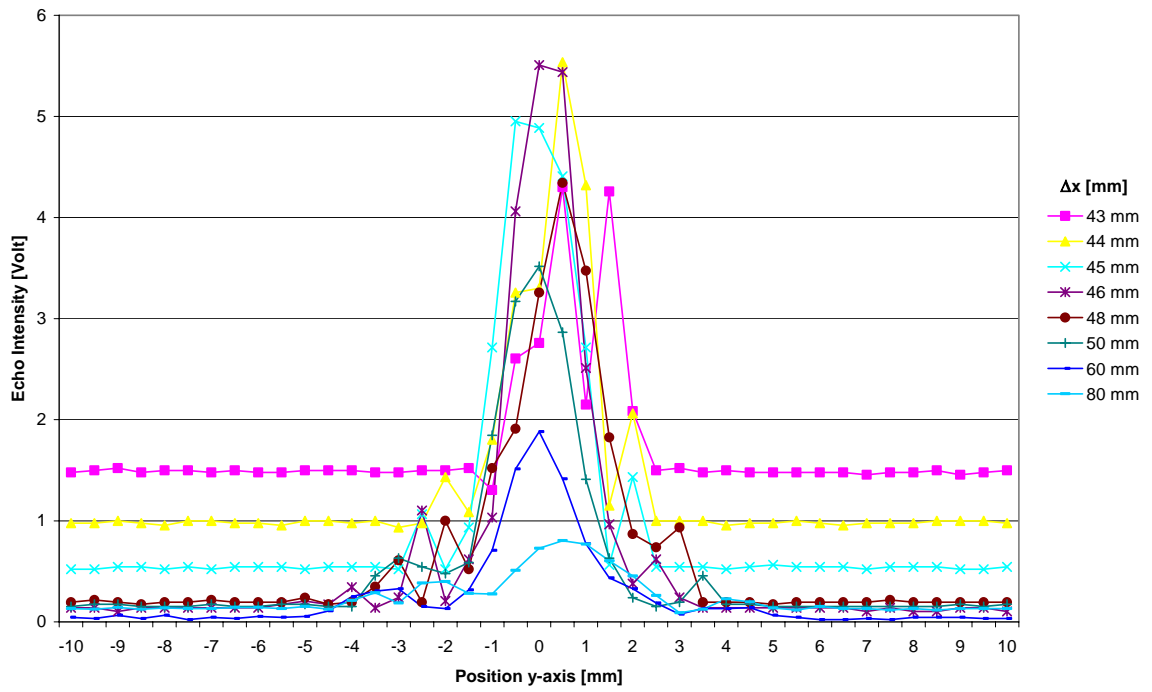
Screen at x = 40 mm:

Figure 4-56: Echo Intensity 4 MHz Focussed Transducer With Screen at x = 40 mm
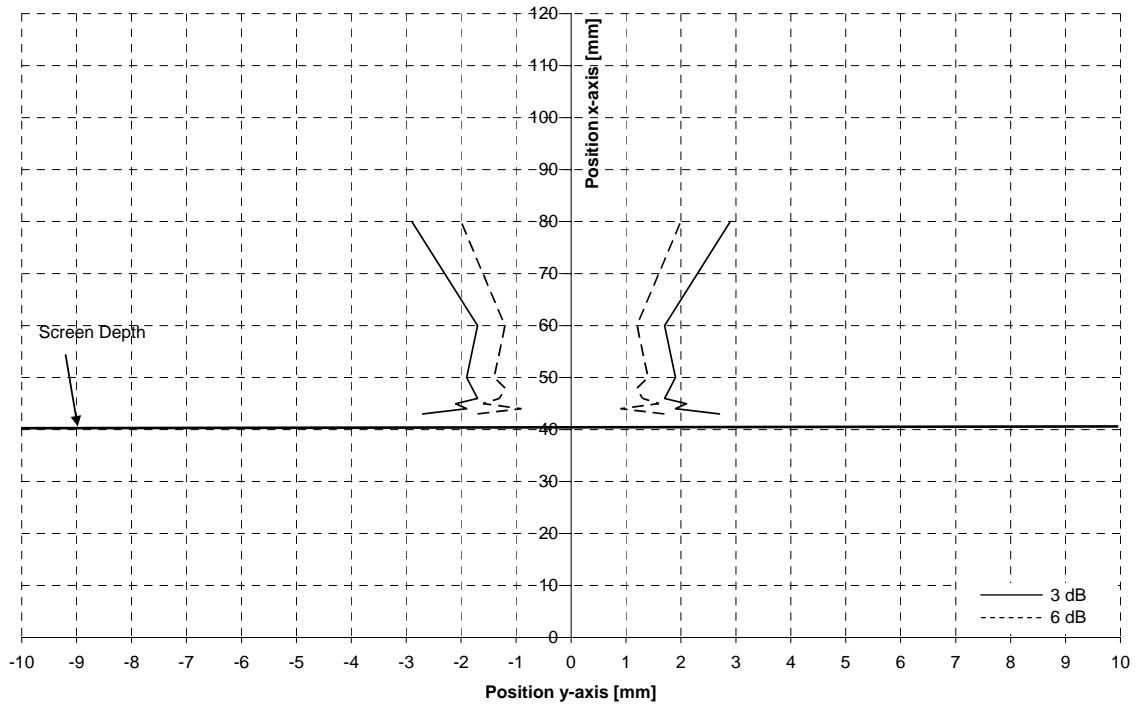
Figure 4-57: Divergence 4 MHz Focussed Transducer With Screen at x = 40 mm

Screen at x = 60 mm:
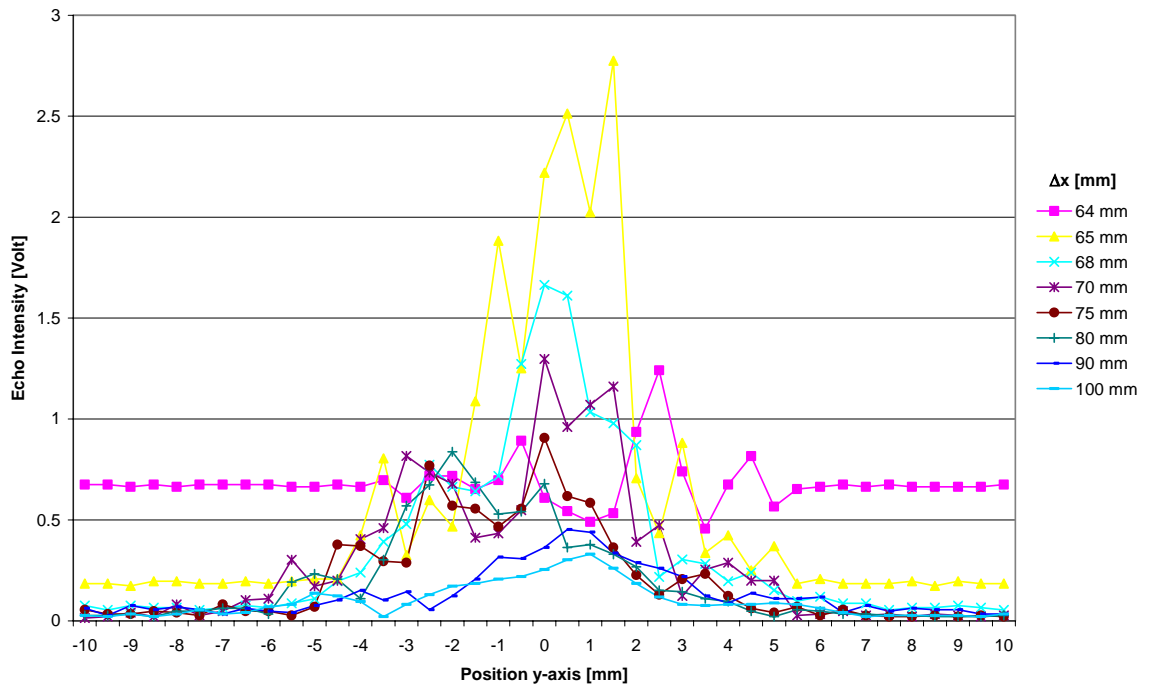
Figure 4-58: Echo Intensity 4 MHz Focussed Transducer With Screen at x = 60 mm
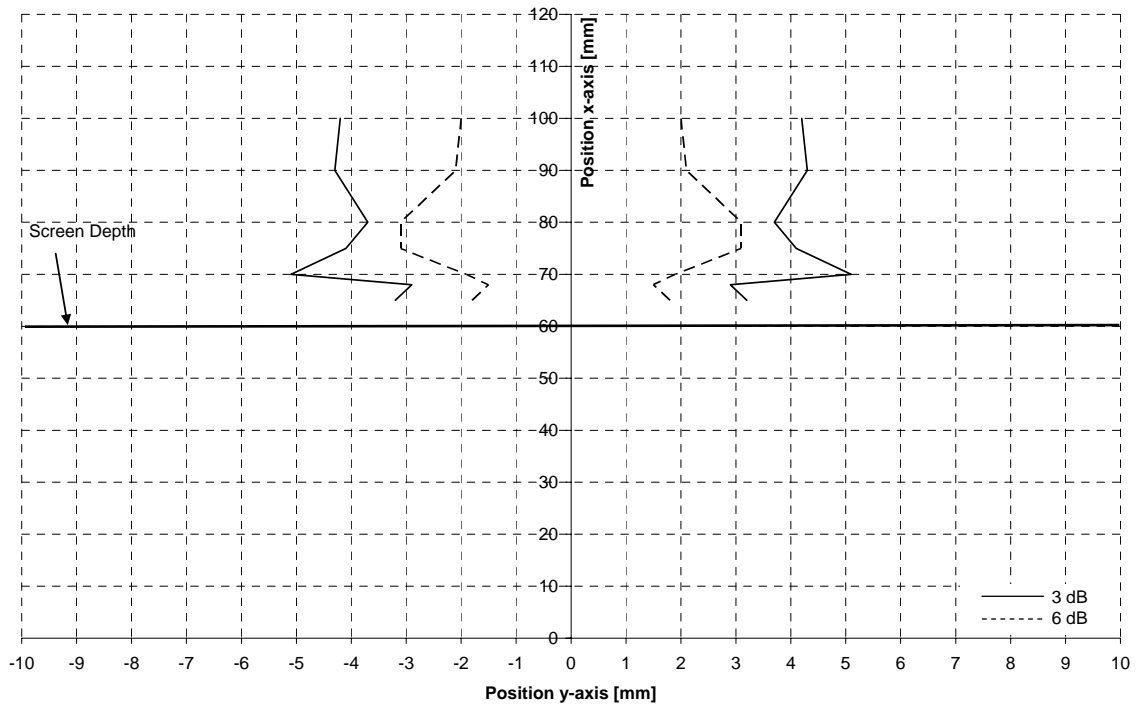
Figure 4-59: Divergence 4 MHz Focussed Transducer With Screen at x = 60 mm

126

4.6 Evaluation of Ultrasonic Beam Measurements

Ultrasonic field measurements were conducted with various transducers to determine the transducer best suited to measure velocity profiles in small channels and capillaries, to compare unfocused and focused ultrasonic transducers and to see the effects of Plexiglas walls and porous forming screens inserted between the transducer and the target (plastic sphere). The effect of Plexiglas walls and porous forming screens on the ultrasonic beam shape can not be generalized for all transducers and should therefore be investigated experimentally for each single transducer at various positions.

The 8 MHz 5 mm and 4 MHz 8 mm focused ultrasonic transducer turned out to be the most promising transducer to measure velocity profiles in small channels and capillaries due to their excellent lateral resolution. When dealing with small geometries, the 8 MHz transducer should be preferred, since its axial resolution is half of the 4 MHz transducer's axial resolution. Knowledge of the focal point of both transducers is crucial to optimize measurement results especially when dealing with flow over a backward facing step.

Much greater amplification must be used in order to get a readable signal when the forming screens or the Plexiglas walls are used. This increase in echo intensity comes with the cost of increased ringing of the ultrasonic signal. This ringing effect causes the minimum measurable distance, the distance from the obstruction to the first measurable point, to increase. Especially at high frequencies, Plexiglas walls and forming screens attenuate more than 90 percent of the ultrasonic signal. The 4 MHz transducer turned out to represent a good tradeoff between the high attenuation of the 8 MHz transducer and the low lateral and axial resolution of the 2 MHz transducer. The closest distance from the plastic sphere to the porous forming screen over the widest range of transducer-screen-distances that produced detectable echoes was also achieved with the 4 MHz transducer. Due to the better lateral resolution (and therefore the greater amount of energy that is reflected from scatterers behind the porous forming screen), the 4 MHz focused transducer turned out to be the most promising transducer to measure velocity profiles closely behind a porous forming screen.

5 Measurement of Velocity Profiles in Small Channels

In Chapter 4, the 8 MHz 5 mm ultrasonic transducer was identified to be the most promising transducer to measure velocity profiles in small channels and capillaries due to its excellent lateral resolution. In this chapter, velocity profiles are non-intrusively measured in a small rectangular channel characterized by a backward facing step to experimentally validate the theoretical limitations of pulsed ultrasound Doppler velocimetry (identified before), investigate further limitations in small channels in a separated flow at low velocities and compare focused with unfocused ultrasonic transducers. At first, the principle of measurement and important parameters of pulsed ultrasound Doppler velocimetry are presented. Then the experimental setup that was solely designed for this purpose is described. Technical drawings of the channel and distributor are listed in Appendix A. After reviewing the fundamentals of flow over a backward facing step, the measurement results are presented and finally evaluated. The effect of Plexiglas walls on the measurement results has been evaluated in detail.

5.1 Principle of Measurement of Pulsed Ultrasound Doppler Velocimetry

In pulsed ultrasound Doppler velocimetry, a transducer is placed on a wall with an angle inclination θ (angle between transducer and flow direction) to ensure a velocity component in the direction of the measuring line. The most important point is to ensure a good coupling between the transducer and the liquid. Any gas interface is not allowed because gas has very low acoustic impedance and therefore reflects all the ultrasonic energy.

The master oscillator generates a reference frequency of from 1 to 10 MHz. This reference frequency is the input to a gating circuit which transmits just a few cycles of the reference frequency at preset intervals. This produces a train of pulses at a frequency called the pulse repetition frequency. The pulse train is the input to the transmitting

piezocrystal to produce acoustic pulses. As the acoustic burst leaves the crystal and propagates through the flow field, a continuous train of echoes is produced.

Figure 5-1 [55] shows an example of the signal of the received echo. Between two emissions of ultrasonic pulses the echo can be observed, backscattered from somewhere on the measuring line. A position axis along the measuring line is thus converted to a time axis. The frequency of an echo signal at any instant is Doppler-shifted due to the fluid motion as far as it is reflected inside the flow.

Since echoes are produced by a single acoustic burst, range information can be obtained. This is accomplished by "range gating" the receiver crystal. The receiver is turned off while a burst is transmitted. Since the acoustic burst propagates at a known acoustic velocity through the medium, the distance which it travels corresponds to a particular time delay. Thus, if the receiver is turned on for an instant after a given time delay from the instant of pulse transmission, the echoes reaching the receiver crystal at that instant will correspond to a particular range distance. At this instant, the phase of the received signal is compared in a phase detector with the reference frequency. The phase-detector output is a voltage pulse proportional in magnitude to the phase difference between the echo and the reference frequency. Repeating the comparison over many pulse repetition frequency cycles results in a train of phase detector output voltages with each pulse proportional to an instantaneous phase difference [59].

In modern devices, after amplification, the echo signal is demodulated to eliminate the component of basic frequency and then digitized. The time series of the digitized data is then filtered digitally to eliminate vibration of the container or from noise, then the Doppler shifts are detected to give a histogram of velocity values and thus the velocity profile (Figure 5-1 (c)).
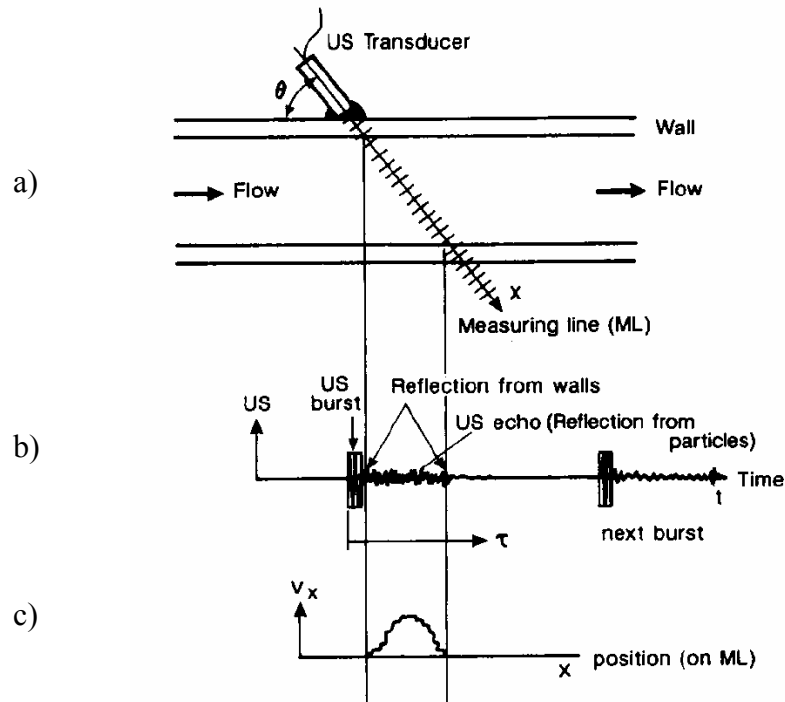
Figure 5-1: Principle of Measurement [55]

The velocity component measured by the velocimeter is always the component in the direction of the ultrasonic beam as shown in Figure 5-2. The measured velocity v_{us} represents the projection of the three dimensional velocity vector onto the ultrasound beam line [16]. When the direction of the real velocity is known, the velocimeter can automatically compute the real velocity value v_{real} by using the value of the Doppler angle θ. In such a case the depth values displayed by the velocimeter are the depths perpendicular to the velocity direction (P_{real}).
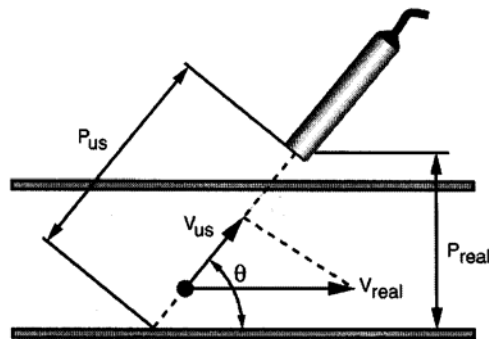
Figure 5-2: Velocity Components [51]

130

The acquisition time of a complete profile depends on three parameters; the sound velocity in the liquid, the maximum depth at which measurements have to be done and the number of ultrasonic emissions used to estimate the velocities.

5.2   Important Parameters of Pulsed Ultrasound Doppler Velocimetry

With respect to the velocimeter architecture, working structure and measurement method identified in Section 2.5 and Section 5.1, the following parameters are essential to correctly determine a velocity profile.

5.2.1   The Emitting Frequency

In making the choice of an emitting frequency the following four factors are crucial. First of all, the desired position of the sampling volume is important in selecting the emitting frequency especially when dealing with small channels and capillaries. The emitting frequency contributes to the definition of the axial and lateral dimension of the sampling volume. As this dimension is linked to the duration of the burst, for a defined number of wave cycles in the burst, a higher emitting frequency will give a better resolution. Besides the sampling volume size, attenuation of the ultrasonic signal is an important factor in making the choice of an emitting frequency. The attenuation of ultrasonic waves depends on their frequencies. Low frequencies are less attenuated than high frequencies. The attenuation coefficient may vary quite a lot and depends on the material. Moreover, the maximum measurable velocity, which is inversely proportional to the emitting frequency, and the energy backscattered by particles depend on the ultrasonic frequency.

5.2.2   Doppler Angle

The velocimeter measures the velocity component in the direction of the ultrasonic beam and gives therefore only one component of the velocity vector. If the direction of the real velocity vector is known, it is possible to compute directly the module of the velocity vector by using the Doppler angle. The Doppler angle is the angle formed by the axis of the ultrasonic beam and the direction of the real velocity vector. When the Doppler angle is used to compute the module of the velocity vector, the depth values, measured in the

direction of the ultrasonic beam are computed perpendicularly to the direction of the velocity.

5.2.3 Pulse Repetition Frequency

The pulse repetition frequency determines the maximum measurable depth as well as the maximum Doppler frequency and therefore the maximum velocity which can be measured unambiguously. The choice of the pulse repetition frequency should be based on the velocity values that have to be measured and not on the depth that has to be reached. The best way to select a correct value is to start with a high value and reduce this value until at least 50 percent of the velocity scale is covered. The desired analyzed depth can then be adapted by changing the resolution, the position of the first gate or the number of gates.

5.2.4 Position of the First Gate, Wall- and Saturation-Effect

In order to correctly determine the velocity profile, the position of the first gate should be chosen carefully to decrease the wall effect and the effect of the saturation region.

The measuring position of each sample volume is located in the center of the sample. When part of the sample volume is located inside the channel wall, this position will not reflect the actual measuring position given by the instrument (wall effect). The actual center of the measurement volume (this part of the sample volume which is in the flow and not in the wall) can be calculated based on the Doppler angle (geometric considerations) and simplifications on the shape of the sample volume (e.g., disk shape sample volume). The position of the first sample volume can consequently be corrected based on this calculation [64]. In the following, the position of the first gate will be set so that the sampling volume begins ideally right behind the channel wall to decrease the wall effect (see also section 5.5.3). Since the position of the first gate can be defined only in specific increments, the starting depth should be set so that only a very small portion (in the order of maximal 0.08 millimeter) of the sample is inside the wall. The position of the first gate is based on the position of the center of the first sample volume which depends on the emitted ultrasonic burst length, the speed of sound in the media located between the transducer face and the first gate, the Doppler angle (geometry) and the starting depth that can be set in the instrument.

132

When the first gates are close to the surface of the transducer, the burst duration and the ringing of the piezoelectric ceramic do not allow any measurement in these gates due to a saturation of the receiver (saturation effect). The saturation region can be visualized in the display of the received echoes, where the levels echoes of gates located at depths near the surface of the transducer stretch over the entire scale.

The position of the first measurable gate therefore depends on the emitting frequency, the burst length, the Doppler angle, the geometry of the experimental setup, the emitted power and the amplification level. The starting depth chosen in the instrument is the distance between the transducer face and the center of the first gate.

5.2.5 The Burst Length

The length of the emitted burst affects the sampling volume. The bandwidth of the electronic receiving unit in the ultrasonic instrument is fixed, but the number of cycles contained in the emitted ultrasonic burst can be selected. The length of the emitted burst depends on the selected emitting frequency and the speed of sound of the medium.

5.2.6 The Resolution

In the ultrasonic instrument, the resolution is defined as the distance between the centers of adjacent sampling volumes. In ultrasonic Doppler velocimetry, the shape and lateral size of the sampling volumes (measured perpendicularly to the ultrasonic beam axis) are defined by the geometry of the ultrasonic beam. The longitudinal size of the sampling volumes on the other hand is defined by the burst length. The borders of the sampling volumes are not well defined since the levels of the ultrasonic echoes increase and decrease "slowly" due to the finite bandwidth of the receiver. Whenever possible, a value for the spatial filter that equals the resolution should be selected to achieve an optimum signal to noise ratio.

5.2.7 The Number of Gates

The number of gates that can be measured depends on the selected pulse repetition frequency, the position of the first gate and the selected resolution. An upper limit can be fixed to ensure a better display of velocity profiles, especially when low pulse repetition values are selected. The position of the first gate and the number of gates define the

measuring range and therefore the analyzed depth. It is often much better to change the number of analyzed gates in order to change the measuring depth or range than to change the pulse repetition values.

5.2.8 The Emitting Power and Sensitivity

The emitted ultrasonic power has to be selected in order to receive enough backscattered energy from the particles and avoid as much as possible saturation in the receiver stage of the instrument. The display of the echo profile may be used to verify this point. A high emitting power should be avoided since it induces more ringing in the transducer and more dissipated energy. Therefore it is generally better to increase the amplification (time gain control) instead of increasing the emitting power. Nevertheless, a too high level of amplification also induces saturation in the receiver stage of the instrument, which induces wrong measurement values.

The algorithm used to measure the Doppler frequency computes the mean frequency of the Doppler spectrum. When the Doppler energy decreases, the mean value become more and more random due to the noise included in the spectrum. In order avoid the apparition of random values on the screen, the instrument computes also the level of Doppler energy received and allows the user to cancel the computation of the Doppler frequency if the level of the Doppler energy is below a user defined value. In such a case the canceled values are replaced by zero values. The sensitivity parameter contains five different values, which define the level below which the computation is canceled. The sensitivity parameter can be used to obtain information on the quality of the measured values. No changes should occur if the sensitivity parameter is modified.

5.2.9 Number of Emissions Per Profile

The measurement of the Doppler frequencies is based on the correlation that exists between different emissions. As each emission can be seen as a particular realization of a random process, more samples are available and lower the variance of the estimated quantity. The algorithm used to estimate the Doppler frequency is based on the assumption that the particles that generate the echoes during the measurement of the Doppler frequency remain inside the ultrasonic beam and their velocities are constant. For low velocities in steady flows this assumption is valid, but for transient ones, with high

velocities, a compromise has to be taken between the quality of the estimation (minimum variance) and the measuring time. The number of emissions per profile should be selected in accordance to the type of flow investigated and on the width of the ultrasonic beam. For low velocities in steady flows, a high number will decrease the variance and therefore should be selected. For high velocities in unstationary flows this number should be adapted to the degree of variation of the velocities versus time.

5.2.10 Speed of Sound

The knowledge of the speed of sound in the medium is necessary to transform the Doppler frequency shifts in mm/s, and the time of flight of the ultrasonic waves in millimeter. A good knowledge of the sound velocity in the medium especially when dealing with suspended particles or fibers is necessary to obtain good quantitative measurement values, as all errors in this parameter are directly transferred to the measured values. Since the speed of sound for different particle or fiber concentrations in water is unknown, the sound velocity is measured in a special unit before each measurement. These measurements are described in Appendix H.

5.2.11 Profiles to Record

In pulsed ultrasound Doppler velocimetry measurements, a certain number of "instantaneous velocity profiles" is used to calculate the mean velocity profile as defined by the instrument parameter "profiles to record". Possible velocity fluctuations, caused by the recirculation of the backward facing step at high Reynolds-numbers and pressure fluctuations caused by the pump and distributor, may lead to small differences between different instantaneous profiles and therefore to a statistical error. Therefore, it is necessary to determine the mean velocity profile based on enough instantaneous velocity profiles.

5.3   Experimental Setup

The experimental setup shown in Figures 5-3 and 5-4 is used for measuring velocity profiles in a small rectangular channel and determining current limitations of the utilized

pulsed ultrasound Doppler velocimetry system (Signal Processing DOP2000 model 1225).
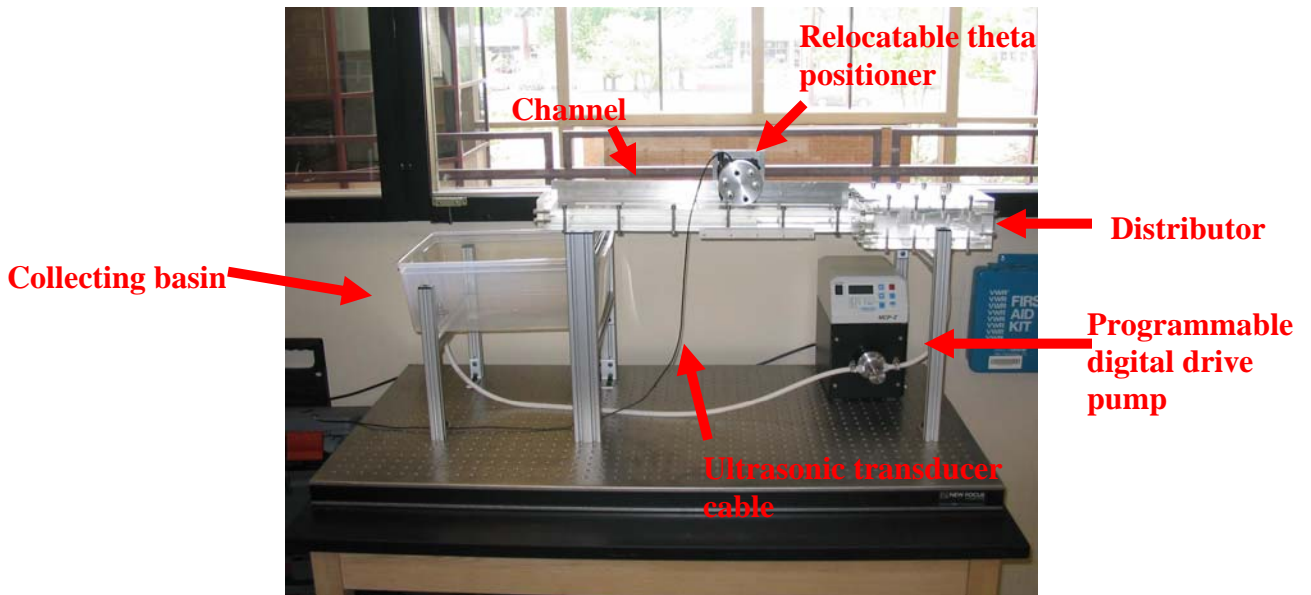
Figure 5-3: Experimental Setup
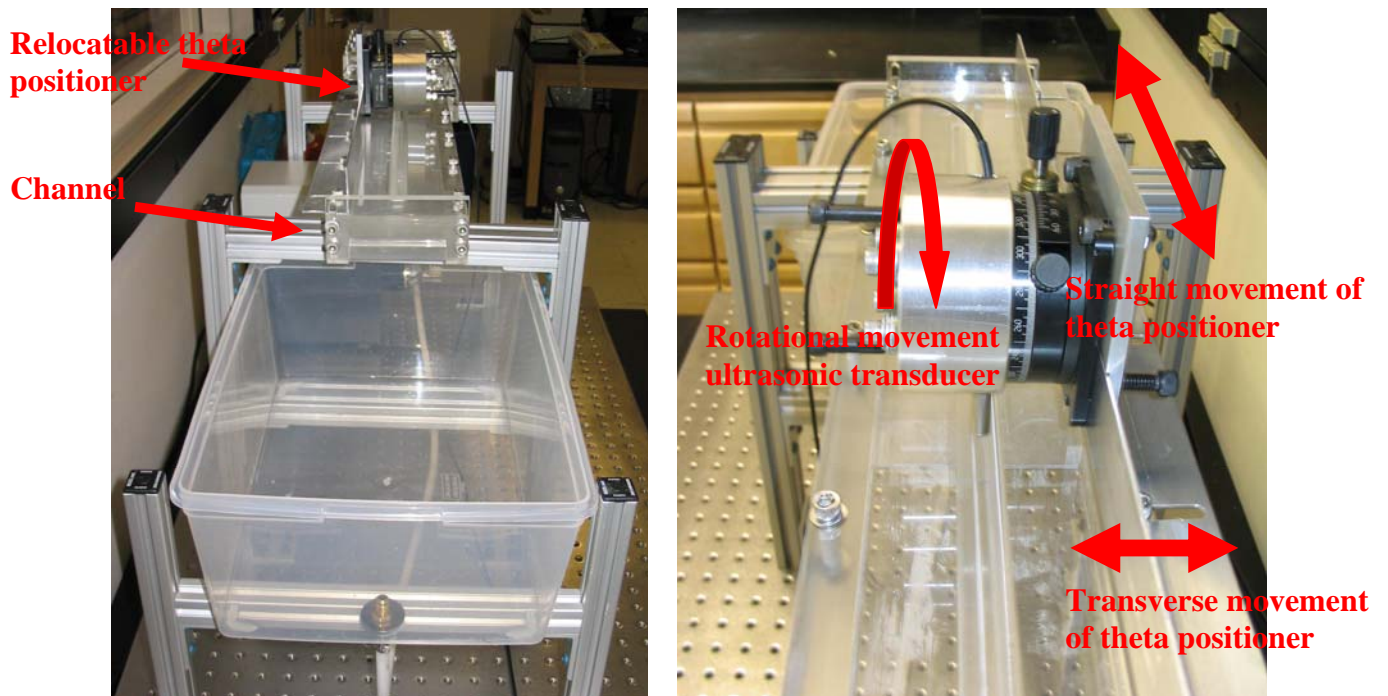
Figure 5-4: Experimental Setup Side Views

Main parts of the experimental setup are the pulsed ultrasound Doppler velocimetry system, the small rectangular channel (10 mm high and 80 mm wide; 0.7 liter volume)

characterized by a 5 mm backward facing step, the distributor (1.5 liter volume), the theta-positioner (relocatable across the entire area of measurement as shown in Figure 5-4 and 5-5) and the pump. To achieve better measurement results and decrease attenuation of the ultrasonic beam while crossing the Plexiglas wall, a slot has been machined in the top wall of the channel. The thickness of the Plexiglas wall in the area of measurement is therefore reduced to 2.5 mm. The pump is dimensioned to allow for Reynold numbers between 1 and 1000.
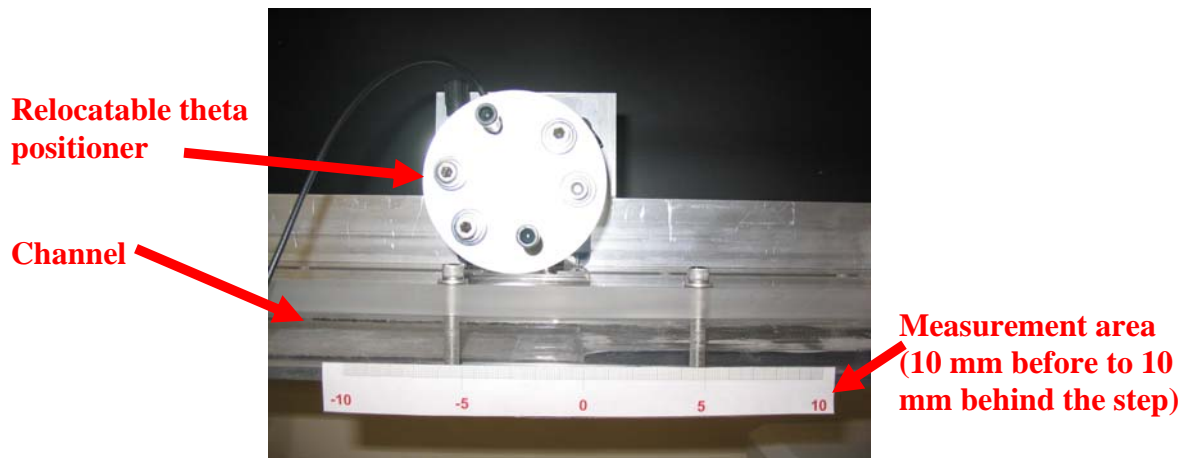
Figure 5-5: Theta-Positioner

Technical drawings of the experimental setup can be found in Appendix A. Technical specifications about the pump are given in Appendix D.

The desired outcome of this thesis is to use pulsed Doppler ultrasound velocimetry to measure velocity profiles in small channels, determine its limitations and develop suggestions for improvement. In the following, transducers with focussed acoustic waves and different frequencies will be used for measuring velocity profiles in the channel described above. Evaluating the measurement results, the current limitations of the utilized instrument (Signal Processing DOP2000 model 1225) will be determined. The primary objective is to develop suggestions for improving the application of pulsed Doppler ultrasound velocimetry to measure velocity profiles especially in small channels and capillaries.

5.4 Backward Facing Step

In this research, ultrasonic transducers with different frequencies will be used for measuring velocity profiles in the small rectangular channel shown above (10 mm high and 80 mm wide) which is characterized by a 5 mm backward facing step. The essential part of the experimental setup can be abstracted as shown in Figure 5-6:
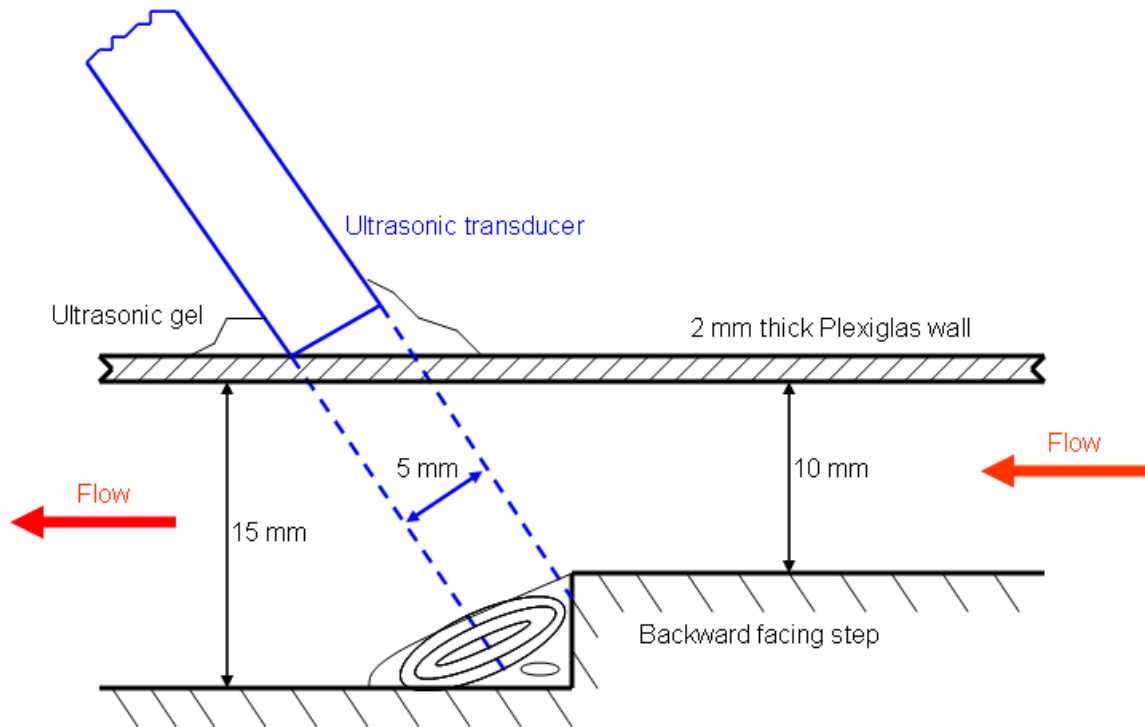
Figure 5-6: Backward Facing Step

Due to the sudden change in surface geometry (5 mm backward facing step), flow separation occurs. In general, separated-reattached flows due to sudden changes in geometry develop in many industrial devices such as fluidic, electronic and turbine blade cooling and many other heat exchanging equipment. Most of these industrial applications exhibit three-dimensional behaviour but most of the published studies are restricted to the two-dimensional case. The size of the reverse flow region characterizes the global features of flow and heat transfer in this geometry [41].

Flow separation often occurs at locations of sudden changes in the surface geometry. A separated shear layer usually develops at the surface discontinuity and reattaches some distance downstream, if the surface geometry permits forming a recirculation bubble. Backward facing step flow is a widely known separated flow geometry. This geometry is

of particular interest because it facilitates the study of the reattachment process by minimizing the effect of the separation process, while for other separating and reattaching flow geometries there may be a strong interaction between the two [35].

The principal flow features of the turbulent backward-facing step flow are described as follows. A turbulent boundary layer which forms on a flow plate encounters a downward step. The sudden expansion due to the change in surface geometry causes the boundary layer to separate at the step edge. Immediately after detachment, the flow essentially behaves as a free shear layer, with high-speed fluid on one side and low-speed fluid on the other. Some distance downstream, the shear layer impinges on the surface and forms a closed recirculation region containing turbulent, upstream moving fluid. A small "corner eddy" of the opposite rotation sense to the main recirculating flow might also exist in this region. Reattachment occurs over a region located about the time-averaged reattachment point. The flow in this zone is found to be unsteady and highly three-dimensional with large-scale structures (of size of the channel height before the step) passing through frequently. Downstream of reattachment, the boundary layer begins to redevelop and undergoes a relaxation to a normal turbulent boundary layer state [35]. Flow in the vicinity of the backward facing step is shown in Figure 5-7 for various Reynolds-numbers.
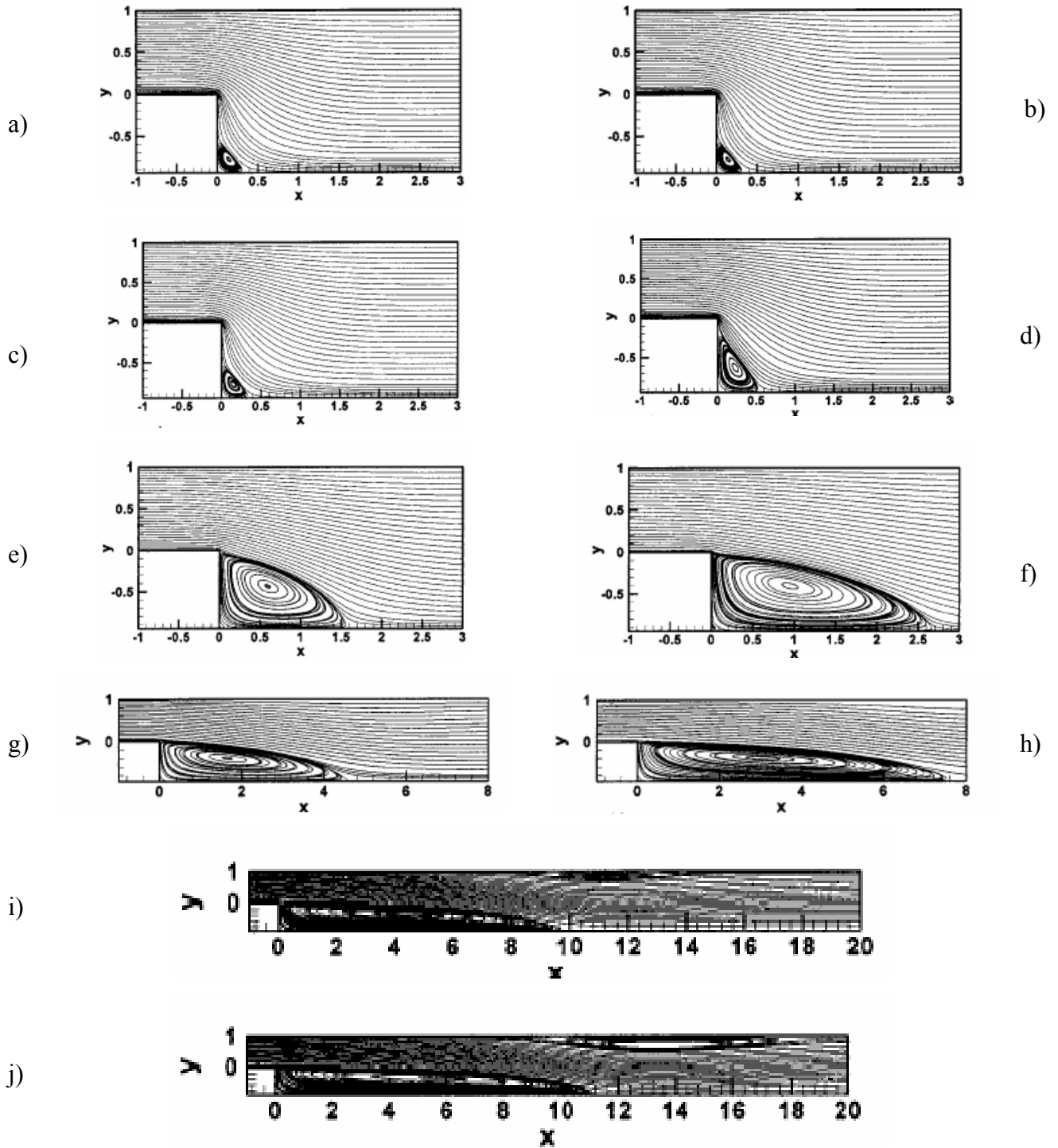
Figure 5-7: Flow Over Backward Facing Step [35]
Flow in the vicinity of the step. Expansion ratio H/h = 2; 10^{-4}; a) Re = 10^{-4}; b) Re = 10^{1};
c) Re = 1; d) Re = 10; e) Re = 50; f) Re = 100; g) Re = 200; h) Re = 400; i) Re = 600;
j) Re = 800

The size of the reverse flow regions increases and moves further downstream in the laminar flow regime (Re < 400); decreases and moves upstream in the transitional flow regime (400 < Re < 3400); and remains almost constant or diminishes in the turbulent flow regime (Re > 3400); as the Reynolds number increases [41].

Usually, recirculation length is obtained from the particle image velocimetry by measuring the distance between the step corner and the point of reattachment on the channel bottom wall. This point is characterized by a zero longitudinal velocity in the extreme vicinity of the bottom wall [10]. In the following, the ability of pulsed ultrasound Doppler velocimetry to measure the recirculation length is evaluated.

5.5 Measurements with Pulsed Ultrasound Doppler Velocimetry

Before actually measuring velocity profiles with pulsed ultrasound Doppler velocimetry, the purpose and necessary measurement preparations are described. The effect of Plexiglas walls and various measurement parameters is discussed. Finally, measurement results of focused and unfocused ultrasonic transducers are compared and evaluated.

5.5.1 Purpose

The desired outcome of this thesis is to use pulsed Doppler ultrasound velocimetry to measure velocity profiles in small channels and capillaries, determine its limitations and, if necessary develop suggestions for improvement. Velocity profiles in the small rectangular channel described above are therefore measured in this section to further determine the current limitations of the utilized pulsed ultrasound Doppler velocimetry system. Measurement results of focused and unfocused ultrasonic transducer are compared.

5.5.2 DOP 2000 Model 2125 Pulsed Ultrasonic Doppler Velocimetry

In this study, a commercially available pulsed ultrasound Doppler velocimetry system (DOP 2000, Model 2125) manufactured by Signal Processing S.A., Switzerland, is used to measure velocity profiles in the experimental setup described above. The basic

function of pulsed ultrasonic Doppler velocimetry is to measure the Doppler shift frequency and time delay between emission and reception of ultrasound scattered back by small particles which are moving with the fluid. The information on velocity and sample volume position is included in the ultrasound echoes. Technical specifications of the digital ultrasonic synthesizer are listed in Appendix B. The ultrasonic synthesizer records data values in a binary or ASCII format. These formats insure a minimum space requirement.

5.5.3 Ultrasonic Transducers

In Chapter 4, the 8 MHz 5 mm ultrasonic transducer turned out to be the most promising transducer to measure velocity profiles in small channels and capillaries due to its excellent lateral and axial resolution. To compare focused and unfocused transducers, velocity profiles measured with the 4 MHz 5 mm unfocused and 4 MHz 8 mm focused transducer are also evaluated. Technical specifications of these single-element ultrasonic transducers manufactured by Signal Processing S.A., Switzerland, are presented in Appendix C.

As mentioned in Section 5.2.6, a value for the spatial filter that equals the resolution should be selected to achieve an optimum signal to noise ratio. The distance along the ultrasonic beam axis, displayed by the instrument, depends on the selected ultrasonic transducer and the selected value of the spatial filter. In order to measure the velocity profile in small geometries, the highest possible axial resolution should be chosen, i.e., the distance between the centers of two sample volumes should be as small as possible. Therefore, the smallest possible spatial filter given by the instrument must be selected to achieve an optimum signal to noise ratio. This in turn leads to an offset in the distance displayed by the instrument along the ultrasonic beam axis. The distance offset caused by the selection of the spatial filter is in the order of 0.5 mm to even 4 mm (when using a lower frequency transducer).

To obtain a precise value of the actual distance of the center of the sample volume, the distance offset must be calibrated. The sound-velocity-measuring unit (described in Appendix H) has been used to calibrate this offset. Since the distance offset also depends on the distance of the sample volume to the transducer face on the ultrasonic beam axis,

the offset has been measured at several distances, which are crucial for measuring the velocity profile in the small channel described above.

In Figure 5-8, the distance displayed by the instrument is plotted over the measured echo intensity. The ultrasonic echo is caused by the micrometer screw. The micrometer screw is placed at the desired distance from the transducer face, in this case 15 mm. The measured distance offset for the 8 MHz 5 mm ultrasonic transducer, with the target (micrometer screw) placed 15 mm away from the transducer face on the ultrasonic beam axis, can therefore be evaluated.

When determining the distance offset, knowledge about the ultrasonic pulse length and resolution is essential. The maximum echo peak is ideally caused by the first sample volume which is (virtually) completely "in" the micrometer screw. This is also explained in Section 2.6.6 and visualized in Figure 2-21. In these measurements, a resolution as small as possible is selected to attain the best possible measurement results. Therefore, the value of the selected resolution equals half the value of the ultrasonic burst length. Consequently, the value of the displacement of the center of this sample volume from the surface of the micrometer screw is the same as the value for the selected resolution. The position of the surface of the micrometer screw consequently coincides with the position of the center of the sample volume right before the sample volume which causes the maximum peak in the echo intensity (in the ideal case). In Figure 5-8, the center of this sample volume is at a distance of 16.29 mm away from the transducer face on the ultrasonic beam axis.
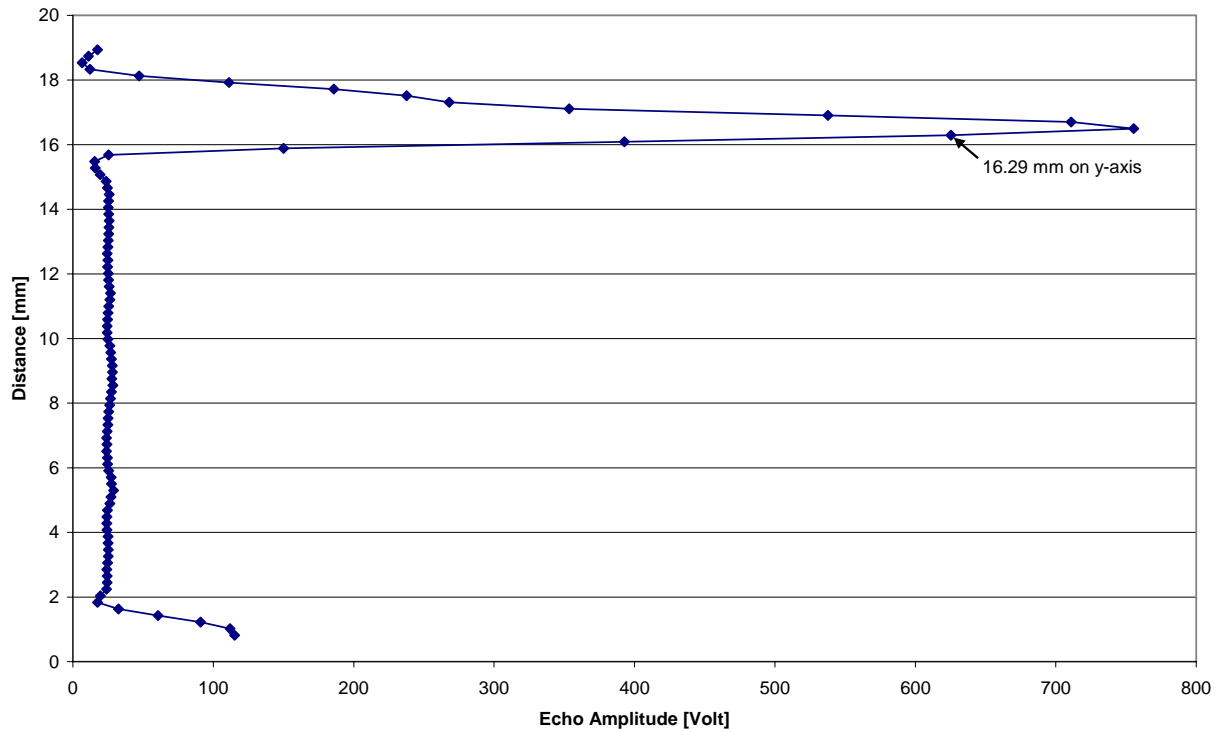
Figure 5-8: Calibration of Transducer Distance Offset

The offset in the distance displayed by the instrument has been measured for each ultrasonic transducer at various distances which are of importance to measuring the velocity profile in the small channel described above. Values for the distance offset with the target (micrometer screw) at different positions, can be found in Table 5-1.

5.5.4 Channel and Probe Geometry

To exactly determine the position of each sample volume, characteristic distances of the experimental setup have been defined and calculated for various Doppler angles θ and ultrasonic transducers as shown in Figure 5-9.
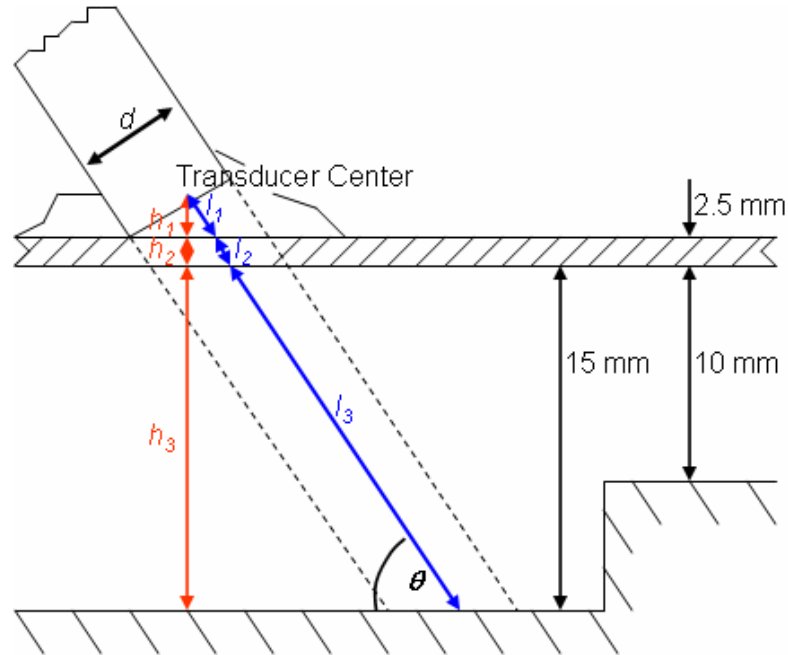
Figure 5-9: Channel and Transducer Geometry

The distance from the center of the ultrasonic transducer (with diameter d) to the outer surface of the Plexiglas channel-top-wall, which is perpendicular to the wall, is denoted as h_1. h_2 is the thickness of the Plexiglas channel-top-wall, whereas h_3 is the channel height.

$$h = h_1 + h_2 + h_3 = \frac{d}{2}\cos\theta + h_2 + h_3$$

Equation 34: Distance Perpendicular to the Flow

The distance from the center of the ultrasonic transducer to the outer surface of the Plexiglas channel-top-wall along the ultrasonic beam axis is denoted as l_1. Respectively l_2 and l_3 are projections of h_2 and h_3 on the ultrasonic beam axis.

$$l = l_1 + l_2 + l_3 = \frac{h_1}{\sin\theta} + \frac{h_2}{\sin\theta} + \frac{h_3}{\sin\theta} = \frac{h}{\sin\theta}$$

Equation 35: Distance in Direction of the Ultrasonic Beam

An exact definition of the characteristic distances is crucial, to understand the effect of Plexiglas walls placed between the sample volume and the ultrasonic transducer.

145

5.5.5 Plexiglas Wall Effect

Placing a Plexiglas wall between the area of interest (sample volume) and the ultrasonic transducer leads to another offset in the distance displayed by the instrument along the ultrasonic beam axis. This distance offset is caused by different sound velocities in Plexiglas, ultrasonic gel and the fluid inside the channel. For example, the inner wall of the Plexiglas-top-wall should be displayed at a distance which equals the sum l_1 and l_2 (given in Table 5-1). Due to different sound velocities, the distance displayed by the instrument (L) differs from the sum of l_1 and l_2.

The distance offset caused by Plexiglas walls at normal incidence is already described in Section 4.4.1. To calculate the distance offset (and therefore the distance L) caused by the effect of the Plexiglas wall, when the ultrasonic transducer is inclined by the Doppler angle, the time which is required for ultrasound to propagate through the ultrasonic gel (distance l_1) and the Plexiglas wall (distance l_2) is compared to the time which is required for ultrasound to propagate the same distance in the fluid inside the channel (the sound velocity of the fluid is set in the instrument). Distance L is given in Table 5-1 for various Doppler angles. Distance L_1 (also mentioned in Table 5-1) is simply the sum of distance L and the specific transducer offset described in Section 5.5.3. Respectively, $L_{2,max}$ and $L_{2,min}$ are the sum of L, the specific transducer offset and the particular value of l_3.

When measuring the velocity of scatterers behind the Plexiglas wall, the ultrasonic transducer must be inclined by the Doppler angle. Normal incidence of the ultrasonic beam is not possible. Therefore, the ultrasonic beam is refracted. Refraction leads to a distance offset along the channel axis in direction of the flow. Since the Plexiglas wall is only 2.5 mm thick, this distance offset will be less than 1 mm and is therefore neglected in this study.

5.5.6 Measurement Parameters 8 MHz 5 mm Transducer

The following parameters (given in Figure 5-1) are chosen to determine the velocity profile in the small channel (described above) with the 8 MHz 5 mm ultrasonic transducer:

Table 5-1: Measuring Parameters 8 MHz 8 mm Transducer

Classifi-cation	Description	Data/Comments						
Instrumentation Parameters	Emission:	Emitting frequency [MHz]:	8					
		Emitting power:	medium					
		Pulse repetition frequency [Hz]:	For Re=200: 4000 For Re=400: 2000 For Re=600: 1200					
			For Re=800: 1000 For Re=1000: 800					
		Emitting burst length [cycles]:	2 (equals 0.41 mm in chosen fluid)					
	Reception:	Resolution [mm]:	0.205					
		Sensitivity:	very high					
		Starting depth [mm]:	distance L1 + resolution					
		Spatial filter [mm]:	0.73					
		Number of gates:	128					
	Processing Condition:	Time gain control [dB]:	Start value:	60				
			End value:	60				
			Overall gain:	20				
		Profiles to record:	256					
		Emissions/profile:	256					
		Skip profile:	0					
		Module scale:	1					
		Velocity scale:	1					
		Doppler angle:	Angle [°]:	80	70	65	60	50
			Distance l_1 [mm]:	0.7	1.46	1.86	2.31	3.35
			Distance l_2 [mm]:	2.54	2.66	2.76	2.89	3.26
			Distance l_3 [mm]:	min. 10.15	min. 10.64	min. 11.03	min. 11.55	min. 13.05
				max. 15.23	max. 15.96	max. 16.55	max. 17.32	max. 19.58
			Distance h_1 [mm]:	0.69	1.37	1.69	2	2.57
			Distance h_2 [mm]:	2.5	2.5	2.5	2.5	2.5
			Distance h_3 [mm]:	min. 10	min. 10	min. 10	min. 10	min. 10
				max. 15	max. 15	max. 15	max. 15	max. 15
		Transducer offset [mm]:	Target at 4 mm:	0.48				
			Target at 5 mm:	0.5				
			Target at 15 mm:	1.29				
			Target at 20 mm:	1.79				
		Corrected Distances [mm]:	Distance L:	2.28	3.18	3.68	4.25	5.61
			Distance L_1:	2.76	3.66	4.16	4.73	6.11
			Distance $L_{2,min.}$:	13.72	15.11	16	17.09	20.45
			Distance $L_{2,max.}$:	19.3	20.93	22.02	23.36	27
		Sound speed [m/s]:	Ultrasonic gel:	1480				
			Plexiglas:	2750				
			Chosen fluid:	1629				
	Transducer:	Piezoelectric element diameter [mm]:	5					
		Transducer case diameter [mm]:	8					
		Focus:	Unfocused					
Fluid Parameters	Kind of fluid:	Water						
	Temperature [°C]:	20						
	Reynolds number:	200, 400, 600, 800, 1000						
	Flow rate [l/min]:	0.96, 1.92, 2.88, 3.84, 4.8						
Fiber/ Particle Parameters	Kind of particles/fibers:	Thermoplastic CoPolyamide resin						
	Shape (simplified):	Spherical						
	Characteristic length:	3 μm diameter						
	Concentration [%]:	0.01						

In the first set of measurements, the velocity profile was measured at 10 different points: 10 mm before step, on the step and 10 – 80 mm behind the step. For example, 10 mm before the step means, that the ultrasonic beams impinges on the inner side of the channel

147

bottom wall at 10 mm before the step viewed from the direction of the flow. The position of some measurement points is shown in Figure 5-10.
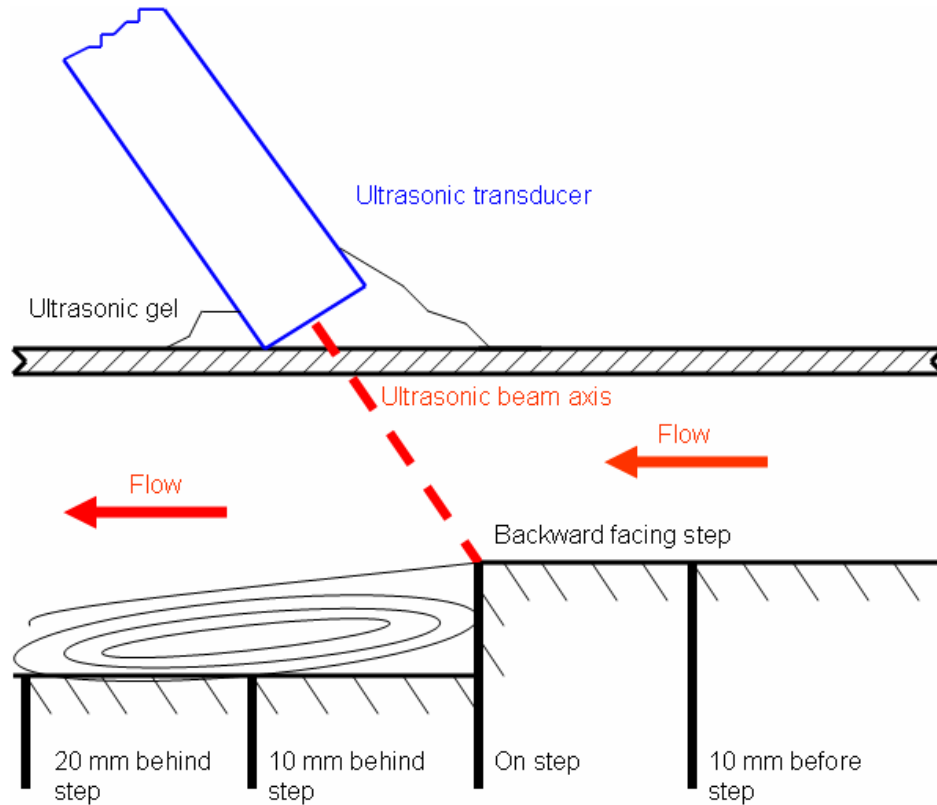
Figure 5-10: Position Measurement Points

5.5.7 Measurement Results 8 MHz 5 mm Transducer

The velocity profiles measured at eight measurement points behind the backward facing step at a Reynolds number of 400 and a Doppler of 70 degrees are presented in Figure 5-11.

In flow over a backward facing step the maximum velocity of the profile behind the step decreases with increasing distance to the step. In Figure 5-11, it can clearly be seen, that the maximum velocity at 10 mm behind the step is higher than the maximum velocity at all the other measurement points behind the step. Having said that, the measurement results do not show that the maximum velocity decreases from one profile to the next profile behind the step. For example, the maximum velocity at 70 mm behind the step is

higher than the maximum velocity 20 mm behind step according to the measurement results.

Besides the decrease in maximum velocity, the height of the recirculation region behind the backward facing step decreases with increasing distance to the step. The center of the velocity profile therefore shifts more to the middle of the channel, which can clearly be identified in Figure 5-11.
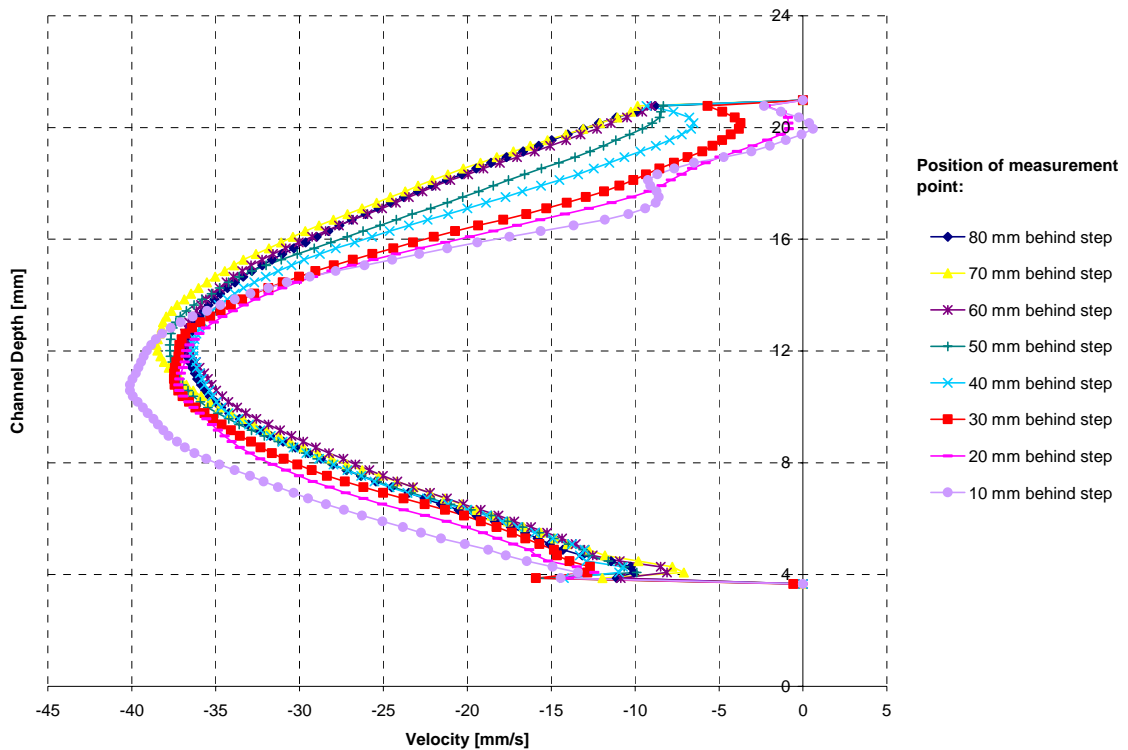
Figure 5-11: Velocity Profiles Behind Step

The velocity profiles measured 10 mm before and on the step are shown in Figure 5-12. Due to the smaller channel height before than after the step, the maximum velocity is higher before than on and behind the step. This can clearly be seen in the measurement results given in Figure 5-11 and Figure 5-12.

In the velocity profile 10 mm before the step distinct drops at a displayed channel depth of 6.3 mm and 8.1 mm are shown. These perturbations in the velocity profile can only be explained by the effect of the Plexiglas wall. At a later point, it will be shown that these perturbations are more likely to occur at lower particle concentrations and specific Doppler angles.

In the velocity profile on the step, the effect of the lateral resolution of the ultrasonic transducer becomes obvious. Theoretically, the velocity should be zero at a channel depth of 15.27 mm. But since the ultrasonic beam is about 2 – 3 mm thick at a depth of 15 mm behind the 2.5 mm thick Plexiglas wall (identified in section 4.3.2), velocities of particles on both sides of the step are measured. Small variation may occur due to the transducer positioning. Nevertheless, the velocity profile is at least 1 mm wider than the velocity profile at 10 mm before the step. Moreover, the instrument should not measure any velocities at channel depths beyond 17 mm. The displayed velocities at these channel depths are due to received echoes from earlier ultrasonic burst emissions. Especially reflections inside the channel bottom wall falsify measurement results especially close to this wall. Therefore, velocities measured close to the bottom channel wall are higher than they should be. This is described in more detail in Section 6.3.
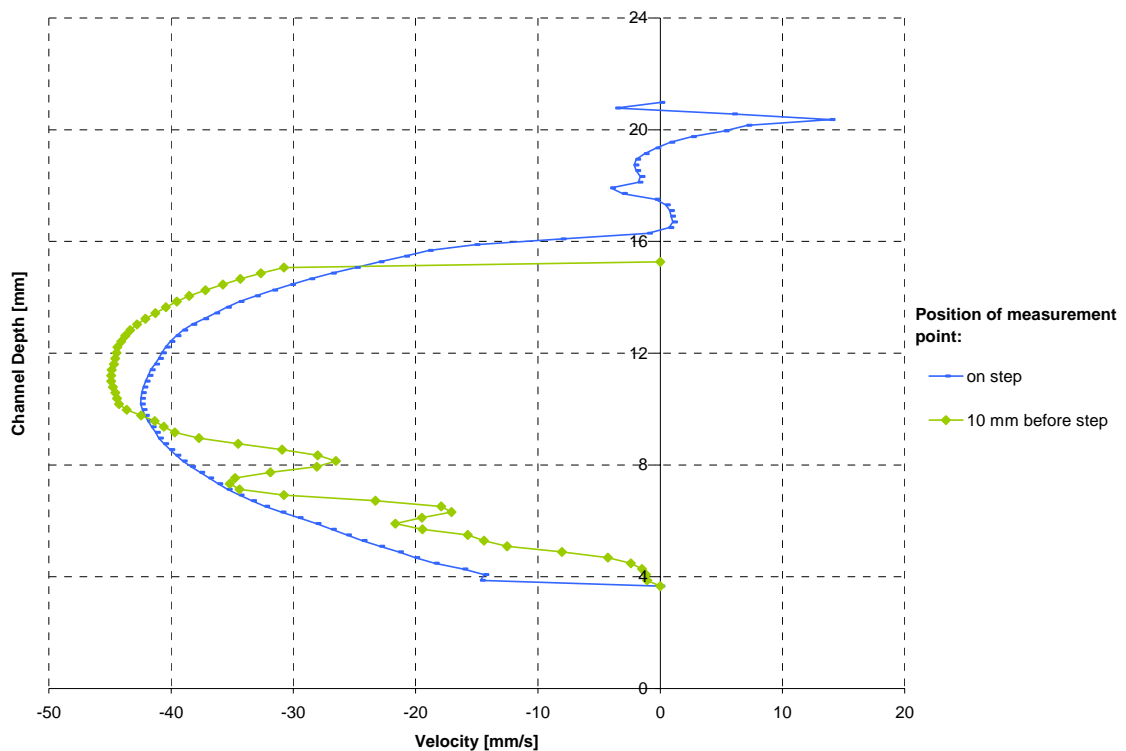
Figure 5-12: Velocity Profile Before and On Step

To more qualitatively evaluate the velocity profile measured by pulsed ultrasound Doppler velocimetry, measurement results are compared to numerical results in the following section.

150

5.5.8 Comparison to Numerical Results

Velocity profiles of flow over the backward facing step described above are numerically determined by the Lattice Boltzmann simulation. The Lattice Boltzmann method is an alternative approach to solving a fluid flow system. It is used to analyze the dynamics of particles suspended in fluid. In Lattice Boltzmann simulations, the interaction rule between the fluid and the suspended particles is developed for real suspensions where the particle boundaries are treated as no-slip impermeable surfaces. This method correctly and accurately determines the dynamics of single particles and multi-particles suspended in the fluid [2, 3]. Results of the Lattice Boltzmann simulation for the measurement points mentioned above are given in Figure 5-13.
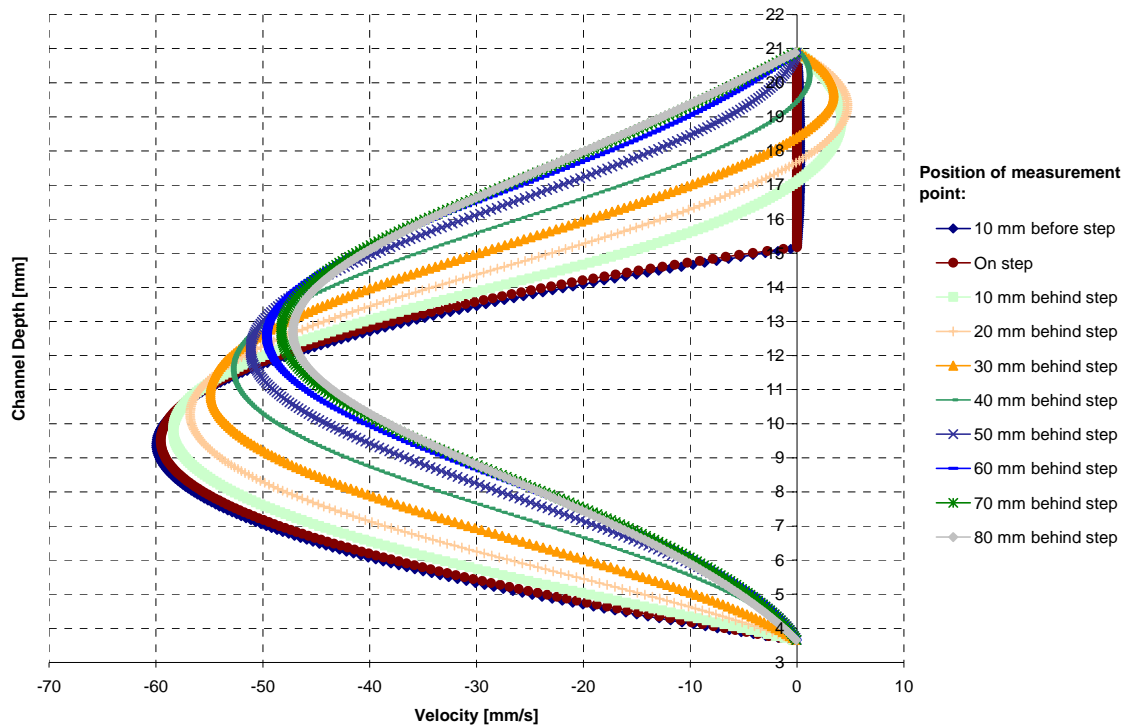
Figure 5-13: Numerical Results

To compare measured and numerical results, the velocity profile 10 mm before the step, 10 mm behind the step (inside the recirculation area) and 80 mm behind the step (outside the recirculation area) are presented in Figure 5-14, Figure 5-16 and Figure 5-15 respectively. In pulsed ultrasound Doppler velocimetry, the velocity component in

direction of the ultrasonic beam is measured. A trigonometric transformation finally yields the velocity component in direction of the flow. Nevertheless, it must be considered that even though the velocity is plotted along a line perpendicular to the flow, it is measured along the ultrasonic beam axis which is inclined by the Doppler angle. In a region of fully developed flow (that may be assumed before the step), this error may be neglected. Nevertheless, this error must be considered in the area behind the step especially in the presence of the recirculation region. In the following figures, the numerical results have been projected on the ultrasonic beam axis. Nevertheless, this assumption is only justified 10 mm before and 80 mm behind the step. Care should be taken when comparing the numerical and measured velocity profiles 10 mm behind the step especially inside the recirculation region. Moreover, the ultrasonic beam does not exactly impinge at the measurement point due to refraction in the Plexiglas wall. This effect causes an offset much smaller than 1 mm along the channel axis in direction of the flow and is therefore neglected.
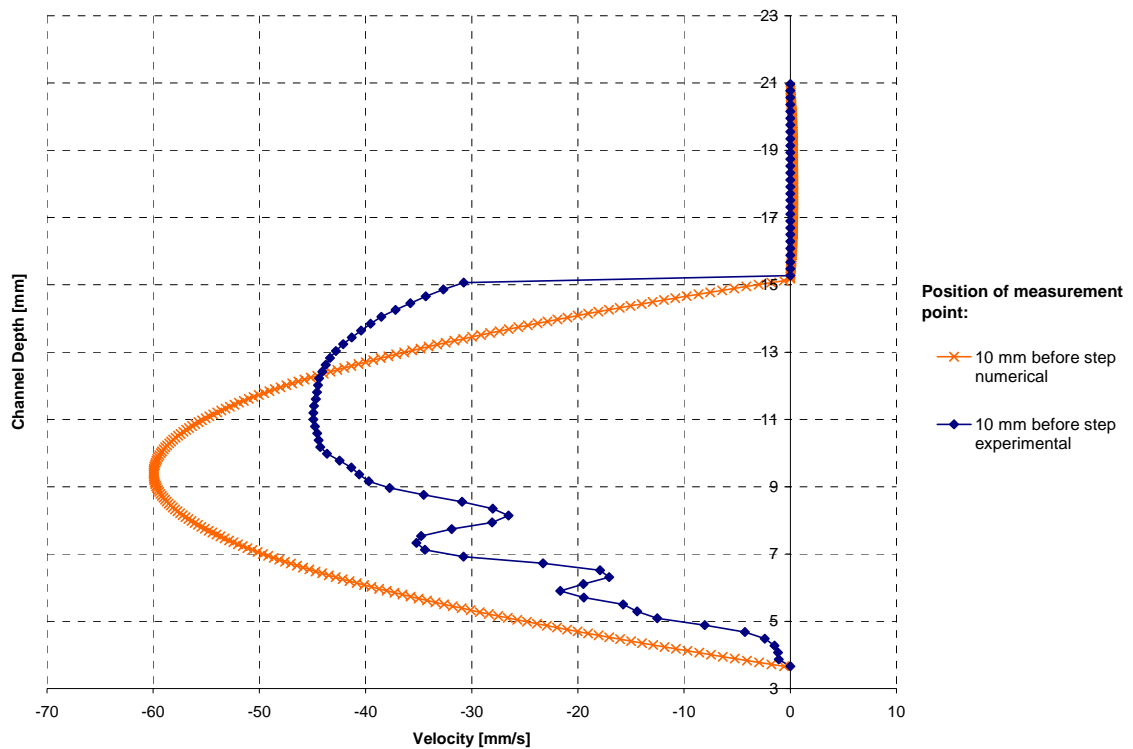
Figure 5-14: Comparison Numerical-Experimental 10 mm Before Step

The discrepancy between the numerical and measured profile becomes obvious in Figure 5-14. Apart from the distinct drops of the measured velocity profile already mentioned in the context of Figure 5-12, the maximum velocity offset of approximately 25 percent is a major shortcoming of the measured velocity profile. Moreover, it can clearly be seen in Figure 5-15, that the measured velocity profile is broadened compared to the numerical velocity profile. The broadening of the measured velocity profile is not obvious in Figure 5-14 due to the perturbations in the profile.
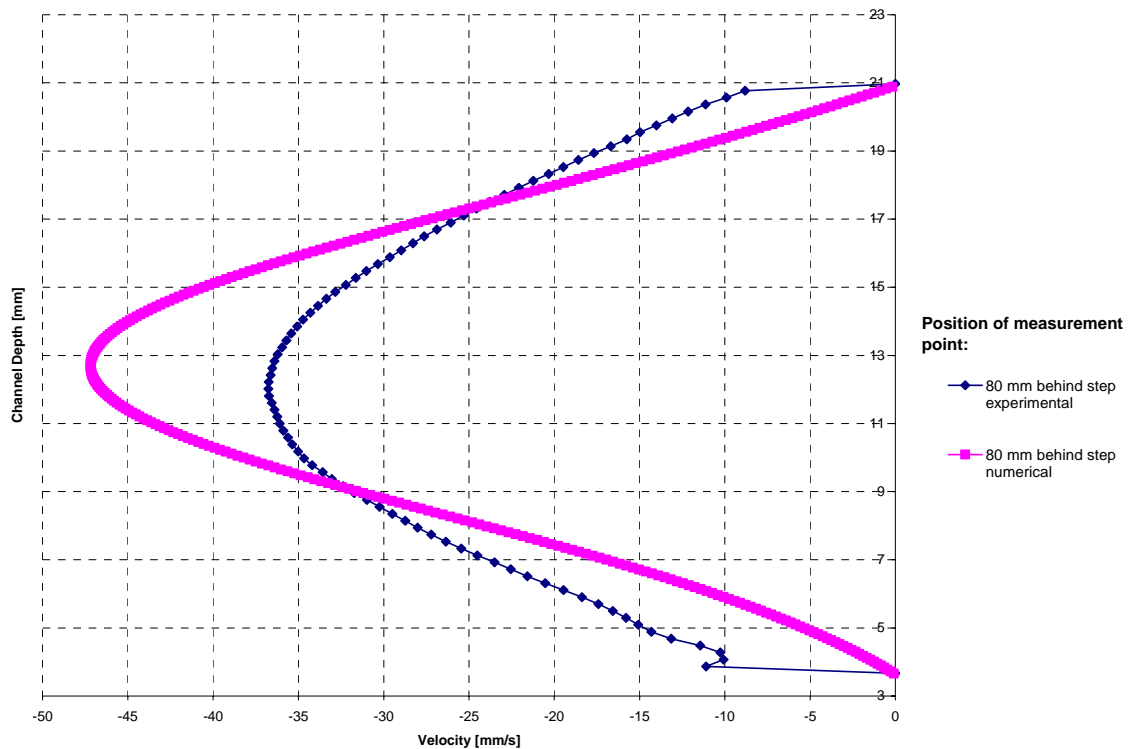
Figure 5-15: Comparison Numerical-Experimental 80 mm Behind Step

As mentioned above, care must be taken when comparing the numerical and measured velocity profile in Figure 5-16. The numerical velocity values are calculated perpendicular to the flow whereas the experimental velocity values are measured along the ultrasonic beam axis, which is inclined by 70 degrees to the direction of the flow. The ultrasonic burst impinges on the bottom channel 10 mm behind the step, but enters the inside of the channel at 15.5 mm behind the step. Even though the numerically calculated velocity profile has been projected on the ultrasonic beam axis, it can still be seen that the measured velocity profile is broadened with respect to the numerical velocity profile. In

Figure 5-16 broadening is also due to an underestimation of the height of the recirculation region in the measured velocity profile because the ultrasonic burst enters the recirculation area at about 13 mm behind the step instead of 10 mm behind the step.
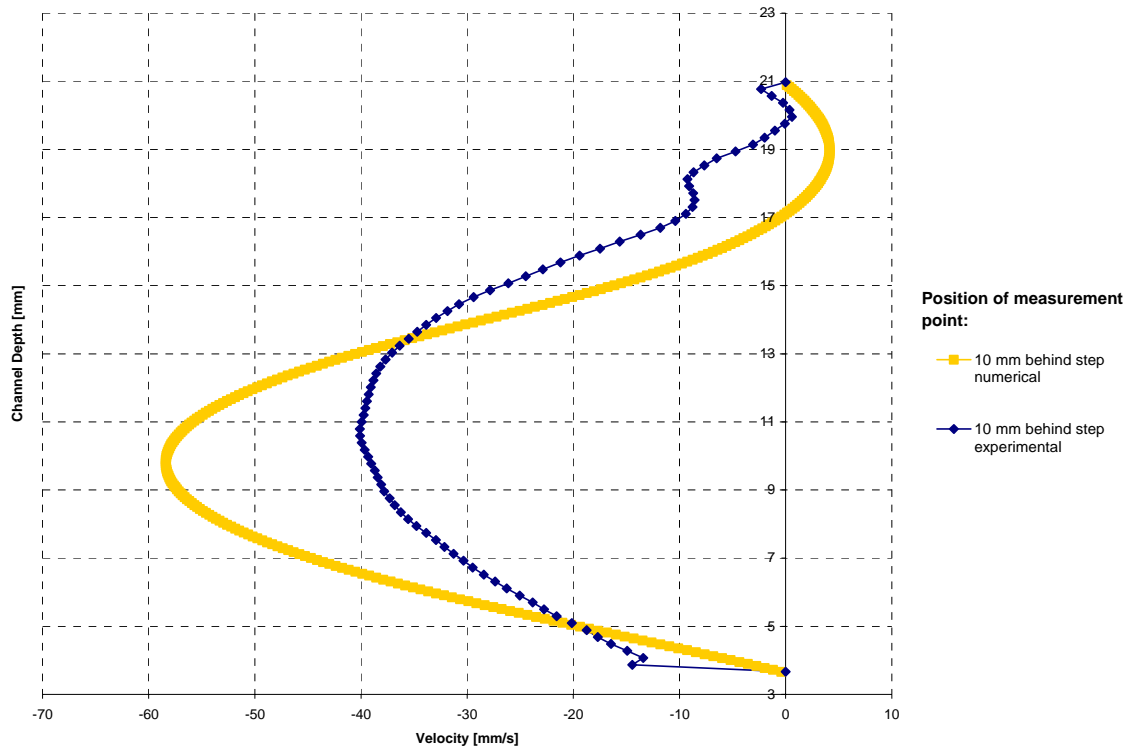
Figure 5-16: Comparison Numerical-Experimental 10 mm Behind Step

The main shortcoming identified in this section is the discrepancy of the measured to the numerically calculated maximum velocity. One explanation for this offset is the relatively small flow rate at a Reynolds number of 400. At small flow rates, the velocity component in direction of the ultrasonic beam, which is measured by the instrument, is very small. Therefore, even small variations in the flow may falsify the measurement results severely. There are two approaches to increase the measured velocity component in direction of the ultrasonic beam: either increasing the flow rate and consequently the Reynolds number or decreasing the Doppler angle. Both approaches are evaluated in the following sections.

5.5.9 Effect of Reynolds Number

To evaluate the effect of the flow rate on the measured maximum velocity, measurements are taken at the same measurement points for the following Reynolds numbers: 200, 400,

600, 800 and 1000. In Figure 5-17 results are shown for the measurement point 10 mm behind the step.
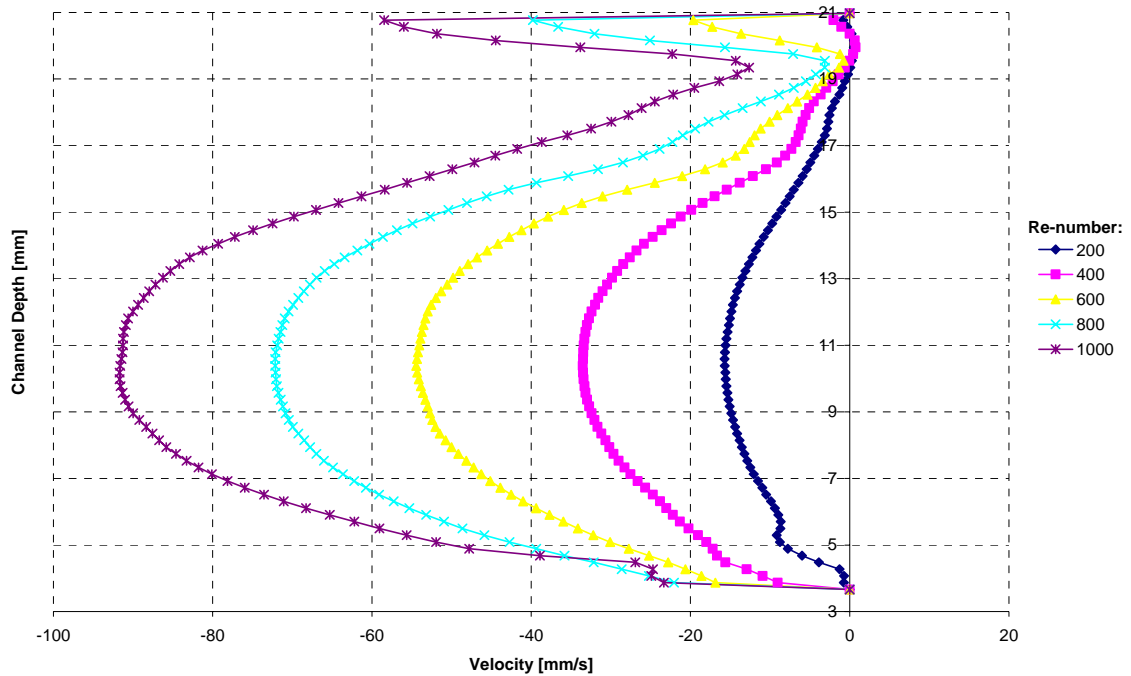
Figure 5-17: Velocity Profile for Different Re-Numbers

Comparing the measurement results at 10 mm before, 10 mm behind and 80 mm behind the step leads to the conclusion that increasing the flow rate, and therefore the velocity component in direction of the ultrasonic beam, does not significantly decrease the discrepancy between the measured and numerically calculated maximum velocity.

In Figure 5-17, it can clearly be seen that for higher Reynolds numbers the velocity in the recirculation area (ranging from a channel depth of approximately 17 mm to 21 mm) is not correctly determined by the instrument. For higher Reynolds numbers, the absolute value of the negative velocities in the recirculation area should increase. In Figure 5-17, no negative velocities can be identified for the higher Reynolds numbers of 600, 800 and 1000. This can be explained by the effect of the channel bottom wall and reflections caused by previous ultrasonic burst emissions. The effect of reflections caused by the far wall is further described in Section 6.3.

5.5.10 Effect of Doppler Angle

Besides increasing the flow rate, the Doppler angle can be decreased in order to increase the measured velocity component in direction of the ultrasonic beam. Results at the measurement point 10 mm before the step are given in Figure 5-18.
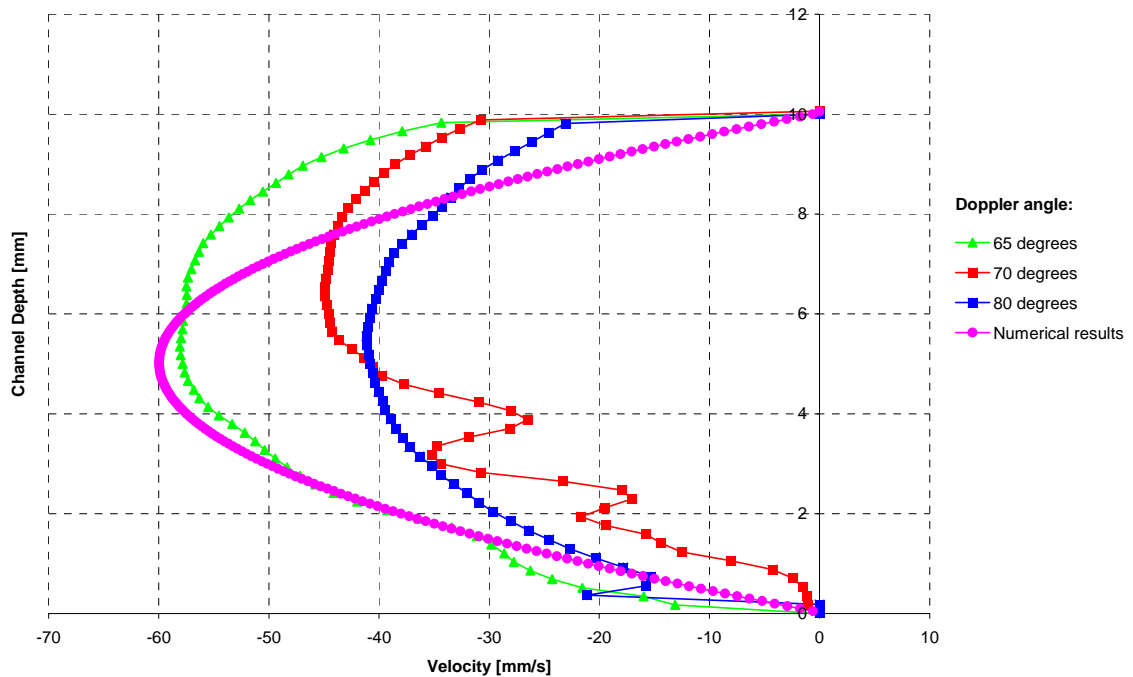
Figure 5-18: Velocity Profiles for Different Doppler Angles

First of all, it can clearly be seen in Figure 5-18 that changes in the Doppler angle eliminate perturbations in the velocity profile. Therefore, changing the Doppler angle may decrease the effect of the Plexiglas wall on the measured velocity profile.

It can also be clearly seen in Figure 5-18 that decreasing the Doppler angle, i.e. increasing the measurable velocity component in direction of the ultrasonic beam axis, reduces the maximum velocity offset. For a Doppler angle of 65 degrees, the measured maximum velocity differs from the numerically calculated maximum velocity by approximately only 3 percent.

For higher or much lower Doppler angles, the measured maximum velocity is further decreased leading to an even higher maximum velocity offset. It is much harder to single emitting and receiving transducers to receive reflections from the targets (particles) for

lower Doppler angles than for angles that ensure that the ultrasonic beam is as close to normal to the medium interface as possible.

Nevertheless, changing the Doppler angle does not reduce the broadening of the measured velocity profile especially close to the bottom channel wall.

5.5.11 Effect of Particle Concentration

Another approach to improve the accuracy of the measured velocity profiles especially close to the bottom channel wall is to increase the particle concentration. By increasing the particle concentration, the intensity of the received ultrasonic echo will increase and may lead to more accurate measured velocity profiles. In order to evaluate the effect of the particle concentration, velocity profiles have been measured 10 mm before the step with 4 different particle concentrations: 0.01 percent, 0.1 percent, 0.5 percent and 1 percent. Measurement results are given in Figure 5-19.
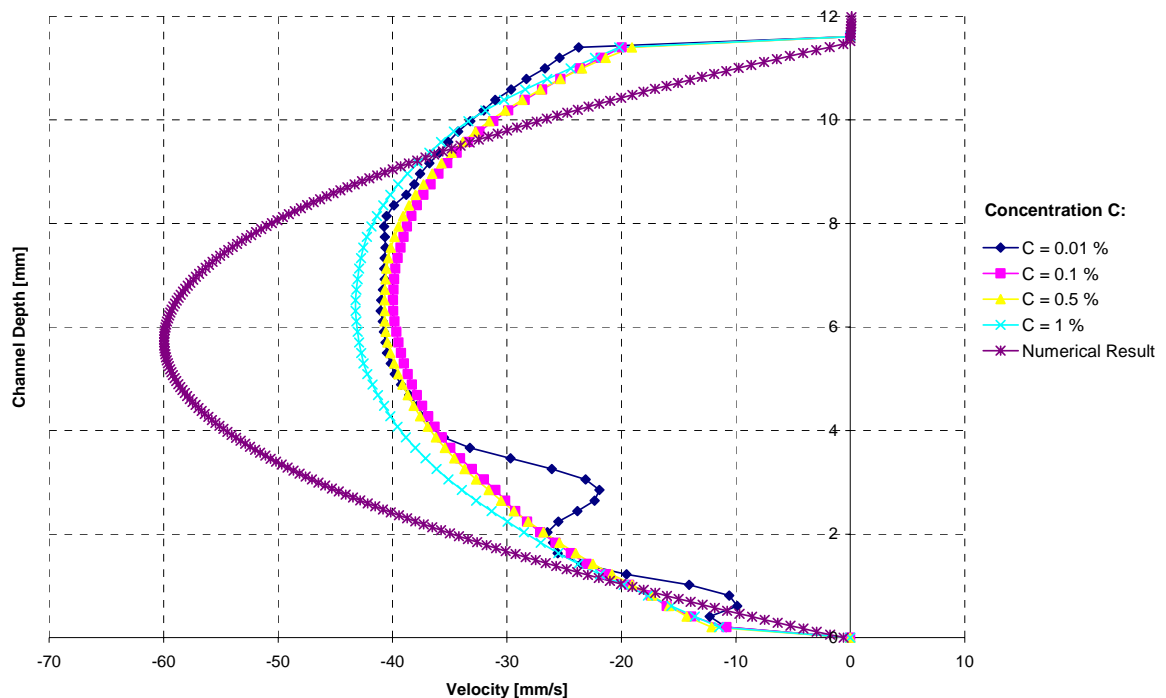
Figure 5-19: Velocity Profiles for Different Particle Concentrations

In Figure 5-19, it can clearly be seen that for increased particle concentrations, perturbations in the velocity profile are eliminated. Looking at Figure 5-19, it becomes obvious that for increased particle concentrations, the measured maximum velocity

increases. Moreover, broadening of the velocity profile is slightly decreased. Due to pump limitations, the particle concentration cannot arbitrarily be increased.

5.5.12 Effect of Spatial Filter and Burst Length

In general, a compromise between the length of the range area and the velocity resolution must be made (see chapter 2.6.6). Therefore, the effect of the spatial filter and the ultrasonic burst length on the measured velocity profile has been evaluated.

Theoretically, if a short pulse is used, a small area is probed, but the pulse spectrum and resulting velocity spectrum are wide and give a low velocity resolution, i.e., increasing the spatial resolution decreases the accuracy of the estimation of the Doppler frequency. For a longer pulse the reverse is true, i.e., an accurate estimation of the target velocity requires a narrow spectrum, and thus a long emitted pulse. On the other hand, such an emission will decrease the depth resolution. A long range gate is employed, and a narrow spectrum evolves. The spectral resolution is also determined by the number of pulses (N) used, as the bandwidth of the narrow spectra is proportional to f_{prf}/N. A long observation time, NT_{prf}, yields a small bandwidth.

In the hope of improving the measurable maximum velocity, the value for the spatial filter and the ultrasonic burst length has been varied. Nevertheless, changing the value for the spatial filter and the ultrasonic burst length did not decrease the discrepancy between the measured and numerically calculated velocity profile, nor did it improve the shape of the measured velocity profile.

5.5.13 Effect of Ultrasonic Transducer

In order to evaluate the effect different ultrasonic transducers and compare unfocused to focused transducers, velocity profiles have been measured with the 4 MHz 5 mm unfocused and 4 MHz 8 mm focused ultrasonic transducer as well. The following parameters are chosen to determine the velocity profile at a Reynolds number of 400 for the 4 MHz 5 mm unfocused transducer and the 4 MHz 8 mm focused transducer respectively. Measurement parameters are given in Table 5-2 and Table 5-3 respectively.

Table 5-2: Measuring Parameters 4 MHz 5 mm Unfocused Transducer

Classifi-cation	Description	Data/Comments		
Instrumentation Parameters	Emission:	Emitting frequency [MHz]:	4	
		Emitting power:	Medium	
		Pulse repetition frequency [Hz]:	3500	
		Emitting burst length [cycles]:	2 (equals 0.82 mm in chosen fluid)	
	Reception:	Resolution [mm]:	0.205	
		Sensitivity:	Very high	
		Starting depth [mm]:	distance L_1 + resolution	
		Spatial filter [mm]:	0.73	
		Number of gates:	128	
	Processing Condition:	Time gain control [dB]:	Start value:	34
			End value:	46
			Overall gain:	6
		Profiles to record:	256	
		Emissions/profile:	256	
		Skip profile:	0	
		Module scale:	1	
		Velocity scale:	1	
		Doppler angle:	Angle [°]:	70
			Distance l_1 [mm]:	1.46
			Distance l_2 [mm]:	2.66
			Distance l_3 [mm]:	min. 10.64
				max. 15.96
			Distance h_1 [mm]:	2.05
			Distance h_2 [mm]:	2.5
			Distance h_3 [mm]:	min. 10
				max. 15
		Transducer offset [mm]:	Target at 4 mm:	0.89
			Target at 15 mm:	1.9
			Target at 20 mm:	2.4
		Corrected Distances [mm]:	Distance L:	3.18
			Distance L_1:	4.07
			Distance $L_{2,min.}$:	5.08
			Distance $L_{2,max.}$:	5.58
		Sound speed [m/s]:	Ultrasonic gel:	1480
			Plexiglas:	2750
			Chosen fluid:	1629
	Transducer:	Piezoelectric element diameter [mm]:	5	
		Transducer case diameter [mm]:	8	
		Focus:	Unfocused	
Fluid Parameters	Kind of fluid:	Water		
	Temperature [°C]:	20		
	Reynolds number:	400		
	Flow rate [l/min]:	1.92		
Fiber/ Particle Parameters	Kind of particles/fibers:	Thermoplastic CoPolyamide resin		
	Shape (simplified):	Spherical		
	Characteristic length:	3 μm diameter		
	Concentration [%]:	0.1		

Table 5-3: Measurement Parameters 4 MHz 8 mm Focused Transducer

Classifi-cation	Description	Data/Comments		
Instrumentation Parameters	Emission:	Emitting frequency [MHz]:	4	
		Emitting power:	Medium	
		Pulse repetition frequency [Hz]:	3500	
		Emitting burst length [cycles]:	2 (equals 0.82 mm in chosen fluid)	
	Reception:	Resolution [mm]:	0.205	
		Sensitivity:	Very high	
		Starting depth [mm]:	distance L_1 + resolution	
		Spatial filter [mm]:	0.73	
		Number of gates:	128	
	Processing Condition:	Time gain control [dB]:	Start value:	42
			End value:	46
			Overall gain:	6
		Profiles to record:	256	
		Emissions/profile:	256	
		Skip profile:	0	
		Module scale:	1	
		Velocity scale:	1	
		Doppler angle:	Angle [^{0}]:	70
			Distance l_1 [mm]:	2.18
			Distance l_2 [mm]:	2.66
			Distance l_3 [mm]:	min. 10.64
				max. 15.96
			Distance h_1 [mm]:	2.05
			Distance h_2 [mm]:	2.5
			Distance h_3 [mm]:	min. 10
				max. 15
		Transducer offset [mm]:	Target at 4 mm:	1.7
			Target at 15.5 mm:	3.84
			Target at 21 mm:	4.25
		Corrected Distances [mm]:	Distance L:	3.97
			Distance L_1:	5.67
			Distance $L_{2,min-}$:	7.81
			Distance $L_{2,max-}$:	8.22
		Sound speed [m/s]:	Ultrasonic gel:	1480
			Plexiglas:	2750
			Chosen fluid:	1629
	Transducer:	Piezoelectric element diameter [mm]:	8	
		Transducer case diameter [mm]:	12	
		Focus:	Focused	
Fluid Parameters	Kind of fluid:	Water		
	Temperature [^{0}C]:	20		
	Reynolds number:	400		
	Flow rate [l/min]:	1.92		
Fiber/ Particle Parameters	Kind of particles/fibers:	Thermoplastic CoPolyamide resin		
	Shape (simplified):	Spherical		
	Characteristic length:	3 μm diameter		
	Concentration [%]:	0.1		

Measuring the velocity profile at 10 mm before the step with the 8 MHz 5 mm transducer, the 4 MHz 5 mm unfocused transducer and the 4 MHz 8 mm focused transducer yields the following results given in Figure 5-20:
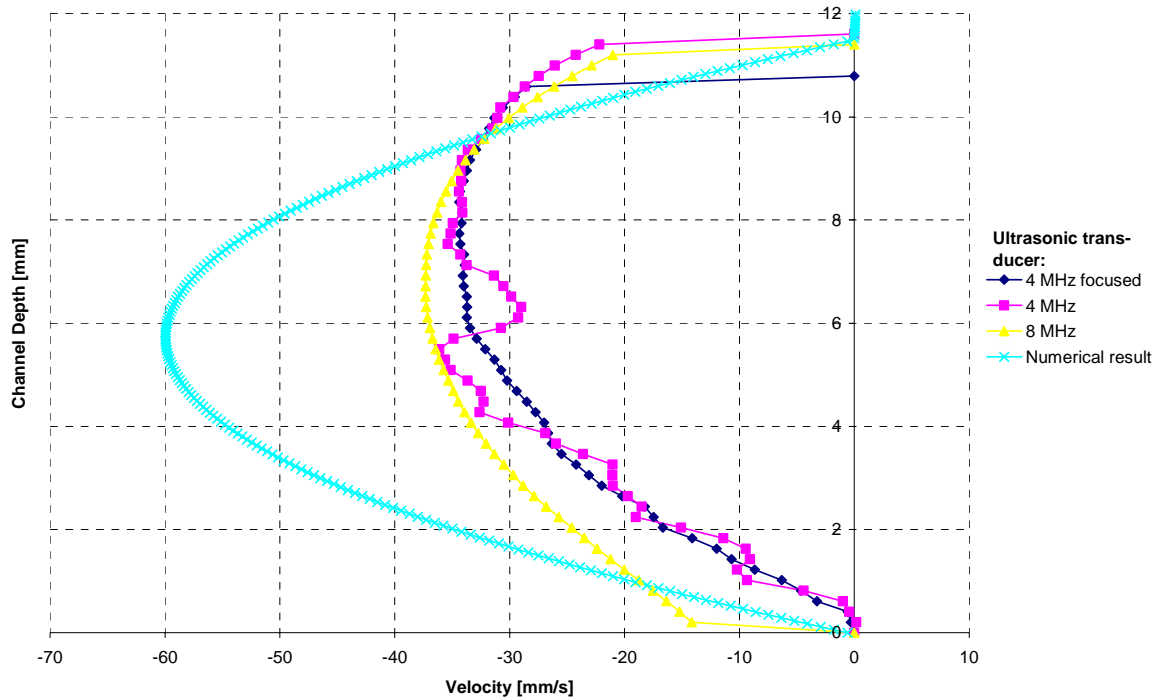
Figure 5-20: Velocity Profiles for Different Ultrasonic Transducers

In Figure 5-20, it can clearly be seen that it is most appropriate to measure velocity profiles in small channels with the 8 MHz ultrasonic transducer. The larger wavelength of the 4 MHz ultrasonic transducers leads to a poorer spatial resolution, both axial and lateral. The effect of the poor lateral resolution of the 4 MHz transducers can clearly be seen in Figure 5-20 by looking at the perturbations in the velocity profile. In general, improved spatial resolution with higher frequency is accompanied by decreased penetration depth as a result of increased attenuation. In the case of measuring the velocity profile in small channels and capillaries, this effect is not important. Due to the broader saturation region of the 4 MHz transducer compared to the 8 MHz transducer (identified in Section 4.4.1), the accuracy of the measured velocity close to the channel top wall is significantly decreased.

Since the lateral resolution is equal to the ultrasonic pulse width, measurement results of the 4 MHz focused transducer are better than the results achieved with the 4 MHz

unfocused transducer. Single element focused transducers use an acoustic lens to effectively shift the location of the focal point toward the transducer face. The end result is a dramatic increase in sensitivity. Moreover, the smaller the beam diameter, the better the lateral resolution and the greater the amount of energy that is reflected by the targets (particles). The measurement results of the 4 MHz focused transducer are therefore better than the measurement results of the 4 MHz unfocused transducer.

5.6 Evaluation of Velocity Profile Measurements with PUDV in Small Channels

Several characteristics and limitations of the Doppler velocity detection method are immediately obvious from the measurement results presented in this chapter. In general, the Doppler profile peak is only about 70% of the actual maximum velocity. This discrepancy between the measured and actual maximum velocity may be decreased by changing the Doppler angle and increasing the particle concentration. Nevertheless, the then still existing discrepancy is ultimately due to averaging by the finite sample volume and to frequency-meter characteristics.

Moreover, the location of the maximum Doppler frequency estimation is slightly down range from the actual maximum-velocity location. This offset is due also to the averaging effect of the sample volume.

Even though all important measurement parameters have been varied, the broadening of the measured velocity profile did not significantly decrease. As mentioned above, broadening of the measured velocity profile may be due to the effect of the bottom channel wall and reflections from previous ultrasonic burst emissions. Another explanation for the broadening of the measured velocity profiles is the observation during measurements that velocities and echoes of the targets (particles) in the ultrasound field changed rapidly with time. This causes a broadening of the Doppler spectrum und therefore decreased velocity resolution (as described in Section 2.6.6). This effect may consequently cause broadening of the measured velocity profile.

Gross disturbances, such as large vortices, may cause irregular spectra with large isolated forward and reverse components. This may also lead to spectral broadening and

decreased velocity resolution. Gross disturbances at higher Reynolds numbers in the recirculation region of the flow over the backward facing step (described in Section 5.5.9) may also be the explanation for the false velocity values in the recirculation area at the measurement point 10 mm behind the step (see Figure 5-17).

Another shortcoming of pulsed ultrasound Doppler velocimetry is that the distances indicated on the measured velocity profiles are greater than the actual channel height (including the orientation angle). The reason for this is the effect of the transducer offset, caused by the selection of the spatial filter, and the effect of the Plexiglas wall, caused by a different speed of sound in the media encountered by the ultrasonic beam. Another reason for the limited range resolution is the sample volume length and therefore limited range resolution.

The effect of a wall and the sample volume length on the determination of the velocity profile is described in Section 2.6.5 and visualized in Figure 2-20. Therefore, the center of the first sample volume inside the channel should be positioned in a way, that the distance from the center of the sample volume equals the value for the resolution. Then, in the ideal case, the sampling volume should be completely inside the channel and not inside the wall. Due to the Doppler angle, the teardrop shape of the sample volume and acoustic ringing, which de facto extends the ultrasonic burst length, this will never be the case. Therefore, an approach to minimize the effect of the wall proposed by Xu and Aidun [64] should be leveraged. Assuming a disc shape sample volume, Xu and Aidun proposed to eliminate zero velocity values measured inside the wall and consequently correct the position of the center of the sample volume and therefore the position of the first measurement point. Following this approach and considering the teardrop shape of the sample volume (as described in Section 2.6.4), the range resolution of the pulsed ultrasound Doppler velocimetry can be further increased. Nevertheless, in order to follow this approach, the transducer offset and the offset caused by different values for the speed of sound in various media along the ultrasonic beam axis must be taken into to account to exactly identify the specific sample volume. Another approach to minimize the effect of the wall is to calculate the ideal position of the first sampling volume and then adjust the positioning of the ultrasonic transducer accordingly. Nevertheless, due to the ringing noise of the ultrasonic transducer, a small part of the first sample volume will always be

inside the wall. In any case, zero velocity values measured inside the wall must be eliminated manually to improve the resolution of the instrument.

Another reason for the lack of range resolution in the experimental results is the problem of wall reflection. As the sample volume reaches the far wall of the channel, some of the acoustic energy is reflected back into the flow field. This reflected energy is scattered by the moving particles to produce detected Doppler shifts. Since they occur after the sample volume has begun to leave the flow field, they give rise to fictitious frequency-versus-range information. In effect, the instrument is beginning to plot an image profile. This is described in more detail in Section 6.3.

The broadening of the measured velocity profile may also be explained by these wall reflections but also to spectral broadening caused by observed velocity fluctuations and gross disturbances in the recirculation region.

A general drawback of ultrasound Doppler velocimetry is that flow perpendicular to the beam is not detected and finding the velocity direction can, in some cases, be problematic. It must always be considered that the velocity profile is measured along the ultrasonic beam axis and not perpendicular to the flow. Therefore, care must be taken when comparing for example a velocity profile measured along the ultrasonic beam axis and a perpendicularly to the flow calculated velocity profile. Especially in the presence of recirculation regions or other gross disturbances, this may lead to distortions of the measured velocity profile. Since the Doppler angle must generally be decreased to avoid perturbations in the measured velocity profile or to increase the velocity component in direction of the ultrasonic beam (to obtain more accurate measurement results for example of the maximum velocity), these distortions may be severe.

Evaluation of the measurement results shows that focused transducers yield better results than unfocused due to higher lateral resolution and increased sensitivity.

The specific limitations of pulsed ultrasound Doppler velocimetry in small channels and separated flow at low velocities identified in this chapter are generalized and summarized in Chapter 6 together with the fundamental limitations identified in previous chapters.

6 Limitations of Pulsed Ultrasound Doppler Velocimetry

Based on the fundamentals of pulsed ultrasound Doppler velocimetry, beam shape measurements of various ultrasonic transducers with and without walls and porous screens and measurements of velocity profiles in the flow over a backward facing step in a small rectangular channel, the limitations of pulsed ultrasound Doppler velocimetry have been determined. After stating the simplifying assumptions of pulsed ultrasound Doppler velocimetry, its accuracy and the effect of artifacts, specific limitations are identified in this chapter.

6.1 Simplifying Assumptions

Three simplifying assumptions must be made in ultrasound Doppler velocimetry. First, the isotropic acoustic velocity is the same throughout the sample volume. Second, the ultrasonic pulse travels in a straight line so echoes returning at later times are interpreted by the range equation as being caused by proportionately distant reflectors. When there are large directional changes of the propagating ultrasonic pulse due to refraction, reflection from oblique highly reflecting interfaces, or reverberations between two highly reflecting interfaces, this assumption is no longer true and image artifacts will result. Third, all detected reflectors are located on the beam central axis. This assumption is mostly untrue but gives reasonably accurate spatial information at image depths where the focused beam pattern is narrow. At image depths where the beam pattern is wide, this assumption leads to blurring of reflector position lateral to the beam central axis for high-contrast reflectors.

Concerning velocity estimation, the following assumption is made. Noise is ignored and the motion of the particle transversal to the direction of the ultrasonic beam (the direction of the measured motion) does not introduce a significant change in the signal received from the particle. Consequently the shift in the position of the particle is assumed to be the dominant source of change in the received signal and the drop in intensity due to either transverse or axial movement of the particle is ignored. The measurements ordinarily require the idealization that the ambient velocity and acoustical properties

appear unidirectional and stratified in the plane that contains transmitter and scatterer and is tangential to the scatterer's velocity vector.

6.2 Accuracy and Noise

The accuracy of the velocity measurement and the resolution in position and time are deeply related to the selection of frequency of ultrasound, its pulse structure and electronic constants for data acquisition. The accuracy in general is largely affected by the system configuration and specifications of the electronic design. It is modified by adapting different basic frequencies, beam diameters, maximum measurable depths, and an algorithm to detect the Doppler shift frequency, as well as by fluid properties [55].

Any erroneous information included in the ultrasonic image can be considered noise. There are many sources of noise. Noise in Doppler systems arises from a number of sources. A very important source is the finite size of the sample volume and the coherent interference of the resulting echo signals of the transducer front surface [44]. Other important sources of noise are:

(i)   The equivalent input noise of the amplifier

(ii)   The demodulator acting as a mixer

(iii)   Reflections from other moving structures apart from those of primary interest, and movements of the transducer

Noise contained in the signal originates from both external and internal sources. All electronic signals returning to the computer for analysis are contaminated by electronic noise as well as by low intensity signals. The electronics used to amplify the weak transducer signal contributes thermal or white noise to the signal and the transducer, although shielded, picks up stray signals through stray coupling to the atmosphere and surrounding noise sources. If the system has too large a bandwidth, random noise will become a factor [47].

Real Doppler signals always contain a certain amount of noise. The cut-off frequency will naturally affect the signal to noise ratio. There is an optimum value of the product of the bandwidth and the impulse duration which will give the maximum signal to noise ratio,

provided the frequency and temporal characteristics of the noise are known. This value also depends on the characteristics of the filter and the signal to be filtered.

6.3 Artifacts

In sonography, an artifact is anything not properly indicative of the structures imaged. It is caused by some characteristic of the imaging technique. Display artifacts include reverberation, refraction, mirror image, shadowing and enhancement.

With two or more reflectors in a sound path (one may be the transducer face), multiple reflections (reverberations) occur. Reverberations are the presence of multiple echoes reflected from the same object. When an echo of relatively strong intensity returns to the transducer surface, a portion of this echo signal is reflected back and hits the same object again before it returns once more to the transducer. Hence, two echoes of the same object are generated from a single ultrasound pulse. The delay inherent in the second echo signal causes the ultrasound unit to display a second image of the object at twice the original depth location. This results in the placement on the image of reflectors that are not real. They are placed beyond the second real reflector at separation intervals equal to the separation between the first and second real reflectors [26].

Refraction can cause a reflector to be positioned improperly on the display. In a mirror-image artifact, objects that are present on one side of a strong reflector are presented on the other side also.

Shadowing is the reduction in an echo's intensity from reflectors that lie behind a strongly reflecting or attenuating structure. Enhancement is the increase in an echo's intensity from reflectors that lie behind a weakly attenuating structure. Shadowing and enhancement result in reflectors being placed on the image with intensities that are too low and too high, respectively.

Another potential artifact is that of side lobes, most commonly noted with phased-array transducers. Ultrasonic waves generated by piezoelectric crystals travel in all directions. A special transducer design, coupled with computer-controlled triggering of these crystals, generates a single beam of ultrasound that travels predominantly in one direction. However, this process is not perfect. Multiple ultrasound beams of weaker

intensity may still originate and will travel in a slightly different direction than the original beam. Because of the weaker intensity, echoes reflected from these secondary ultrasound beams are also weak and commonly rejected in the final image processing. However when such weak ultrasound beams are reflected from a strong interface, the resulting echoes may be of sufficient intensity to be recorded. Hence, the final echocardiographic image will display a strong echo originating from the main ultrasound beam together with weaker, ill-defined echoes on either side, extending throughout the edges of the sweep.

As described above, interfaces reflect and modify the acoustic field. The intensity of the acoustic field received in a point depends on the material, on the shape and on the number of interfaces crossed by the ultrasonic waves. This means that it is often very difficult to have a good knowledge of the ultrasonic intensity. This lack of knowledge does not allow a precise determination of the size of the measuring volume. The interfaces may generate, in certain situations, artifacts and induce modifications in the velocity profiles.

The ultrasonic beam reflected by the far interface of Figure 6-1 transforms this interface in a transmitter. The same particles contained in the liquid will backscatter a second time energy in the direction to the transducer. The depth associated to the path ABC is located outside the flowing liquid. Imaginary velocity components are added to the real velocity profile. The measurement of velocities near the far interface is affected by this phenomenon. The size of the ultrasonic beam determines mainly the level of this artifact. The effect mentioned above explains why it is impossible to obtain a zero velocity value at the far wall as shown in Figure 6-1.
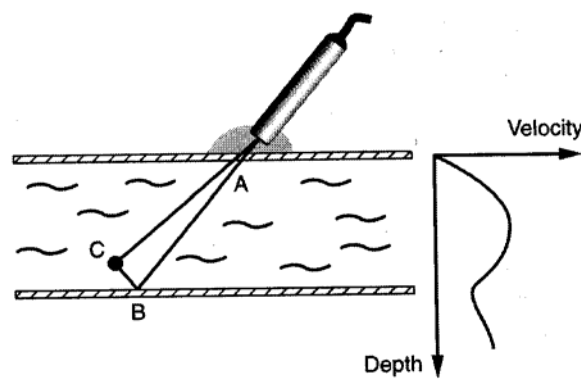
Figure 6-1: Imaginary Velocity Components at the Far Wall [51]

Figure 6-2 displays another situation often encountered. The reflected ultrasonic waves inside a wall enlarge the ultrasonic beam and complicate the determination of the depth of the gates. This phenomena appears if the difference in the acoustic impedance between the liquid and the interface is high, as for instance in steel. In such a case, a lot of acoustic energy remains in the steel, which induces longer saturation of the receiver and a loss in depth resolution [51].
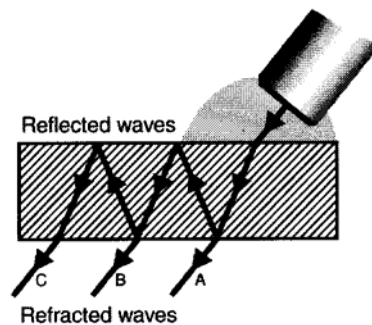
Figure 6-2: Reflection and Refraction [51]

The reflections in both cases mentioned above disturb the determination of the size and the shape of the measuring volume. The thickness, the acoustical impedance and the attenuation coefficient of the interface determine the level of this phenomenon.

6.4   Specific Limitations of Pulsed Ultrasound Doppler Velocimetry

Specific limitations that have been identified by reviewing the fundamentals of pulsed ultrasound Doppler velocimetry and by measuring the ultrasonic beam shape as well as velocity profiles in a small rectangular channel are presented in the following.

6.4.1   Maximum Depth and Velocity

With continuous ultrasound Doppler velocimetry (as well as Laser Doppler Velocimetry) there is no practical limit on the maximum velocity that can be measured. This is not so with pulsed ultrasound Doppler velocimetry because of the finite sampling rates employed.

In order to extract a Doppler shift from the ultrasound signal, the velocimeter compares the phase relationships between a signal from a reference oscillator and each successive returning ultrasound pulse.

The maximum phase change that can be observed between two pulses is limited to the range $-\pi$ to $+\pi$ radians (since angular measurements repeat themselves every 2π radians). Because phase is cyclic, if the Doppler shift frequency is not sampled sufficiently, the phase change between samples may exceed $+/- \pi$ radians but, in the absence of additional information will still be interpreted as lying within this range. Therefore if the target moves a distance of more than $\lambda/4$ between samples (equivalent to a round-trip distance of $\lambda/2$ for the ultrasound pulse) its velocity may be interpreted incorrectly.

This limitation is simply an expression of the sampling theorem (Shannon theorem), which states that it is necessary to sample a signal at least twice the highest frequency present in the signal to avoid ambiguity. Mathematically this may be stated as: $f_{D,max} = f_s/2$ where $f_{D,max}$ is the maximum Doppler shift that can be unambiguously detected, and f_s is the pulse repetition frequency or sampling frequency. The critical frequency $f_s/2$ is commonly known as the Nyquist frequency. This limitation arises because each transmitted pulse is identical and therefore echoes form different transmitted pulses cannot be distinguished. Basically, in order to avoid range ambiguity it is necessary that only one ultrasound pulse is in flight at any given moment.

Consequently, the maximum detectable velocity is determined by the maximum measurable Doppler shift frequency. Unfortunately, as the information is available only periodically, this technique suffers from the Nyquist theorem. As mentioned above, according to Nyquist sampling theory, to adequately describe a signal, it must be sampled at a frequency equal to, or higher than twice the highest frequency present. This requirement places a restriction on the maximum detectable Doppler frequency f_{max}:

$$f_{max} = \frac{1}{2 \cdot T_{prf}}$$

Equation 36: Sampling Frequency

where T_{prf} is the pulse repetition period. This means that a maximum velocity exists for each pulse repetition frequency. If the time between two emissions is too long, fast

particles have moved too much to yield echoes that correlate. At the other extreme, slow particles show no detectable displacements between two emissions if the repetition frequency is too high. Substituting Equation 36 into the Doppler shift equation, the maximum detectable velocity v_{max} will be:

$$v_{max} = \frac{c}{4 f_e \cos\theta \, T_{prf}}$$

Equation 37: Maximum Velocity

where c is the speed of sound, f_e is the emitting frequency and θ the Doppler angle. To some extent, the operator can increase v_{max} by choosing a low carrier frequency or a large Doppler angel. To avoid range ambiguities, the signal must be received before the next subsequent transmission, limiting the maximum value of the pulse repetition frequency.

If the measured velocity is higher than this maximum velocity, a phenomenon named aliasing appears. In general, aliasing is the measurement of an incorrect or false frequency (just as an alias refers to an assumed or false name). In Figure 6-4, the solid line represents a sound wave with a period of T seconds and frequency $f = 1/T$ Hertz. Let the wave be sampled at intervals of T_s seconds corresponding to a sampling rate (sampling frequency) of $f_s = 1/T_s$. It can be seen from the figure that the selected sampling rate is too low. The frequency would be incorrectly identified as that of the dashed line. Aliasing can occur when fast Fourier transformation analyzers and other digital signal processing instrumentation are used. If the measured noise contains frequency components above the Nyquist frequency (half the sampling rate), then aliasing may occur. If those high-frequency components are of interest to us, we must increase the sampling rate. In some cases, high frequency signal components may result from electrical "noise" or other artifacts. Low-pass anti-aliasing filters may be incorporated into fast Fourier transformation and other analyzers to prevent spurious results due to high-frequency signal components that we do not wish to measure [61].
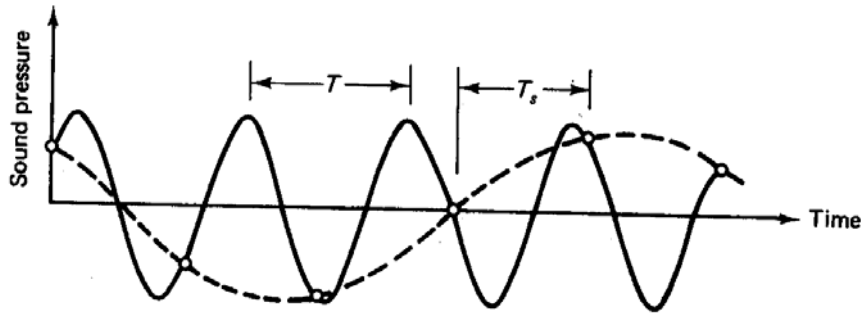
Figure 6-3:Aliasing [61]

The problem of aliasing in pulsed wave Doppler systems arises because the Doppler shift signal is reconstructed by determining the phase changes that occur between the returns from each successive transmitted pulse. Aliasing is a phenomenon that appears when an analog signal is sampled at a frequency which is lower than the half of its maximum frequency (as described above). In such a situation, all Doppler frequencies above the half of the sampling frequency ($1/T_{prf}$), the Nyquist frequency, are folded back in the low frequency region. This phenomenon is called aliasing. In Figure 6-4 the effects of aliasing encountered in pulsed ultrasound Doppler velocimetry is illustrated.
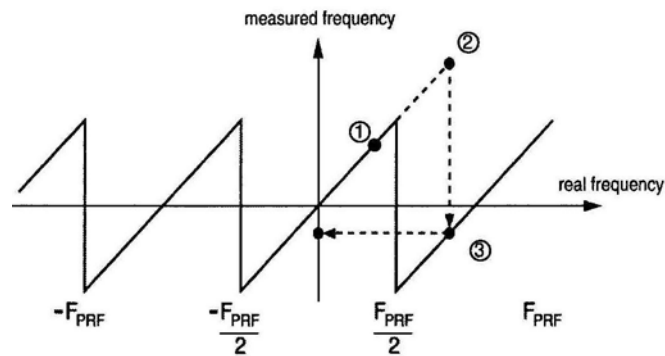
Figure 6-4: Aliasing Frequency Backfolding [51]

At point 1, the real Doppler frequency is below the Nyquist limit ($F_{prf}/2$), so the measured frequency is equal to the real frequency. At point 2, the real Doppler frequency is much above the Nyquist limit. Point 2 is then back folded to point 3, which gives negative velocity. This negative frequency is equal to the real frequency from which the sampling frequency is subtracted. For an analog signal it is possible to avoid aliasing by filtering the signal before sampling it. The filter removes all the frequencies above the Nyquist

limit. Unfortunately for pulsed Doppler ultrasound only samples are available and therefore it is not possible to remove the aliasing. The only solution is to adapt the sampling frequency which is nothing but the pulse repetition frequency of the emitted pulses. An easy way to check the presence of aliasing is to examine the evolution of the measured Doppler frequency when the pulsed repetition frequency is changed.

The effect of aliasing in a directional pulsed Doppler ultrasound system (the incorrect interpretation of frequencies above the Nyquist limit) is that as soon as the Doppler shift frequency exceeds $f_s/2$, it is interpreted as being $-f_s/2$ and the top of the velocity profile appears at the bottom of the reverse channel. This situation is shown in Figure 6-5. Although the Doppler shift is normally interpreted as being between $-f_s/2$ and $+f_s/2$, it may be interpreted as any other range of frequencies provided that the total range is only f_s.
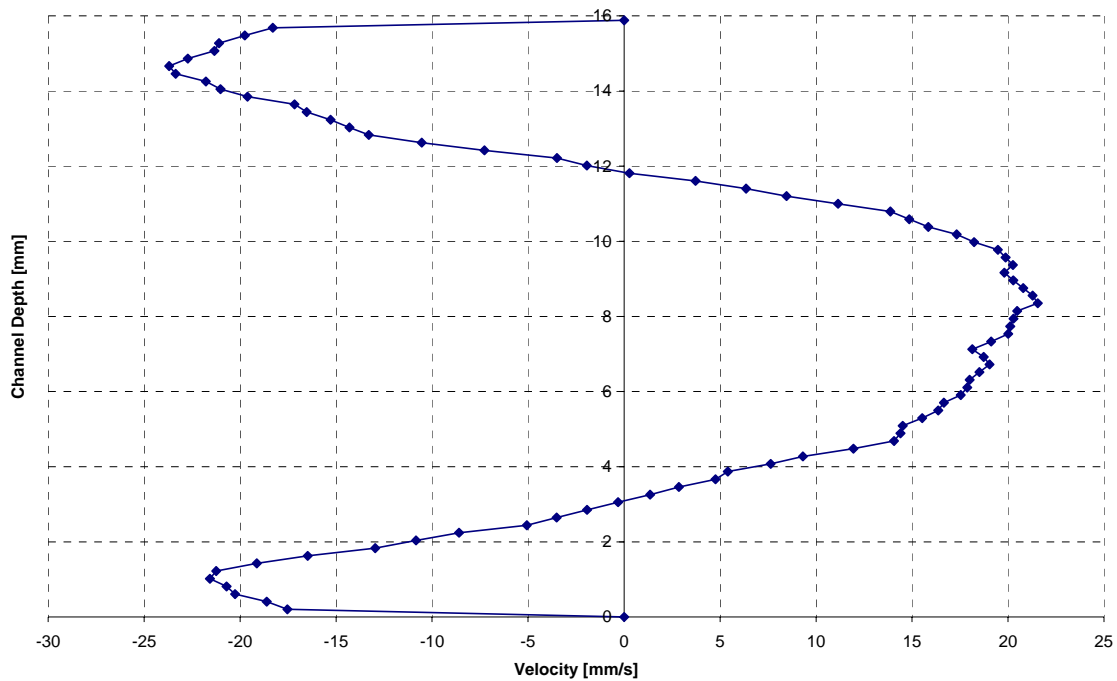
Figure 6-5: Measured Aliasing

By changing the way in which the frequencies map onto the frequency scale (not a change in the permissible frequencies), a shift in the frequency range may result in the correct interpretation of the signal and therefore the correct velocity profile. If possible,

aliasing can easily be corrected by changing the pulse repetition frequency in the instrument.

In other words, if the reflected ultrasound wave is superimposed on the original ultrasound wave, it is clear that they are not identical. This is due to the frequency shift. The phase lag ΔQ between these two sound waves can be measured as shown in Figure 6-6. If the phase lag is greater than 180 degrees in one direction, confusion may arise as to whether this phase lag is truly greater than 180 degrees in one direction, or less than 180 degrees but in the opposite direction.
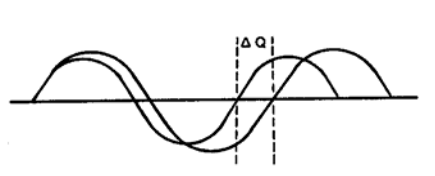
Figure 6-6: Phase Lag [26]

In this situation, flow patterns in both directions will be displayed. This physical phenomenon is frequency aliasing. The Nyquist limit is the numerical value of one-half the pulse repetition frequency. If f exceeds f_{max} (Nyquist limit), then frequency aliasing will occur and the resultant signal will be distorted with respect to the magnitude and direction of the flow being examined. With pulsed ultrasound Doppler velcoimetry, aliasing problems are more troublesome at high frequencies [18]

In general, aliasing is the generation of artifactual lower-frequency signals when the sampling frequency drops below two times the Doppler signal. It results in apparent reversal of flow direction and false interpretation of velocities. Increasing the spectral velocity range produces an accompanying increase in the pulse repetition frequency, and can eliminate aliasing when present. Also adjusting the spectral baseline can eliminate the effect of aliasing, as long as flow is only in a single direction. Reducing the transducer frequency and adjusting the Doppler angle closer to 90 degrees also helps reduce aliasing because these steps result in lower frequency Doppler signals for the same flow velocity.

The obvious solution to overcome aliasing is to sample the signal more frequently, but in pulsed Doppler applications there is an upper limit to this because of the finite propagation time of ultrasound, and the fact that range ambiguity will arise if an ultrasound pulse is transmitted before the previous pulse has had time to return from

targets at the maximum range of interest. Combining the requirements that the sampling frequency must be at least twice the maximum Doppler shift frequency and that each pulse must have time to return from the target before another is transmitted, results in a maximum velocity that can be unambiguously measured at any depth (Equation 39). Various techniques for overcoming aliasing were developed and are described byEvans [18].

In addition to the maximum velocity limitation, there is a maximum depth at which a velocity can be measured. This limit is determined by the time needed for the ultrasonic signal to travel from the transducer to the target and back. This time is fixed by the pulse repetition frequency of the ultrasonic pulses. This maximum depth is equal to:

$$P_{max} = \frac{T_{prf}\,c}{2}$$

Equation 38: Maximum Depth

The range gate in a pulsed Doppler ultrasound system is determined by the time delay between transmission and the commencement of signal acquisition. In fact, there is a degree of range ambiguity since the signals arriving at the transducer at a given time may be echoes from the latest transmission pulse, the previous pulse, or even earlier pulses. Signals are therefore collected from ranges located around P_n given by: $P_n = (c/2)(T_{prf} + nT_{prf})$ where T_{prf} is the time between subsequent pulse transmissions and n is zero or any non-negative integer. In practice, because of attenuation, the signals returning from deeper sample volumes are weaker than signals from the more superficial sample volumes, and if f_s is low they may be negligible. If f_s is high, two or more significant gates may exist and it is for this reason that f_s cannot be increased at will to overcome the maximum velocity limit discussed in the last section.

Another way of viewing this is that, as f_s is increased, pulsed Doppler ultrasound tends to be continuous Doppler ultrasound, where there is no maximum velocity limit but neither is there any depth resolution. If a flowmeter is to use pulses that return during the same transmission cycle and thus avoid ambiguity, the maximum range at which it can operate is given by P_{max}. In practice, v_{max} is effectively independent of transmitted frequency, because at higher frequencies attenuation decreases the range from which significant

echoes can be detected [18]. Some commercial pulsed Doppler ultrasound systems that do not incorporate a continuous Doppler ultrasound facility attempt to overcome the problem of measuring high velocities by deliberately increasing their pulse repetition frequency beyond the maximum required to prevent range ambiguity. Doubling the pulse repetition frequency will cause the device to monitor not only velocities at the depth of interest, but also velocities at a depth which is in between the transducer and the depth of interest. Continuing to increase the pulse repetition frequency will add more equally spaced sample volumes between the transducer and initial depth of interest, but this often does not present a problem as the higher velocities usually only occur at one point in the beam. Reducing the sampling frequency (increasing T_{prf}) will increase the maximum measurable depth, but will also reduce the maximum Doppler frequency that can be measured. The maximum velocity and the maximum depth are thus linked according to the following relation:

$$P_{max} v_{max} = \frac{c^2}{8 f_e}$$

Equation 39: Relation Maximum Depth and Velocity

This shows that the larger the velocity to be measured, the smaller the maximum detectable depth. By using a suitable combination of basic ultrasound frequency, measuring depth and inclination angles, pulsed ultrasonic Doppler velocimetry can be adjusted to the problem at hand. The penetration length of the ultrasonic wave into the fluid depends on the sound absorption of the fluid [29].

At any given instant, an echo signal can come from many different depths, corresponding to echoes from previously emitted signals. The presence of several acoustic interfaces also causes several reflections which could cause a false determination of the target depth. Nevertheless, if the pulse repetition frequency is sufficiently low (a few kHz) the attenuation of previously emitted pulses will render them indiscernible. The same goes for reflected signals. With a large increase in the pulse repetition frequency, pulsed Doppler ultrasound approaches the properties of continuous wave Doppler, with a loss of axial resolution but no maximum velocity limitation.

Generally speaking the higher frequency ranges offer a higher spatial resolution and higher velocity resolution than the lower. Thus high frequency use is ideal for small geometries with small velocity range. 8 MHz is for instance a frequency that would be selected to measure a blood flow. On the other hand the low frequencies allow higher Doppler shift frequency detection corresponding to larger velocities and larger probing distance. Moreover they have better propagation abilities through the measured liquid as well as through walls when non-intrusive probing is required. In return lower frequency means larger waveform and thus poorer spatial resolution, but because of larger measurement volume in a higher velocities environment the flux of reflectors is increased resulting in a higher sensitivity of the related transducer.

6.4.2   Spatial Versus Velocity Resolution

As mentioned earlier, a compromise between the length of the range area and the velocity resolution must be made. If a short pulse is used, a small area is probed, but the pulse spectrum and resulting velocity spectrum are wide and give a low velocity resolution, i.e., increasing the spatial resolution decreases the accuracy of the estimation of the Doppler frequency. For a longer pulse the reverse is true, i.e., an accurate estimation of the target velocity requires a narrow spectrum, and thus a long emitted pulse. Such an emission will decrease the depth resolution. A long range gate is employed, and a narrow spectrum evolves.

Unfortunately, it is impossible to increase the intensity of the emitted pulse beyond a certain threshold with risking the appearance of unwanted phenomena such as cavitation. If ultrasonic waves are focused into water, tiny bubbles will be produced, forming a fractal structure and radiating sound by themselves as shown in Figure 6-7 [57]. This phenomena is called acoustic cavitation.
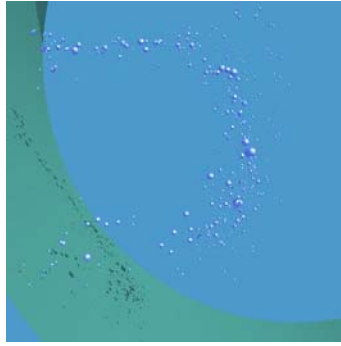
Figure 6-7: Acoustic Cavitation [57]

Reducing the length of the emitted pulse will reduce the signal to noise ratio of the Doppler signal if it is not possible to increase the intensity [51]. The duration of the impulse determines the depth resolution by determining the longitudinal size of the sample volume. The other dimensions are determined by the beam pattern of the transducer.

The spectral resolution is also determined by the number of pulses used, as the bandwidth of the narrow spectra is proportional to f_{prf}/N. A long observation time, NT_{prf}, yields a small bandwidth.

Velocity resolution not only depends on the length of the range area, but also on the time resolution of the ultrasound system. Especially in the case of turbulence and gross disturbances, time resolution is essential.

6.4.3 Focused Transducer Limitations

Different architectures of focused transducers are described in detail in chapter 3.4. In pulsed wave Doppler systems, accurate frequency measurements require minimal spectral broadening. Highly focused beam patterns can cause excessive spectral broadening [44], which is discussed in detail in chapter 2.6.6.

Spectral broadening can be understood physically from two equivalent viewpoints, one considering the Doppler signals received with a finite array aperture and the other considering the time of flight of the scatterers through the focused beam. With a finite aperture transducer, each portion of its front (or each element in a multi-element array) has a different Doppler angle with the direction of flow and a different detected Doppler shifted frequency. The larger the aperture, the greater the spread of Doppler angles and detected Doppler shifted frequencies. Or, the finite time of flight through the narrowest

beam width leads to a commensurate uncertainty in the measured Doppler shifted frequency. The stronger the focus, the smaller the spot size and the larger the frequency uncertainty.

There are limitations on focal lengths for transducers of particular frequency and element diameter combinations and target designations. According to Papdakis, the maximum practical focal length for a point target focal designation is 0.8 multiplied with the near field length due to spectral broadening [44]. Transducers with focal lengths beyond these maximums, but less than the near field are called weakly focused units. In other words, there may not be an advantage to a focused transducer over that of a flat transducer. In addition to the limitations on maximum focal lengths, there are limitations on the minimum focal lengths. These limitations are typically due to the mechanical limitations of the transducer.

Theoretically, ultrasonic beams can be strongly focused and beam widths smaller than 0.1 millimeter can be achieved [51]. In the case of focused single element transducers, the theoretical limit depends on the material of the lens and the side effect. The side effect simply describes the fact that the piezoelectric element never vibrates in one mode. Other modes exist and the vibration is never in a pure "piston" mode. Therefore, the emitted ultrasonic waves are not exactly plane waves, especially at the border (side) of the transducer.

For single element transducers, the theoretical focal length depends on the diameter of the piezoelectric element. For example, larger diameter piezoelectric elements lead to a small focal zone. The measured focal length of a transducer is dependent on the material in which it is being measured. This is due to the fact that different materials have different sound velocities. When specifying a transducer's focal length it is typically specified for water. Since most materials have a higher velocity than water, the focal length is effectively shortened. This effect is caused by refraction (according to Snell's Law) and must be considered to obtain more accurate measurement results.

In addition, the curvature of the surface of the test piece can affect focusing. Depending on whether the entry surface is concave or convex, the sound beam may converge more rapidly than it would in a flat sample or it may spread and actually defocus.

Focused immersion transducers use an acoustic lens to effectively shift the location of the focal point toward the transducer face. The end result can be a dramatic increase in sensitivity.

6.4.4 Doppler Angle

A general limitation of ultrasound Doppler velocimetry is that flow perpendicular to the beam is not detected and finding the velocity direction can, in some cases, be problematic. It must always be considered that the velocity profile is measured along the ultrasonic beam axis and not perpendicular to the flow. Especially in the presence of recirculation regions or other gross disturbances, this may lead to distortions of the measured velocity profile. Since the Doppler angle must generally be decreased to avoid perturbations in the measured velocity profile or to increase the velocity component in direction of the ultrasonic beam (to obtain more accurate measurement results for example of the maximum velocity), these distortions may be severe. Refraction, as mentioned in section 6.3, may even facilitate this distortion.

Another limitation to further decreasing the Doppler angle is the angle of total reflection. Setting the Doppler angle smaller than the critical angle allows one to use only the transverse wave for the measurement. In fluids, only longitudinal waves exist, but in solids, even at small incident angles, another mode of ultrasonic wave called transverse wave exists (see section 2.6). For example, part of the longitudinal wave is converted into the transverse wave at the outer surface of the Plexiglas wall. This transverse wave is sufficient to measure the velocity in the sample volume.

6.4.5 Distance Offset

Another general limitation of pulsed ultrasound Doppler velocimetry is the distance offset along the ultrasonic beam axis caused by the ultrasonic transducer (depending on the spatial filter) and by acoustic interfaces with different values for the speed of sound encountered by the ultrasonic beam (as described in section 4.4.1, 5.5.3 and 5.5.5). Exact calculations of the distances displayed by the instrument are therefore necessary in advance to correctly interpret the measured velocity profile. Refraction may moreover cause a distance offset along the axis in direction of the flow.

6.4.6 Ringing Effect and Saturation Region

The transducer's ringing effect and the saturation region caused by the transducer's acoustic ringing or highly absorbing acoustic interfaces impedes measurements close to the transducer face or close to the highly absorbing acoustic interfaces (as described in chapter 4.2). The ringing effect (saturation region) can only be decreased by decreasing the amplification or decreasing the emitted ultrasonic power. This might not be possible, when measuring the velocity profile behind highly absorbing acoustic interfaces or in highly absorbing media. If the amplification or emitted power is decreased beyond a certain minimal value, the intensity of ultrasonic echoes from scatterers inside the sample volume may be too low to be received by the transducer.

6.4.7 Ultrasound Scatterers

Ultrasound Doppler velocimetry requires some amount of reflection particles suspended in the liquid, which may disturb its flow or change its fundamental properties. Nevertheless, due to attenuation and reflection, upper limits of particle concentration exist (e.g., 50 percent in blood, 30 percent in mud). If the particle concentration is too low, the received echo may be too weak and measurement results may easily be perturbed or falsified by slight variations in the liquid.

The ultrasonic waves generated by the transducer are more or less confined in a narrow cone. As they travel in this cone they may be reflected or scattered when they touch a particle having different acoustic impedance. The scatterers are assumed to be in the far field, so that the waves emitted by the transducer are planar when they impinge on the reflector. If the size of the particle is bigger than the wave length, the ultrasonic waves are reflected and refracted by the particle. In such a case the direction of propagation and the intensity of the ultrasonic waves are affected. But if the size of the particle is much smaller than the wave length another phenomenon appears, which is named scattering. In such a case, a very small amount of the ultrasonic energy is reflected in all directions. The intensity and the direction of propagation of the incoming waves are practically not affected by the scattering phenomena. Thus, the transducer also receives a plane wave. In ultrasound Doppler velocimetry particles smaller than the wavelength are therefore required.

Particles in the presence of a sound field will experience forces associated with the acoustic wave field which may falsify measurement results. The acoustic radiation pressure is customarily interpreted as the time-averaged pressure acting on an object in a sound field, which results in a unidirectional force that moves the object [22]. It is exactly this movement of the object which is important for the accuracy of measurement results with pulsed ultrasound Doppler velocimetry. Since in pulsed ultrasound Doppler velocimetry the shift in position of suspended objects in the sample volume is measured, i.e., the movement of these suspended objects, any movement enforced by the acoustic wave may falsify the measurement results. This limitation has to be further investigated in future research.

Having identified the limitations of pulsed ultrasound Doppler velocimetry based on reviewing the fundamentals of the methods and on measuring the actual beam shape, the echo intensity and the velocity in small channels, suggestions for improvement and future research are given Chapter 7.

7   Suggestions for Improvement and Future Research

Based on the fundamentals of pulsed ultrasound Doppler velocimetry, on the measurements of ultrasonic beam shapes and velocity profiles in the flow over a backward facing step in a small rectangular channel and on the limitations of pulsed ultrasound Doppler velocimetry presented in Chapter 6 suggestions for improving the measurement system and for future research are made in the following. The ultrasonic transducer has been identified as the most critical component of the measurement system in Section 2.5. To improve especially the spatial resolution of the measurement system, it is suggested to use annular phased array transducers and modify the measurement system accordingly. Through electronic focusing, ultrasonic beam steering and automatic variations in the aperture size, annular phased array transducers enhance the spatial resolution of the system significantly. Research on a new ultrasonic transducer architecture combining the advantages of standard pulsed ultrasound Doppler velocimetry and the ultrasound phased array technique is therefore crucial. The necessity of future research on the interaction between acoustic waves and acoustic interfaces encountered by the ultrasonic beam and suspended objects in the flow is emphasized in the following sections. A literature review on the interaction of acoustic waves with cylindrical and spherical objects is then undertaken in Section 7.3 to frame future research in this area.

7.1   Transducer Architecture

The ultrasonic transducer has been identified as the most critical component of the measurement system. The main suggestion for improving pulsed ultrasound Doppler velocimetry therefore is to combine the advantages of standard pulsed ultrasound Doppler velocimetry systems (e.g., real time velocity profile determination) with the advantages of the ultrasound phased array technique (e.g., dynamic beam control, dynamic depth focusing, … described in detail in Section 3.2.2) and enhance the measurement system accordingly (e.g., allow for dynamic focusing, …). Therefore, detailed research on the most appropriate transducer and system architecture is essential.

Most of the applications of the ultrasound phased array technique are currently in the area of ultrasonic testing of components and structures and nondestructive materials characterization. Using the ultrasound phased array technique for the determination of velocity profiles in fluid flow would requires further processing the incoming ultrasonic echo (e.g., dynamic focusing, …). After consultation with the head probe designer of R/D TECH, using the ultrasound phased array technique for the determination of velocity profiles in fluid flow is generally feasible.

According to R/D TECH (www.rd-tech.com), ultrasonic phased array transducers are in the price range of 10,000 to 15,000 US-Dollars. A portable ultrasonic phased array system would be in the price range of 60,000 to 100,000 US-Dollars. Prices ultimately depend on the application and specific requirements (e.g., transducer diameter, number of annular elements, shape of piezoelectric element, level of damping (of piezoelectric element), transducer housing specifications, system electronics, …). Nevertheless, the ultrasonic phased array transducer technique is significantly more expensive than standard pulsed ultrasound Doppler velocimetry (prices of standard pulsed ultrasound Doppler velocimetry and experimental setup are given in Appendix F, Table F-1). This is especially due to the required dynamic focusing technique in phased array systems.

Annular phased array systems, but also phased array systems in general, consist of small piezoelectric elements. Another feature besides dynamic focusing, beam steering etc. of small piezoelectric elements is their energy transfer efficiency (as described in detail in Section 3.2.2). Smaller elements take less energy to excite and are more efficient receivers due to the lower mass to be energized. Lower energy consumption is crucial when measuring over longer distances or through highly absorbing media (e.g., paper forming screens).

To further improve the spatial resolution of pulsed ultrasound Doppler velocimetry especially when dealing with small geometries (small channels or capillaries), it is suggested to investigate the feasibility of emitting frequencies higher than 8 MHz. Higher emitting frequencies lead to improved axial and also lateral resolutions (at a given transducer radius, the beam width decreases with decreasing wavelength). Absorption of the emitted ultrasonic signal will increase with higher ultrasonic frequencies. Since suggestion to improve pulsed ultrasound Doppler velocimetry to measure velocity profiles in especially small channels and capillaries are developed, higher absorption is

not vitally important. Improved axial resolution (shorter ultrasonic burst length) will also be beneficial to minimize the wall effect.

To further minimize the wall effect, but also to minimize the saturation region and maximize the measurable minimal distance, damping of the piezoelectric element and therefore minimizing of the transducer's ringing must be improved.

7.2   Interaction of Acoustic Waves with Forming Screens

On the one hand, the ultrasonic beam shape was determined in chapter 4 to identify the most appropriate transducer to measure velocity profiles in small channels and capillaries. On the other hand, results of the ultrasonic beam shape measurements will be used to evaluate the possibility of applying pulsed ultrasound Doppler velocimetry to measure the velocity through porous screens, i.e., paper forming screen.

7.2.1   Forming Screen Properties

To evaluate the interaction of acoustic waves with the forming screen, its acoustic properties must precisely be determined (e.g., acoustic impedance, pore shape factor, tortuosity, etc.). Numerical simulations with the Lattice Boltzmann method of the propagation of an acoustic wave through the forming screen may also be useful to further investigate the effect of the forming screen on the ultrasonic beam.

Moreover, laboratory experiments to optimize the acoustic-wire impedance matching are essential to improve the signal to noise ratio. Other reports show that the main problem is the power required to run the system. Once the laboratory experiments are complete, the information to make conclusions about the required power consumption is available. The feasibility of using the ultrasonic phased array technique instead of standard pulsed ultrasound Doppler velocimetry may then be evaluated.

7.2.2   Modification Existing Experimental Setup

In order to investigate the possibility of using pulsed Doppler ultrasound velocimetry to measure the velocity profile of watery pulp through the forming board and the forming screen, the experimental setup described in chapter 3 is modified. The fluid leaving the

channel flows over a forming screen. The forming screen will be mounted on the steps in both side walls of the section attached to the channel (Figure 7-1). Various ultrasonic transducers are then used to measure the velocity profile through the forming screen. Outcome of this research will be the information, if and how pulsed Doppler ultrasound velocimetry can be used for this application.
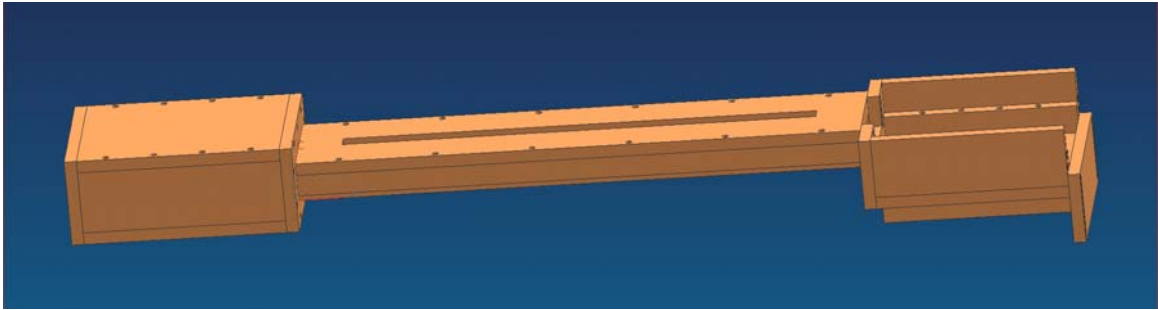
Figure 7-1: Modified Experimental Setup

7.2.3   General Effect of Moving Interfaces

After pulsed Doppler ultrasound velocimetry has been successfully used to measure velocity profiles through stagnant forming screens, the effect of moving interfaces (e.g., moving forming screens as encountered in paper machines) must be investigated.

As the ultrasonic waves propagate, they encounter different structures which may create strong echoes (e.g., Plexiglas, forming screen). Furthermore, some of these structures may themselves be moving (e.g., forming screen). Despite of the many reflections which are necessary to reach the transducer, the energy reflected by these interfaces is often stronger than the energy coming from the particles flowing with the liquid. When some interfaces are in movement, the correct estimation of the velocity field is more difficult. The echoes generated by such interfaces may affect the velocity profile in some places due to the combination of many reflections. The Doppler frequency induced by these movable interfaces can not be removed if their values are the same as the values of the flowing particles. If their values are different, the echo signal may contain a certain number of stationary and quasi-stationary echoes of low frequency and high intensity, as well as the echoes from the particles within the fluid at higher frequencies but of smaller intensities. The difference between the intensities of these two types of signals may be 20

to 60 dB. For the case of moving flow boundaries, the velocity of the wall creates a Doppler effect which must be filtered out. These low frequency components may be eliminated by the wall motion filter. Unfortunately, this high-pass filter also diminishes the intensities of the already weak Doppler signals coming from the particles within the fluid [51].

Moving screens also represent moving free surfaces and are therefore more like to introduce perturbations in the velocity profile as can be seen in Figure 5-14. Moreover, moving screens will lead to significant spectral broadening.

Besides the effect of large scale acoustic interfaces (e.g., Plexiglas walls, forming screens, etc.) on the ultrasonic wave packet, its interaction with the suspended objects (particles or fibers) in the fluid must be investigated. Especially since the acoustic wave packet, or acoustic waves in general, exert forces on the suspended objects, this interaction and its effect on the measurement results must be investigated.

7.3 Interaction of Acoustic Waves with Suspended Objects

When evaluating the effect of acoustic waves on the accuracy of the measurement results in pulsed Doppler ultrasound velocimetry, an investigation of the dynamics of the acoustic wave interaction with suspended objects in the sample volume is crucial. An object in the presence of a sound field will experience forces associated with the acoustic wave field which may falsify measurement results.

The so called acoustic radiation force is the time-average force exerted by an acoustic field on an object ("target") or on a boundary surface. In scientific practice it occurs as an unintentional effect under various circumstances. So far, its importance lies in its intentional and quantitative use for which at least three main areas can be identified, namely: (a) The radiation force on a balance and serving as a measure of the ultrasonic power; (b) the radiation force on a small target as measured by a sphere radiometer and serving as a measure of the ultrasonic intensity; (c) the radiation force on small liquid and solid samples for purpose of separation techniques and for levitation and positioning purposes, with the aim of a containerless processing [11].

The acoustic radiation pressure is customarily interpreted as the time-averaged pressure acting on an object in a sound field, which results in a unidirectional force that moves the object [22].

It is exactly this movement of the object which is important for the accuracy of measurement results with pulsed ultrasound Doppler velocimetry. Since in pulsed ultrasound Doppler velocimetry the shift in position of suspended objects in the sample volume is measured, i.e., the movement of these suspended objects, any movement enforced by the acoustic wave may falsify the measurement results.

To identify future research opportunities, the following literature review about the acoustic radiation pressure is undertaken. Since in the applications of importance to us (e.g., paper industry, bioengineering) objects suspended in the fluid are mainly spherical particles or cylindrical fibers, I will focus in this literature review on research on the acoustic radiation pressure acting on spheres or cylinders.

7.3.1   Acoustic Radiation Pressure Acting on Spherical Objects

In general, much theoretical and experimental work has been performed on the acoustic radiation pressure acting on spherical or cylindrical objects. Kundt was one of the earliest to study the effect of acoustic forces through measurements on dust particles' motion in resonant tubes in 1866 [36].

A detailed calculation of the acoustic pressure on spheres in a plane standing or progressive wave field in an ideal fluid was first presented by King in 1934 [32]. King calculated the radiation force by summing the effect of acoustic pressures acting on each surface element of rigid spheres freely suspended in a non-viscous fluid. King's method is to solve exactly the problem of the flow in an ideal fluid around a small sphere in the field of a sound wave. The radiation pressure is expressed as a function of the intensity (or a quantity related to the velocity potential) of the sound, the relative densities of the sphere and the medium, and a parameter $\alpha = 2\pi r/\lambda$ where r is the radius of the sphere and λ is the acoustic wave-length in the liquid. For large α, King's model approaches a limiting value. Fox therefore used simple approximations to quickly determine the radiation pressure beyond this limiting value for all values of α from zero to infinity with an accuracy of better than one percent [19].

Since the work on the acoustic radiation force on a rigid sphere in an axisymmetric wave field by King in 1934, the radiation force on a sphere with different properties in different wave field has been reported. Extending and elaborating King's approach, the radiation force on a rigid sphere in a progressive, diverging spherical or cylindrical wave field was reported by Embleton in 1954 [17]. Yosioka and Kawasima extended this method to include the effects of a compressible sphere, i.e., to calculate the radiation force on fluid spheres suspended freely in a plane traveling wave or plane standing wave [66]. According to their theory, the radiation force on a spherical particle in the stationary standing-wave field is proportional to the wavenumber, the ultrasound energy density and the cube of the particle radius. The radiation force on a fluid sphere in a plane traveling wave was later reported again by Maidanik in 1957 [39]. The special case of a rigid sphere in a plane traveling wave was reported by Maidanik and Westervelt in 1957 [40].

Gor'kov, using a different approach than King, derived a simple method to determine the forces acting on a particle in an arbitrary acoustic field in 1962 [21]. The force on a small sphere was expressed as a function of mean square fluctuations of the pressure and velocity at the point where the particle is located. Gorkov derived an expression for the potential of the acoustic force that acts on a small spherical particle in an arbitrary acoustic field in an ideal fluid. He showed that his expression was equivalent to King's in the case of a plane standing wave.

Nyborg also derived simple expression for the acoustic force on a small rigid sphere in an axisymmetric wave by extending the methods of King and Embleton in 1967 [42]. He expressed the radiation force as a function of spatial gradients of potential energy density and kinetic energy density, and suggested that only the field in the vicinity of the sphere needs to be axisymmetric. In the case of standing waves, Nyborg's expression reduced to that of Gor'kov.

In 1969, Hasegawa et al. [24] developed a theory for the acoustic radiation pressure acting on an elastic sphere in a plane progressive sound field, which includes the solution for elastic spheres with complex wave speeds later used for calibration of plane-wave fields [23]. Since then, the subject of the radiation pressure on spheres has been extensively studied [9, 37, 38, 48, 62]. Barmatz and Collas applied the method of Gor'kov for deriving the acoustic radiation potential on a sphere in an arbitrary sound field. Generalized potential and force expression are derived for arbitrary standing wave

modes in rectangular, cylindrical and spherical geometries for the case where the sphere radius is much smaller than the wavelength. The developed expressions were analyzed primarily for a rigid sphere but are also applicable to the general case of samples with arbitrary density and compressibility. A general expression for the acoustic radiation force on a small compressible sphere in a focused beam has been derived and expressed in terms of the time-averaged densities T_i and V_i of kinetic and potential energies, respectively, in the incident sound field by Wu and Du in 1990 [62]. The results have been applied to two focused beams: Gaussian beams and piston beams. The effect of viscosity and surface tension on radiation force due to a plane traveling or standing wave were discussed by Lofstedt and Putterman in 1991 [38]

In most of the studies cited above, a plane incident wave was used due to its simplicity. For the nonplanar incident wave only the rigid sphere has been studied. Various approximations are used by different authors. In 1996, Chen and Apfel unify the various treatments of the radiation force on an elastic sphere (which includes other types of sphere as limiting cases) and provide a general formulation suitable for any axissymmetric incident wave, regardless of the size of the sphere [14]. The sphere is described in general by its density, compressional wave speed and shear wave speed. Other types of spheres, including the rigid and immovable sphere and the infinitely soft sphere (void), are treated as limiting cases. Specialized formulations of the radiation force function are provided for several types of incident waves of common interest. A low-frequency expansion for each case is provided for comparison with results form the literature.

Yasuda and Kamakura correlated predictions made by the theory of the acoustic radiation force as proposed by Yosioka and Kawasima with actual experimental data in 1997 [65]. They measured the radiation force on micrometer-sized polystyrene spheres through observation of the sphere's microscopic movement in a 500 kHz ultrasonic standing wave.

7.3.2   Acoustic Radiation Pressure Acting on Cylindrical Objects

Very little is known about the acoustic radiation force on a small-diameter rigid cylinder, although the subject of the radiation pressure on spheres has been extensively studied.

Awatani [6] and Hasegawa [22] have derived numerical results for acoustic radiation forces on rigid and elastic cylinders in a plane progressive sound field. Simple and general analytical expressions for the acoustic radiation force of any acoustic field, that is symmetrical about its axis, on a rigid cylinder, whose diameter is much smaller than the wavelength of the sound wave and whose axis is perpendicular to the wave propagation, are derived by Wu et al. in 1990 [63]. Wu et al. follow King and Nyborg's approach to derive acoustic radiation forces on the rigid cylinder. Results are expressed in terms of the time-averaged densities of kinetic and potential energies of the incident sound field. They show that for the case of a standing wave field, the theoretical results agree well with the experimental observations of the acoustic radiation force exerted on a glass microneedle in a standing-wave field of megahertz frequency.

The radiation force-per-length on an infinitely long circular, compressible cylinder in an acoustic plane standing wave is expressed in terms of partial-wave scattering coefficients for the corresponding traveling wave scattering problem by Wei, Thiessen and Marston in 2004 [58]. This information allows a dimensionless radiation force function to be expressed using coefficients available from two-dimensional scattering theory. Wei et al. also examine a long-wavelength approximation for the force, which is analogous to one for the radiation force on compressible spheres giaven by Yosioka and Kawasima [66].

7.3.3   Acoustic Radiation Pressure Acting on Shells

Hasegawa et al. [22] theoretically investigate the acoustic radiation pressure resulting from a plane wave incident on spherical shells and cylindrical shells immersed in a fluid in relation to the thickness of the shell and the contents of the hollow region in 1988. The spherical and cylindrical shell is placed freely in a plane progressive sound field in a nonviscous fluid. Numerical calculations showed that the differences between the frequency dependence of the acoustic radiation pressure on spherical shells and that on cylindrical shells are more remarkable than those between spheres and cylinders.

8 Conclusion

Based on a review of the fundamentals of pulsed ultrasound Doppler velocimetry, on the measurements of ultrasonic beam shapes of focused and unfocused ultrasonic transducers emitting ultrasonic wave packets at different ultrasonic frequencies and on the measurements of velocity profiles in the flow over a backward facing step in a small rectangular channel (small compared to the transducer diameter), the limitations of pulsed ultrasound Doppler velocimetry have been determined. Moreover, suggestions to improve the measurement system and its spatial resolution have been made. Future research to enhance pulsed ultrasound Doppler velocimetry has been framed.

The accuracy of the measured velocity field mainly depends on the shape of the acoustic beam through the flow field and the intensity of the echo from the incident particle where the velocity is being measured. With ultrasonic beam measurements the actual beam shape and echo intensity was investigated to select the most promising transducer to measure the velocity in small channels. The 8 MHz 5 mm ultrasonic transducer was identified to be the most promising single element transducer due to its excellent spatial (lateral and axial) resolution. Since application of pulsed ultrasound Doppler velocimetry for measurements often involves the propagation of the emitted acoustic field and the returning echo through a Plexiglas wall, the effect of Plexiglas walls on the measured velocity profile has been analyzed and quantified in detail. The distance offset displayed in the instrument, which is caused by the Plexiglas wall, and the echo intensity reduction has been determined. To minimize the effect of Plexiglas walls, wall corrections based on the calculated distance offset are introduced. Evaluating the effect of porous screens (forming screens), the 4 MHz 8 mm focused ultrasonic transducer turned out to be most promising single element transducer to measure velocity profiles closely behind highly absorbing porous screens. In general, the shape of the ultrasonic beam varies depending on the frequency and diameter of the emitter as well as the characteristics of the acoustic interfaces that the beam encounters.

By comparing measurement results in a small rectangular channel characterized by a backward facing step to numerically calculated results, further limitations of the method have been identified. It was not possible to determine velocities correctly throughout the

whole channel at low flow rates, in small geometries and in flow separation regions. A discrepancy between the absolute value and position of the maximum measured velocity, broadening of the velocity profile, various distance offsets displayed in the instrument, perturbations in the velocity profile and wrong velocity determination at the far channel wall and in the recirculation region were main shortcomings. Measurement results have been improved by changes in the Doppler angle, the flow rate, the particle concentration and the use of focused ultrasonic transducers (when compared to unfocused transducers). The effect of Plexiglas walls on the measurement results has been quantified and minimized by correcting the position of the first sample volume.

Analyzing the fundamentals of the method and working structure of the instrument revealed limitations in the measurable maximum velocity due to aliasing, in the measurable maximum depth due to frequency dependent absorption of ultrasound, in the spatial resolution due to emitting frequency constraints, in the time resolution due to spectral broadening as well as in the appropriate amount of ultrasound scatterers. After having measured the ultrasonic beam shape of various transducers with and without walls and porous screens, the transducer's ringing effect and the saturation region caused by highly absorbing acoustic interfaces have been identified as further limitations that restrict measurements close to the transducer face or close to highly absorbing acoustic interfaces. Evaluation of measured velocity profiles in a small rectangular channel (small compared to the transducer diameter) revealed further fundamental limitations concerning the measurement of the velocity component along the ultrasonic beam axis (inclined by the Doppler angle), the appropriate amount of ultrasound scatterers, the displayed distances, the velocity determination close to the far wall and the right selection of the Doppler angle.

Nevertheless, pulsed ultrasound Doppler velocimetry turned out to be a feasible method for quantitatively determining velocity profiles in small channels (compared to the transducer diameter). Especially when dealing with flow at low velocities in small channels and flow separation, pulsed ultrasound Doppler velocimetry revealed several limitations. The ultrasonic transducer turned out to be the most critical component of the ultrasonic system. It determines the frequency of ultrasound, the sensitivity of the velocimeter and the achievable spatial resolution. To improve especially the spatial resolution, it is suggested to use annular phased array transducers and modify the

measurement system accordingly. Through electronic focusing, ultrasonic beam steering and automatic variations in the aperture size, annular phased array transducers enhance the spatial resolution of the system significantly. Research on a new ultrasonic architecture combining the advantages of standard pulsed ultrasound Doppler velocimetry and the ultrasound phased array technique is essential. The necessity of future research on the interaction between acoustic waves and acoustic interfaces encountered by the ultrasonic beam and suspended objects in the flow is emphasized. A literature review on the interaction of acoustic waves with cylindrical and spherical objects has been undertaken to frame future research in this area in order to enhance pulsed ultrasound Doppler velocimetry for accurate measurement of velocity profiles especially in small channels and capillaries.

Appendix A: Technical Drawings Experimental Setup

TECHNICAL DRAWINGS OF THE RECTANGULAR CHANNEL AND

DISTRIBUTOR:

This Appendix contains the computer aided design drawings of the rectangular channel and distributor (Figures A-0-3 to A-0-15). The technical drawings are generated using the program Unigraphics NX 2.0.0.21. A list of parts is given in Table A-1, assembly drawings in Figure A-0-1, A-0-2 and A-0-7.

Table A-1: Parts List Experimental Setup

| Request: PUDV	Title: Parts List Experimental Setup			Originator: Matthias Messer	Issued on: 1-Jun-05
Piece Number	Number of Pieces	Material	Title	Comments	
1	1	PC (Polycarbonate)	Channel Bottom Wall		
2	2	PMMA (Clear Plexiglas)	Channel Side Wall		
3	1	PMMA (Clear Plexiglas)	Channel Top Wall		
4	1	PMMA (Clear Plexiglas)	Channel Pressure Part		
5	1	PMMA (Clear Plexiglas)	Distributor Bottom Wall		
6	1	PMMA (Clear Plexiglas)	Distributor Back Wall		
7	2	PMMA (Clear Plexiglas)	Distributor Side Wall		
8	1	PMMA (Clear Plexiglas)	Distributor Top Wall		
9	1	PMMA (Clear Plexiglas)	Distributor Front Part		
10	1	AlMg1.5 (Aluminum)	Theta Positioner L-Profile		
11	1	AlMg1.5 (Aluminum)	Theta Positioner Transducer Holder		
12	1	AlMg1.5 (Aluminum)	Theta Positioner Support Part		

Assembly Drawing Experimental Setup:
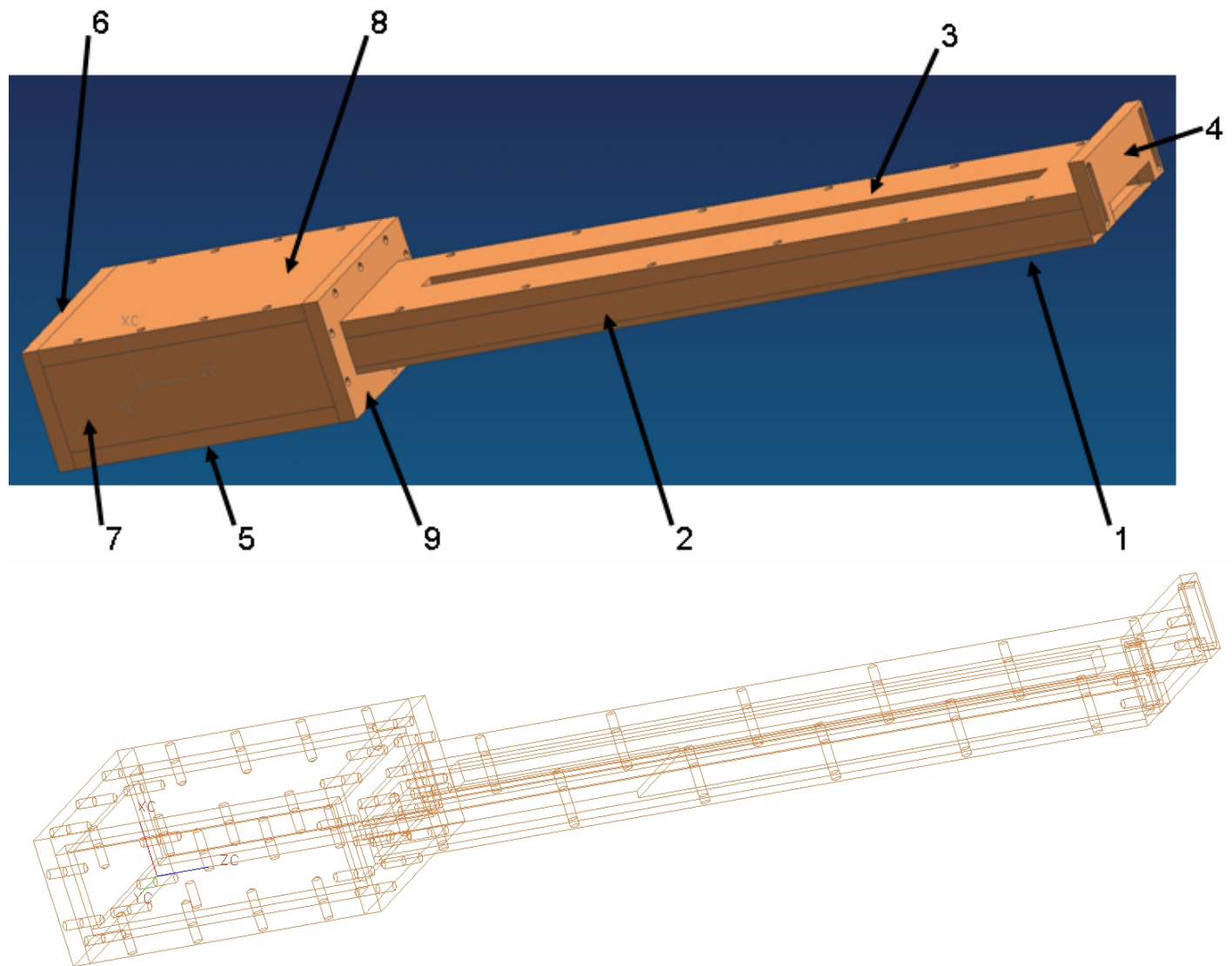
Figure A-0-1: Assembly Drawing Experimental Setup
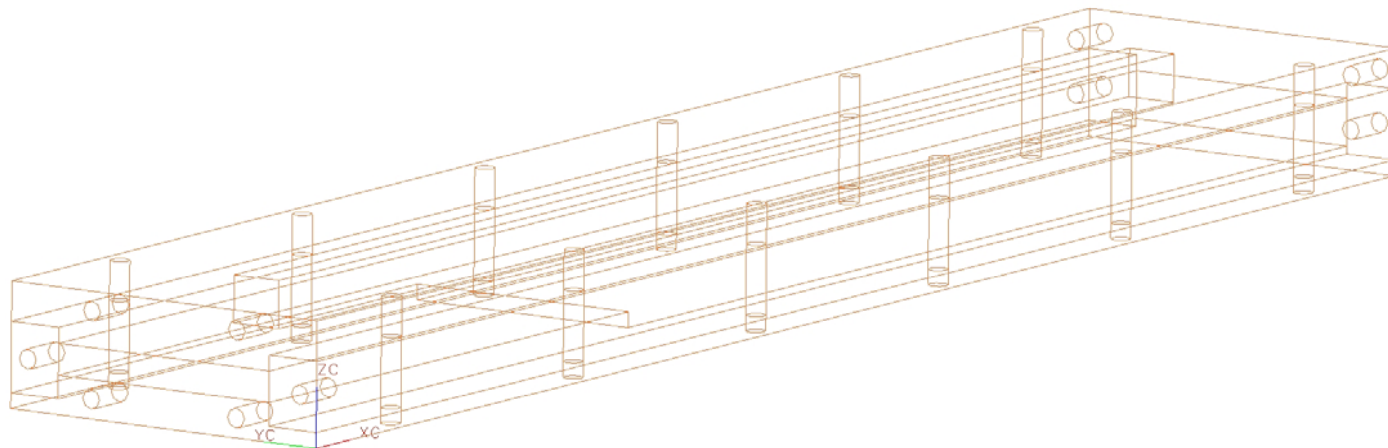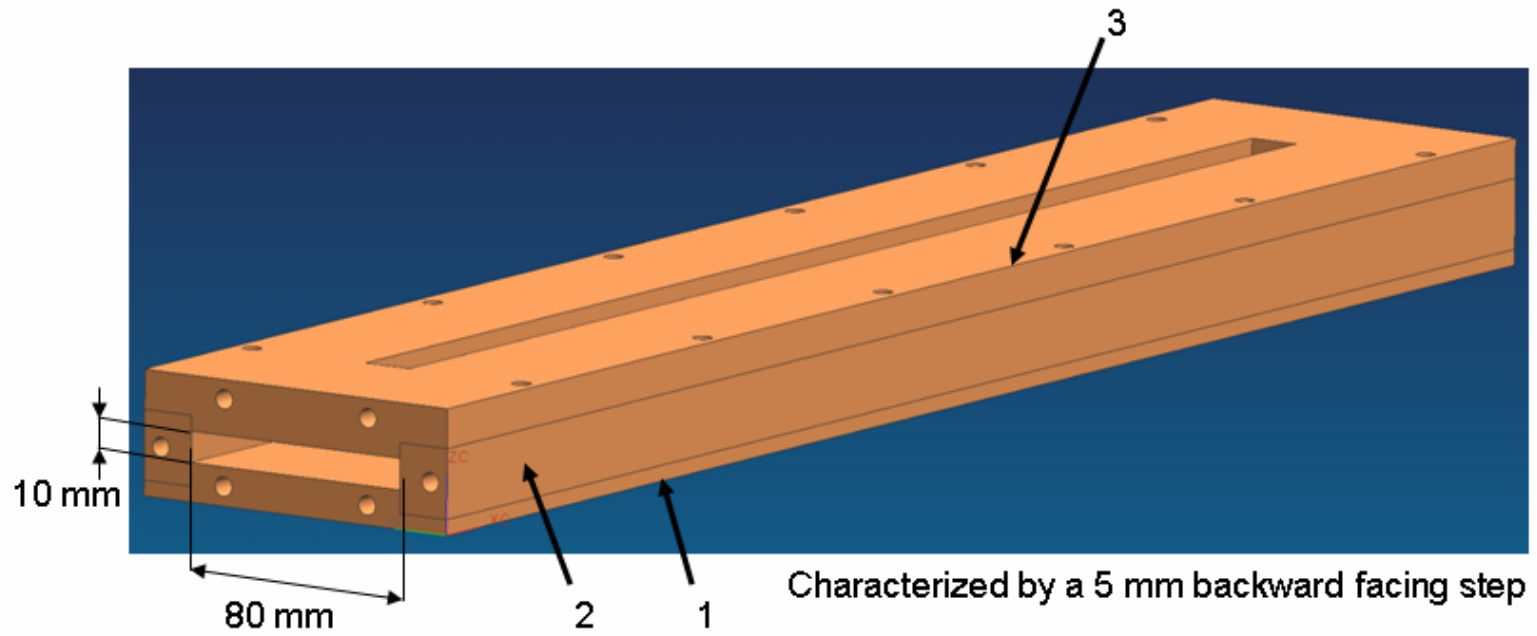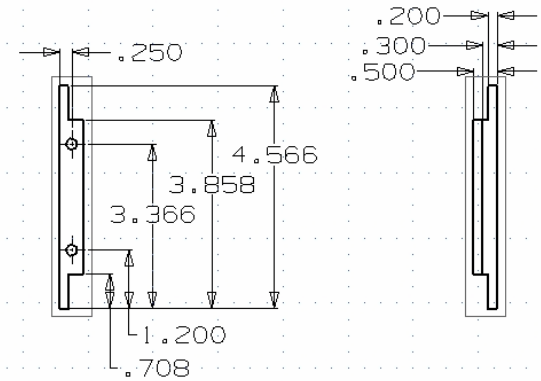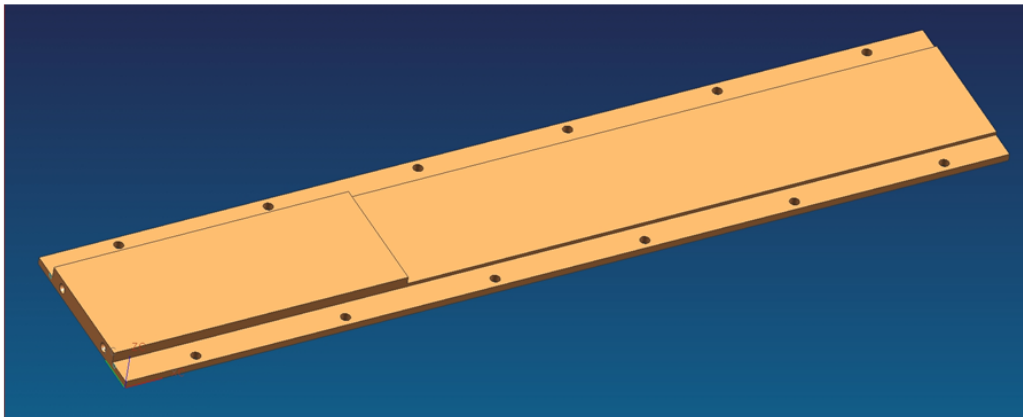
Assembly Drawing Channel:

Figure A-0-2: Overview Channel

1/4 tap, 0.625 inch deep, 2 places   1/4 inch hole, through, 12 places

.250
.250

1.620
5.620
9.620
13.620
15.750
17.620
21.620
23.620

.200
.300
.500

.250

4.566
3.858
3.366

1.200
.708
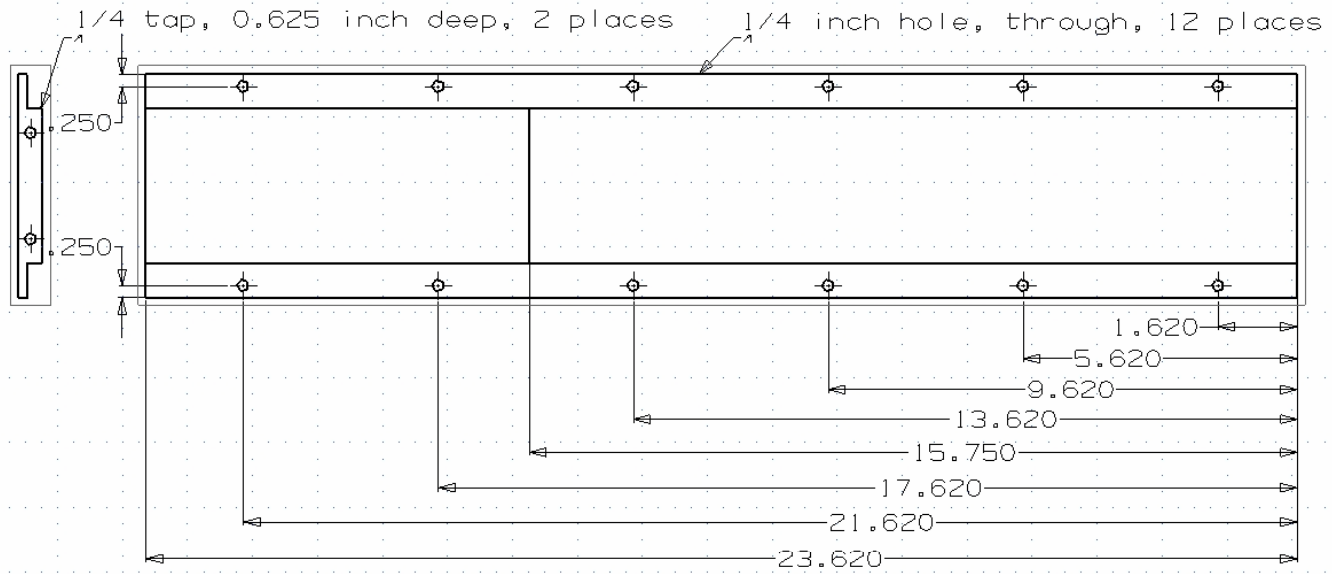
Originator:	Matthias Messer	Date:	1-Jun-2005
Scale:	3 : 1	Dimensions:	Inch
Material:	PC	Part-Number:	1
Title:	Channel Bottom Wall		

Figure A-0-3: Technical Drawing Channel Bottom Wall

199

Notes:
1) Break sharp corners
2) Surface finish of 6.3 μm or better
3) Bore diameter variations and fit tolerances: 0.1 mm overallowance and 0.2 mm underallowance

23.620
21.620
17.620
13.620
9.620
5.620
1.620

1/4 inch hole, through, 6 places

.708
.250

.250

.450
.900

Originator:	Matthias Messer	Date:	1-Jun-2005
Scale:	3 : 1	Dimensions:	Inch
Material:	PMMA	Part-Number:	2
Title:		Channel Side Wall	

Figure A-0-4: Technical Drawing Channel Side Wall

200
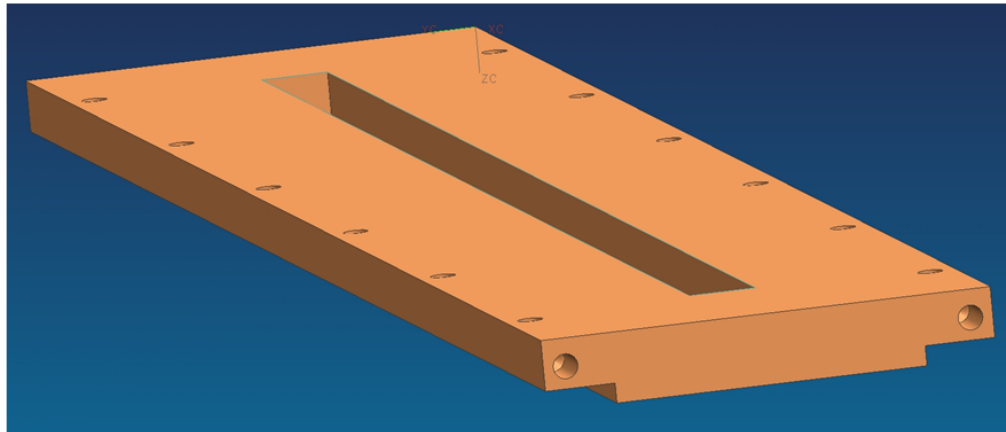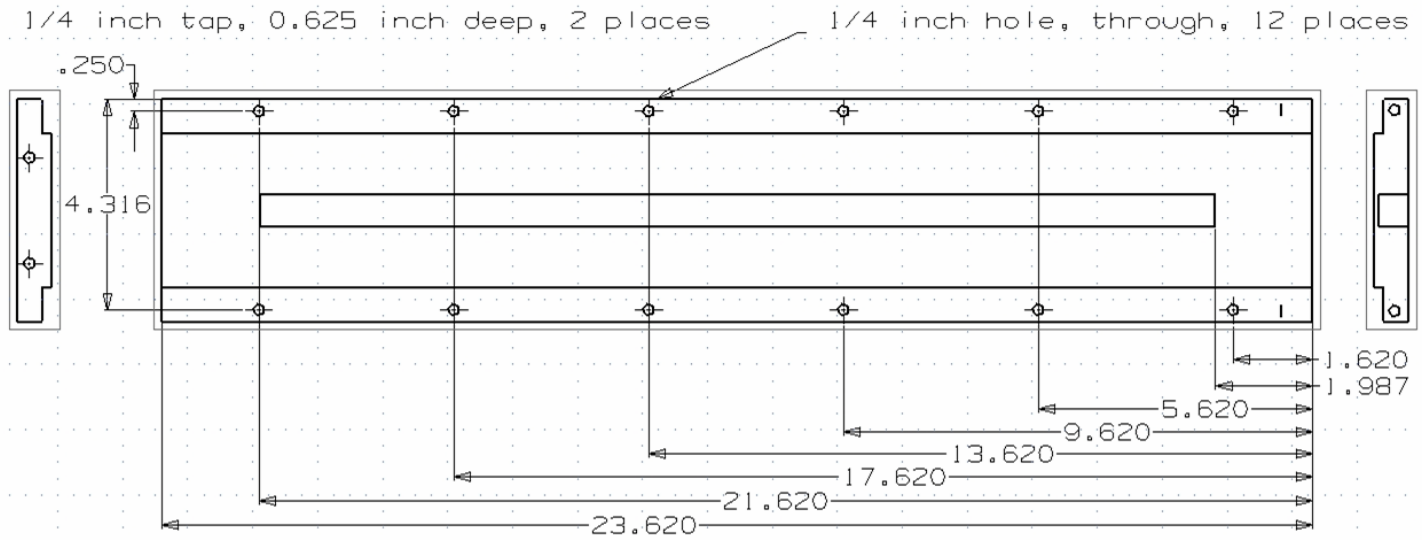
Figure A-0-5: Technical Drawing Channel Top Wall

Notes:
1) Break sharp corners
2) Surface finish of 6.3 μm or better
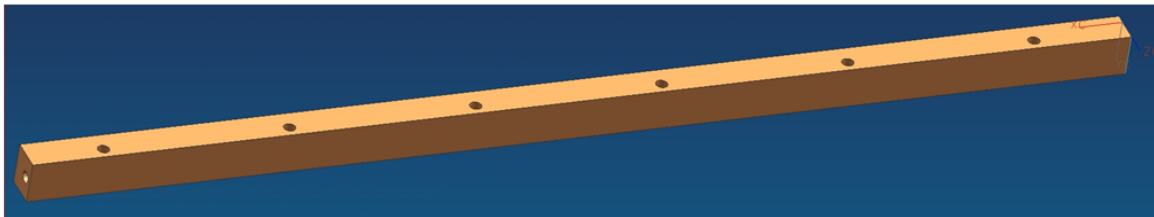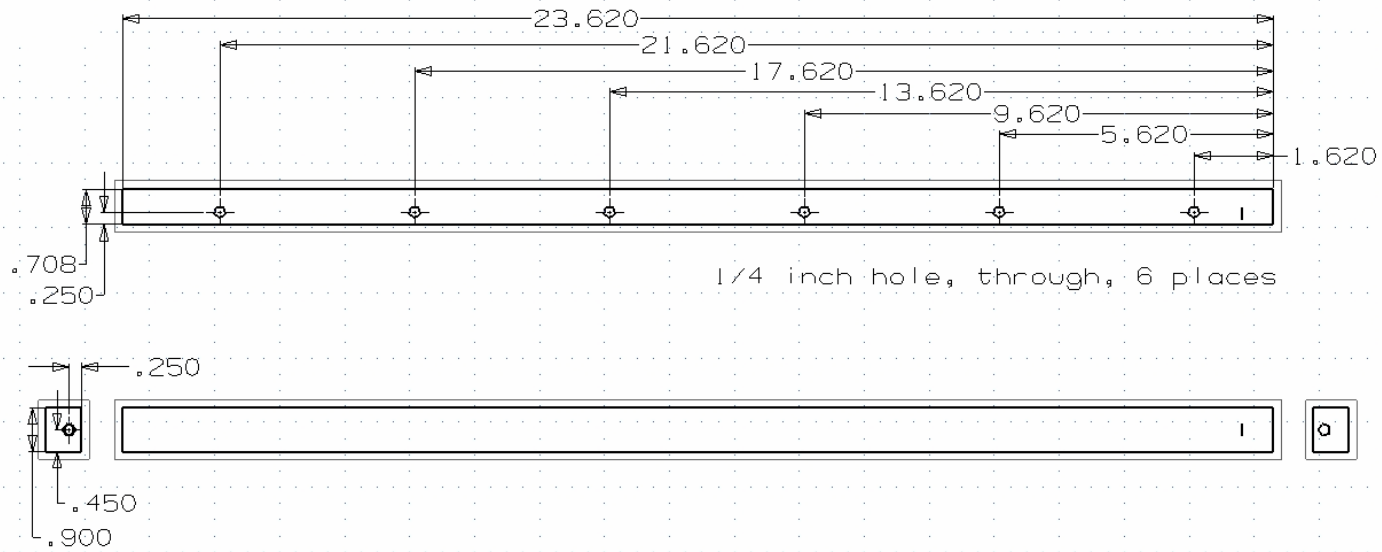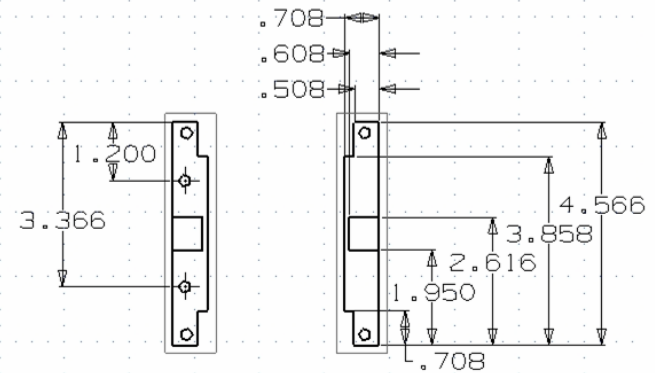3) Bore diameter variations and fit tolerances: 0.1 mm overallowance and 0.2 mm underallowance

.283

1.608

1.983

2.208

.100
.225
.350

.500

.708

3.858

4.218

4.341

4.465

4.566
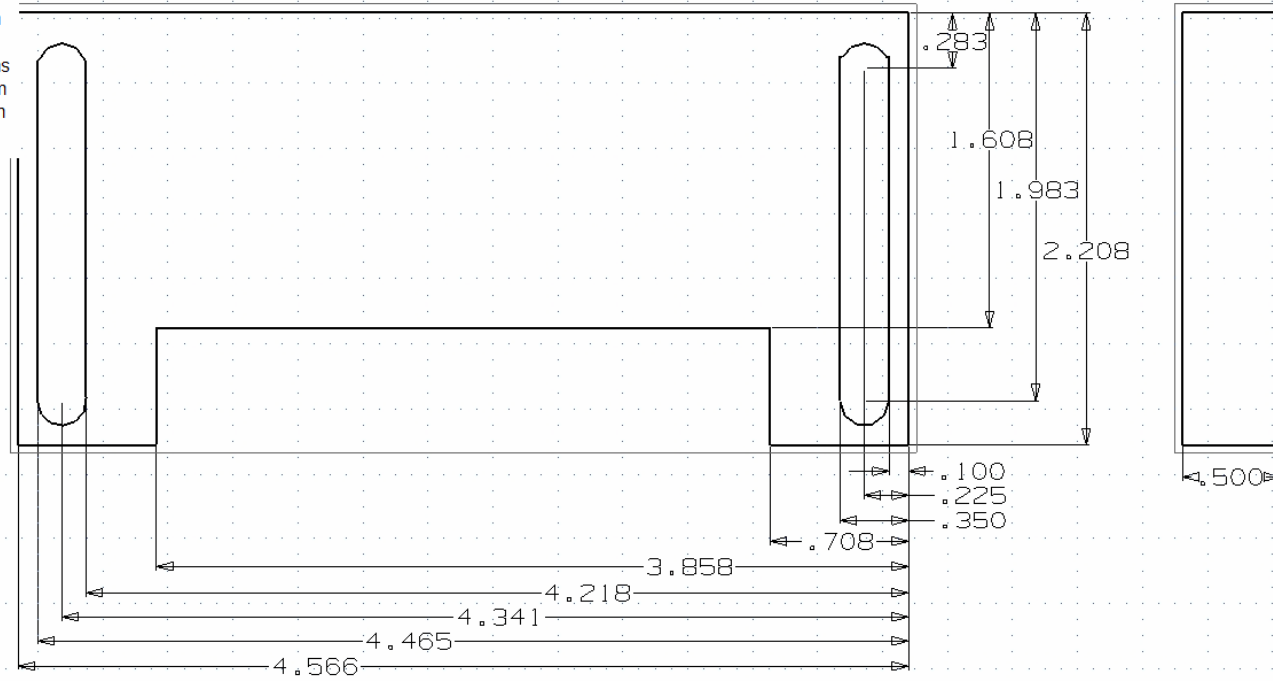
1/4 hole, through, 4 places
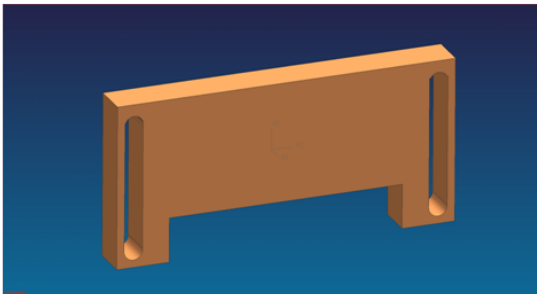
Originator:	Matthias Messer	Date:	1-Jun-2005
Scale:	1 : 1	Dimensions:	Inch
Material:	PMMA	Part-Number:	4
Title:	Channel Pressure Part		

Figure A-0-6: Technical Drawing Channel Pressure Part

Assembly Drawing Distributor:
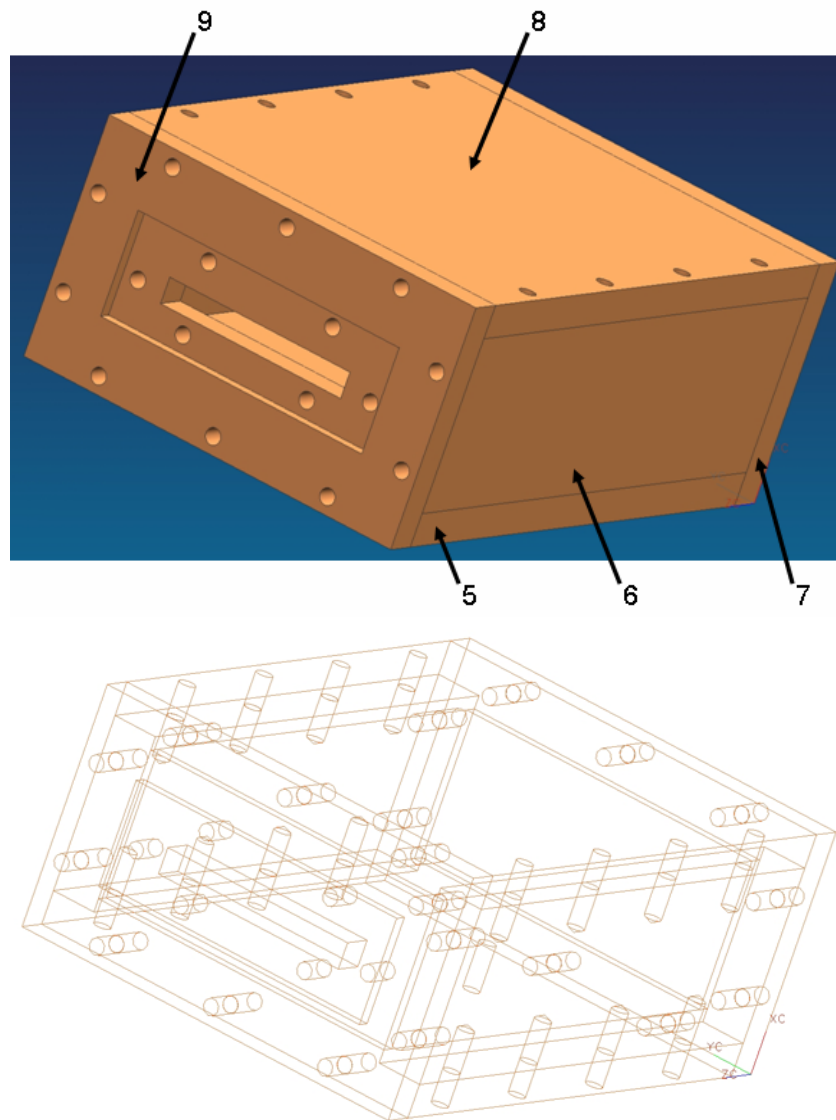
Figure A-0-7: Overview Distributor
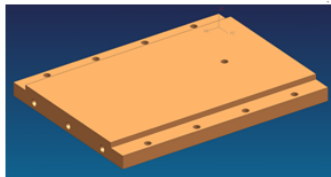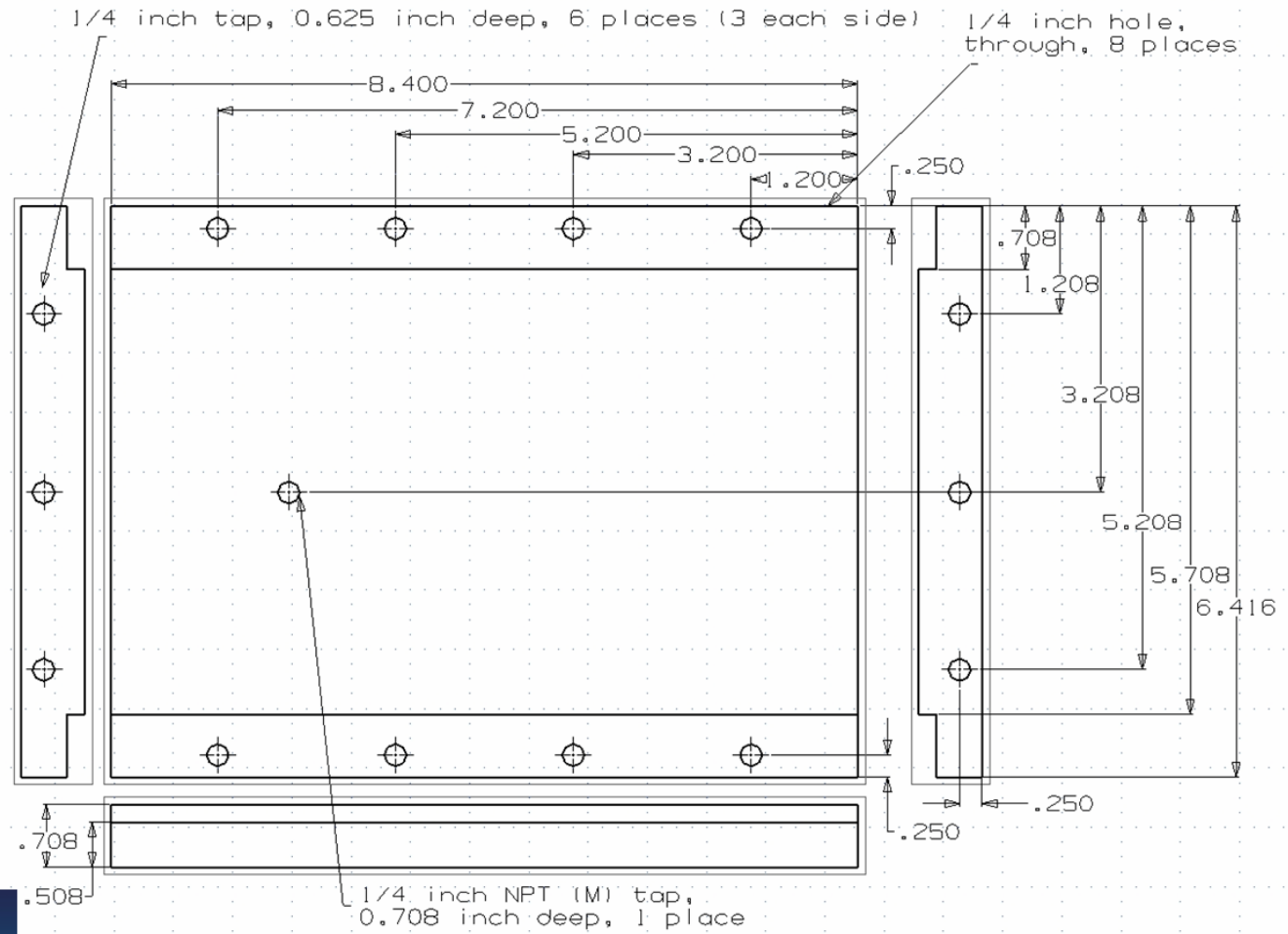
Figure A-0-8: Technical Drawing Distributor Bottom Wall

Figure A-0-9: Technical Drawing Distributor Side Wall

3.666
2.958
.708
.508
.708
.708

1/4 inch hole, through, 10 places

.250
1.200
3.200
5.200
6.166

5.708
6.416

.250
1.083
2.583
3.416

Originator:	Matthias Messer	Date:	1-Jun-2005
Scale:	2 : 1	Dimensions:	Inch
Material:	PMMA	Part-Number:	7
Title:	Distributor Back wall		

Figure A-0-10: Technical Drawing Distributor Back Wall

206
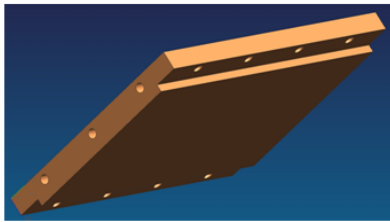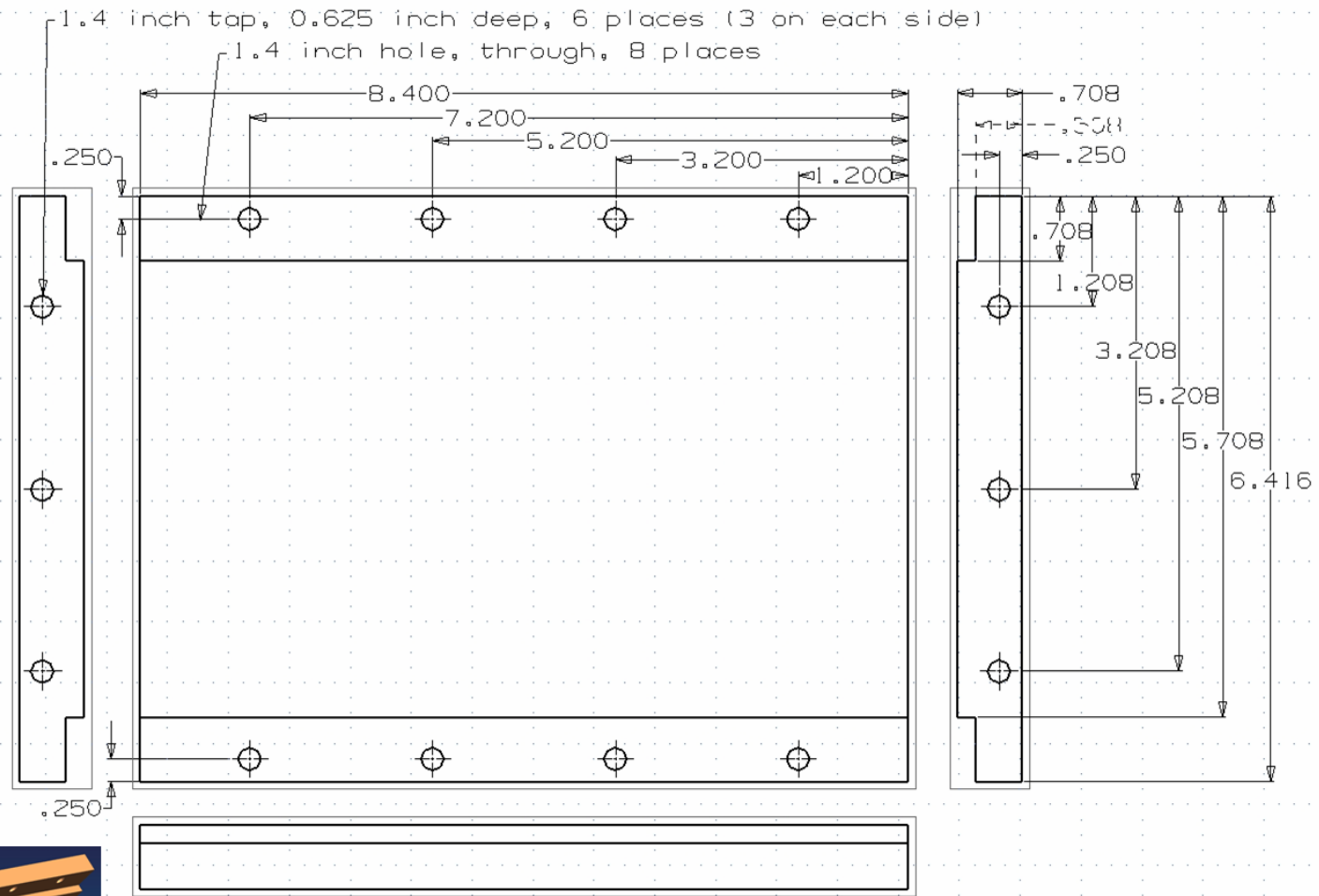
Figure A-0-11: Technical Drawing Distributor Top Wall

Notes:
1) Break sharp corners
2) Surface finish of 6.3 μm
or better
3) Bore diameter variations
and fit tolerances: 0.1 mm
overallowance and 0.2 mm
underallowance

.708
.508
.200

.708
.925

1.633

4.783

5.491

5.708

6.416

A - A
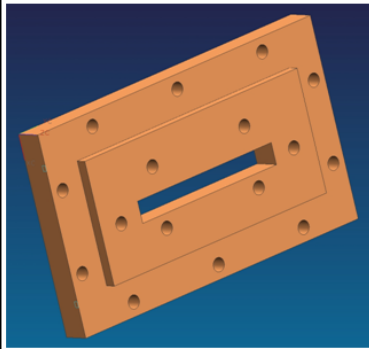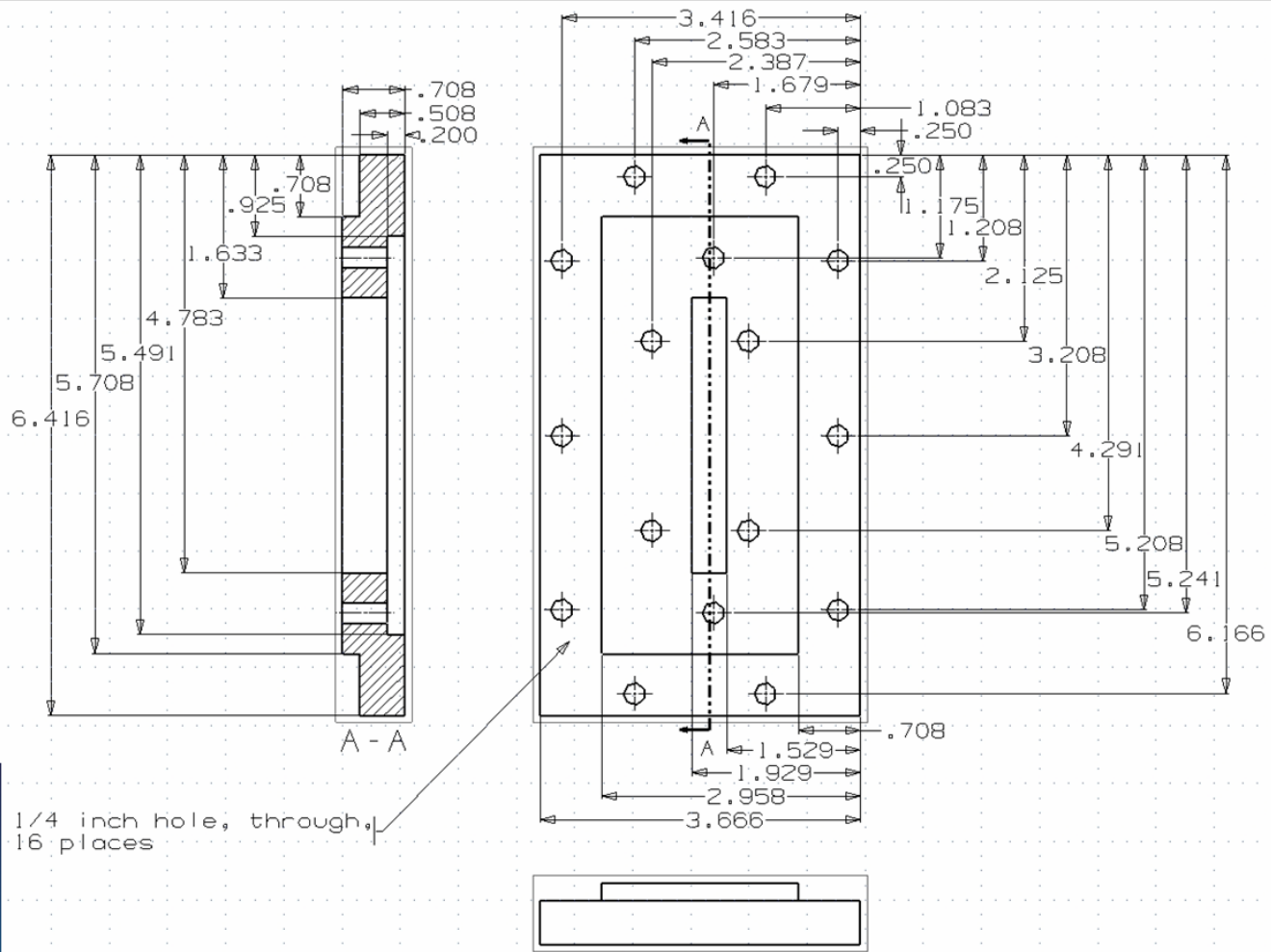
1/4 inch hole, through,
16 places

3.416
2.583
2.387
1.679
1.083
.250
.250
1.175
1.208
2.125
3.208
4.291
5.208
5.241
6.166

.708

A 1.529
1.929
2.958
3.666

Originator:	Matthias Messer	Date:	1-Jun-2005
Scale:	2 : 1	Dimensions:	Inch
Material:	PMMA	Part-Number:	9
Title:		**Distributor Front Part**	

Figure A-0-12: Technical Drawing Distributor Front Part

TECHNICAL DRAWINGS OF MOUNTING PARTS

Technical Drawings of Mounting Parts required to attach a theta-positioner to the top channel wall are presented in the following. These parts can be seen in Figure 5-3.

Notes:
1) Break sharp corners
2) Surface finish of 6.3 μm or better
3) Bore diameter variations and fit tolerances: 0.1 mm overallowance and 0.2 mm underallowance

23.62
22.00
18.00
14.00
10.00
6.00
2.00

1.438
.100
.250

1.500
1.438
.062
1.500

23.62
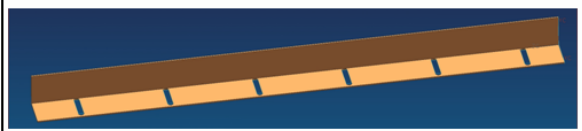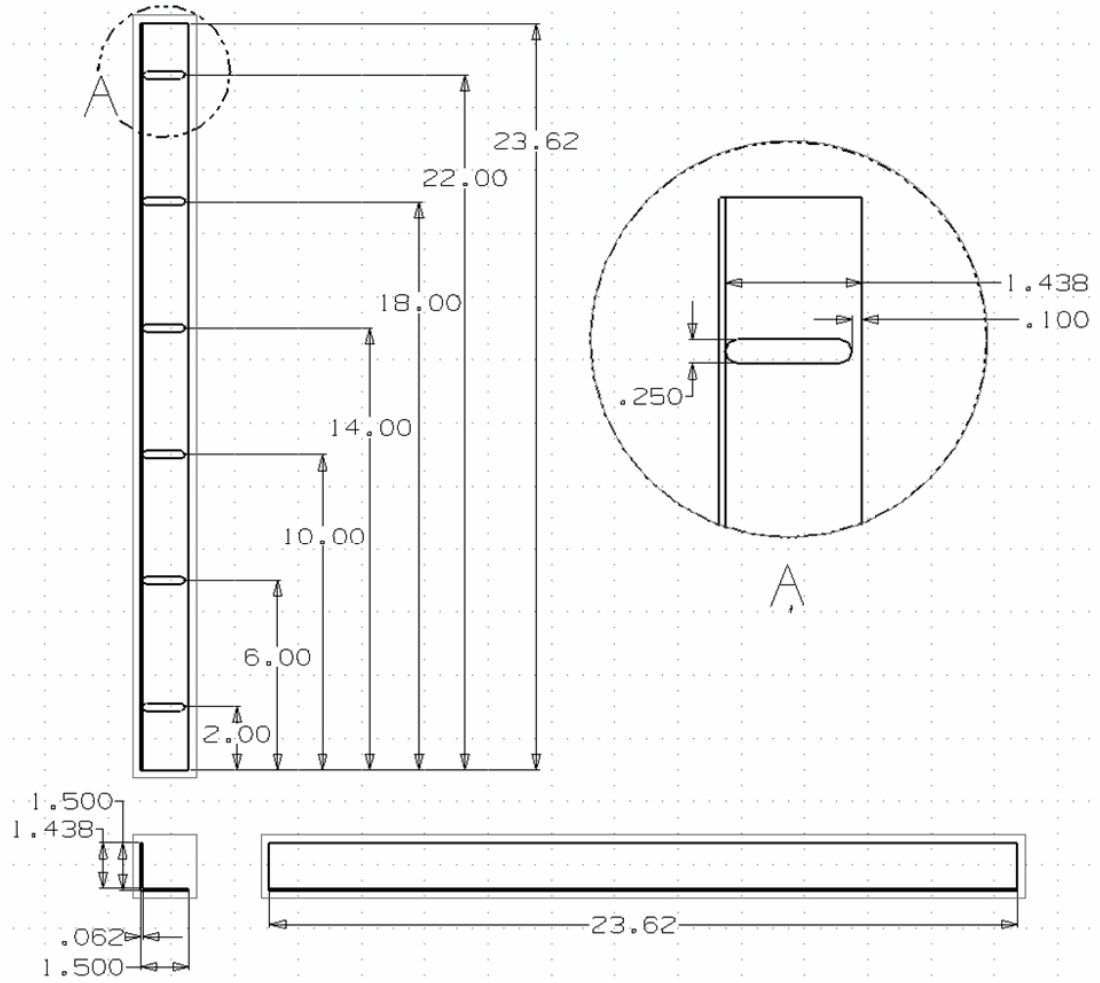
Originator:	Matthias Messer	Date:	1-Jun-2005
Scale:	4 : 1	Dimensions:	Inch
Material:	AlMg 1.5	Part-Number:	10
Title:	Theta Positioner L-Profile		

Figure A-0-13: Technical Drawing Theta Positioner L-Profile

1/4 inch tap, 0.65 inch deep,
2 places

Ø .28
0.28 inch hole, through,
4 places

2.63
1.63
.63
2.62
2.16
1.08
.62

Ø .50
0.5 inch hole, through,
1 place

1.00
.34
1.63
3.26
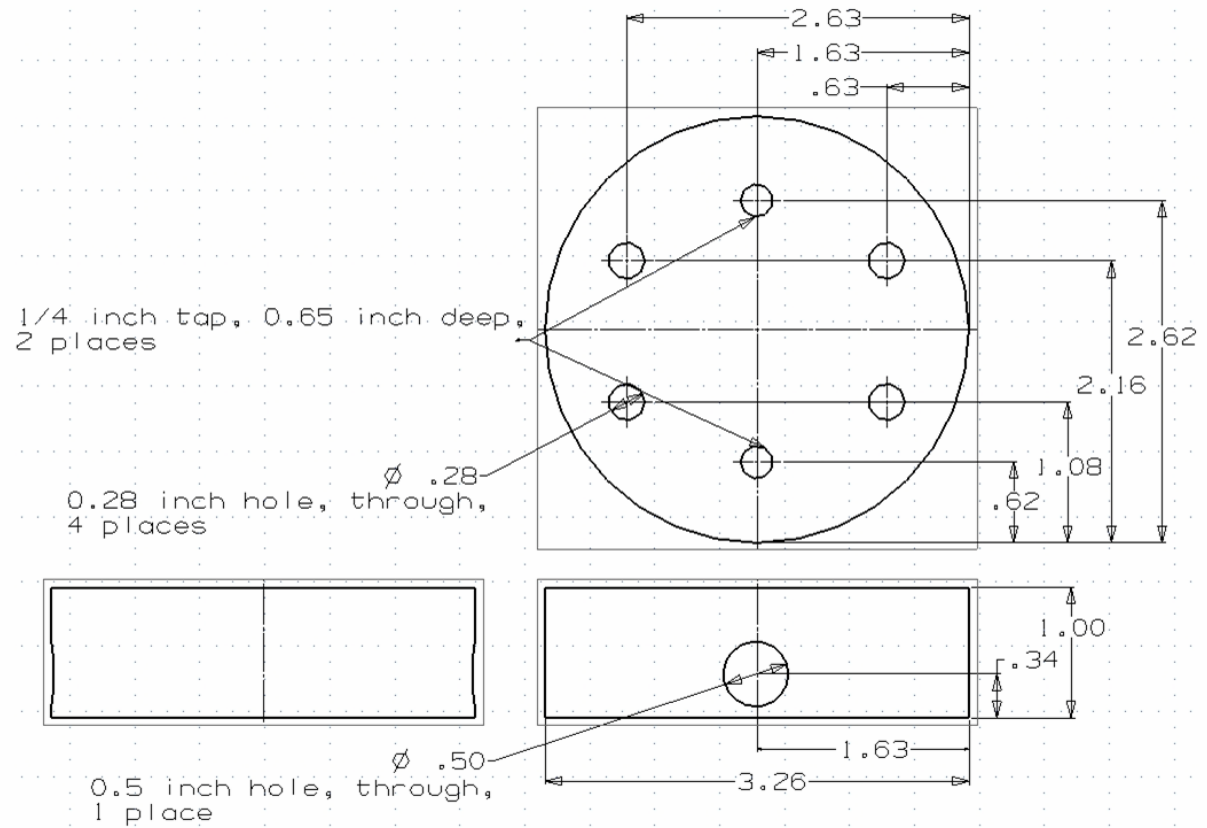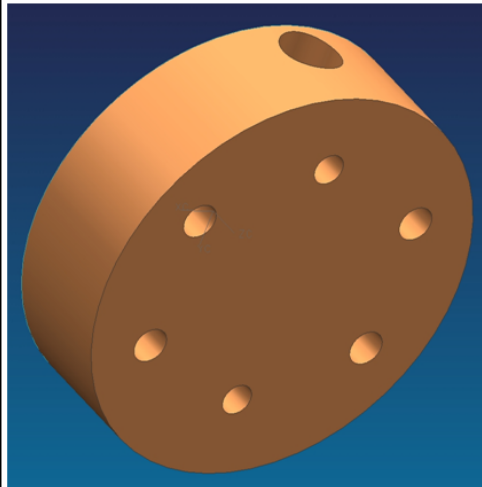
Originator:	Matthias Messer	Date:	1-Jun-2005
Scale:	2 : 1	Dimensions:	Inch
Material:	AlMg 1.5	Part-Number:	11
Title:			
	Theta Position Transducer Holder		

Figure A-0-14: Technical Drawing Theta Positioner Transducer Holder

Notes:
1) Break sharp corners
2) Surface finish of 6.3 μm or better
3) Bore diameter variations and fit tolerances: 0.1 mm overallowance and 0.2 mm underallowance

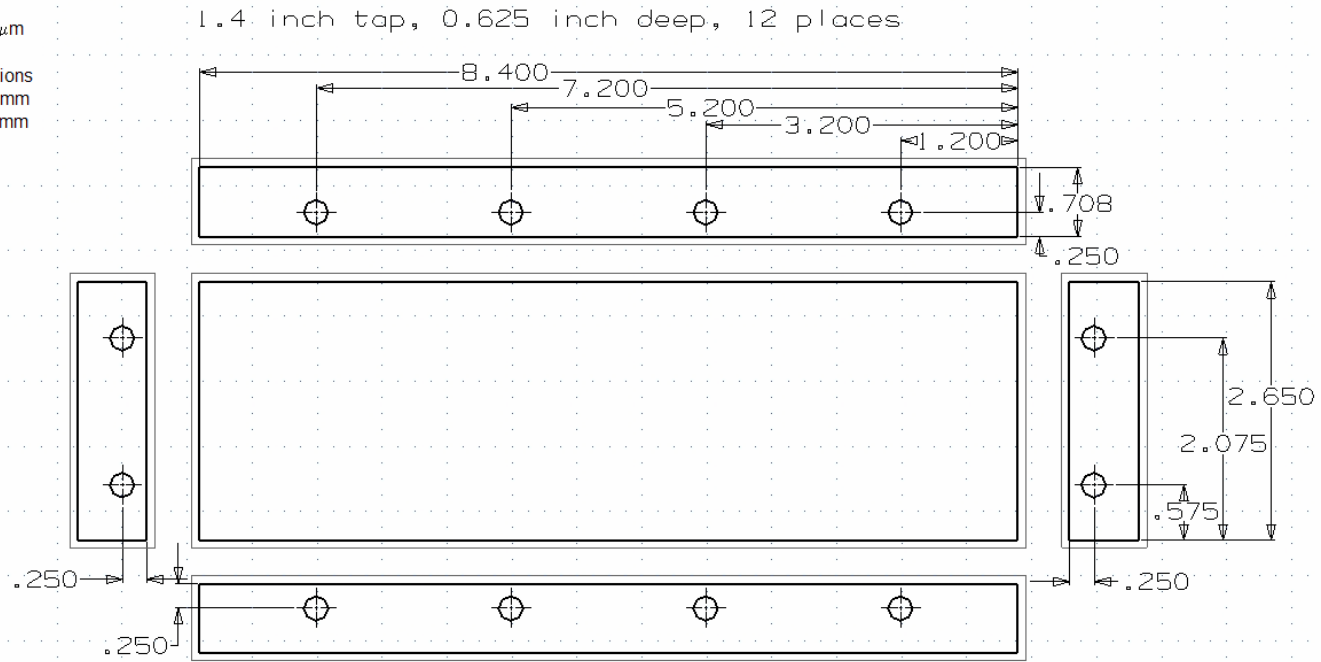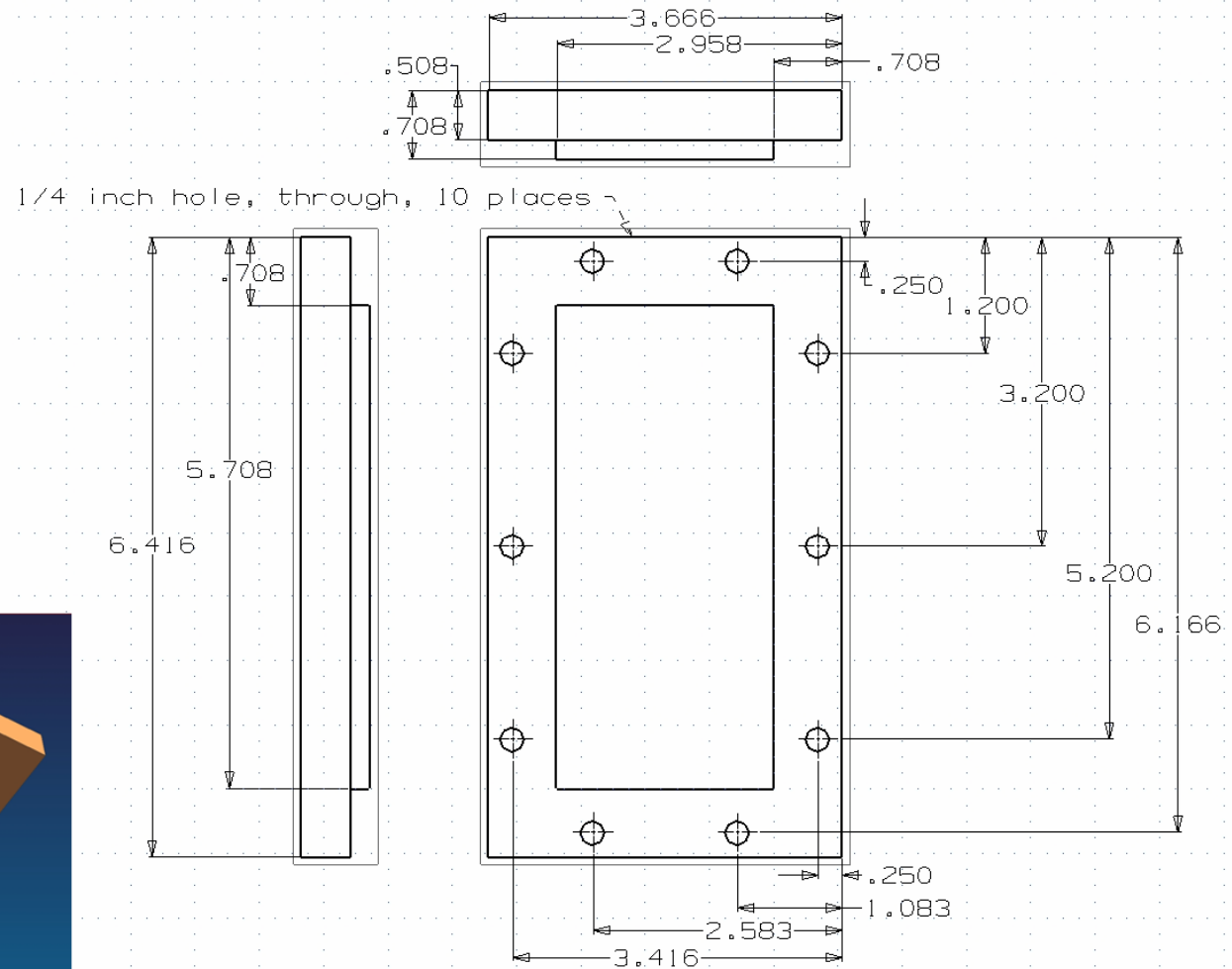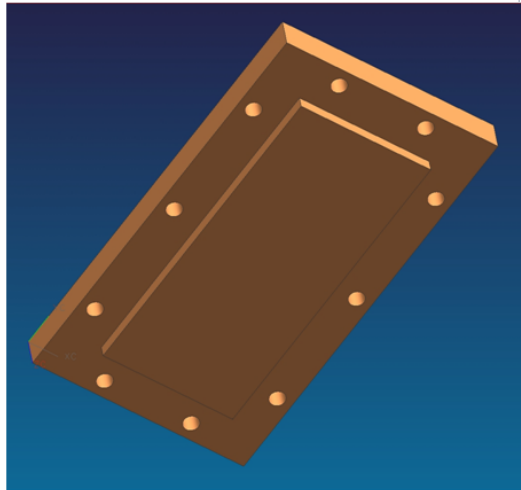1/4 inch tap, 0.188 inch deep, 2 places

.250
.188

3.500
2.800
2.300
.725

0.3 inch hole, through, 2 places

.5
1.0
3.0
3.5
4.0
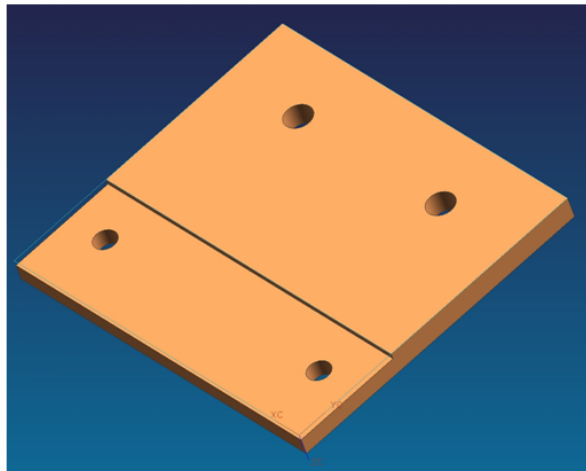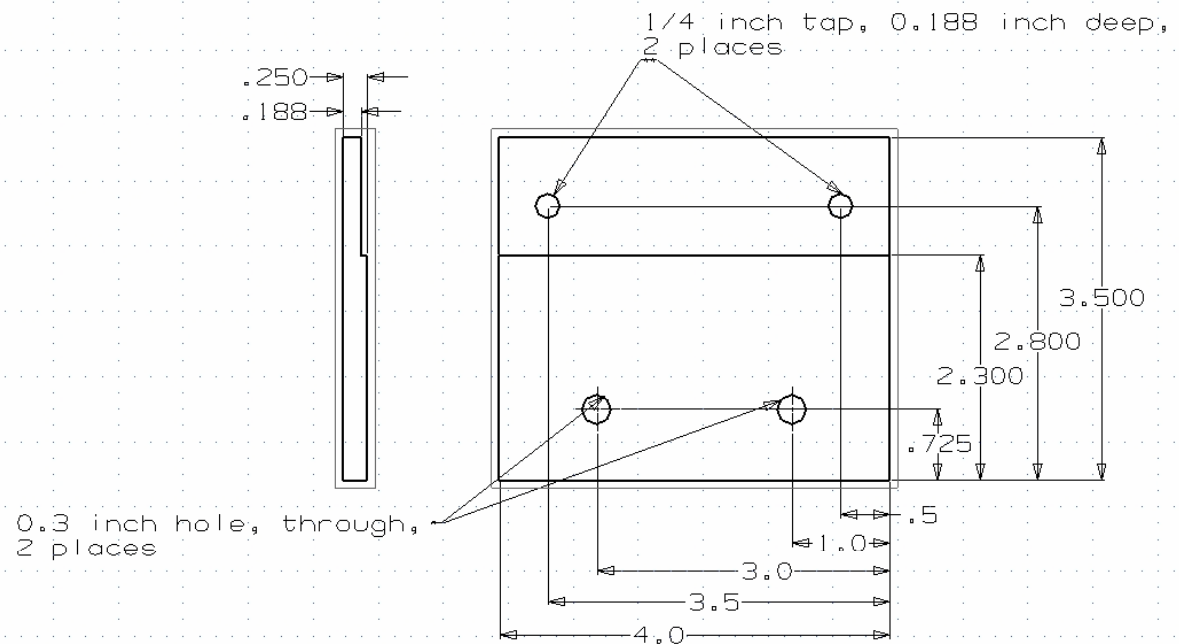
Originator:	Matthias Messer	Date:	1-Jun-2005
Scale:	2 : 1	Dimensions:	Inch
Material:	AlMg 1.5	Part-Number:	12
Title:	Theta Positioner Support Part		

Figure A-0-15: Technical Drawing Theta Positioenr Support Part

212

Appendix B: Technical Specifications Pulsed Ultrasound Doppler Velocimetry System

The digital ultrasonic synthesizer (Figure B-0-1) can generate any emitting frequencies between 0.45 MHz and 10.5 MHz. Associated to this performance, the DOP2000 includes a variable spatial resolution filter that allows to adapt the size of the sampling volume to the application and therefore improves the signal to noise ratio of the measurements.
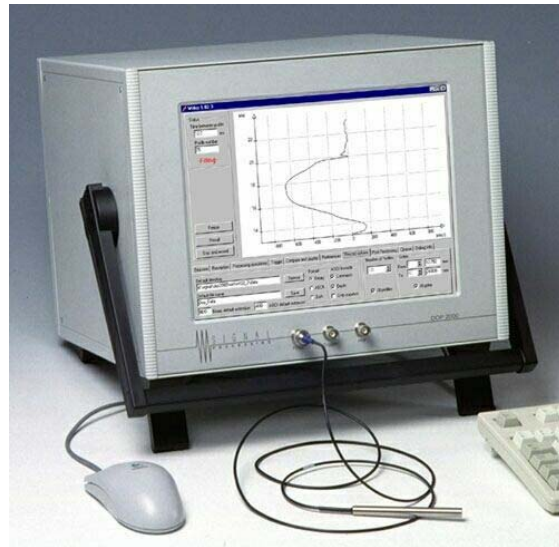
Figure B-0-1: Digital Ultrasonic Synthesizer [51]

All the ultrasonic parameters (Frequency, PRF, Tgc..) and the processing conditions (number of gates, filters ...) are set by the user. The smart trigger capability of the instrument allows to synchronize the acquisition to any periodic or non periodic event. This high flexibility applies to the 10 channels multiplexer and up to 32'000 profiles could be recorded in binary and/or ASCII format.

If desired, the DOP2000 can record simultaneously two types of data profiles, such as the velocity profiles and the Doppler energy profiles. A separate emitter output connector enables to use two different transducers for emission and reception.

Operating in a Windows 9x® environment, the measured profiles are displayed on screen and are recorded in its internal memory or send through the build-in Ethernet connection to any storage device within few milliseconds.

Technical specifications DOP2000 Model 2125

Emission:

Emitting frequencies	from 0.45 MHz to 10.5 MHz, step of 1 kHz
Emitting power	3 levels
Burst length	2, 4 or 8 cycles
PRF	between 64 µs (48 mm) and 10'500 µs (7'875 mm), step of 1 µs

Reception:

Number of gates	between 3 and 1000, step of 1 gate
Position of the first channel	movable by step of 250 ns
Amplification (TGC)	Uniform, Slope, Custom
	Slope mode exponential amplification between two defined depth values. Value at both depths variable between -40dB and +40dB
	Custom mode user's defined values between -40dB and +40dB in cells. Variable number, size and position of the cells.
Sensitivity	>-100 dBm

Resolution:

Lateral resolution	defined by the transducer
Longitudinal resolution	minimum value of 0.85 s (0.64 mm) depends on spatial filter and burst length. (approximate value, defined at 50% of the received)
Spatial filter	from 50 KHz (3.9 mm) to 300 KHz (0.7 mm) , step of 50 KHz
Display resolution	distance between the center of each sample volume selectable between 0.25 s (0.187 mm) and 20 s (15 mm), step of 0.25 s
Velocity resolution	1 LSB (maximum = 0.0091 mm/s; minimum = 91.5 mm/s), Doppler frequency given in a signed byte format

Ultrasonic Processor:

Doppler frequency	computation based on a correlation algorithm
Wall filter	stationary echoes removed by IIR high-pass filter 2nd order
Number of emissions per profile	between 1024 and 8, any values
Detection level	5 levels of the received Doppler energy may disable the computation
Acquisition time per profile	depends on PRF and number of emissions per profile, minimum arround 2 to 3 ms
Filters on profiles	moving average: based on 2 to 32000 profiles, zero values included or rejected median, based on 3 to 32 profiles
Maximum velocity	11.72 m/s for bi-directional flow, 2 times more for unidirectional flow (at 0.5 MHz)
Velocity scale	variable positive and negative velocity range.

Computation:

Compute and display	velocity profile Doppler energy echo modulus velocity profile with echo modulus or Doppler energy velocity profile with velocity versus time of one selected gate velocity profile with flow rate versus time (circular section assumed) velocity profile with real time histogram echo modulus with real time histogram Doppler energy with real time histogram power spectrum of one selected gated
Statistics	mean, standard deviation, minimum, maximum
Velocity component	automatic computation of the projected velocity component
Replay mode	replays a recorded measure from the disk
Utility	freeze/run mode

Advanced features:

	measurement of the ultrasonic field
	extended velocity range (aliasing correction). Option
	acquisition of I and Q signals (8000 values can be recorded)

216

acquisition in real time of a complet 3 dimensional velocity field (UDVF mode). Option

emission and reception can be realized on separated connectors

Trigger:

Input	external signal (TTL) or keyboard action
Configuration parameters	high, low level, internal pull-up 4 K
Delay	between 1 and 10'000 ms, step of 1ms
Acquisition procedure	selectable number of blocks of profiles automatic record capability

Memory/Files:

Internal memory	variable size, memorization from 2 to 32000 profiles
Configuration parameters	10 saved configurations
Data file	Binary (include: ASCII short info blocks, comments, all parameters, all data profiles) ASCII(statistical information available)

Environment(may be changed):

Operating system*	Windows$^{®}$ 95 or 98
Processor*	VIA Eden 400MHz
RAM*	128 MBytes (up to 512 Mbytes in option)
Storage devices*	Hard disk 20 GBytes 1'44 MBytes Floppy CD-ROM Read/Write (40x/12x/48x)
Screen	12.4" TFT Color display (800x600) VGA
Communication	2 serial ports 1 parallel port (printer port) 1 Ethernet 10 base T, RJ45 1 external SGVA (simultaneous with TFT) 2 PS2 port (mouse and keyboard) 1 USB (Rev 1.10, type A)
US interface	Echo, (max 0.7 Vp), output impedance of 50 ohm, BNC TTL high level pulse of 100 ns at each emission, BNC Logic level trigger input, pull up by 330 ohm, BNC US probe In/Out, BNC US emission connector, BNC

Power supply   220-110 VAC, selectable, 50 - 60 Hz
Humidity   =< 80%
Temperature   5 - 35 °C
Size   340x265x305 cm
Weight   13 Kg

Options:

Multiplexer   10 probes, internal or external multiplexer

Sound speed unit   measure the sound velocity within 2%

* may be adapted to the market
All values computed with a sound velocity of 1500 m/s (water),in the direction
of the ultrasonic beam

Appendix C: Technical Specifications Ultrasonic Transducers

Technical Specifications Ultrasonic Transducers

Technical specifications of ultrasonic transducers are given in Figure C-0-1 and C-0-2.

Frequencies and diameters:

Figure C-0-1: Available Ultrasonic Transducers Signal Processing [51]

Cases:
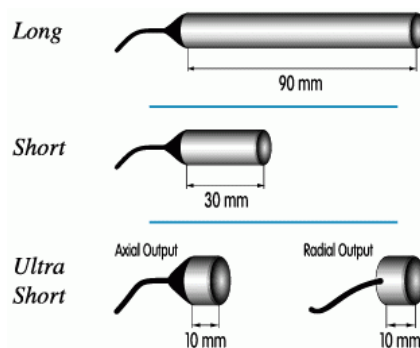
Figure C-0-2: Available Cases Ultrasonic Transducers Signal Processing [51]

Technical specifications

Maximum pressure : 1.5 bars
Impedance :   Matched around 50
Cable type :   RG174
Cable length :   1.5 m (other length upon request)
Cable output :   Axial, Radial available on Ultra-Short Execution
Connector :   BNC
Housing :   Stainless Steel
Front surface :   Epoxy

Appendix D: Technical Specifications Pump

PUMP DRIVE

Technical Specification Ismatec Programmable Digital Drive

Table D-1: Pump Drive Technical Specifications

Duty cycle		continuous from 60 to 6000 rpm
Max rpm		60 to 6000
Motor type		24 VDC, PMDC
Motor (hp)		1/5
Max flow rate with indicated pump head	Pump head 07002-25	1.02 to 102 mL/min
	Pump head 07002-26	2.52 to 252 mL/min
	Pump head 07002-27	5.04 to 504 mL/min
	Pump head 07002-14	5.52 to 552 mL/min
	Pump head 07002-17	19.2 to 1920 mL/min
	Pump head 07003-02	34.8 to 3480 mL/min
	Pump head 07002-23	38.4 to 3840 mL/min
	Pump head 07001-80	38.4 to 3840 mL/min
	Pump head 07001-70	38.4 to 3840 mL/min
	Pump head 07001-40	54.6 to 5460 mL/min
	Pump head 07003-04	70.2 to 702 mL/min
Temp range		104°F (40°C)

Remote control	Input	speed control:0-5 or 0-10 VDC, 0-20 or 4-20 mA (DB15 female) On/off control: TTL contact (DB15 female) RS-232: 9600 or 1200 baud, 8 bit, 1 stopbit, no parity (DB9 female)
	Output	2 valve control outputs (DB15 female), additional RS-232 output for cascading (DB9 female)
Power	VAC	115/230
	Hz	50/60
Dimensions		6"L x 10-1/4"H x 9-1/2"W

PUMP HEAD

Technical Specifications Micropump A Mount Suction Shoe gear Pump Head

Table D-2: Pump Head Technical Specifications

Wetted parts	Body: 316 SS, PPS gears, Viton® seals
mL/rev	1.17
Flow rate (min)	58.5 mL/min at 50 rpm 5850 mL/min at 5000 rpm
Max system pressure	300 psi
Differential pressure (Max)	55 psi
Temp range	-50 to 350°F

Port size	1/8" NPT(F)
Suction lift	24" H_2O (at 1750 rpm)
Viscosity	100 cp
Particulates	none
Run dry	under 30 seconds
Relief valve	yes
Reversible	no
Duty cycle	continuous (from 150 to 5000 rpm)
Motor rpm	10,000
Internal bypass	Yes

PUMP DIMENSIONING

Cross-sectional area: Minimal: 8 cm^2 = 0.0008 m^2 (3.15 inch^2)

Maximal: 12 cm^2 = 0.0012 m^2 (4.72 inch^2)

Characteristic length: L_{min} = 10 mm = 10^{-2} m

L_{max} = 15 mm = 1.5 10^{-2} m

Volume: $V_{distributor}$ = 1.5 l

$V_{channel}$ = 0.7 l

Density: ρ_{water} = 1000 kg/m^3

Kinematic viscosity: ν_{water} = 10^{-6} m^2/s

Reynolds number: Re = $\rho UL/\eta$ = UL/ν = $V_t L/A\nu$

Re_{min} = 1

Re_{max} = 1000

Required minimal flow rate:

$$V_{t,min} = ReAv/L = 8 * 10^{-8} \text{ m}^3/\text{s} = 4.8 * 10^{-3} \text{ l/min} \qquad (1.666 * 10^{-5} \text{ m}^3/\text{s} = 1 \text{ l/min})$$

Required maximal flow rate:

$$V_{t,max} = 8 * 10^{-5} \text{ m}^3/\text{s} = 4.8 \text{ l/min}$$

Minimal velocity:

$$U_{min} = V_{t,min}/A_{max} = 0.0000666 \text{ m/s}$$

Maximal velocity:

$$U_{max} = V_{t,max}/A_{min} = 0.1 \text{ m/s}$$

Appendix E: Technical Specifications Particles

TECHNICAL DATA SHEET GRILTEX 2A PARTICLES

In Table E-1 and E-2, properties and processing information of Griltex 2A (CoPolyamide hotmelt adhesive) particles from EMS-GRILTECH Americas are listed.

Table E-1: Particles Properties

Property	Value
Melting range [^{o}C]	120 – 130
Glass transition temperature [^{o}C]	15
Melt viscosity [Pa s]	600
Melt volume rate [cm^3/10 min]	18
Density [g/cm^3]	1.05
Tensile E-modulus [MPa]	570
Characteristic length (diameter) [μm]	3
Form of delivery	Granules

Table E-2: Particles Processing Information

Processing Information	Value
Hot melt application temperature [^{o}C]	170 – 210
Film extrusion temperature [^{o}C]	180 – 220
Lamination temperature [^{o}C]	130 – 160

Appendix F: Cost Analysis Experimental Setup

In Table F-1, a cost analysis of the experimental setup is given:

Table F-1: Cost Analysis Experimental Setup

Component Experimental Setup	Price US-Dollars (without taxes and without shipping)
Pulsed Ultrasound Doppler Velocimeter DOP2000 Model 2125	42742
External Keyboard	121
Sound Speed Measuring Unit	968
Unfocused 2 MHz 10 mm probe TR0210LS	708
Unfocused 4 MHz 5 mm probe TR0405LS	708
Unfocused 8 MHz 5 mm probe TR0805LS	708
Focused 4 MHz 8 mm probe	800
Ultrasonic Gel 250 ml	17
Particles	0
Breadboard	828
Profile Mounting Parts	240
Tubing, Adapter, Fitting, Tape	185
Pump Drive	1540
Pump Head	450
Beaker	47
Machine Shop Channel and Distributor	2500
Machine Shop Slot in Channel Top Wall	350
Machine Shop Theta Positioner	300
Machine Shop End Piece Channel	220
Laptop	2700
Sum	**56132**

Appendix G: Measurement of Flow Resistivity of Forming Screen

INTRODUCTION:

The flow resistivity of the forming screen was measured by determining the air flow through the sheet at a specified pressure drop. The "air permeability tester" (Figure G-0-1 and G-0-2) is an instrument capable of drawing air through a sheet having an adequate area, at sufficient speed, to make a pressure drop of 0.5 inch (12.7 mm) of water across the sheet, with means for measuring this pressure drop and the corresponding flow rate.

DESCRIPTION OF THE AIR PERMEABILITY TESTER AND ITS OPERATION:

Figure G-0-1: Air Permeability Tester

The air, which is drawn through the fabric by a given suction, is measured with orifice-type flowmeters. The instrument is mounted in the top of a table. The orifice over which the fabric is placed is mounted in the top of a table. The area of the opening is 0.0412 square feet. A ring weighing 3 lb. and having a beveled surface with an inside diameter of 5 inch fits over a similar beveled surface of the orifice rim. The beveled ring is placed over the fabric to hold it across the orifice in a smooth condition and with a slight tension in all directions. The clamp for holding the fabric against the orifice is pivoted in its supporting frame so that it will press uniformly against the upper surface of the orifice. The frame is hinged at the back of the table and locks at the front. It can be raised to

231

permit cloth to be drawn from a bolt across the orifice. In order to prevent air leakage, silicone was spread on the forming screen and the forming screen was placed in between two layers of gasket material.

The speed of the motor which draws air through the aria of fabric under test is adjusted by a dial type rheostat. Manometers filled with a special oil furnished with the instrument are used to indicate the pressure drops across the fabric under test and across the orifice for measuring the air flow. The inclined manometer, which indicates the pressure drop across the fabric, is provided with leveling screws and a a micrometer plunger for adjusting the meniscus to zero when no air is being drawn through the fabric. This manometer functions smoothly and dependably. The vertical manometer, which indicates the pressure drop across the orifice for measuring the air flow, is connected to a reservoir having a large area compared with the cross-sectional area of the manometer so that the oil level in the reservoir remains sufficiently constant.

The amount of air flowing through a fabric under test is determined from the pressure drop indicated by the vertical manometer and the calibration of the orifice which is used. A set of nine orifices covers the range of air permeability from 1 to 700 cubic feet per minute per square foot of fabric. The orifices are easily inserted through a door opening into chamber B of Figure G-2. The air permeability is usually measured for a pressure drop across the fabric of 0.5 inch of water, but it may be measured at any pressure drop between 0.1 and 1.0 inch of water or at a series of pressure drops between these limits. The appropriate size of orifice to use for a fabric whose approximate air permeability is not known is determined by a trial run. The pressure drop indicated by the vertical manometer should be greater than 3 inch. If it is less, a smaller orifice should be used to obtain precision in the measurement.

The inclined manometer is graduated to read pressure in inches of water, one division equaling a pressure difference of 0.01 inch of water. The scale is readily readable to 0.002 inch of water. The pressures indicated by the scales of eight inclined manometers were checked against the values obtained with a sensitive differential pressure gage. In making the calibration, a given volume of air, measured by means of a calibrated gasometer, was drawn through the instrument. The pressure drop across the orifice, as indicated by the vertical manometer, was maintained at a constant value during this period. The

appropriate air permeabilities which can be measured with each of the nine orifices are given in specific tables [50].
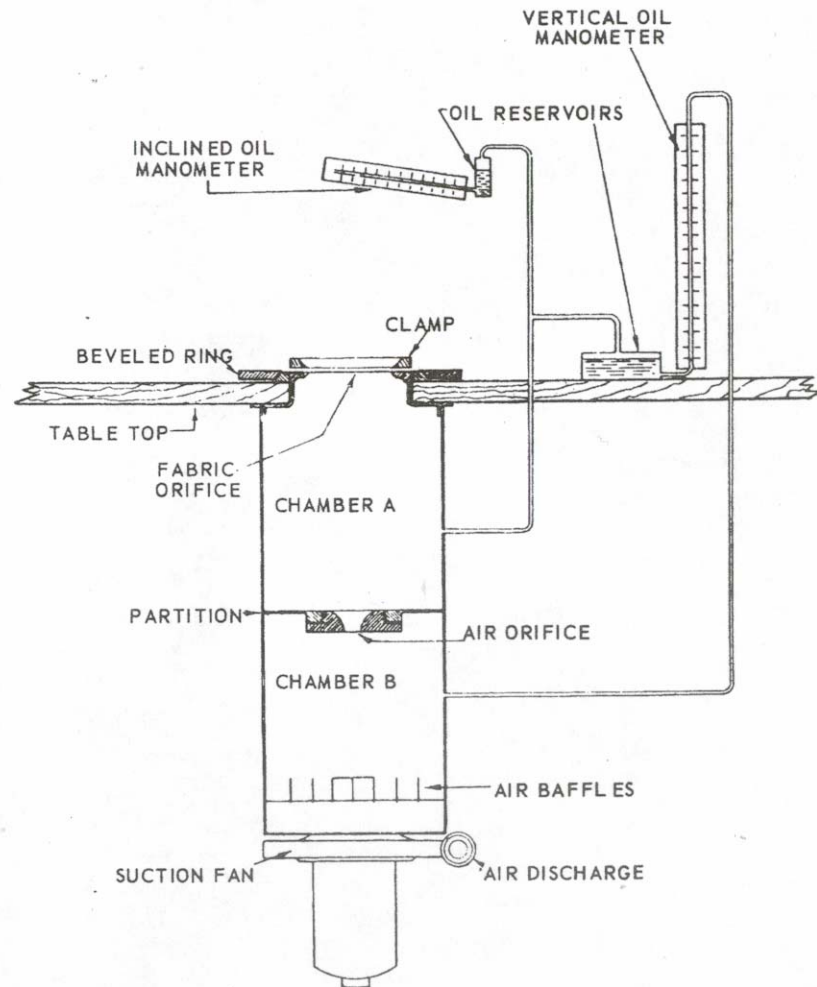
Figure G-0-2: Schematic Diagram of the Air-Permeability Instrument [50]

Air permeability tests were conducted in a room at 73 degree Fahrenheit (22.7 degree Celsius) and 50 relative humidity.

MEASUREMENT RESULTS:

Measurement results are given Table G-1.

Table G-1: Air Permeability Measurement Results

Sample Number and Positioning	Air Permeability	
	Cubic Feet / Square Foot / Minute	Rayls
Sample 1	478.8	94.2278
Sample 1 – 90 degree converted	477.1	93.8933
Sample 1 – upside down	472	92.8896
Sample 1 – upside down 90 degree converted	475.4	93.5587
Sample 2	492.4	96.9043
Sample 2 – 90 degree converted	492.4	96.9043
Sample 2 – upside down	492.4	96.9043
Sample 2 – upside down 90 degree converted	492.4	96.9043
Sample 3	489	96.2352
Sample 3 – 90 degree converted	487.3	95.9006
Sample 3 – upside down	487.3	95.9006
Sample 3 – upside down 90 degree converted	485.6	95.5661

Conversion cubic feet per square foot per minute in Rayls:

$$Rayl = \frac{\frac{N}{m^2}}{\frac{m}{s}} = \frac{kg\,m}{m^2\,s^2}\frac{s}{m} = \frac{kg}{m^2\,s} = \frac{60\,l}{m^2\,min} = \frac{2.118\,cu\,ft}{10.7639\,sq\,ft\,min} = 0.1968\frac{cu\,ft}{sq\,ft\,min}$$

$1\ cu\ ft = 28.3168466\ l$

$1\ sq\ ft = 0.09290304\ m^2$

EVALUATION OF RESULTS:

In general, a knowledge of the flow-resistance of a material permits the relevant acoustic impedence to be predicted, although care must be taken to ensure that a representative

value of flow-resistance is used, as many practical materials are subject to considerable variation between and within batches. However, for many purposes high accuracy is not required for instance, in the initial design stages where selection of a potentially suitable absorbing material is the objective. Unfortunately, manufactures do not usually include data on flow-resistance in their technical literature. It is emphasized that the purpose of these flow resistivity measurements is solely to provide an indication of the order of magnitude of the flow-resistance to be expected for a given material.

Therefore, the value used for predicting the flow resistivity of the forming screen is the average over all given measurement results (for three different samples and various orientations). The mean value therefore is: 95.4824 Rayls.

Appendix H: Measurement of Speed of Sound

Technical Specifications Sound Speed Measuring Unit:

The sound speed measuring unit (Figure H-0-1) allows to measure the sound speed in any kind of liquid by measuring with precision the time that is taken by an ultrasonic burst to propagate over a define distance. Therefore, the transducer is connected to the DOP 2000 velocimeter. The measurement is based on a phase analysis of an echo generated by a mobile plate when this plate is moved over a known distance. Any transducers having a case diameter of 8mm or 12mm can be used, which enables the measurement of the sound speed at different ultrasonic frequencies. The sound speed unit is delivered with a special software module which is installed in the WDOP software of the velocimeter.

Figure H-0-1: Sound Speed Measureing Unit [51]

Appendix I: Measurement of the Insertion Loss

INTRODUCTION:

The insertion loss characterizes the sensitivity of a transducer, and is given by:

$$I_L \ [dB] = 20 \log \frac{Vpp \ echo}{Vpp \ emitted}$$

Equation 40: Insertion Loss

In order to measure the insertion loss, an ultrasonic burst is emitted by a transducer. The same transducer receives an echo issued from a plane perpendicular target, which acoustic impedance differs very much from the liquid used as a transmitting media. The voltage ratio between the echo and the emitted burst, expressed in logarithm, is called Insertion Loss [53]. Signal Processing's transducers have an IL between 10 and 20 dB, depending on the type of transducer. To measure the Insertion Loss of your transducer, you need the following equipment:

- 1 burst generator
- 1 oscilloscope
- 2 coaxial cable
- 1 water container, with a transducer holder
- 1 target (stainless steel preferred)

SET UP:

Connect the transducer, the burst generator and the oscilloscope as shown in Figure I-0-1. You can trig the Echo signal by using the TTL output signal coming from the burst generator (if available).
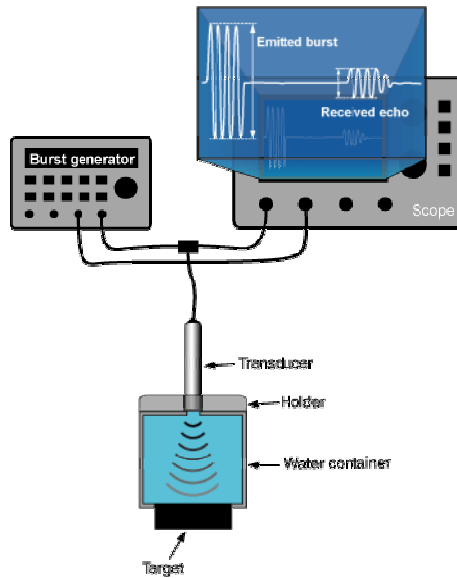
Figure I-0-1: Insertion Loss Setup [51]

To prevent any damage to the burst generator, we recommend to check the specifications of the instrument in order to verify that it can support the connection of a very low impedance (<50 ohm) during a long time.

MEASURING PROCEDURE:

1. Be sure that the contact between the front surface of the transducer and the water is good (no air bubbles).
2. Be sure that the transducer is perpendicular to the target (max echo voltage).
3. Measure the voltage of the emitted burst.
4. Measure the voltage of the echo.
5. Compute the Insertion Loss.

The distance between the transducer and the target must be enough in order to avoid the disturbances generated by the ringings (the ringing effect results in saturation of the transducer preventing measurements at depths located just a few mm behind the surface of the transducer), but not too long to be sure to collect all the emitted energy (divergence of the ultrasonic beam).

The thickness of the target must also be considered. To avoid any interferences generated by second echo, coming from the far wall of the target, a minimum thickness is required. As the amount of the energy that penetrates inside the target depends on the difference in acoustic impedance between the target and the transmitting media, it is recommended to use a target with the highest acoustic impedance as possible.

Appendix J: Delany-Bazley-Model and Allard-Champoux-Model

The Delany-Bazley-Model and the Allard-Champoux-Model were used to model the acoustic impedance of the porous forming screen. Both models and the results are described in the following.

DELANY-BAZLEY MODEL (MIKI CORRECTION)

The equations of Delany and Bayley, presented for the first time in 1970, have since been widely used to describe sound propagation in fibrous materials. These laws have been used in various applications such as sound attenuation in ducts, room acoustics, the calculation of transmission loss through walls, and primarily in models describing sound propagation above various types of ground. Slightly different but similar laws were later suggested to handle specific fibrous materials, and also to improve the low-frequency behavior of the Delany and Bazley equations. The geometry of fibrous materials, in spite of its apparent simplicity has however not been taken into account in these works [5].

The power laws of Delany and Bazley involve eight adjustable parameters that are the same for all fibrous materials. According to Delany and Bazley, the acoustic impedence is predicted by:

$$Z = R + iX = \rho_0 c_0 \left[1 + AF^\alpha + iBF^\beta \right]$$

with the constants:

$A = 0.057$

$B = 0.087$

$\alpha = -0.75$

$\beta = -0.732$

Equation 41: Delany-Bazley-Model

where f is the frequency, ρ_0 is the density of the fluid, $\sigma = \Delta p/(U\, l)$ is the flow resistivity, Δp is the pressure drop, U is the fluid velocity, l is the material thickness, c_0 is the speed of sound in the fluid and the constant F is $\rho_0 f/\sigma$.

In general, knowledge of the flow-resistance of a material permits the relevant acoustic impedance to be predicted, although care must be taken to ensure that a representative

value of flow-resistance is used, as many practical materials are subject to considerable variation between and within batches. However, for many purposes high accuracy is not required for instance, in the initial design stages where selection of a potentially suitable absorbing material is the objective. Unfortunately, manufactures do not usually include data on flow-resistance in their technical literature. It is emphasized that the purpose of these flow resistivity measurements (see appendix) is solely to provide an indication of the order of magnitude of the flow-resistance to be expected for a given material. Manufacturers do not necessarily control the flow-resistance of their product and it will usually be necessary to sample-test a specific material before final evaluation. The main factors influencing the flow-resistance of fibrous materials are the fiber size and the bulk density, and it is known that for given fiber size the relation between bulk density and flow-resistance approximates closely to a simple power law [15].

The formulas given above were implemented in the following MATLAB code to calculate the acoustic impedance from 2 to 8 MHz.

```matlab
%Acoutic Impedance Description of the Forming Screen

clear all

%Forming screen roperties:
rhop=1620; %density of polyester in kg/m3
Omega=0.95; %porosity
sigmae=95.5; %specific flow resistivity in MKS-Rayls
l=0.00056; %thickness in m
sigma=sigmae/l; %flow resistivity in MKS-Rayls/m

%Fluid properties:
rho0=1000; %density of water in kg/m3
c0=1482; %speed of sound in water at 20 degree celsius in m/s

%Specific Acoustic Impedance Zs

%a) Delany-Bazley model:

N1=2000000;
N2=8000000;
f=N1:1:N2; %frequency in Hertz

A=0.057;
B=0.087;
F=f.*rho0/sigma; %Non-dimensional frequency
alpha=-0.750;
beta=-0.732;
Zs=rho0*c0*(1+A*F.^alpha+i*B*F.^beta);

figure(1)
subplot(2,2,1)
semilogx(f,real(Zs),'b')
```

```
xlabel('Frequency [log]')
ylabel('Real Part Spec. Ac. Impedance')
title('Delany-Bazley Model')

subplot(2,2,2)
semilogx(f,imag(Zs),'b')
xlabel('Frequency [log]')
ylabel('Imaginary Part Spec. Ac. Impedance')
title('Delany-Bazley Model')

hold on
```

The results are shown in Figure J-1 and discussed in chapter 4.5.

ALLARD-CHAMPOUX-MODEL

Jean-F. Allard and Yvan Champoux developed new expressions that can be used instead of the phenomenological equations of Delany and Bazley. They provide similar predictions in the range of validity of these equations, and in addition are valid at low frequencies where the equations of Delany and Bazley provide unphysical predictions. These new expressions have been worked out by using the general frequency dependence of the viscous forces in porous materials proposed by Johnson et al. [J. Fluid Mech. 176, 379 (1987)], with a transportation carried out to predict the dynamic bulk modulus of air. The model used suggests how sound propagation in fibrous materials can depend both on the diameter of the fibers and on the density of the material [5].

Typical fibers are modeled here as infinite circular-cylindrical rods of radius r that lie in planes parallel to the surface of the layers. Only the case where the velocity of the fluid for from the fibers is perpendicular to the direction of the fibers is considered here. The detailed description of the model which will be used to describe the propagation of sound through the porous forming screen and the derivation of the equations which will be applied in the following can be found in the paper of Allard et al. [5]. The acoustic impedance Z is:

$$Z = \sqrt{\rho_b(\omega) K_b(\omega)}$$

Effective dynamic density of material ρ_b:

$$\rho_b(\omega) = \rho_0 \left[1 - \frac{\sqrt{1 - \dfrac{i\omega\tau}{2}}}{i\omega\tau} \right]$$

Effective dynamic bulk modulus K_b:

$$K_b(\omega) = \gamma P_0 \left[\gamma - \frac{\gamma - 1}{1 - \dfrac{\sqrt{1 - i\omega 2N\tau}}{i\omega 4N\tau}} \right]$$

Equation 42: Allard-Champoux-Model

where ρ_0 is the density of the fluid, $\omega = 2\pi f$ is the angular frequency, τ equals ρ_0/σ, $\sigma = 4\Omega\sigma_e/S_f^2$ is the flow resistivity, $\Omega = V_p/V_S$ is the porosity (V_p is the volume of the sample and V_s is the volume of the fibers), σ_e is the specific flow resistivity, S_f is the pore shape factor, γ is the ratio of the specific heats, P_0 is the atmospheric pressure and N is Prandtl number.

The predictions obtained from the laws of Delany and Bazley as well as from Allard and Champoux, are very similar in the range of validity of the laws of Delany and Bazley. The expressions given by Allard and Champoux are, however, also valid at low frequencies and can be used to describe the steady flow of air through fibrous media. The Allard-Champoux-model predicts a dependence of the dynamic density and the bulk modulus as a function of the bulk density of the material and the diameter of the fibers, that can be neglected at low frequencies, but is measurable at high frequencies.

The formulas given above were implemented in the following MATLAB code to calculate the acoustic impedance from 2 to 8 MHz.

```
%Acoutic Impedance Description of the Forming Screen

clear all

%Forming screen roperties:
rhop=1620; %density of polyester in kg/m3
Omega=0.95; %porosity
sigmae=95.5; %specific flow resistance in MKS-Rayls
l=0.00056; %thickness in m
s=1; %pore shape factor
sigma=sigmae/l; %flow resistivity in MKS-Rayls/m
```

```
%Fluid properties:
rho0=1000; %density of water in kg/m3
c0=1480; %speed of sound in water at 20 degree celsius in m/s
cpw=4.186; %specific heat at constant pressure for water in J/(gK)
cvw=4.186; %specific heat at constant volume for water in J/(gK)
gamma=cpw/cvw; %heat capacity ratio
P0=101300; %atmospheric pressure
N=7; %Prandtl number for water


%Specific Acoustic Impedance Zs (real and imaginery part of the specific acoustic
impedance)

%b)Allard-Champoux Model:

N1=2000000;
N2=8000000;
i=sqrt(-1);

for j=N1:100000:N2 %frequency in Hertz
    f(j)=j;
    omega=f(j)*2*pi;
    tau=rho0/sigma;
    rhob=rho0*(1+((1/(i*2*pi))*(1/(tau*f(j)))*(1+i*pi*(tau*f(j)))^0.5));
    Kb=gamma*P0*(gamma-((gamma-1)/(1+(1/(i*8*pi*N))*(1/(tau*f(j)))*((1+i*pi*
        (tau*f(j)))^0.5)*((1+i*pi*4*N)^0.5)))));
    Zs(j)=(rhob*Kb)^0.5;
end

figure(1)
subplot(2,2,3)
semilogx(f,real(Zs),'b')
xlabel('Frequency [log]')
ylabel('Real Part Spec. Ac. Impedance')
title('Allard-Champoux Model')

subplot(2,2,4)
semilogx(f,imag(Zs),'b')
xlabel('Frequency [log]')
ylabel('Imaginary Part Spec. Ac. Impedance')
title('Allard-Champoux Model')

hold on
```

The results are shown in Figure J-1 and discussed in chapter 4.5.

RESULTS OF THE DELANY-BAZLEY-MODEL AND ALLARD-CHAMPOUX-MODEL:

Results of the Delany-Bazley-Model and the Allard-Champoux-Model are given in Figure J-0-1. The results are discussed in chapter 4.5.
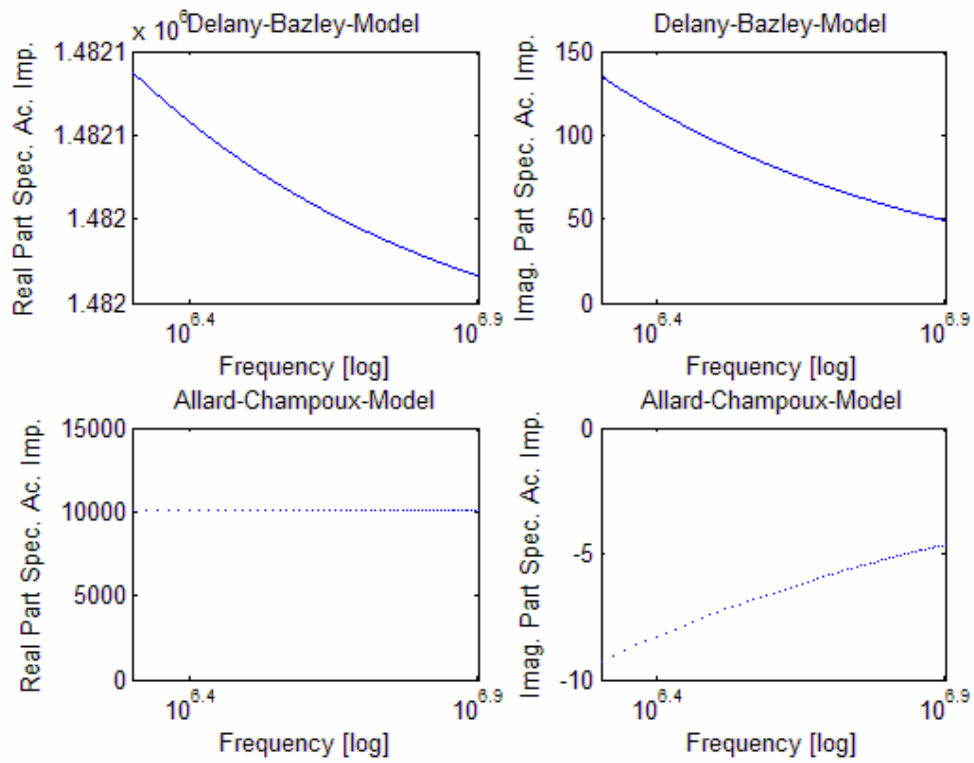
Figure J-0-1: Results Acoustic Impedance Models

References

1. Adrian, R. J. (2004). "Twenty Years of Particle Image Velocimetry." 12th International Symposium on Applications of Laser Techniques to Fluid Mechanics.

2. Aidun, C. K.; Lu, Y. (1995). "Lattice Boltzmann Simulation of Solid Particles Suspended in Fluid." Journal of Statistical Physics 81.

3. Aidun, C. K.; Lu, Y.; Ding, E.-J. (1998). "Direct Analysis of Particulate Suspensions with Inertia Using the Discrete Boltzmann Equation." Journal of Fluid Mechanics 373: 287-311.

4. Alfonsi, G.; Brambilla, S.; Chiuch, D. (2003). "The Use of an Ultrasonic Doppler Velocimeter in Turbulent Pipe Flow." Exepriments in Fluids 35: 553-559.

5. Allard, J.-F.; Champoux, Y. (1992). "New Empirical Equations for Sound Propagation in Rigid Frame Fibrous Materials." J. Acoust. Soc. Am. 91(6).

6. Awatani, J. (1955). "Study on Acoustic Radiation Pressure, Radiation Pressure on a Cylinder." Mem. Inst. Sci. Ind. Osake Univ. 12: 95-102.

7. Baker, D. W. (1965). "The Doppler Shift Principle Applied to Flow and Displacement Measurement, Proceedings of the 18th Annual Conference on Engineering in Medicne and Biology.

8. Baker, D. W. (1973). "Characteristics and Mathematical Modeling of the Pulsed Ultrasonic Flowmeter." Medical and Biological Engineering(July): 404-421.

9. Barmatz, M.; Collas, P. (1985). "Acoustic Radiation Force Experienced by a Solid Cylinder in a Plane Progressive Sound Field." J. Acoust. Soc. Am. 77(9280945).

10. Beaudoin, J.; Cadot, O.; Aider, J.; Wesfreid, J. (2004). "Three-Dimensional Stationary Flow over a Backward-Facing Step." European Journal of Mechanics B-Fluids 23(1): 147-155.

11. Beissner, K. (1998). "The Acoustic Radiation Force in Lossless Fluids in Eulerian and Lagrangian Coordinates." J. Acoust. Soc. Am. 103(5): 2321-2332.

12. Brito, D.; Nataf, H. C.; Cardin, P.; Aubert, J.; Masson, J. P. (2001). "Ultrasonic Doppler Velocimetry in Liquid Gallium." Experiments in Fluids 31(6): 653-663.

13. Brodeur, P. H.; Lewis, E. L. (1993). "Ultrasonic Characterization of Forming Fabrics." IPST Technical Paper Series.

14. Chen, X. C.; Apfel, R. E. (1996). "Radiation Force on a Spherical Object in an Axisymmetric Wave Field and Its Application to the Calibration of High-Frequency Transducers." J. Acoust. Soc. Am. 99: 713-724.

15. Delany, M. E.; Bazley, E. N. (1970). "Acoustical Properties of Fibrous Absorbent Materials." Applied Acoustics 3.

16. Eckert, S.; Gerbeth, G. (2002). "Velocity Measurements in Liquid Sodium by Means of Ultrasound Doppler Velocimetry." Experiments in Fluids 32(5): 542-546.

17. Embleton, T. F. W. (1954). "Mean Force on a Sphere in a Spherical Sound Field." J. Acoust. Soc. Am. 20: 40-45.

18. Evans, D. H.; McDicken, W. N. (2000). "Doppler Ultrasound - Physics, Instrumentation and Signal Processing." Wiley.

19. Fox, F. E. (1940). "Sound Pressure on Spheres." J. Acoust. Soc. Am. 12: 147-149.

20. Fry, F. J. (1978). "Ultrasound: Its Applications in Medicine and Biology." Amsterdam, Elsevier Scientific Pub. Co.

21. Gorkov, L. P. (1962). "On the Forces Acting on a Small Particle in an Acoustic Field in an Ideal Fluid." Sov. Phys. Kokl. 6: 772-775.

22. Hasegawa, T.; Saka, K.; Inouse, N.; Matsuzawa, K. (1988). "Acoustic Radiation Force Experienced by a Solid Cylinder in a Plane Progressive Sound Field." J. Acoust. Soc. Am. 83: 1770-1775.

23. Hasegawa, T.; Watanabe, Y. (1978). "Acoustic Radiation Pressure on an Absorbing Sphere." J. Acoust. Soc. Am. 46: 1733-1737.

24. Hasegawa, T.; Yosioka, K. (1969). "Acoustic Radiation Force on a Solid Elastic Sphere." J. Acoust. Soc. Am. 46: 1139-1143.

25. Hueter, T. F.; Bolt, R. H. (1954). "Sonics - Techniques for the Use of Sound and Ultrasound in Engineering and Science." John Wiley & Sons, Inc.

26. Jawad, I. A. (1996). "A Practical Guide to Echocardiogrpahy and Cardiac Doppler Ultrasound." John Wiley & Sons, Inc.

27. Jensen, J. A. (1996). "Estimation of Blood Velocities Using Ultrasound." Cambridge University Press.

28. Kerut, E. K.; McIlwain, E. F.; Plotnick, G. D. (1996). "Handbook of Echo-Doppler Interpretation." John Wiley & Sons, Inc.

29. Kikura, H.; Takeda, Y.; Durst, F. (1999). "Velocity Profile Measurement of the Taylor Vortex Flow of a Magnetic Fluid Using the Ultrasonic Doppler Method." Experiments in Fluids 26(3): 208-214.

30. Kikura, H.; Takeda, Y.; Sawada, T. (1999). "Velocity Profile Measurements of Magnetic Fluid Flow Using Ultrasonic Doppler Method." Jorunal of Magnetism and Magnetic Materials 201: 276-280.

31. Kikura, H.; Yamanaka, G.; Aritomi, M. (2004). "Effect of Measurement Volume Size on Turbulent Flow Measurement Using Ultrasonic Doppler Method." Experiments in Fluids 36(1): 187-196.

32. King, L. V. (1934). "On the Acoustic Radiation Pressure on Spheres." Proc. R. Soc. London Ser. 147: 212-240.

33. Kino, G. S. (1987). "Acoustic Waves: Devices, Imaging and Analog Signal Processing." Engelwood Cliffs, N.J., Prentice-Hall.

34. Kinsley, L. E.; Frey, A. R. (1982). "Fundamentals of Acoustics." John Wiley & Sons, Inc.

35. Kostas, J.; Soria, J.; Chong, M. (2002). "Particle Image Velocimetry Measurements of a Backward-Facing Step Flow." Experiments in Fluids 33(6): 838-853.

36. Kundt, A. (1866). "Ueber Eine Neue Art Akustischer Staubfiguren Und Ueber Die Anwendung Derselben Zur Bestimmung Der Schallgeschwindigkeit in Festen Koerpern Und Gasen." Ann. Phy. (Leipzig) 127(497).

37. Leung, E.; Jacobe, N.; Wang, T. (1981). "Acoustic Radiation Force on a Rigid Sphere in a Resonance Chamber." J. Acoust. Soc. Am. 70: 1762-1767.

38. Lofstedt, R.; Putterman, S. (1991). "Theory of Long Wavelength Acoustic Radiation Pressure." J. Acoust. Soc. Am. 90: 2027-2033.

39. Maidanik, G. (1957). "Acoustic Radiation Pressure Due to Incident Plane Progressive Waves in Spherical Objects." J. Acoust. Soc. Am. 29: 738-742.

40. Maidanik, G.; Westervelt, P. J. (1957). "Acoustic Radiation Pressure Due to Incident Plane Progressive Waves on Spherical Objects." J. Acoust. Soc. Am. 29: 936-940.

41. Nie, J.; Armaly, B. (2004). "Reverse Flow Regions in Three-Dimensional Backward-Facing Step Flow." International Journal of Heat and Fluid Flow 47(22): 4713-4720.

42. Nyborg (1967). "Radiation Pressure on a Small Rigid Sphere." J. Acoust. Soc. Am. 42: 947-952.

43. Panametrics, I. (2004). "Technical Notes." http://www.panametrics-ndt.com/ndt/ndt_transducers/downloads/transducer_technotes.pdf.

44.   Papadakis, E. P. (1999). "Ultrasonic Instruments and Devices." Academic Press.

45.   Pierce, A. D. (1981). "Acoustics: An Introduction to Its Physical Principles and Applications." New York, McGraw-Hill.

46.   Prasad, A. K. (2000). "Particle Image Velocimetry." Current Science 79(1).

47.   Reneman, R. S. (1973). "Cardiovascular Applications of Ultrasound." McGraw-Hill.

48.   Rudnick, I. (1977). "Measurement of the Acoustic Radiation Pressure on a Sphere in a Standing Wave Field." J. Acoust. Soc. Am. 62: 20-22.

49.   Sabbagha, R. (1994). "Diagnostic Ultrasound: Applied to Obstetrics and Gynecology." McGraw-Hill.

50.   Schiefer, H. F.; Boyland, P. M. (1942). "Improved Instrument for Measuring the Air Permeability of Fabrics." Journal of Research of the National Bureau of Standards 29.

51.   Signal-Processing (2004). "Introducing Ultrasonic Doppler Velocimetry." www.signal-processing.com.

52.   Skolnik, M. I. (1990). "Radar Handbook." McGraw-Hill.

53.   Skolnik, M. I. (2001). "Introduction to Radar Systems." New York, McGraw-Hill.

54.   Takeda, Y. (1986). "Velocity Measurement by Ultrasound Doppler Shift Method." International Journal Heat and Fluid Flow 7(4): 313-318.

55.   Takeda, Y. (1995). "Velocity Profile Measurement by Ultrasonic Doppler Method." Experimental Thernal and Fluid Science 10(4): 444-453.

56.   Takeda, Y. (1999). "Ultrasonic Doppler Method for Velocity Profile Measurement in Fluid Dynamics and Fluid Engineering." Experiments in Fluids 26(3): 177-178.

57.   Technische-Universitaet-Darmstadt (2005). "Acoustic Cavitation and Nonlinear Dynamics." http://www.physik.tu-darmstadt.de/nlp/cavitation.html.

58.   Wei, W.; Thiessen, D.; Marston, P. (2004). "Acoustic Radiation Force on a Compressible Cylinder in a Standing Wave." J. Acoust. Soc. Am. 116(1): 201-208.

59.   Wells, P. N. T. (1969). "Physical Principle of Ultrasonic Diagnosis." Academic Press.

60.   Wells, P. N. T. (1977). "Biomedical Ultrasonics." Academic Press.

61.   Wilson, C. E. (1994). "Noise Control." Krieger Publishing Company.

62.   Wu, J.; Du, G. (1990). "Acoustic Radiation Force on a Small Compressible Sphere in a Focused Beam." J. Acoust. Soc. Am. 87: 997-1003.

63.   Wu, J.; Du, G.; Work, S.; Warshaw, D. (1990). "Acoustic Radiation Pressure on a Rigid Cylinder - an Analytical Theory and Experiments." J. Acoust. Soc. Am. 87(2): 581-586.

64.   Xu, H. (2003). Measurement of Fiber Suspension Flow and Forming Jet Velocity Profile by Pulsed Ultrasonic Doppler Velocimetry. Atlanta, Institute of Paper Science and Technology. Ph.D.

65.   Yasuda, K.; Kamakura, T. (1997). "Acoustic Radiation Force on Micrometer-Size Particles." Applied Physics Letters 71(13): 1771-1773.

66.   Yosioka, K.; Kawasima, Y. (1955). "Acoustic Radiation Pressure on a Compressible Sphere." Acoustica 5: 167-173.